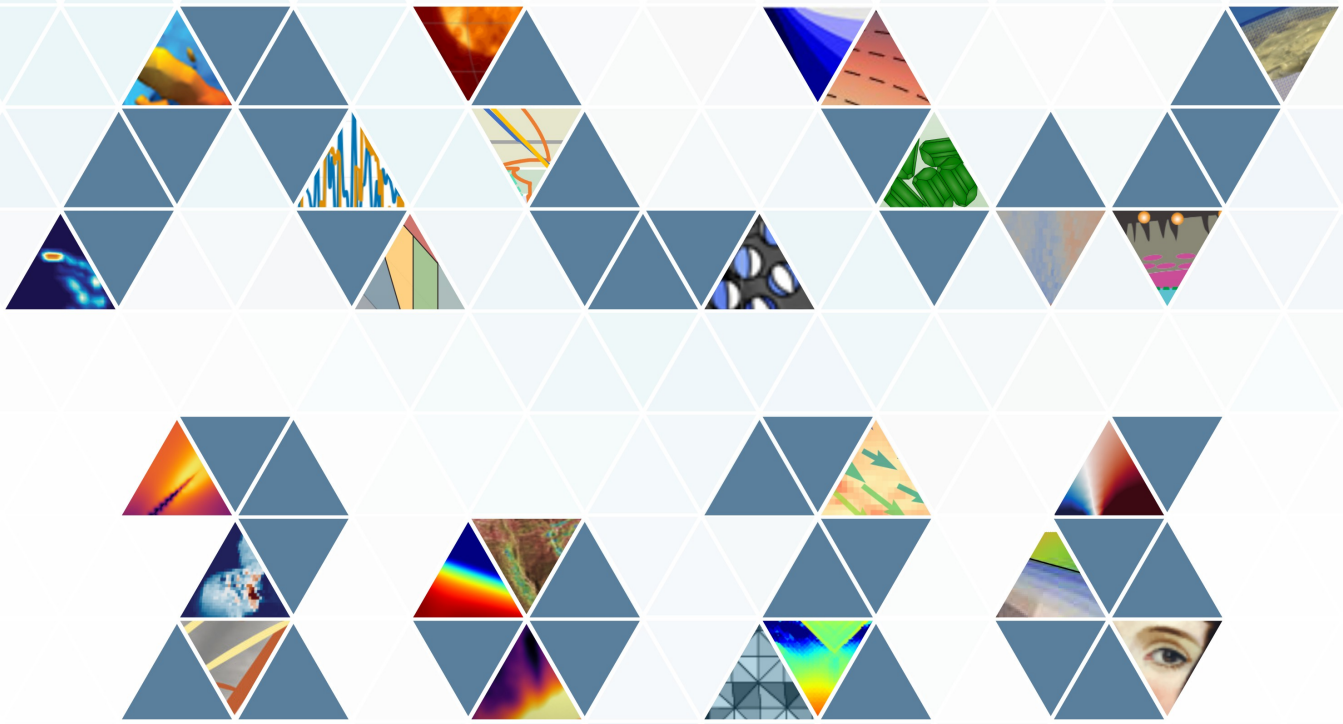
Abstracts



EGU

Charles University

1919 CZECH GEOLOGICAL SURVEY

Contents

Invited speakers **1**

Susanne Buiter: A discussion of rifted continental margins in a plate tectonic context . . . 1
Denise Degen: Interpretable Physics-Based Machine Learning for Geodynamic Modeling . . . 2
Oğuz Hakan Göğüş: Lithospheric Dripping Across Tectonic Regimes: From Earth's Orogens to Venusian Tectonics . . . 3
Anthony Jourdon: Coupling long-term geodynamics and dynamic rupture: Deformation of the lithosphere across scales . . . 4
Tobias Keller: Numerical modelling of multi-phase flows in magmatic systems . . . 5
Madeleine C. Kerr et al.: Effects of mineral phase transitions on mantle dynamics and heat flow in Venus 6
Martin Kihoulou et al.: Remote-controlled tectonics: How does Io drive "rifting" and "subduction" on Europa? . . . 8
Ágnes Király: Towards efficient modeling of rock texture related mechanical anisotropy during large-scale dynamic processes . . . 9
Diogo L. Lourenço: Rocky Planets as Heat Engines: Global Tectonomagmatic Regimes and Planetary Evolution . . . 10
Julian Lowman et al.: Plate generation from mantle convection and feedback with the deep interior . . . 11
Adina E. Pusok: Melt generation and transport from the mantle to the surface . . . 12
Christian Sippl et al.: Processes in subducting slabs: how can seismology inform models? . . . 13
Christophe Sotin: Laboratory experiments on the creep behavior of ices: implications for the interior dynamics of icy worlds . . . 14
Arne Spang et al.: Ductile instability, strain localization, and rupture propagation by thermal runaway . 15
Sebastian G. Wolf et al.: Quantifying the interaction between tectonic deformation and climate-driven surface processes using coupled geodynamic-landscape evolution models . . . 17

Posters **1**

Andrea Adams et al.: 3D Modeling of Peel Back Delamination on Venus . . . 1
Riva Alkahal et al.: Investigating mantle flow on Mars . . . 3
Amita Anand et al.: Can porosity waves create long-period seafloor topography? Investigating the topographic expression of transient mid-ocean ridge magma supply . . . 4
Valentin André et al.: Investigating Partial Melting in Europa's Mantle Using 3D Convection Models . . 6
Maëlis Arnould et al.: Influence of Mantle Rheology on Plume Morphology and Dynamics . . . 8
Maëlis Arnould et al.: Geodynamica: a new community-led Diamond-Open Access Journal dedicated to Earth and (Exo)Planets dynamics . . . 10
Daniel Astudillo Manosalva et al.: Forming the Lunar crustal Dichotomy from Terrestrial Tides . . . 11
Adrian Bakoč et al.: Why is Enceladus so stressed? . . . 12
Vít Beran et al.: A parameterized model of a solidifying magma reservoir: the microstructural record of crystal settling dynamics . . . 13
Priyanka Biju Sindhu et al.: Experimental Insights into Effusive Cryovolcanism: Boiling and Freezing of Saline Water under Low Pressure Conditions . . . 14
Sascha Brune et al.: Semi-automated analysis of fault and plate boundary networks using Fatbox . . . 16
Arijit Chakraborty et al.: Towards thermo-chemical geodynamic modelling: surrogate models for coupling ASPECT with thermodynamics . . . 17
Byung-Dal So et al.: Efficient GPU Uzawa algorithms with projection strategies for geodynamic Stokes flow . . . 18
Hee Choi et al.: Estimating Archean Oceanic Crust Composition and Its Role in Water Delivery in Subduction Settings . . . 20
András Cserép et al.: Transient Seafloor Uplift at Mid-Ocean Ridges Driven by Mush Zone Buoyancy . . 21
Ritabrata Dasgupta et al.: Automatic detection and time tracking of mantle plumes using topological data analysis . . . 22
Anne Davaille et al.: On the importance of melt to localize large-scale deformation on Venus . . . 23
Luc de Hoÿm de Marien et al.: Combined petrology and physical modelling reveal the thermal evolution of translithospheric diapirs in the French Massif Central . . . 24
Albert de Montserrat Navarro: RheologyCalculator.jl: automatically solving arbitrary constitutive relationships . . . 26
Alexandr Dizov et al.: Role of water in mantle-lithosphere interactions in the context of Venus . . . 27
Daniel Douglas et al.: Linking surface and deep earth processes in geodynamic models: Coupling ASPECT and LandLab . . . 28
Valeria Fedeli et al.: Subduction initiation across a magma-poor to magma-rich passive margin transition: preliminary results from 3D numerical modelling . . . 29
Menno Fraters et al.: Intermediate-complexity modeling of magma–tectonic interaction in continental rifts . . . 30

Fanny Garel et al.: Thermal structure and deformation state of folding slabs : relationship with subduction zones' deep seismicity . . . 31
Catherine Gower et al.: Testing Compositional Asymmetry Between the African and Pacific LLVPs Using a Bayesian Inversion Framework . . . 32
Guido Gianni et al.: Pacific double-subduction drives Gulf of California rifting . . . 33
Tianyu Hu et al.: Linking the lower seismic layer in double seismic zones to the oceanic mid-lithospheric discontinuity . . . 34
Yangfan Huang et al.: Kinematics and Dynamics of Trumpet-Shaped Strike-Slip Fault Systems: The Western Himalayan Syntaxis Case Study . . . 36
Theo Häußler et al.: The Coupling of Mechanical Anisotropy to Post Glacial Rebound . . . 37
Pejvak Javaheri et al.: Implementing PlateRecipy: an open-access tool utilizing graph theory for detecting tectonic plate boundaries in geophysical datasets and model output . . . 39
Gabriel Johnston et al.: A Global Voxel-Based Analysis of Residence Time and Flux from Backward in Time Mantle Convection . . . 40
Buchanan Kerswell et al.: Beyond Equilibrium: Kinetic Thresholds and Rheological Feedbacks Create a Potentially Complex 410 in Slab Regions . . . 41
Hyunseong Kim et al.: Investigating the roles of laterally variable surface temperature and tidal heating in Europa's ice shell . . . 42
Inyup Kim et al.: Assessment of the Applicability of Smoothed Particle Hydrodynamics to Geodynamic Thermal Convection . . . 43
Terézia Košíková et al.: The Role of Geophysical Constraints in Assessing of Europa's Interior . . . 44
Ondřej Krýza et al.: Evolution of hot partially molten orogenic crust during lateral compression: Insights from coupled numerical and analogue models . . . 46
Yusuke Kubota et al.: The role of the mantle decompaction layer in Hadean volcanism . . . 47
Sreenidhi Kuruvamana Satheeshbabu et al.: Afar Plume Transport Beneath Arabia: Towards Constraining Controls on Sublithospheric Flow . . . 48
Laetitia Le Pourhiet et al.: 3D modelling of double out-dip subduction initiation in triangular oceanic basins: the role of slab bending . . . 50
Laëtitia Lebec et al.: Cracking Europa: Dilational bands formation . . . 52
Artem Lebedev et al.: Estimation of Gravity Field Parameters by thermal evolution modelling of Uranus's icy satellites . . . 53
Jieun Chang et al.: Effects of the balance between grain-size reduction and growth on lithosphere–basin evolution and mantle upwelling during continental rifting . . . 55
Kyeong-Min Lee et al.: The Effect of Multiple Impact Scenarios on the Thermo-Hydrodynamic Evolutionary Path and Core Formation Timing in Terrestrial Planets . . . 56
Victor Lherm et al.: Subduction dynamics in colloidal suspension convection experiments . . . 57
Zhong-Hai Li et al.: Contrasting slab decarbonation patterns control deep carbon cycling efficiency in hot vs. cold subduction zones . . . 58
Ranpeng Li et al.: Modeling Thermodynamically Consistent Phase Transitions in a Heterogeneous Mantle: A Multi-Component Entropy Method . . . 59
Xinnuo Li et al.: Crust–Mantle Separation at the Top of the Lower Mantle: Insights From Numerical Modeling . . . 60
Yingying Li et al.: Mantle plume formation and dynamics under Central Europe . . . 61
Yida Li et al.: From Slab Dynamics to Seismicity: A Global Perspective . . . 63
Mohit Lohani et al.: Geodynamic models of the Hellenic slab: implications for seismicity and stress . . . 65
Julian P. Lowman et al.: Impact of numerical model dimensionality on stagnant-lid convection in extreme curvatures and the influence of dynamically-varying thermal conductivity . . . 66
Tianyang Lyu et al.: Mantle flow acceleration drives episodic mobile-lid tectonics in Earth-like planets . . . 67
Ziqi Ma: Revisiting Plume-Induced Oceanic Hotspot Swells and Global Plume Buoyancy Fluxes . . . 68
Antonio Manjón-Cabeza Córdoba et al.: The differentiation of the growing mantle-magma ocean system: the primacy of thermodynamic properties . . . 69
Enrico Marzotto: Variable Thermal Conductivity Induces the Formation of Low-Conductivity Zones in Mantle Convection Models . . . 70
Ana Carolina Maurício Gomes et al.: From Constant to Nonlinear: Assessing the Role of Rheology in Subduction Interface Behavior . . . 73
Marla Metternich et al.: Rheological Controls on the Plate-Mantle System: Self-Consistent vs. Kinematically Constrained Models . . . 74
Nickolas Moccetti Bardi: Effects of Surface Mobility on Relevant Mantle H_2O Fluxes and Distribution . . . 76
Gwynfor T. Morgan et al.: Explaining d410-d660 correlation using MCMs? . . . 77
Gwynfor T. Morgan et al.: Strain Localisation in 2D models of continental rifting coupled to surface processes. . . . 78
Kim Moutard et al.: Sensitivity of hydrothermal vent temperatures to changes in crustal permeability profiles . . . 79

Laura Murzakhmetov et al.: How surface temperature changes surface magmatism and the tectonic regime . . . 81
Maria Elisa Muñoz et al.: Exploring geodynamic controls of orogenic gold systems under Paleoproterozoic and Phanerozoic thermal conditions. . . . 82
Ivan Navarrete et al.: A cyclo-steady-state model for inter-rifting deformation in magmatic rifts . . . 83
Derek Neuharth et al.: Dynamics of Carbonated Melt Migration in an Evolving Continental Rift . . . 84
Tina Neumann et al.: Lithospheric mechanisms leading to rift failure . . . 86
Vojtěch Patočka et al.: Layered bubble-rich structures on icy worlds: near-vacuum experiments with large volumes of low-salinity water . . . 87
Barbora Piláriková et al.: Coupled Damage and Ocean Overpressure Dynamics in Enceladus' Ice Shell . 88
Abigail Plimmer et al.: Controls on the spatio-temporal distribution of plume-related excess melting during continental rifting . . . 89
Michael Pons et al.: Surface expression of global tectonic regimes on Earth and Venus . . . 90
Hang Qian et al.: Modeling True Polar Wander from Time-Dependent Mantle Convection Using Self-Gravitating Geoid and Dynamic Topography in ASPECT . . . 92
Alessandro Regorda et al.: Understanding the Evolution of Venusian Rifts through Integrated Observations and Modeling . . . 93
Marko Repac et al.: Petit-Spot Volcanism: Flexure-Driven Melt Transport in the Oceanic Lithosphere . . 94
Neil M. Ribe et al.: Flexural and Membrane Stresses in Doubly Curved Subducting Slabs . . . 95
Sandrine Ritter et al.: From Mantle to Atmosphere: Quantifying the Geodynamic and Climatic Impacts of Large Igneous Provinces . . . 96
Maxwell Rudolph et al.: Broad thermochemical plumes - morphology, melt production, and volatile release . . . 97
Sabatino Santangelo et al.: Updated lunar crustal thickness distribution from global geodynamic models 99
Arushi Saxena et al.: Role of Local and Far-Field Forces in Central and Eastern U.S. Intraplate Seismicity 101
Felipe Sáez Leiva et al.: Two-phase flow modelling with FEniCSx: benchmarking and first steps into studying deformation and fluid flow feedback in simple shear . . . 103
Minji Seong et al.: Thermal structure modeling of subduction zones incorporating two-phase fluid flow 104
Kun Shang et al.: Did supracrustal materials build Archean continents? Evidence from coupled S-Si isotopes . . . 105
Brandon Lopez et al.: Volatile distribution in a Crystallizing Venusian Magma Ocean with hydrodynamic escape . . . 106
Henry W. Sitte et al.: Investigating the Stability of Thermochemical Piles for Different Origins . . . 107
Stephanie A. Sparks et al.: From Thermochronology to Geodynamics - Adapting Uncertainty Analysis for Lithosphere and Mantle Modeling . . . 108
Dave Stegman et al.: Revisiting Thermal Evolution Models of Rocky Planets using Asymmetric Thermal Boundary Layers . . . 109
Bernhard Steinberger and Shipboard Party SO319: A new approach to estimate oceanic upper mantle viscosity structure . . . 110
Simran Suresh et al.: Using ASPECT to construct a fully coupled 3D geodynamic landscape evolution model - Preliminary results and Outlook . . . 111
Shona A. Swan et al.: Tracking the Geochemical Evolution of the Oceanic Crust Using a Multi-Component Geodynamic Model of Mid-Ocean Ridge Magmatism . . . 113
Klára Anna Šindlerová et al.: Viscous response of Enceladus' ice shell to hydrothermal vents . . . 114
Catherine Thoraval et al.: Strength and sensitivity: Toward an a priori quantification of deformation localization potential in the ductile lithosphere . . . 116
Sushilkumar Thounaojam et al.: Modeling Iron Droplets Settling in Magma Ocean: Timescales of Core Formation . . . 117
Andréa Tommasi et al.: Modelling ductile strain localization with evolutive stochastic rheologies . . . 118
Andrea Tommasi et al.: Linking elastic and viscous anisotropy in the upper mantle through neural networks . . . 120
Leevi Tuikka et al.: How do you drive sinking and translation of a warm, oceanic plate? A geodynamic-petrological model of Paleoproterozoic flat-slab subduction . . . 122
Etienne Van Broeck et al.: Diagnosing rheological feedbacks during plate boundary formation . . . 123
Nhat Le Vo et al.: Topographic diffusion parameterization for rift dynamics: application to an ultraslow Arctic ridge . . . 124
Michaela Walterová: The effect of Mercury's spin rate and eccentricity variations on past tidal heating . 125
Yang Wang et al.: Maximum Decoupling Depth controls the Point of No Return in oceanic subduction zones . . . 127
Yijun Wang et al.: Composition-dependent erosion in subduction zones: Implications for slab dynamics and Andean margin evolution . . . 129
Zhensheng Wang et al.: The dense MORB fraction controls the dynamic stability and water-storage potential of the Mantle Transition Zone . . . 130

Tatjana Weiler et al.: Pure necking or strain localization: Rheological and geometrical controls of the lower crust on slab detachment . . . 132
Chenying Yu et al.: Thermomechanical modeling of the Archean thermal state: Evidence for a hot, thin lithosphere . . . 133
Alan J. Yu et al.: Geodynamic controls on the Upper Rhine Graben: from transtensional basin architecture to thermo-hydro-mechanical processes . . . 134
Filippo Zarabara et al.: Strain localisation in anisotropic materials . . . 136
Lilou Zeller et al.: Adeli2024 : The new version of a 3D versatile software for elasto-visco-plastic deformations on geological time scales . . . 137
Lilou Zeller et al.: Multiscale modeling of viscous strain localization : from rocks sample to lithospheric scale . . . 138
Rui-Min Zhang et al.: Numerical Simulation of Fully Compressible Two-Phase Flow in Subduction Zones 140
Yu Zhang et al.: Applying geodynamic tools to 3D large-scale ice-sheet modelling . . . 142
Wenbo Zhang et al.: Invert for the length scale of lunar mantle heterogeneity in the source region of Chang'E-5 mare basalts . . . 143

Invited speakers

A discussion of rifted continental margins in a plate tectonic context

Susanne Buiter*[1,2]

[1]GFZ Helmholtz Centre for Geosciences, Potsdam, Germany
[2]Tectonics and Geodynamics, RWTH Aachen University, Aachen, Germany
*buiter@gfz.de

Keywords: continental rifting, Wilson Cycle, mantle plumes, microcontinents

Rifted plate margins form as continental stretching evolves into continental breakup. Since Wegener's depiction of an abrupt boundary between ocean and continent, we have come to appreciate the intrinsic dynamics of continental rifting as part of the interactions between Earth's mantle and lithosphere. This is reflected in rifted margin processes and architectures that share common features, but also seem to point to a certain level of uniqueness among rift systems.

In this overview presentation, I aim to examine curiosity-driven questions regarding rifting, such as: Which factors and processes determine the localisation of rifting in a Wilson Cycle perspective, where rifts open at or near former sites of ocean closure? What is the role of mantle plumes? How can active ocean spreading centres jump, leading to the formation of microcontinents? Why do some rifts fail?

Interpretable Physics-Based Machine Learning for Geodynamic Modeling

Denise Degen[*1,2]

[1]TU Darmstadt
[2]GFZ Helmholtz Centre for Geosciences
[*]degen@geo.tu-darmstadt.de

Characterizing the influence of geodynamical models is important to improve our understanding of the development and current state of subsurface properties. Which are, in turn, of great societal relevance, for questions such as renewable energy. However, enabling a quantifiable characterization is a major challenge in Geodynamics, due to the high computational cost associated with both the model and the analysis for characterizing the influential parameters. The high cost of the model is caused by a high dimensionality in space, and time and a large number of input parameters. The cost of the probabilistic analyses is related to the large number of individual model solves required for performing the characterization.

To address the computational demand, we introduce the usage of surrogate models. Surrogate models comprise data-driven and physics-based approaches. While data-driven techniques, such as neural-networks, well capture complex system responses, they typically lack interpretability, hindering the degree of reliability of the model outcomes. This, in turn, poses challenges for the integration into digital twins especially in applications where risks need to be assessed. In contrast, physics-based approaches are fully interpretable, but often limited to elliptic and parabolic partial differential equations. Hence, they cannot capture the full complexity of the systems dynamics. To overcome the limitations of both data-driven and physics-based techniques, we introduce a hybrid approach namely the non-intrusive reduced basis method within the class of projection-based model order reduction techniques.

In this contribution we illustrate the benefits of these interpretable AI-assisted surrogate models to characterize the variability of geodynamic processes. To demonstrate the opportunities and challenges across multiple applications, we present the approach for examples from the field of mantle convection and lithospheric dynamics.

Lithospheric Dripping Across Tectonic Regimes: From Earth's Orogens to Venusian Tectonics

Oğuz Hakan Göğüş*[1]

[1]Eurasia Institute of Earth Sciences, Istanbul Technical University (ITU)
*goguso@itu.edu.tr

Keywords: drip tectonics, plateaus, Venus, biogeodynamics

This presentation explores the dynamics of viscous lithospheric dripping and its profound impact on surface topography and crustal deformation. Drawing on thermo-mechanical and analogue modeling across diverse settings, we will examine how these gravitational instabilities trigger rapid topographic uplift and crustal flow in active orogens like the Central Andes and the Anatolian Plateau. We will also review the mechanisms behind these drips, including eclogitization in magmatic arcs, and outline their diagnostic thermal and structural signatures. Finally, the talk will extend these geodynamic concepts beyond Earth, highlighting how similar drip mechanisms may drive crustal evolution and topographic features on Venus as well as their crucial role in biogeodynamic cycle.

Coupling long-term geodynamics and dynamic rupture: Deformation of the lithosphere across scales

Anthony Jourdon*[1]

[1]Université Côte d'Azur, Nice, France
*

Tectonic deformation plays a crucial role in shaping Earth's surface. Strain localization leads to the formation of shear zones at depth and faults at the surface, accommodating a significant portion of plate displacement within plate boundaries. Over millions of years, deformation can be considered as a spatially and temporally continuous process of visco-plastic strain localization. At shorter timescales, strain localization involves the alternation of continuous visco-elastic deformation and discontinuous, almost instantaneous elasto-plastic deformation events rapidly releasing strain energy: earthquakes. Linking long-term plate boundary formation and short-term earthquake mechanics is a challenging active field of research. In this presentation I will provide an overview of concepts, methods and advances in linking long-term geodynamics and short-term earthquake dynamics.

Numerical modelling of multi-phase flows in magmatic systems

Tobias Keller*[1]

[1]School of Geographical & Earth Sciences, University of Glasgow, UK
*Tobias.Keller@glasgow.ac.uk

Keywords: magma dynamics, igneous processes, numerical modelling, geodynamics

Magmatic systems in the Earth's mantle and crust exert important controls on planetary differentiation and long-term evolution, crust formation tied to tectonic regimes, and both hazards and resources associated with volcanism. These systems range from melt-poor partially molten rock, to mush bodies at intermediate melt fractions, and lenses of melt-rich, eruptible magma suspensions. Previous process-based models tended to represent magmatic systems as either porous flows (melt fraction < 20 %) or suspension flows (melt fraction > 60%). A lack of theoretical basis to represent mush flows at intermediate phase fractions has thus far hindered investigations into the dynamics of cumulate layers during magma ocean solidification as well as crustal mush bodies mediating magma ascent and petrogenesis in diverse tectonic settings. Moreover, previous theories were formulated specifically for two-phase flows of melt-solid mixtures and did not account for additional, volatile or other fluid phases despite their crucial role in driving volcanic activity and magmatic ore genesis.

My contribution addresses these gaps in theoretical understanding and modelling capacity by presenting a comprehensive theory [1] of magmatic multi-phase flows across all phase fractions at the system scale, rooted in mixture theory. I demonstrate its applicability with a numerical implementation using a finite-difference staggered-grid approach [2].

Numerical experiments replicate expected behaviours for two-phase flows including rank-ordered porosity wave trains in 1D, and porosity wave breakup in 2D in the porous flow regime, as well as particle concentration waves in 1D, and mixture convection in 2D in the suspension flow regime. In the mush regime, numerical experiments show strong melt localisation into lenses and stress-aligned melt-shear bands. A further application to a three-phase flow problem of immiscible melt segregation from a crystallising magma body demonstrates the versatility of the theoretical model and its numerical implementation.

References

[1] Keller & Suckale, GJI, 2019. https://doi.org/10.1093/gji/ggz287.
[2] Wong & Keller, GJI, 2022. https://doi.org/10.1093/gji/ggac481.

Effects of mineral phase transitions on mantle dynamics and heat flow in Venus

Madeleine C. Kerr*[1,2], Dave R. Stegman[2], Suzanne E. Smrekar[3,4], and Andrea C. Adams[3,4]

[1]University of California, Los Angeles
[2]Scripps Institution of Oceanography, University of California, San Diego
[3]Jet Propulsion Laboratory, Pasadena CA
[4]California Institute of Technology
*mckerr@ucla.edu

Keywords: Venus, mineral phase transition, ASPECT, coronae, mantle dynamics, heat flow

Among the many observed differences between the surfaces of Earth and Venus, the apparent lack of present-day plate tectonics as well as the abundance of volcano-tectonic features called coronae on Venus are among the starkest. These observations may be connected. The surface expression of both large-scale mantle upwellings (plumes from the core-mantle boundary) and downwellings, as well as smaller scale upwellings and downwellings (which manifest as coronae) can be understood within the framework of a terrestrial mantle undergoing a complex array of mineral phase transitions beneath a wholly connected lithosphere [1]. The mineral phase transition from wadsleyite to majorite and ferropericlase (WMF), which occurs at ~600 km depth in Venus, is relevant for planetary mantles with potential temperatures greater than 1700 K [1,2,3]. Two-dimensional mantle convection models that incorporate multiple phase transitions in pyrolite under Venus-like temperatures and pressures are explored using the geodynamic code ASPECT [4,5,6] and by employing the projected density approximation [7] and the entropy formulation of the energy equation [8]. The equation of state for the pyrolite composition is generated from the thermodynamic modelling software HeFESTo [9,10,11]. This talk will discuss the role that the WMF transition may play in explaining the complex surface expression of multi-scale mantle plumes on Venus in the present-day [1] as well as discuss the role that changing mineral phase transitions play in affecting how heat flows through the mantles of stagnant lid planets [12]. We will show how the WMF phase transition creates a regime of partially layered convection in a 2D stagnant lid model and how this state of layered convection creates upwellings and downwellings of multiple scales. We will also show that the WMF transition enhances the magnitude and variability of surface heat flow compared to an expected Rayleigh-Nusselt scaling relation. Finally, the dynamic topography from our modeling results for Venus are consistent with observations of a mid-wavelength (≈ 600 km) spatial frequency in the recent surface deformation history along the 7,000 km long Baltis Vallis lava channel [13]. The dynamical effect of the WMF phase transition may work in concert with melt-induced heat flow and lithospheric thinning (in the case of a "squishier" lithosphere [14]) to explain Venus's present-day surface.

References

[1] Kerr, M. C., D. R. Stegman, S. E. Smrekar, and A. C. Adams (2025), The glass-ceiling convective regime and the origin and diversity of coronae on Venus, Proceedings of the National Academy of Sciences, 122(38), e2504491,122.
[2] Kerr, M. C., & Stegman, D. R. (2024). Mantle avalanches in a Venus-like stagnant lid planet. Earth and Planetary Physics, 8(5), 686-702.
[3]Li, R., Dannberg, J., Gassmöller, R., Lithgow-Bertelloni, C., & Stixrude, L. (2025). How phase transitions impact changes in mantle convection style throughout Earth's history: From stalled plumes to surface dynamics. Geochemistry, Geophysics, Geosystems, 26(2), e2024GC011600.
[4] Timo Heister, Juliane Dannberg, Rene Gassmöller, and Wolfgang Bangerth. 2017. "High Accuracy Mantle Convection Simulation through Modern Numerical Methods – II: Realistic Models and Problems." Geophysical Journal International 210 (2) (May 9): 833–851. doi:10.1093/gji/ggx195. http://dx.doi.org/10.1093/gji/ggx195.
[5] Martin Kronbichler, Timo Heister, and Wolfgang Bangerth. 2012. "High Accuracy Mantle Convection Simulation through Modern Numerical Methods." Geophysical Journal International 191 (1) (August 21): 12–29. doi:10.1111/j.1365-246x.2012.05609.x. http://dx.doi.org/10.1111/j.1365-246X.2012.05609.x.
[6] Wolfgang Bangerth, Juliane Dannberg, Menno Fraters, Rene Gassmoeller, Anne Glerum, Timo Heister, Robert Myhill, and John Naliboff. 2024. *ASPECT v3.0.0* (version v3.0.0). Zenodo. https://doi.org/10.5281/ZENODO.14371679.
[7] Rene Gassmöller, Juliane Dannberg, Wolfgang Bangerth, Timo Heister, and Robert Myhill. 2020. "On Formulations of Compressible Mantle Convection." Geophysical Journal International 221 (2) (February 13): 1264–1280. doi:10.1093/gji/ggaa078. http://dx.doi.org/10.1093/gji/ggaa078.
[8] Dannberg, J., Gassmöller, R., Li, R., Lithgow-Bertelloni, C. and Stixrude, L. 2022. An entropy method for geodynamic modelling of phase transitions: capturing sharp and broad transitions in a multiphase assemblage.

Geophysical Journal International, 231(3), pp.1833-1849. doi:10.1093/gji/ggac293. https://doi.org/10.1093/gji/ggac293.
[9] Stixrude, L., & Lithgow-Bertelloni, C. (2022). Thermal expansivity, heat capacity and bulk modulus of the mantle. Geophysical Journal International, 228(2), 1119-1149.
[10] Stixrude, L., & Lithgow-Bertelloni, C. (2005). Thermodynamics of mantle minerals—I. Physical properties. Geophysical Journal International, 162(2), 610-632.
[11] Stixrude, L., & Lithgow-Bertelloni, C. (2011). Thermodynamics of mantle minerals—II. Phase equilibria. Geophysical Journal International, 184(3), 1180-1213.
[12] Kerr, M. C., Stegman, D. R., Smrekar, S. E. (2026). Heat flow and velocity scaling in the "glass-ceiling" convective regime and implications for Venus. Geodynamica (Accepted)
[13] Conrad, J. W., & Nimmo, F. (2023). Constraining characteristic morphological wavelengths for Venus using Baltis Vallis. Geophysical Research Letters, 50(10), e2022GL101268.
[14] Lourenço, D. L., Rozel, A. B., Ballmer, M. D., & Tackley, P. J. (2020). Plutonic-squishy lid: A new global tectonic regime generated by intrusive magmatism on Earth-like planets. Geochemistry, Geophysics, Geosystems, 21(4), e2019GC008756.

Remote-controlled tectonics: How does Io drive “rifting” and “subduction” on Europa?

Martin Kihoulou*[1] and Ondřej Čadek[1]

[1]Department of Geophysics, Faculty of Mathematics and Physics, Charles University, Prague, Czech Republic
*martin.kihoulou@matfyz.cuni.cz

Keywords: Europa, Io, tectonics, rifting, subduction, bands, eccentricity

The geologically young surface of Jupiter’s icy moon Europa exhibits multiple lines of evidence for both divergent and convergent tectonic activity: dilation bands, where fresh ice has been emplaced, and regions interpreted as “subduction” zones, where ice appears to have descended under the surface [1]. Although these features were initially compared to terrestrial mid-ocean ridges and subduction zones, Europa’s tectonic motions are likely driven by a fundamentally different mechanism: by cyclic global expansion and contraction of the ice shell [2,3,4].

These volumetric changes are thought to result from long-term variations of Europa’s orbital eccentricity, as periods of enhanced tidal heating promote melting of the ice shell, whereas reduced tidal heating leads to freezing of the subsurface ocean [4]. Through this process, Europa’s tectonics may enable vertical transport of chemical compounds across the ice shell, possibly allowing for transient habitable conditions within the subsurface ocean. The efficiency of this exchange depends on the amplitude and frequency of eccentricity variations [3].

Our estimate based on the difference in surface area between fully liquid and fully solid hydrosphere reveals that the present-day area of Europa’s dilation bands (900,000 km^2) can only be explained by multiple episodes of ice shell thinning and thickening [5]. However, given that the age of Europa’s surface is only $\sim$180 Myr, this interpretation is inconsistent with thermo-orbital models, which predict the eccentricity variation cycles on time scales of hundreds of millions of years [4,6]. One possible explanation is that the thermo-orbital evolution of the Jovian satellites, particularly that of Io, operates on much shorter time scales than previously assumed [5]. Consequently, investigation of Europa’s dilation bands might provide insight not only into Europa’s internal dynamics, but also into Io’s orbital evolution, heat transfer and volcanic activity.

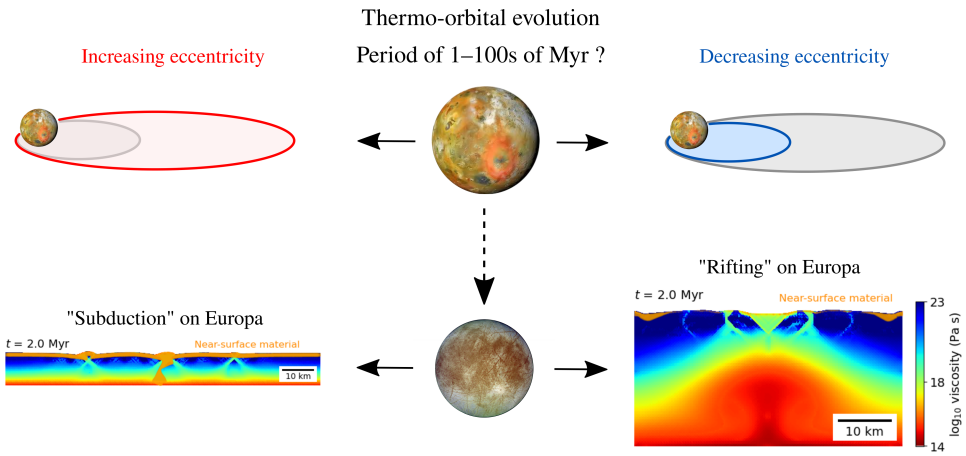


Figure: The link between Io’s thermo-orbital evolution and Europa’s tectonic deformation. Periods of rising eccentricity trigger a subduction-like process on Europa, while periods of decreasing eccentricity give rise to ”rifting” (band formation).

References

[1] Collins, G. et al. (2022) Episodic plate tectonics on Europa: Evidence for widespread patches of mobile-lid behavior in the Antijovian hemisphere. J. Geophys. Res. Planets 127, e2022JE007492.
[2] Rudolph, M. L. , Manga, M., Walker, M., Rhoden, A. R. (2022) Cooling crusts create concomitant cryovolcanic cracks. Geophys. Res. Lett. 49, e2021GL094421.
[3] Kihoulou, M., Choblet, G., Tobie, G., Kalousová, K. and Čadek, O. (2025). Subduction-like process in Europa’s ice shell triggered by enhanced eccentricity periods. Science Advances 11, eadq8719.
[4] Hussmann, H. and Spohn, T. (2004). Thermal-orbital evolution of Io and Europa. Icarus, 171, 391–410.
[5] Kihoulou, M. and Čadek, O. (2026). Unresolved circumstances of Europa’s dilation bands formation. Under review in Geophysical Research Letters.
[6] Ojakangas, G. W. and Stevenson, D. (1986). Episodic volcanism of tidally heated satellites with application to Io. Icarus, 66 (2), 341–358.

Towards efficient modeling of rock texture related mechanical anisotropy during large-scale dynamic processes

Ágnes Király*[1]

[1]University of Oslo, Oslo, Norway
*kiraly@uio.no

Keywords: anisotropy, CPO, modeling

All crystals exhibit symmetry, which often leads to direction-dependent (i.e., anisotropic) intrinsic properties at the grain scale. Here, we focus on the viscous anisotropy of two prevalent Earth-forming crystals: ice and olivine. Olivine has orthorhombic symmetry, with three main slip systems that accommodate creep deformation. In particular, dislocation creep occurs more than an order of magnitude more easily along the [100](001) and [100](010) slip systems than along the [001](010) slip system. Similar to olivine, ice is highly anisotropic when deforming via dislocation creep; however, due to its hexagonal symmetry, deformation generally activates only the basal slip system.

During large-scale deformation, rock-forming crystals may rotate, deform, or recrystallise, leading to a systematic alignment of crystallographic axes. This is referred to as crystallographic preferred orientation (CPO), and can be inferred from seismic or radar observations in different regions of the Earth, including ice sheets at the surface and the upper mantle at depth. When CPO is well developed, the intrinsic anisotropy of individual crystals averages in such a way that the macroscopic properties of the aggregate also become direction-dependent. Consequently, anisotropic viscosity and texture evolution are tightly coupled and should be modelled in a fully coupled framework.

To incorporate texture-related viscous anisotropy into large-scale geodynamic models, one requires: i) a micromechanical model that describes how a single crystal responds to different loading conditions, ii) a texture evolution model that describes how the orientations (and grain sizes) of individual grains evolve during large-scale deformation, and iii) a homogenisation method that averages the micromechanical behaviour of the grains based on their orientations.

These components must then be used to incorporate the direction-dependent rheology into the constitutive equations.

In this presentation, I will introduce a statistical method that simplifies steps (i) and (iii) by inferring the parameters describing anisotropic viscosity directly from the CPO. This method has been applied to olivine and has the potential to be extended to ice. Accounting for anisotropic viscosity in both the mantle and ice can significantly affect modelled ice-sheet dynamics, for example, through modified post-glacial rebound rates and through time- and space-dependent internal ice dynamics.

Rocky Planets as Heat Engines: Global Tectonomagmatic Regimes and Planetary Evolution

Diogo L. Lourenço*[1]

[1]Institute of Geophysics, Department of Earth and Planetary Sciences, ETH Zurich, Switzerland
*diogo.lourenco@eaps.ethz.ch

Keywords: rocky planets, heat engines, habitability, evolution and dynamics

Rocky planets function as heat engines, with internal heat driving mantle convection, tectonics, and magmatism. In this talk, I will examine how these processes are coupled and how their feedbacks control the long-term thermal and chemical evolution of rocky planets. Variations in heat production, rheology, crustal buoyancy, volatile content, surface conditions, and melt generation can lead to distinct global tectonomagmatic regimes, including plate tectonics, stagnant-lid, episodic-lid, and plutonic–squishy-lid behavior. These regimes regulate planetary heat loss, crustal recycling, volcanic outgassing, and the generation and longevity of magnetic fields, ultimately shaping the evolution of planetary surface and atmospheric conditions. Placing Earth within a broader comparative planetary framework, I will show how interior dynamics shape the present-day states of rocky planets in the Solar System and beyond.

Plate generation from mantle convection and feedback with the deep interior

Julian Lowman[*1], Pejvak Javaheri[2], Chad Fairservice[1], Joshua Guerrero[3], Sean Langemeyer[2], and Paul Tackley[4]

[1]University of Toronto Scarborough, Department of Physical and Environmental Sciences
[2]University of Toronto, Department of Physics
[3]Institute of Earth Sciences, Academia Sinica
[4]Department of Earth and Planetary Sciences, ETH Zurich
[*]julian.lowman@utoronto.ca

Keywords: plate generation, convection, Euler poles, LLVPs, mantle viscosity

Efforts to understand the generation of plate-like surface behaviour from a vigorously convecting mantle have included studies focused on both investigating the feedback between the plates and the deep mantle, and the ability of the mantle to generate plates, regardless of their influence on the planet's interior. As computational power has increased, and spherical 3D models have become commonplace, the problem of investigating the control parameters affecting plate generation first necessitates determining a way to identify the contiguous surface segments that may comprise distinct plates. Confirmation that plates have indeed been generated then requires verifying that each candidate plate's motion on the spherical surface is equivalent to rotation about an associated Euler pole. Plate generation is profoundly impacted by mantle viscosity structure, which includes a strong temperature-dependence that results in feedback between the lowermost mantle and the surface. Accordingly, LLVPs and the formation of plates may be intertwined, such that the surface motion impacts the distribution of the LLVPs but the properties of the provinces may affect the mantle's overall viscosity structure and therefore plate formation itself. Here, we shall discuss some of the progress in modelling and verifying plate generation in mantle convection calculations, as well as feedback between the deep mantle and surface.

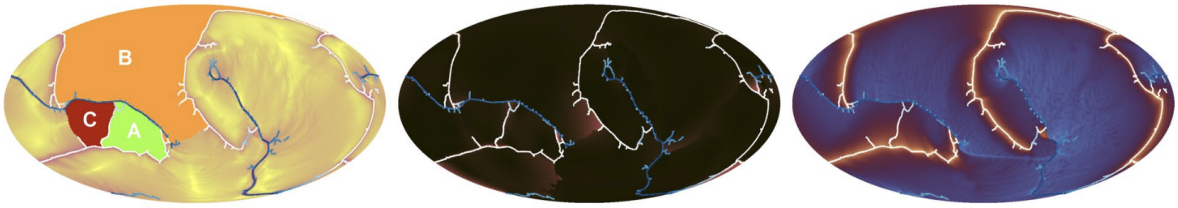


Figure: Plate identification, surface deformation and plate interior temperature from a mantle convection calculation

Melt generation and transport from the mantle to the surface

Adina E. Pusok[*1]

[1]Department of Earth Sciences, University of Oxford, Oxford, United Kingdom
[*]adina.pusok@earth.ox.ac.uk

Magmatism plays a key role in the operation of plate tectonics, yet the details of magma generation in the mantle and transport to the surface remain unclear. In this talk, I will give a brief introduction to the growing evidence that melt is more widely distributed in the asthenosphere-lithosphere system, which questions our classical models of mid-ocean ridges and the lithosphere-asthenosphere boundary. Then, I will talk about recent progress in understanding how melts may be extracted across the ductile–brittle lithosphere to the surface. Magma transport changes from porous flow in the hot, ductile mantle to fluid-filled fractures, known as dikes and sills, in the cold, brittle crust. Accurate representation of these processes in geodynamic models is crucial for understanding lithospheric deformation and planetary dynamics, as magma transports heat and alters lithospheric stresses.

Processes in subducting slabs: how can seismology inform models?

Christian Sippl[*1], Nooshin Najafipour[1,2], Nazia Hassan[1,2], Guido Gianni[1], Andres Tassara[3], Bernd Schurr[4], Jacob Geersen[5], and Armin Dielforder[6]

[1]Institute of Geophysics, Czech Academy of Sciences, Prague, Czech Republic
[2]Department of Geophysics, Faculty of Mathematics and Physics, Charles University, Prague, Czech Republic
[3]Universidad de Concepcion, Concepcion, Chile
[4]Helmholtz-Zentrum fuer Geoforschung (GFZ), Potsdam, Germany
[5]Leibniz-Institute for Baltic Sea Research, Warnemunde, Germany
[6]University of Greifswald, Greifswald, Germany
*sippl@ig.cas.cz

Thermomechanical models of subduction zones have contributed significantly to understanding a large range of geodynamic processes. Many of the observations that link these models to plate tectonic reality come from seismology, which as all geophysical methods is restricted to the observation of the "now" state, and comes with sometimes considerable uncertainties. In this talk, we will present some recent seismological results related to intermediate-depth earthquakes in the uppermost ~200 km of subduction zones, and their possible implications for ongoing geodynamic processes.

Intermediate-depth seismicity in subduction zones often forms double seismic zones, two parallel layers of earthquake hypocenters parallel to the slab dip. Moment tensors from these earthquakes thus allow a glimpse at the intraslab stress field at two different depth levels inside the downgoing plate. A global compilation of moment tensor observations shows that while the lower plane seismicity consistently shows downdip extension everywhere, upper plane seismicity shows either uniform compression or uniform extension along the slab dip, depending on the subduction zone segment. This likely hints at a complex interplay between bending and unbending stresses and "in-plane stresses" (mostly slab pull), leading to a dominance of one over the other depending on current local conditions.

Secondly, intermediate-depth earthquakes are intimately linked to the hydration of the downgoing oceanic lithosphere in the Outer Rise region, and its dehydration at depth. While many modeling attempts assume a fixed hydration for oceanic crust and uppermost mantle, we observe that initial hydration of the downgoing plate likely varies considerably along strike, dependent on bathymetric features being subducted. We will present evidence from recent high-resolution studies along the South American subduction zone that highlight the variability of oceanic plate hydration as well as its likely concentration near subducted bend-faults.

Laboratory experiments on the creep behavior of ices: implications for the interior dynamics of icy worlds

Christophe Sotin*[1]

[1]Nantes University, France
*christophe.sotin@univ-nantes.fr

Keywords: ice rheology, convection, tidal dissipation, icy moons

Deformation of ice has been studied in laboratory since the pioneering work of Glen et al. [1]. These experiments were carried out to better understand the deformation of terrestrial glaciers. More recent experiments (e.g. Goldsby & Kohlstedt [2], McCarthy & Cooper [3]) were carried out to better understand the dynamics of icy worlds. Merging these different data sets is important to define the deformation laws relevant to processes such as subsolidus convection and tidal dissipation which play a critical role in shaping the geological evolution of icy worlds. These two processes involve different frequencies. While convection processes are best described by the secondary creep of ice (or even tertiary creep), primary creep should be used to describe tidal dissipation. The different creep laws will be described and discussed. Then application to icy worlds such as Europa, Ganymede, Enceladus, and Titan will be described.

One ingredient of icy moons is organic molecule. As the interior temperature increases, these organic molecules degrade, releasing soluble organics and more volatiles compounds such as CO2, CH4, and N2. Thermochemical evolution models will be described. They suggest that clathrate hydrates may form. Their influence on interior processes and global evolution is reviewed.

Among these icy worlds, the Galilean icy moons and Titan will be explored by the upcoming space missions JUICE, Europa Clipper, and Dragonfly. Information on the thickness of their ice crust, depth of their oceans, and deformation should provide key measurements to constrain models of their present interior structure.

References

[1] Glen, J. W. (1955). The creep of polycrystalline ice. Proceedings of the Royal Society London, Series A, 228, 519–538. https://doi.org/10.1098/rspa.1955.0066
[2] Goldsby, D.L., Kohlstedt, D.L., (1997). Grain boundary sliding in fine-grained ice I. Scr. Mater.37, 1399–1406.
[3] McCarthy C., and R.F. Cooper (2016) Tidal dissipation in creeping ice and the thermal evolution of Europa; Earth Planet. Sci. Lett., 443, 185-194. http://dx.doi.org/10.1016/j.epsl.2016.03.006

Ductile instability, strain localization, and rupture propagation by thermal runaway

Arne Spang*[1], Marcel Thielmann[2], Albert de Montserrat[3], and Thibault Duretz[4]

[1]Bayerisches Geoinstitut, Universität Bayreuth, Bayreuth, Germany
[2]Universität Bonn, Bonn, Germany
[3]ETH Zürich, Zürich, Switzerland
[4]Goethe-Universität Frankfurt, Frankfurt am Main, Germany
*arne.spang@uni-bayreuth.de

Keywords: ductile deformation, strain localization, thermal runaway, rupture propagation, deep earthquakes

Ductile deformation is usually associated with slow and uniform deformation such as mantle convection. Yet, it is also sensitive to temperature and strain rate and therefore prone to the development of instabilities which can result in strain localization and faster deformation. Examples of ductile localization include mylonites, slow-slip events and deep earthquakes. The latter are detected in depths of up to 700 km and exhibit slip velocities in the range of 10^{-3} to 10^{1} m s^{-1}. Such rapid deformation is usually associated with brittle failure, but the conditions under which deep earthquakes occur suggest that it is predominantly ductile.

Reaching slip velocities on the order of mm s^{-1} requires a specific localization mechanism. One such mechanism is thermal runaway, a feedback loop of shear heating (the conversion of elastic energy to thermal energy during irreversible deformation), temperature-dependent viscosity and localization. Several one-dimensional (1D) thermomechanical studies support the viability of thermal runaway to cause rapid ductile slip. Two-dimensional (2D) studies have also demonstrated the ability of thermal runaway to propagate through a previously intact host rock, weakening it locally, and resulting in narrow shear zones.

Here, we present new 2D thermomechanical models of thermal runaway in olivine under simple and pure shear conditions in line with the cold cores of subducting slabs. The models employ a composite visco-elastic rheology including diffusion creep, dislocation creep, and low-temperature plasticity. Adaptive time stepping and local grid refinement allow us cover length scales from centimeters to kilometers and time scales from milliseconds to thousands of years in one model.

Our models capture the nucleation and transient propagation of ductile ruptures through a previously intact host rock. The ruptures initiate in zones of reduced strength and under plate tectonics deformation rates (~ 10 cm yr^{-1}). During propagation, they self-localize and accelerate to reach slip velocities in the range of earthquakes ($>$ 1 mm s^{-1}). The magnitude of maximum slip velocity depends on a nondimensional ratio between elastic energy and thermal energy in the host rock prior to rupture nucleation. This is in line with the location of deep-focus earthquakes at the bottom of the mantle transition zone where phase transitions and slab deformation due to the resistance of the lower mantle can cause stress increases. Considering the latent heat of melting reveals that the local temperature surge due to thermal runaway is fast enough to completely melt a thin layer of peridotite during rupture propagation.

The ruptures nucleate in the cold slab core and self-consistently run out in its high-temperature/low-stress edges. Our models suggest that thermal runaway provides a plausible explanation for the location, propagation, and arrest of deep-focus earthquake ruptures.

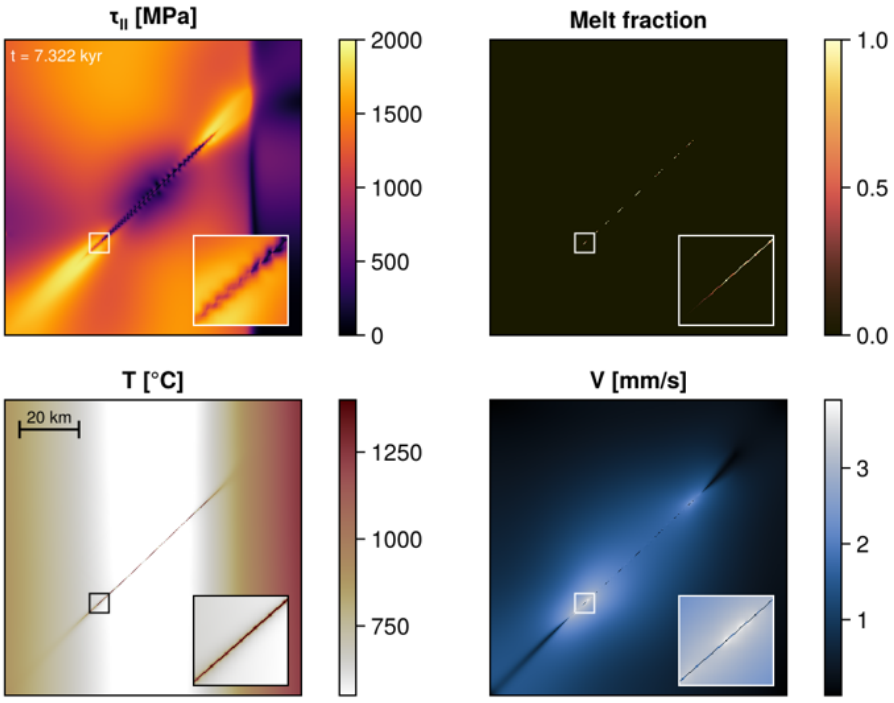


Figure: Ductile rupture propagation by thermal runaway under mantle transition zone conditions. Upper left shows deviatoric stress field, upper right shows melt fraction, lower left shows temperature field, and lower right shows velocity field. Insets zoom into the area around the ruptures.

Quantifying the interaction between tectonic deformation and climate-driven surface processes using coupled geodynamic-landscape evolution models

Sebastian G. Wolf*[1], Ritske S. Huismans[1], Jean Braun[2,3], Thomas Theunissen[1], and Dave A. May[4]

[1]Department of Earth Science, University of Bergen, Bergen, Norway
[2]Helmholtz Centre Potsdam, German Research Centre for Geosciences, Potsdam, Germany
[3]Institute of Geosciences, University of Potsdam, Potsdam, Germany
[4]Institute of Geophysics and Planetary Physics, Scripps Institution of Oceanography, University of California San Diego, La Jolla, CA, USA
*sebastian.wolf@uib.no

Topography on Earth results from the couplings and feedbacks that exist between tectonic deformation and climate-fueled surface processes. In this coupled system, fluvial and glacial erosion are not merely a decoration on top, but have the potential to modify and even fully counteract tectonic deformation. This raises the question of how different tectonic and erosional settings are expressed on Earth. This talk will provide an overview of how the interaction between tectonic deformation and surface processes can be quantified with the help of coupled geodynamic-landscape-evolution models, with a focus on mountain belts on Earth. To this end, we will first introduce the underlying physics of mountain building and fluvial erosion. Second, we will show how to couple 2D and 3D geodynamic models with landscape evolution models, and where the main challenges lie. Third, we will use these coupled models and non-dimensional analysis to quantify the interaction between surface processes and tectonics during mountain building. Finally, the modelling results are compared to several orogenic systems on Earth, highlighting how tectonics and climate determine mountain belt shape, size, and height.

Posters

3D Modeling of Peel Back Delamination on Venus

Andrea Adams*[1,2], Sue Smrekar[1,2], Mike Gurnis[2], Dave Stegman[3], and Paul Tackley[4]

[1]Jet Propulsion Laboratory, California Institute of Technology
[2]California Institute of Technology
[3]University of California San Diego
[4]ETH Zürich
*andrea.c.adams@jpl.nasa.gov

Keywords: Venus, tectonics, delamination, plume-lithosphere interactions

Although Venus lacks Earth-like plate tectonics, trench-outer rise systems identified at coronae and other features have been interpreted as evidence for localized lithospheric recycling [1,2]. These sites exhibit substantial geometric variability, including the large quasi-circular trench system at Artemis Corona, the smaller dual-trench morphology of Latona Corona, and the elongated trench at Derceto Plateau. Flexural topography associated with these features has been used to estimate elastic thickness (Te), providing constraints on lithospheric mechanical strength and thickness. In particular, the large flexural amplitude and high inferred Te at Artemis Corona suggests a thicker and mechanically stronger lithosphere than at other proposed recycling sites. While previous models of plume-induced subduction primarily focused on thin, weak lithosphere, the observed flexural signatures at Artemis suggest that rollback-style lithospheric recycling may also occur in thicker, stronger lithosphere. Previous 2D models have shown that peel-back delamination (PBD) may be a viable mechanism for recycling thicker lithosphere on Venus [3,4], but it remains unclear whether PBD is viable in 3D and whether it can reproduce the range of observed trench geometries and flexural signatures at proposed recycling sites.

Here, we present a suite of three-dimensional numerical models of PBD induced by plume-rift interactions under Venus-like conditions to investigate the evolution of its surface expression in 3D. Models are computed using the finite-volume mantle convection code, StagYY [5]. Simulations are performed in a spherical-patch geometry using a viscoplastic rheology with diffusion creep and temperature- and depth-dependent viscosity. A low-density sticky-air upper boundary condition allows the development of realistic topography. Crustal densities are calculated using Perple_X [6] phase equilibria calculated for Venusian basalt compositions. The initial condition includes a hot mantle plume head placed 700 km below a finite-length rift zone. We vary lithospheric thickness, rift length, mantle temperature, and lithospheric strength to evaluate the conditions under which PBD occurs and whether it can reproduce the observed trench geometries and flexural signatures of Artemis Corona, Latona Corona, and Derceto Plateau.

Results show that lithospheric thickness exerts the primary control on whether PBD occurs. Models with thin lithosphere remain stable while thicker lithosphere (TL $\geq$ 150 km) undergoes sustained PBD driven by the negative buoyancy of the lithospheric mantle and eclogitized lower crust. Rift geometry strongly influences the resulting trench morphology where short rifts (L = 600 km) produce quasi-circular trench systems like Artemis and Latona Corona, and longer rifts (L = 1800 km) produce elongated arcuate geometries like Derceto Plateau. Although the weak flexural signature at Derceto Plateau suggests that PBD is unlikely to be the dominant recycling mechanism in that region, PBD successfully reproduces the observed elastic thickness and trench outer rise structure at Artemis Corona (Figure) and the dual-trench morphology of Latona Corona.

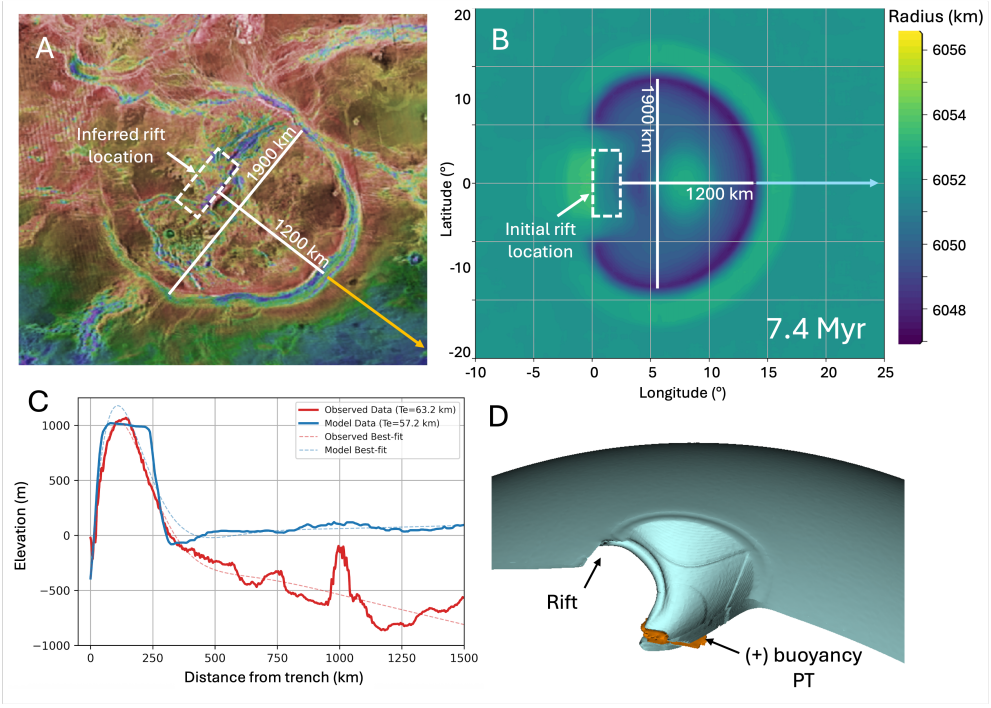


Figure: Comparison between observed Artemis Corona topography and the best-fit 3D PBD model at 7.4 Myr. The model reproduces the large quasi-circular geometry, flexural topography, and inferred elastic thickness of Artemis Corona.

References

[1] Sandwell, D. T., Schubert, G. (1992). Evidence for Retrograde Lithospheric Subduction on Venus, Science, 257(5071), 766–770. https://doi.org/10.1126/science.257.5071.766

[2] Schubert, G., Sandwell, D. T. (1995). A Global Survey of Possible Subduction Sites on Venus, Icarus, 117, 173–196. https://doi.org/10.1006/icar.1995.1150

[3] Adams, A. C., Stegman, D. R., Smrekar, S. E., Tackley, P. J. (2022). Regional-scale lithospheric recycling on Venus via peel-back delamination. JGR:Planets, 127, e2022JE007460. https://doi.org/10.1029/2022JE007460

[4] Adams, A. C., Stegman, D. R., Mohammadzadeh, H., Smrekar, S. E., Tackley, P. J. (2023). Plume-Induced Delamination Initiated at Rift Zones on Venus, JGR: Planets, 128, e2023JE007879. https://doi.org/10.1029/2023JE007879

[5] Tackley, P. J. (2008). Modelling compressible mantle convection with large viscosity contrasts in a three-dimensional spherical shell using the yin-yang grid, Physics of Earth and Planetary Interiors, 171(1–4), 7–18. https://doi.org/10.1016/j.pepi.2008.08.005

[6] Connolly, J. A. D. (2005), Computation of phase equilibria by linear programming: A tool for geodynamic modeling and its application to subduction zone decarbonation, Earth Planet. Sci. Lett., 236, 524–541, doi:10.1016/j.epsl.2005.04.033.

Investigating mantle flow on Mars

Riva Alkahal[*1], Bart Root[1], and Cedric Thieulot[2]

[1]Delft University of Technology, Delft, the Netherlands
[2]Utrecht University, Utrecht, the Netherlands
[*]r.alkahal@tudelft.nl

Keywords: Mars, plumes, 2D spherical annulus

Understanding the present-day internal dynamics of Mars requires bridging the gap between sparse observational constraints and the vast, poorly constrained, parameter space of mantle plume physics. The Tharsis rise, host to the largest volcano in the solar system, Olympus Mons, is characterized by a free-air gravity anomaly reaching up to 3,540 mGal that cannot be explained by lithospheric flexure alone, requiring a substantial mantle mass anomaly [1,2]. Additionally, a long-term acceleration in Mars' rotation rate detected by InSight's RISE experiment points to a possible ongoing redistribution of mass in the Martian interior [3]. Together, these constraints motivate a systematic modeling effort to characterize the state of a possible mantle plume beneath Tharsis.

Therefore, we simulate the long-term geophysical evolution of the Martian mantle using the ASPECT code, introducing a deep thermal anomaly beneath the Tharsis region to drive plume development from initiation to the present day. The computations are performed in a 2D geometry (chunk and spherical annulus), assuming an incompressible flow under Boussinesq approximation. We investigate depth and temperature dependent viscosity profiles drawn from the literature, spanning from 10^{20} to 10^{23} Pa·s. We explore how these profiles control plume longevity and the amplitude of the resulting time-variable gravity observations. For each scenario, we forward-model the gravity-rate signature and compare outputs against existing InSight and orbital gravity constraints.

Predicted gravity-rate signals in the most favorable configurations reach approximately 20 nGal/year [4], sitting at the detection threshold of current satellite tracking. We evaluate how detectability varies across the parameter space, to identify which plume configurations would be resolvable with existing missions and which would require improved instrumentation or longer observation baselines, such as the proposed MaQuIS concept mission [5].

By systematically narrowing the plausible parameter space, our results provide refined constraints on the viscosity structure and thermal state of the Martian mantle, and assess the extent to which a present-day plume or its remnant is consistent with available observations.

References

[1] Root, B. C., Qin, W., van der Tang, Y., Thieulot, C. (2026). Describing the global gravity field of Mars with lithospheric flexure and deep mantle flow. Journal of Geophysical Research: Planets, 131, https://doi.org/10.1029/2024JE008765

[2] Redmond, H. L., and King, S. D. (2004). A numerical study of a mantle plume beneath the Tharsis Rise: Reconciling dynamic uplift and lithospheric support models. Journal of Geophysical Research: Planets, 109, E09008. https://doi.org/10.1029/2003JE002228

[3] Le Maistre, S., et al. (2023). Spin state and deep interior structure of Mars from InSight radio tracking. Nature, 619, 733–737. https://doi.org/10.1038/s41586-023-06150-0

[4] Alkahal, R., Root, B. C., Dirkx, D., Thieulot, C., Fayolle, S., Goossens, S. (under review) Investigating gravity trends from realistic simulated satellite orbits. Icarus.

[5] Wörner, L., Root, B. C., Bouyer, P., Braxmaier, C., Dirkx, D., Encarnação, J., Hauber, E., Hussmann, H., Karatekin, Ö., Koch, A., Kumanchik, L., Migliaccio, F., Reguzzoni, M., Ritter, B., Schilling, M., Schubert, C., Thieulot, C., Klitzing, W. v., & Witasse, O. (2023). MaQuIs—Concept for a Mars Quantum Gravity Mission. Planetary and Space Science, 239, 105800. https://doi.org/10.1016/j.pss.2023.105800

Can porosity waves create long-period seafloor topography? Investigating the topographic expression of transient mid-ocean ridge magma supply

Amita Anand*[1], Shi Joyce Sim[1], and Jean-Arthur Olive[2]

[1]School of Earth and Atmospheric Sciences, Georgia Institute of Technology, Atlanta, GA, USA
[2]Laboratoire de Géologie, CNRS, École normale supérieure, PSL University, Paris, France
*aanand307@gatech.edu

Keywords: mid-ocean ridges, oceanic lithosphere, seafloor topography

The seafloor fabric is a vast geologic feature of Earth, yet the underlying controls remain debated. Studies have proposed Milankovitch glacial cycles with periods of 23, 41, and 100 kyr as a control on hydrostatic pressure at the ridge-axis, thus controlling melt flux, crustal thickness, and topography. However, bathymetric and crustal thickness observations have produced a wide range of periods, including those longer than 100 kyr that fall outside the range explainable by Milankovitch forcing alone [1]. This discrepancy suggests that additional mechanisms must be at work in producing these longer-period signals.

At mid-ocean ridges (MORs), new oceanic crust is created and physically transformed through mainly a combination of magmatic emplacement and faulting. Recent observations suggest that seafloor relief contains periodic components from 10s to 100s of kyrs, not easily explained by standard models of oceanic lithosphere formation. Furthermore, two-phase flow models have shown that at slow to intermediate spreading rates, MOR magma supply varies significantly with time in the form of wave-like instabilities.

To understand if fluctuating MOR melt supply can explain the wide range of seafloor topography and crustal thickness periodicities, we simulate seafloor spreading in a visco-elasto-plastic lithosphere subject to magma injection rates derived from two-phase flow model data. We use a Fast Lagrangian Analysis of Continua (FLAC) model of magma emplacement and faulting at slow to intermediate spreading rates subjected to inputs of magma flux from two-phase flow models with different mantle permeabilities [2, 3]. From comparing the spectra of the crustal thickness produced by two-phase models alone to FLAC models including two-phase model data, we observe that brittle deformation processes systematically dampen nearly all periodicities shorter than 100 kyr while promoting longer ones across spreading rates. Future work will involve an exploration of the parameter space to determine which periods of magmatic fluctuation are best expressed at various MOR settings.

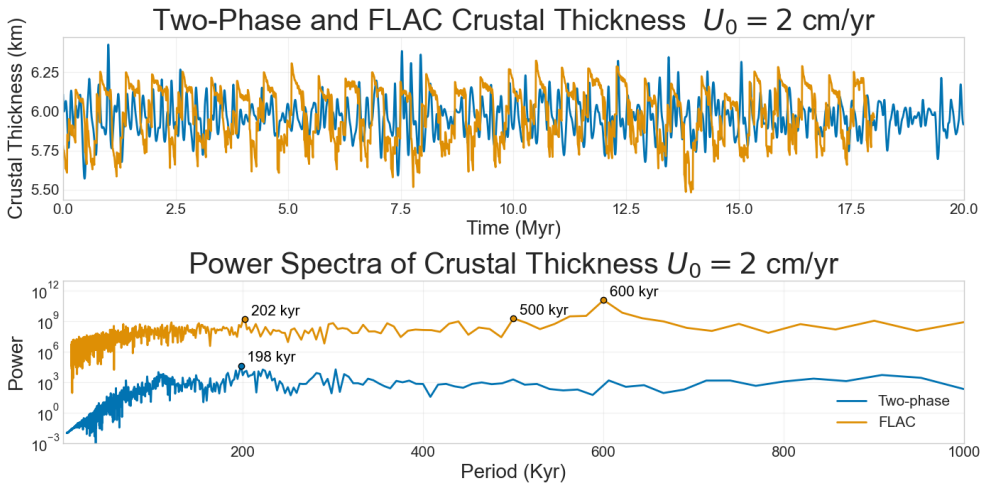


Figure: Top: Crustal thickness over time of two-phase model and FLAC with two-phase model data as inputs for a half spreading rate of 2 cm/yr. Bottom: Power spectra of crustal thickness for two-phase and FLAC models with spectral peaks marked.

References

[1[Boulahanis, B., Carbotte, S. M., Huybers, P. J., Nedimović, M. R., Aghaei, O., Canales, J. P., & Langmuir, C. H. (2020). Do sea level variations influence mid-ocean ridge magma supply? A test using crustal thickness and bathymetry data from the East Pacific Rise. Earth and Planetary Science Letters, 535, 116121.

[2] Olive, J. A., Behn, M. D., Ito, G., Buck, W. R., Escartín, J., & Howell, S. (2015). Sensitivity of seafloor bathymetry to climate-driven fluctuations in mid-ocean ridge magma supply. Science, 350(6258), 310–313.
[3] Sim, S. J. (2022). Persistent magma-rich waves beneath mid-ocean ridges explain long periodicity on ocean floor fabric. Geophysical Research Letters, 49(12), e2022GL098110.

Investigating Partial Melting in Europa's Mantle Using 3D Convection Models

Valentin André*[1], Marie Běhounková[2], Gabriel Tobie[1], Gaël Choblet[1], and Mathilde Kervazo[1]

[1]Nantes Université, Univ Angers, Le Mans Université, CNRS, Laboratoire de Planétologie et Géosciences, LPG UMR 6112, 44000 Nantes, France
[2]Charles University, Faculty of Mathematics and Physics, Department of Geophysics, Praha, Czech Republic
*valentin.andre2@univ-nantes.fr

Keywords: Europa, thermal evolution, partial melting, stagnant lid

Europa is a primary candidate for habitability due to the presence of a liquid subsurface ocean in direct contact with its rocky mantle [1]. Chemical exchanges favored by hydrothermal activity associated to magmatic phenomena could bring compounds suitable for the ocean's habitability [2]. The occurrence and timescale of magmatic activity at the seafloor of Europa, however remains debated. Some studies suggested a hot scenario, where partial melting in Europa's mantle occur during most of the moon's history, with melt generation triggered and sustained by radioactive heating and tidal dissipation alongside limited heat removal by thermal convection [3]. Other studies proposed that Europa had a colder thermal evolution [4], implying delayed magmatism and much more modest amounts of melt. Even if magmatism is significant at depth, it might not result in seafloor volcanism [5]. However, the feedback of melting on mantle rheology as well as the different modes of extraction or retention of the melt were not entirely investigated. Such effects might have considerable implications on the dynamics of convection and thermal evolution of Europa's mantle.

In this study, the thermal evolution and melt production in Europa's silicate mantle is investigated using a three-dimensional (3D) numerical model that solves for thermal convection considering radiogenic and tidal heating [6, 7]. The timescale and location of melt production in the mantle is analyzed by considering several melt treatments as well as the feedback of melting on mantle rheology and solidus temperatures [8]. Melt treatments involve (1) instantaneous melt extraction once the temperature is above the solidus with removal of excess thermal energy; (2) melt retention where melt is advected with the solid matrix and can crystallise once the temperature drops below the solidus; (3) an intermediate melt extraction where melt migrates upward and can heat its surroundings. Our results show that melt generation and production rates in Europa's mantle strongly depend on the considered melt treatment and the subsequent effect on mantle rheology. In the instantaneous melt extraction case, melting predominantly occurs at great depths below a thick lithosphere with relatively low melting rates. If melt remains with the solid matrix, the average melting rate can be ten times higher, with local partial melting up to 20% under favorable conditions. The retention of melt impacts the vigor of convection as local buoyancy and viscosity are respectively increased and decreased. As such, upwelling plumes develop more quickly and can significantly affect the thermal structure of the stagnant lid (Figure). These hot plumes could be able to erode the cold lithosphere, thus reducing the local thickness of the stagnant lid and allowing melt to be generated closer to the seafloor. This effect is even more prominent in the reactive melt extraction treatment, which may suggest that melt could be generated at shallower depths than previously anticipated. Tidal dissipation, amplified in partially molten regions, could further enhance this effect. The weakening of the stagnant lid rheology due to the penetrating plumes could potentially favor dyke development and the transport of melt at Europa's seafloor.

References

[1] W. B. Moore, H. Hussmann (2009). Thermal evolution of Europa's silicate interior, in: R. T. Pappalardo, W. B. McKinnon, K. K. Khurana (Eds.). Europa, University of Arizona Press, Tucson,, pp. 369–380. doi: https://doi.org/10.2307/j.c
[2] Vance, S. D. et al. (2016). Geophysical controls of chemical disequilibria in Europa. Geophysical Research Letters 43 4871–4879. doi: https://doi.org/10.1002/2016GL068547
[3] Běhounková, M. et al (2021). Tidally induced magmatic pulses on the oceanic floor of Jupiter's moon Europa. Geophysical Research Letters, 48, e2020GL090077. https://doi.org/10.1029/2020GL090077
[4] Petricca, F. et al. (2025). Partial differentiation of Europa and implications for the origin of materials in the Jupiter system. Nature Astronomy, pages 1–11. doi: https://doi.org/10.1038/s41550-024-02469-4
[5] Green, A. P et al.. (2025). No magmatic driving force for Europan sea-floor volcanism. Nature Astronomy 9 (2025) 640–649. doi: https://doi.org/10.1038/s41550-025-02508-8
[6] G. Choblet (2005). Modelling thermal convection with large viscosity gradients in one block of the 'cubed sphere'. Journal of Computational Physics 205 269–291. doi: https://doi.org/10.1016/j.jcp.2004.11.005
[7] Choblet, G. et al. (2007). ŒDIPUS: a new tool to study the dynamics of planetary interiors, Geophysical Journal International 170 9–30. doi: https://doi.org/10.1111/j.1365-246X.2007.03419.x
[8] Běhounková, M. et al (2010). Coupling mantle convection and tidal dissipation: Applications to Enceladus

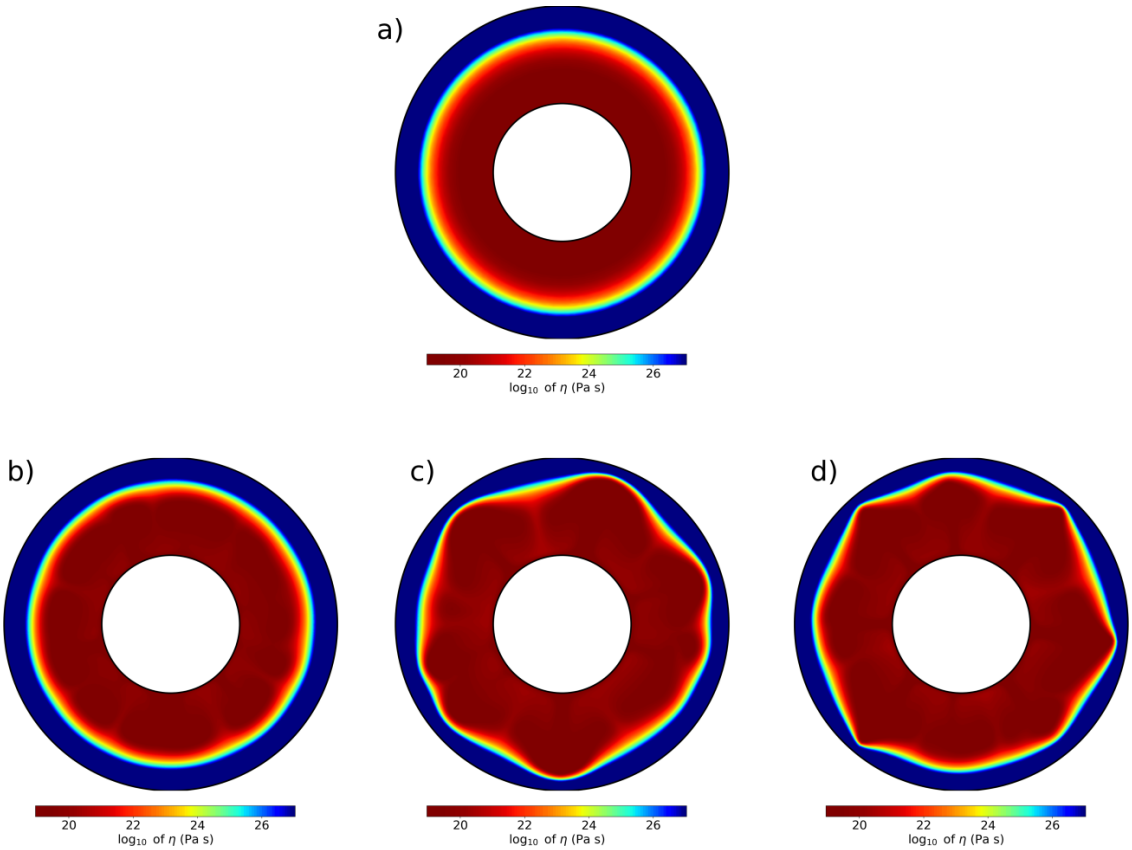


Figure: Vertical cross-sections of Europa's mantle viscosity. a) Initial state. b) Instantaneous melt extraction case. c) Case where melt remains and is advected with the solid matrix. d) Melt percolation case.

and Earth-like planets, Journal of Geophysical Research: Planets 115 2009JE003564.
doi: https://doi.org/10.1029/2009JE003564.

Influence of Mantle Rheology on Plume Morphology and Dynamics

Maëlis Arnould*[1], Alexandre Koessler[1], Jean-Philippe Perrillat[1], and Vincent Famin[2,3]

[1]LGL-TPE, University Lyon 1, France
[2]Laboratoire GéoSciences Réunion, Université de la Réunion, France
[3]IPGP, Paris, France
*maelis.arnould@univ-lyon1.fr

Keywords: mantle plume, mantle rheology, Réunion hotspot, geodynamic modelling

Recent high-resolution seismic tomography and receiver function studies have revealed a variety of mantle plume morphologies [1]. Lateral ponding between 1000 km and 660 km depths can be seen below Réunion and Comores [2] and tree-like plume morphologies can be found beneath major hotspots such as La Réunion [3], Afar [4, 5] or Azores [6], characterized by multiple secondary plume branches (plumelets) with varying sizes and temperatures. The physical mechanisms controlling the generation of these structures and their temporal variability are not well understood. Previous studies suggested that plume morphology is sensitive to the viscosity structure near the mantle transition zone (between 410 km and 660 km depth) and/or to the Clapeyron slope of the ringwoodite/perovskite 660-km phase change [7, 8, 9], or to the thermochemical nature of plumes [10, 11]. However, most related numerical studies rely on setups with a circular plume imposed via a thermal and/or thermochemical anomaly and without self-consistent plate tectonics.

Here, we use 3D compressible spherical-cap convection models (StagYY, [12]) with pseudo-plastic rheology producing self-consistent plate-like tectonics to investigate how viscosity structure and phase transitions control the morphology and dynamics of purely thermal plumes arising from self-consistent convection. We consider an Arrhenius-type viscosity law with an optional 10 to 100-fold viscosity jump at 660 km [13] or 900 km [14], combined with up to three olivine phase transitions at 410, 520 and 660 km depth [15]. The surface yield stress is tuned independently for each viscosity profile to ensure plate-like behavior. We also developed an automated algorithm to detect and track plumes through depth and time, defining them as the ~96th-highest percentile of upward vertical advective heat transport, and computing plume diagnostics (buoyancy flux, section, mean temperature) using Gaussian-weighted averages to reduce sensitivity to detection thresholds.

We identify four distinct plume morphology types. Type 1 exhibits conduit necking driven by the viscosity jump and/or the exothermic phase transitions at 410 and 520 km, which enhance upward buoyancy via a sucking effect. Type 2 shows mild bulging at the endothermic 660-km transition with a broad penetration of the plume into the transition zone. Types 3 and 4 consist of tree-like plumes showing respectively mild or large lateral ponding at 660 km, from which 2–6 or more than 10 secondary plumelets emerge respectively. The transition between these types is primarily controlled by the viscosity at the 660-km depth: sufficiently high viscosity enables plume penetration, while a larger density jump strengthens the barrier. Remarkably, including all three transition zone phase changes completely suppresses the tree-like types within the parameter range explored. For these types, detected plumelets are shorter-lived (~10–50 Myr) than the parent plume (~1 Gyr) and exhibit temporal variability uncorrelated with it. They display distinct mean temperatures, which may result in different degrees of partial melting and distinct geochemical signatures at the surface.

References

[1] Lu, Q. and Rudolph, M. L. (2024). A synoptic view of mantle plume shapes enabled by virtual reality. Geochemistry, Geophysics, Geosystems, https://doi.org/10.1029/2023GC011254
[2] Dongmo Wamba, M., Montagner, J.-P. and Romanowicz, B. (2023). Imaging deep-mantle plumbing beneath La Réunion and Comores hot spots: Vertical plume conduits and horizontal ponding zones. Science Advances, https://doi.org/10.1126/sciadv.ade3723
[3] French, S. W. and Romanowicz, B. (2015). Broad plumes rooted at the base of the Earth's mantle beneath major hotspots. Nature, https://doi.org/10.1038/nature14876
[4] Civiero, C. et al. (2015). Multiple mantle upwellings in the transition zone beneath the northern East-African Rift system from relative P-wave travel-time tomography. Geochemistry, Geophysics, Geosystems, https://doi.org/10.1002/2015GC005988
[5] Tsekhmistrenko, M., Sigloch, K., Hosseini, K. and Barruol, G. (2021). A tree of Indo-African mantle plumes imaged by seismic tomography. Nature Geoscience, https://doi.org/10.1038/s41561-021-00762-9
[6] Saki, M. et al. (2015). Topography of upper mantle seismic discontinuities beneath the North Atlantic: The Azores, Canary and Cape Verde plumes. Earth and Planetary Science Letters, https://doi.org/10.1016/j.epsl.2014.10.052

[7] Li, Y., Wang, Y., Zhao, L., Chen, L. and Huang, J. (2023). The role of mantle viscosity heterogeneities on the development of secondary plumes in the upper mantle. Geophysical Journal International, https://doi.org/10.1093/gji/ggad412
[8] Liu, H., Wang, W., Jia, X., Leng, W., Wu, Z. and Sun, D. (2018). The combined effects of post-spinel and post-garnet phase transitions on mantle plume dynamics. Journal of Geophysical Research: Solid Earth, https://doi.org/10.1029/2
[9] Liu, H. and Leng, W. (2020). Plume-tree structure induced by low-viscosity layers in the upper mantle. Geophysical Research Letters, https://doi.org/10.1029/2019GL086508
[10] Davaille, A. and Romanowicz, B. (2020). Deflating the LLSVPs: Bundles of mantle thermochemical plumes rather than thick stagnant "piles". Tectonics, https://doi.org/10.1029/2020TC006265
[11] Zhu, X., Balázs, A., Gerya, T. and Sun, Z. (2025). Secondary plumes formation controlled by interaction of thermochemical mantle plumes with the mantle transition zone. Journal of Geophysical Research: Solid Earth, https://doi.org/10.1029/2024JB029882
[12] Tackley, P. J. (2008). Modelling compressible mantle convection with large viscosity contrasts in a three-dimensional spherical shell using the yin-yang grid. Physics of the Earth and Planetary Interiors, https://doi.org/10.1016/j.pepi.2008.08.005
[13] Panasyuk, S. V. and Hager, B. H. (1998). A model of transformational superplasticity in the upper mantle. Geophysical Journal International, https://doi.org/10.1046/j.1365-246X.1998.00560.x

Geodynamica: a new community-led Diamond-Open Access Journal dedicated to Earth and (Exo)Planets dynamics

Maëlis Arnould[*1], Mandy Bethkenhagen[2], Thibault Duretz[3], Mohamed Gouiza[4], Lorraine Hwang[5], Stefano Maffei[6], and Iris van Zelst[7]

[1]LGL-TPE, University Lyon 1, France
[2]LULI, Ecole Polytechnique, Saclay, France
[3]Faculty of Earth Sciences, Goethe University, Frankfurt, Germany
[4]School of Earth, Environment and Sustainability, University of Leeds, UK
[5]CIG, University of California Davis, USA
[6]Department of Earth and Planetary Sciences, ETH Zurich, Switzerland
[7]School of Geosciences, University of Edinburgh, UK
*maelis.arnould@univ-lyon1.fr

Keywords: diamond open-access journal, geodynamics, open science

The past decade has seen the consolidation of open access practices in scientific publishing, with funding bodies, international agencies and academic institutions requiring free access to not only scientific papers but also other output such as datasets and computer codes. The transition to open access practices has led multiple academic publishers to offer Gold Open Access (GOA) schemes, under which scientific papers are free-to-read. Compared to the traditional publication models, GOA comes at a much higher cost for authors. These practices have had a documented negative impact on the scientific publishing landscape, from the rise of predatory journals to the broadening of the economic divide between academic institutions.

Partly in response, different fields of Earth Sciences have seen the rise of several community-led Diamond Open Access journals (DOAJ). These journals are free-to-publish and free-to-read. The aim is to remove financial barriers to scientific publishing by making peer-reviewed articles available at no cost to both authors and readers, thus offering a platform for true open science. DOAJs are created and maintained by the very same scientific community they aim to serve, thus removing economical and business considerations that drive a large fraction of the modern publishing landscape. These community-led journals offer a high-quality alternative to classical for-profit scientific journals.

We are pleased to announce a new DOAJ initiative called Geodynamica. Coordinated by a core committee of seven scientists, Geodynamica aims at promoting academic discourse and disseminating research pertaining to the quantitative study of Earth and (exo-)planetary internal structure, dynamics, and evolution from observational to modelling perspectives.

Geodynamica, which has launched in July 2025 and now successfully published its first articles, enjoys the support of eScholarship (University of California), and hugely benefits from the experience of existing community-led journals within the geoscience field, such as Volcanica, Tektonika and Seismica, as well as the help of an editorial team composed of established volunteer scientists.

In this contribution, we will provide the vision behind this initiative, report on the structure of this journal, its scope, and the remarkable community effort that made this new DOAJ a reality, as an inclusive alternative to traditional paywall scientific publishing journals.

Forming the Lunar crustal Dichotomy from Terrestrial Tides

Daniel Astudillo Manosalva*[1], Paul Tackley[1], Diogo Lourenço[1], and Albert de Montserrat Navarro[1]

[1]ETH Zürich
*daniel.astudillo@eaps.ethz.ch

Keywords: magma ocean, moon, tides

The Lunar crustal dichotomy, which is composed of the farside and nearside differences in crustal thickness, volcanism and surface composition, does not have a clear origin so far. Multiple mechanisms can be found in literature that attempt to explain aspects of the dichotomy, but none have managed to fully explain the entirety of the dichotomy. Our work starts from the hypothesis that all aspects of the dichotomy must be related and should originate from the solidification of the Lunar Magma Ocean (LMO). Given that the dichotomy is aligned in reference to Earth, we investigate if Earth's influence can explain this, through its tidal effect on the LMO when the Moon was in proximity to the Roche limit.

Using a version of StagYY [1] modified with a 3-dimensional gravity that accounts for tidal effects, we model the LMO solidification starting from a fully molten Moon.

Our models show that an asymmetric degree two convection pattern can emerge during the beginning of solidification. This tide-drive magma ocean convection is characterized by two massive plumes on the nearside and farside and subduction in the perpendicular plane at the poles. The nearside plume is faster than the farside one given the asymmetries in the tidal forces between each side. This convection pattern inhibits the solidification of the LMO as well as any sort of compaction its solid fraction towards the bottom. As the Moon's orbit recedes, the asymmetries between each plume become more pronounced, resulting in significant differences in degree of crystallization, chemical differentiation and crust formation rates. All of these differences eventually become all of the aspects we know today that form the lunar crustal dichotomy.

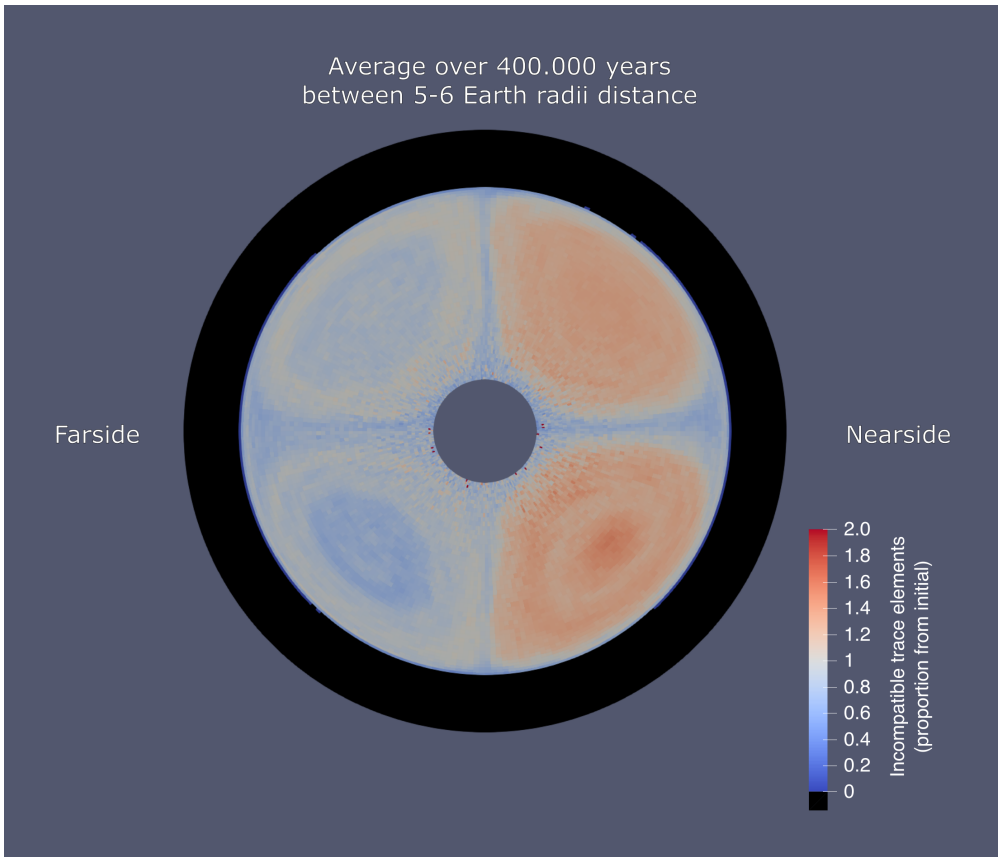


Figure: Concentration of incompatible trace elements in an average of 400,000 years at 5-6 Earth radii distance.

References

[1] Tackley, P. J. (2008). Modelling compressible mantle convection with large viscosity contrasts in a three-dimensional spherical shell using the yin-yang grid. Physics of the Earth and Planetary Interiors, 171(1–4), 7–18.

Why is Enceladus so stressed?

Adrian Bakoč*[1], Barbora Pilářiková[1], Marie Běhounková[1], Ondřej Souček[2], Gaël Choblet[3], and Gabriel Tobie[3]

[1]Department of Geophysics, Charles University, Prague, Czech Republic
[2]Mathematical Institute, Charles University, Prague, Czech Republic
[3]Laboratoire de Planétologie et Géosciences, Nantes University, Nantes, France
*bakoc@karel.troja.mff.cuni.cz

Enceladus, a small moon of Saturn, is considered one of the most geologically active bodies in the Solar system. Its numerous surface features, anomalously high heat flux, and large variations in ice-shell thickness are the result of both internal and external processes over a wide range of temporal scales.

Here, we investigate the contribution of eccentricity-driven diurnal tides, non-synchronous rotation, and viscous flow to the stress state of Enceladus' ice shell.

At short timescales (orbital period, i.e., 1.37 d), we examine stresses induced by tidal forcing, considering elastic rheology and the influence of frictionless faults. At much longer timescales (10 kyr –10 Myr), we assess the effect of non-synchronous rotation assuming viscoelastic behaviour, a process proposed to occur in Enceladus [1]. Additionally, we investigate the long-term effect of viscous flow induced by the lateral variations in ice-shell thickness.

We model the response of Enceladus' ice shell to tidal forcing and non-synchronous rotation, as well as the viscous flow, using a three-dimensional finite-element approach [2–4]. The ice shell thickness model is based on [4], assuming a mean ice shell thickness of 20 km. The geometry of faults, which represent Tiger Stripes in the southern polar region, is parametrised following [5]. Temperature and viscosity profiles are described using a simplified one-dimensional conductive model with an Arrhenius-type temperature dependence of viscosity. We consider reference viscosities at the melting point in the range of 10^{13-15} Pa s and activation energy of $E^* = 60$ kJ/mol.

Diurnal tides induce the lowest stress among the investigated mechanisms. In the absence of faults, the maximum surface stress, reaching up to 100 kPa, occurs within the south polar terrain, where the ice shell is thinnest. When frictionless faults are included, the combined effects of mechanical decoupling associated with the faults and shell thinning further amplify the stresses. This combination also produces a depth-dependent change in the stress regime, particularly in the direction parallel to the faults, due to the bending stresses.

If present, non-synchronous rotation is the dominant source of surface stress, generating stresses of up to ten MPa. These surface stresses are approximately two orders of magnitude higher than those induced by diurnal tides when assuming an elastic ice shell, and even higher when viscoelastic rheology is used.

Finally, the viscous flow generates surface stresses up to ~500 kPa within the southern polar region, largely independent of the viscosity considered at the bottom of the ice shell. The resulting stress field includes both compressional and extensional stresses, with compression associated with locally thinned ice. Moreover, the flow pattern depends on the imposed maximum viscosity contrast, transitioning from predominantly radial flow at low viscosity contrasts to low-velocity tangential flow at high viscosity contrasts.

This work was supported by the Ministry of Education, Youth, and Sports of the Czech Republic through e-INFRA CZ (ID:90254), and by the Czech Science Foundation (project No. 26-21877S).

References

[1] Patthoff et al. (2019). doi: 10.1016/j.icarus.2018.11.028
[2] Alnæs et al. (2015). doi: 10.11588/ans.2015.100.20553
[3] Souček et al. (2019). doi: 10.1016/j.icarus.2019.02.012
[4] Čadek el al. (2019). doi: 10.1016/j.icarus.2018.10.003
[5] Porco et al. (2014). doi: 10.1088/0004-6256/148/3/45

A parameterized model of a solidifying magma reservoir: the microstructural record of crystal settling dynamics

Vít Beran*[1], Vojtěch Patočka[1], Václav Špillar[2], and Marian Holness[3]

[1]Faculty of Mathematics and Physics, Charles University, Prague, Czech Republic
[2]Faculty of Science, Institute of Petrology and Structural Geology, Charles University, Prague, Czech Republic
[3]Department of Earth Sciences, University of Cambridge, United Kingdom
*vit.beran@matfyz.cuni.cz

Keywords: thermal convection, magmatic and igneous systems, CSDs, microstructure

Many processes involved in the formation of plutonic bodies are currently unresolved or poorly constrained, due to the inherent complexity of igneous systems. In particular, only limited quantitative tools are available to address the extent to which the settling of crystals within magma affects the microstructure of igneous rocks. Building upon [1], we present a new parameterized model of a convecting and solidifying magma reservoir, based on experimentally supported kinetics of crystal nucleation and growth [2], in which crystals nucleate in the upper thermal boundary layer, undergo growth while suspended in the convecting magma, before deposition on the floor. The presented framework accounts for coupling with the host rock, enabling a self-consistent calculation of the extracted heat flux that controls the convective vigor and thermal evolution of the reservoir. Incorporating the results of 3D simulations of particle-laden convection [3], we introduce a probabilistic framework for the settling of size-evolving particles to quantify the crystal size distributions in the cumulate pile and in the convecting bulk interior. The vigor of the convection controls the crystal size distributions in the cumulate: weak convection results in rapid sinking and a narrowing of the resultant size distribution, whereas vigorous convection results in a broadening of the size distribution. In contrast, the mean crystal size is relatively unaffected by variation in the settling regime. Additionally, the stratigraphic (temporal) evolution of the mean crystal size within the cumulate is reported and we show that it is controlled primarily by the temperature dependence of magma viscosity, by the initial composition of the magma, and by magma cooling history.

Acknowledgements

VB has been supported by the Charles University Research Centre program No.UNCE/24/SCI/005.

References

[1] Jarvis, R. A. & Woods, A. W., 1994. The nucleation, growth and settling of crystals from a turbulently convecting fluid, Journal of Fluid Mechanics, 273, 83–107, doi: 10.1017/S0022112094001850.
[2] Hort, M., 1997. Cooling and crystallization in sheet-like magma bodies revisited, Journal of Volcanology and Geothermal Research, 76(3), 297–317, doi: https://doi.org/10.1016/S0377-0273(96)00079-0.
[3] Patocka, V., Tosi, N., & Calzavarini, E., 2022. Residence time of inertial particles in 3d thermal convection: Implications for magma reservoirs, Earth and Planetary Science Letters, 591, 117622, doi: https://doi.org/10.1016/j.epsl.2022.117622.

Experimental Insights into Effusive Cryovolcanism: Boiling and Freezing of Saline Water under Low Pressure Conditions

Priyanka Biju Sindhu[*1,2], Petr Brož[1], Vojtěch Patočka[2], Mark Fox-Powell[3], Frances Butcher[4], Manish Patel[3], and Matthew Sylvest[3]

[1]Institute of Geophysics of the Czech Academy of Sciences, Prague, Czech Republic
[2]Department of Geophysics, Charles University, Prague, Czech Republic
[3]School of Physical Sciences, The Open University, Milton Keynes, United Kingdom
[4]School of Geography and Planning, University of Sheffield, Sheffield, United Kingdom
*priyanka@ig.cas.cz

Several icy worlds show surface features interpreted as products of effusive cryovolcanism (e.g., [1–3]), yet the behaviour of saline liquids exposed to low-pressure environments remains poorly constrained. The coupled effects of boiling, evaporative cooling, freezing, and salt precipitation are difficult to observe under planetary conditions. This study presents sixteen experiments investigating how large volumes of water and saline solutions behave during depressurisation.

Experiments were conducted in the Large Dirty Mars Chamber ("George") at the Open University, UK, building on previous work [4]. Each run used a 40 × 40 × 40 cm glass tank containing 40 kg of liquid placed inside a cylindrical vacuum chamber capable of reaching pressures of about 1 mbar. Deionised water was used as a reference, alongside NaCl, $MgSO_4$, and mixed NaCl–$MgSO_4$ solutions. Salinities ranged from 0.5 wt% to 5.0 wt%, with near-eutectic solutions of approximately 23.3 wt% NaCl and 17.4 wt% $MgSO_4$. Each salt–salinity combination was repeated twice for consistency. The study focuses on static or weakly mixed systems; turbulent flow experiments are presented separately [5].

The experiments evolved through three stages: initial boiling-driven cooling, a transition marked by ice nucleation and ice-lid formation, and later progressive porous ice growth. During early depressurisation, vigorous boiling dominated heat loss through latent heat of vaporisation. Despite intense surface activity, vertical temperature gradients initially remained small. Ice crystals appeared after sufficient cooling lowered surface temperatures below each solution's freezing point. Freezing onset was delayed with increasing salinity, and near-eutectic NaCl solutions did not freeze even after six hours. However, near-eutectic NaCl and $MgSO_4$ experiments showed salt crystal nucleation at the surface and later within the liquid.

Ice initially formed as thin translucent patches that nucleated locally, expanded, merged, and were repeatedly disrupted by vapour escaping from below. With continued cooling, these patches developed into a mechanically coherent ice lid. At higher salinities, this lid retained vents and did not fully seal the surface, altering heat and mass transfer by limiting direct liquid exposure to the chamber atmosphere.

Unlike previous studies focused mainly on end-member compositions [6,7], this dataset reveals systematic effects of salinity and salt composition on ice morphology and mechanics. Low-salinity solutions produced brittle, highly porous, multilayered ice crusts [4,6], whereas higher-salinity solutions formed more ductile, compact ice with reduced porosity and more stable vapour vents. At high salinity, $MgSO_4$ and NaCl systems diverged: 17.4 wt% $MgSO_4$ produced ductile salty ice containing trapped salt and ice crystals, while 23.3 wt% NaCl formed a disrupted pseudo-lid of precipitated salt crystals that partially suppressed evaporation and cooling [7].

Increasing salinity delayed freezing, extended the boiling-dominated stage, increased evaporative mass loss before freezing, and reduced cooling rates. These measurements provide constraints for numerical models, including preliminary results showing that evaporative cooling during the pure evaporation stage can be calculated from measured mass loss.

Overall, the experiments show that salinity controls the morphology, porosity, and mechanical stability of ice crusts forming during effusive cryovolcanism on icy worlds such as Europa, Enceladus, Titan, and possibly Pluto.

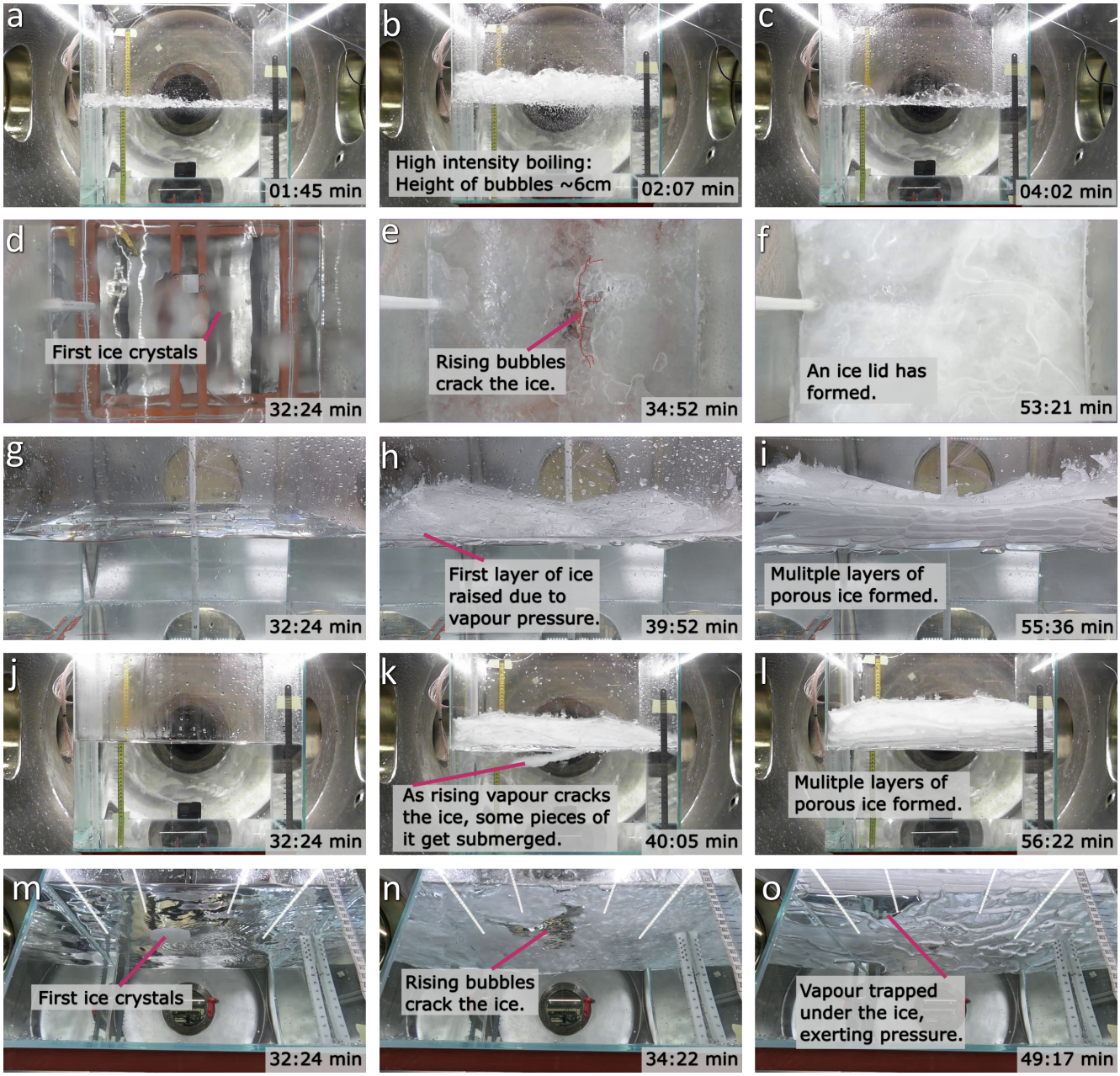


Figure: Progression of boiling and freezing in solution with 0.5% NaCl, when exposed to a low pressure environment. Exp6

References

[1] Fagents, JGR, 108, E12 (2003).
[2] Lesage et al., Nat Comm, 16, 1886 (2025).
[3] Wilson, JGR, 102, E4 (1997).
[4] Brož et al., EPSL, 668 (2025).
[5] Brož et al., EPSC abstract EPSC2026-190 (2026).
[6] Patočka et al., EPSL, 685 (2026).
[7] Fox-Powell et al., EGU abstract 26-21408 (2026).

Semi-automated analysis of fault and plate boundary networks using Fatbox

Sascha Brune[*1,2], Pauline Gayrin[1,2], Alessandro La Rosa[3], Kai Li[4], Michaël Pons[5], Anne C. Glerum[1], and John Naliboff[6]

[1]GFZ Helmholtz Centre for Geosciences, Potsdam, Germany
[2]University of Potsdam, Potsdam, Germany
[3]University of Pisa, Pisa, Italy
[4]University of Sydney, Australia
[5]Roma Tre University, Rome, Italy
[6]New Mexico Institute of Mining and Technology, Socorro, New Mexico, United States of America
*sascha.brune@gfz.de

Keywords: plate boundary dynamics, rifting, faulting, software

Quantifying the spatial arrangement, connectivity, and temporal evolution of faults or plate boundaries is fundamental for understanding strain distribution in active tectonic settings. Yet the density and complexity of deformation—in field data and numerical models alike—pose major challenges for automated analysis, and fault interpretation often remains a time-intensive manual process. Here we present Fatbox, the Fault Analysis Toolbox [1], an open-source python library that integrates semi-automated fault extraction with systematic geometric and kinematic characterisation of fault networks. As a post-processing tool independent of any particular modelling software, Fatbox uses 2D fields such as topography, strain, strain rate, or velocity to derive discrete fault locations and properties such as slip rate, displacement, and length, facilitating direct comparison between model outputs and geological observations. We demonstrate the capabilities of the toolbox through two rift-related case studies and an outlook on its extension to global spherical geometries: (1) We use satellite-based elevation data from the Afar rift (East Africa), mapping ~4,000 individual faults [2]. Combined with rock dating and geodetic data, our results reveal that strain has progressively migrated toward the rift axis since ~4.5 Ma, potentially enhanced by magmatic weakening of the crust. (2) We analyse normal fault network evolution in 3D numerical rift models of oblique extension using ASPECT [3]. Tracking fault geometry and kinematics from surface strain rates, we document a characteristic sequence of rapid fault growth and linkage, inter-fault competition and network stabilisation, and ultimately strain migration toward the rift axis accompanied by border fault disintegration and intra-basin fault nucleation. (3) We present a spherical adaptation of Fatbox for global-scale models, deriving plate boundary networks from surface strain rate fields and tracking plate boundary initiation and relative plate velocities through time. These three applications highlight Fatbox as a versatile framework for analysis of fault system and plate boundary networks across spatial scales and data types.

References

[1] Gayrin, P., Wrona, T., Brune, S., Neuharth, D., Molnar, N., La Rosa, A., & Naliboff, J. (2026). Fatbox: the Fault Analysis Toolbox. Solid Earth, 17(3), 555–572. https://doi.org/10.5194/se-17-555-2026
[2] La Rosa, A., Gayrin, P., Brune, S., Pagli, C., Muluneh, A. A., Tortelli, G., & Keir, D. (2025). Cross-scale strain analysis in the Afar rift (East Africa) from automatic fault mapping and geodesy. Solid Earth, 16(10), 929–945. https://doi.org/10.5194/se-16-929-2025
[3] Bangerth, W., Dannberg, J., Fraters, M., Gassmöller, R., Glerum, A., Heister, T., et al. (2024). ASPECT: Advanced Solver for Planetary Evolution, Convection, and Tectonics, User Manual. https://doi.org/10.6084/m9.figshare.4865333

Towards thermo-chemical geodynamic modelling: surrogate models for coupling ASPECT with thermodynamics

Arijit Chakraborty[*1], Jeroen van Hunen[1], Andrew Valentine[1], Sergio Zlotnik[2,3,4], and Alberto García González[3,4,5]

[1]Department of Earth Sciences, Durham University, Durham, UK
[5]ETSECCPB, Universitat Politècnica de Catalunya - BarcelonaTech (UPC), Campus Nord UPC, 08034 Barcelona, Spain
[3]LaCàN, Universitat Politècnica de Catalunya - BarcelonaTech (UPC), Campus Nord UPC, 08034 Barcelona, Spain
[4]Centre Internacional de Metodes Numerics en Enginyeria (CIMNE), Campus Nord UPC, 08034 Barcelona, Spain
[*]arijit.chakraborty@durham.ac.uk

Keywords: neural networks, mantle melting, ASPECT, MAGEMin

Mantle melting is a critical process governing the thickness and composition of crust, the stability of cratonic lithosphere, and the broader thermochemical evolution of the mantle. It is also a key control on the sources of critical minerals and metals. These melting processes are governed by complex phase equilibria, which determine proportions and compositions of mineral assemblages, depending on pressure, temperature, and bulk composition. Gibbs Free Energy Minimization (GFEM) provides a robust framework for predicting these equilibria, but integrating it into large-scale geodynamic simulations remains a significant computational challenge.

We investigate computational strategies for coupling mantle convection codes such as ASPECT with thermodynamic equilibrium calculations tools like MAGEMin. While a direct coupling would provide accurate phase equilibria predictions, it comes at a significant computational cost for large-scale geodynamic models. Our research explores developing surrogate models using machine learning and neural network techniques to approximate these thermodynamic calculations more efficiently.

We present our preliminary research involving methodological approaches and discuss the computational trade-offs involved in different coupling strategies. A simplified geodynamic model demonstrates potential workflows for this approach. This research is a step towards a more integrated computational framework for thermochemical geodynamic modelling, with implications for a range of applications, including melt generation, lithospheric evolution, and modelling critical mineral formation in complex geodynamic settings.

Efficient GPU Uzawa algorithms with projection strategies for geodynamic Stokes flow

Byung-Dal So[*1,2], Deok-Kyu Jang[3], Kyeong-Min Lee[1], Cedric Thieulot[4], and Whan-Hyuk Choi[3,5]

[1]Interdisciplinary Program in Earth Environmental System Science & Engineering, Kangwon National University, Chuncheon, Republic of Korea
[2]Department of Geophysics, Kangwon National University, Chuncheon, Republic of Korea
[3]KNU Research Institute of Mathematical Sciences, Kangwon National University, Chuncheon, Republic of Korea
[4]Department of Earth Sciences, Utrecht University, Princetonlaan 8A, The Netherlands
[5]Department of Mathematics, Kangwon National University, Chuncheon, Republic of Korea
*bdso@kangwon.ac.kr

Keywords: Stokes solvers, numerical methods, GPU, geodynamics

Stokes equations are often difficult to handle in geodynamic modelling because they form a saddle-point system and involve strong variations in viscosity. Uzawa-type solvers are straightforward to implement, but their convergence may become slow if a suitable preconditioner is not used. Although these are no more considered to be the state-of-the-art in computational geodynamics we have revisited and improved them and show that they are robust and still competitive with other approaches.

In a first article [1] we introduce two adjustments that improve stability and efficiency. Residuals are evaluated in weak form, giving an effect similar to that of a mass-matrix preconditioner. We also add a projection step so that the velocity field remains nearly divergence-free. These updates made the solver converge faster and behave more stably than the standard Uzawa method. The modified approach was tested in several cases, including ABC flow, SolCx, mantle convection, block sinking, and compressible convection under the Anelastic Liquid Approximation.

In a second article [2] we implement this solver on GPUs by coupling CUDA-enabled PETSc with FEniCS. The algorithm is dominated by sparse matrix-vector products, vector inner products, vector updates, and repeated velocity subproblem solves, all of which map onto GPU architectures. PETSc AIJCUSPARSE matrices with CUDA vectors keep operators and field vectors resident in VRAM, which limits CPU-GPU transfers during iterations. The P_1 mass matrix, the gradient operator, and the divergence operator are reused in the pressure-correction L^2-projection step. HYPRE BoomerAMG was adopted for preconditioning the velocity-only subproblem. Accuracy and performance are evaluated on manufactured solutions, the SolCx benchmark, the sticky-air benchmark, 2D and 3D Rayleigh-Taylor instabilities, 3D thermal convection, and a 2D subduction model with nonlinear viscosity.

We confirm that the GPU-based implementation reproduces CPU solutions. We distinguish between the execution time, which includes only the pressure correction step, and the wall time, which includes the workflow from mesh generation to Stokes solves. A single-GPU environment achieves a 5–11× reduction in execution time relative to a 32-core CPU. For nonlinear viscosity cases with per-step matrix updates, the wall time is reduced by 1.14–3.46× on a single GPU relative to a 32-core CPU. Using Multi-Process Service to coordinate two-GPU with a 16-core CPU reduces the wall time by 5.83× compared to a 32-core CPU.

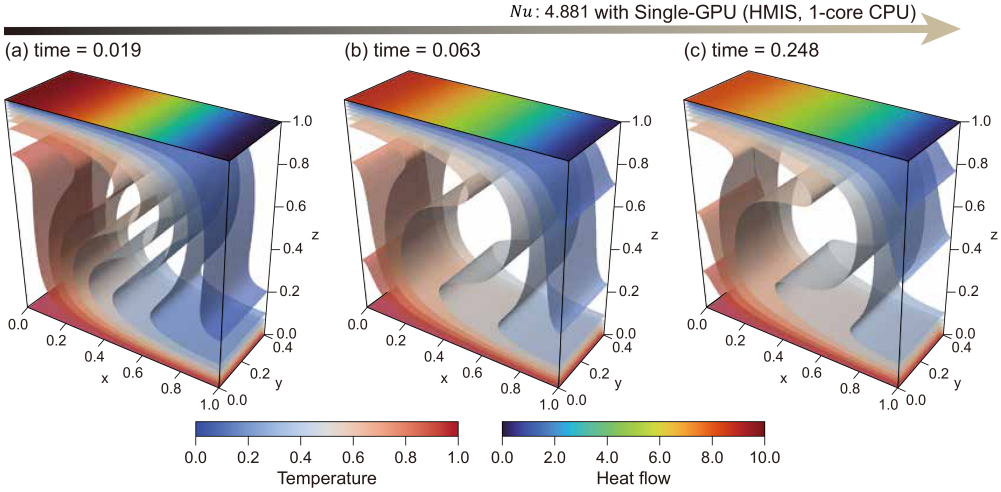


Figure: Time evolution of the temperature field from the single-GPU (HMIS) with 1-core CPU. Snapshots of 3D temperature isosurfaces at nondimensional times t = 0.019, 0.063, and 0.248 (from left to right).

References

[1] Efficient Uzawa algorithms with projection strategies for geodynamic Stokes flow, Deok-Kyu Jang, Kyeong-Min Lee, Cedric Thieulot, Whan-Hyuk Choi and Byung-Dal So, submitted to Solid Earth.
[2] High-Performance Geodynamics on GPUs Using the PETSc's CUDA Backend, Kyeong-Min Lee, Deok-Kyu Jang, Cedric Thieulot, Byung-Dal So, submitted to GMD.

Estimating Archean Oceanic Crust Composition and Its Role in Water Delivery in Subduction Settings

Hee Choi*[1] and Joyce Shi Sim[1]

[1]Georgia Institute of Technology, Atlanta, GA, United States
*hchoi342@gatech.edu

Archean oceanic crust is one of the least directly constrained components of the early Earth, since virtually none of it is preserved. Its composition nevertheless governs a process central to early Earth evolution: the delivery of water to the deep mantle. Where subduction operated in the Archean, the volume and timing of water cycled through these early convergent margins would bear on mantle rheology, melt generation, felsic (TTG) crust formation, and the long-term evolution of the surface ocean. Because the capacity of subducting crust to deliver water depends on which hydrous phases are stable along a given pressure-temperature path, composition and water delivery cannot be evaluated independently.

Here we estimate plausible Archean oceanic crust compositions using a Bayesian framework calibrated against komatiitic basalt from the Yilgarn craton. Since no direct sample of Archean oceanic crust exists, candidate compositions are drawn from this prior and propagated through a thermodynamic model (Perple_X) to test how water budget responds to compositional variability. We consider two end-member scenarios: a homogeneous crust and a vertically layered crust with distinct upper and lower compositions. For each sampled composition, we compute equilibrium phase assemblages across Archean subduction P-T conditions and extract the distribution of structurally bound water. These P-T-H_2O results are then used as inputs to a numerical subduction zone model to track water transport and release through the slab. Preliminary results show lower bound water contents in candidate Archean oceanic crust compositions than in modern oceanic crust. While preliminary, it suggests that early subduction delivered less water than its modern counterpart, with consequences for the deep water cycle and the conditions under which felsic crust formed.

Transient Seafloor Uplift at Mid-Ocean Ridges Driven by Mush Zone Buoyancy

András Cserép*[1], Jean-Arthur Olive[1], and Einat Aharonov[2]

[1]Laboratoire de Géologie de l'ENS, CNRS - École normale supérieure - PSL University, Paris, France
[2]Institute of Earth Sciences, The Hebrew University of Jerusalem, Jerusalem, Israel
*cserep@geologie.ens.fr

Keywords: mid-ocean ridges, mush, magma, seafloor

Seismic imaging of magmatically robust mid-ocean ridges (MORs) reveals the presence of mush zones located a few kilometres below the seafloor, capped by and interspersed with sill-shaped melt lenses (AMLs). These are increasingly seen as dynamic features which must undergo rapid melt replenishment to provide the heat that fuels high-temperature hydrothermal convection. Furthermore, ocean-bottom pressure sensors have documented up to tens of centimetres per year of seafloor uplift above AMLs. This rapid uplift is sustained over decadal timescales, is partially or completely reversed during MOR eruptions, and has thus been interpreted as a direct manifestation of AML replenishment. Previous studies of such phenomena have typically modelled seafloor displacements by imposing overpressurisation rates in a tensile deformation source embedded within a (visco-)elastic half-space. However, few have focused on the physical mechanisms that drive AML inflation / overpressurisation.

To address this gap, we test the hypothesis that mush buoyancy, regulated by melt influx, drives uplift. We model the displacement of an elastic sheet over a viscous half-space due to buoyant loading applied along a finite cross-axis width. By systematically varying the instantaneous loading, steady loading rates, and viscosity, and comparing the results with data from the East Pacific Rise at 9°50′N, we constrain the range of melt fluxes capable of driving such uplift. Our findings suggest that the observed deformation is likely driven by periodic bursts of melt into the mush zone. Such a process could be explained by porosity waves forming at the Mohorovičić discontinuity. Future work will investigate the effect of mush rheology on the development of these melt supply bursts.

Automatic detection and time tracking of mantle plumes using topological data analysis

Ritabrata Dasgupta[*1], Maëlis Arnould[1], Maxim Ballmer[2], and Julien Tierny[3]

[1]LGL-TPE, Université Claude Bernard Lyon 1, Lyon, France
[2]University College London, Department of Earth Sciences, UK
[3]CNRS, Laboratoire d'Informatique de Paris 6, Sorbonne Université, Paris, France
*ritabrata.dasgupta@univ-lyon1.fr

Keywords: Mantle Plume, Topological Data Analysis, Buoyancy flux

Describing mantle plume geometry and dynamics is important in order to calculate the plume heat/buoyancy flux, their effects on surface topography, their magmatic flux and potential effects on climate (e.g. via their volcanic outgassing). However, precise detection of 3D plume shapes from 3D mantle convection models and high-resolution tomography remains a challenge. Previous studies dealing with plume flux mostly focused on the detection of regions of anomalously high temperature and/or radial advection at one specific depth (2D cross-section of plumes) and are highly dependent on preassigned thresholds.

Here, we present an automated method for detecting and characterizing mantle plumes in 3D spherical convection models with plate-like behaviour [1] using topological data analysis. The workflow, using Python and Topology Toolkit [2], processes the temperature field from simulation outputs. 3D iso-volumes of anomalously hot regions are first defined. The resulting geometries are then simplified based on a threshold on the persistence of the critical points (local maxima, minima and saddle points of the iso-volume) in order to remove topological noise. Finally, using Reeb Graphs (shape descriptor for objects defined by functions), central skeletal structures of the iso-volumes are retrieved, allowing efficient tracking of complex plume geometries such as branching. This method robustly detects thick/thin, purely thermal/thermochemical and juvenile/mature plume structures, consistently depicting tilts, branches and merging events, and was successfully tested both on 3D portions of spheres and fully-spherical models of incompressible/compressible convection. We extend this method using a Hungarian/Munkres Algorithm [3] to track the temporal evolution of all the plumes in one spherical model of incompressible mantle convection with plate-like tectonics [1]. In this model, plume characteristics (sectional area, excess temperature, rising speed, volume, buoyancy and heat fluxes) are systematically tracked throughout their lifetime, by applying a Gaussian-weighted average on anomalously hot and upwelling areas in order to precisely describe plume contours.

At any time, the total buoyancy flux for all the model plumes falls within the reported ranges of Earth's mantle plumes estimated from their dynamic topographic swells [4]. However, the buoyancy flux of plumes shows some variations through depth and time in our models. We identified that the entrainment of surrounding mantle material into the plume conduits plays a pivotal role on the increase of buoyancy flux of individual plumes towards the surface. As expected, temporal variations are controlled by the stage of the plume (juvenile/mature), as juvenile plume heads tend to show higher buoyancy flux compared to mature plume conduits [5]. Furthermore, we test the role of "plume clustering" on the buoyancy flux using a nearest-neighbor formulation.

The proposed methodology is simple, robust, and computationally inexpensive, while producing precise plume geometry detection in any geometry (cartesian/spherical). It currently works for plume geometries connected to the Core-Mantle Boundary (CMB). In the future, we plan to extend its versatility to address more complex shapes, such as the detection of disjoint plume/melt structures and slabs in both seismic tomography and 3D mantle convection models.

References

[1] Arnould, M., Coltice, N., Flament, N., & Mallard, C. (2020). Plate tectonics and mantle controls on plume dynamics. Earth and Planetary Science Letters, 547, 116439.
[2] Tierny, J., Favelier, G., Levine, J. A., Gueunet, C., & Michaux, M. (2017). The topology toolkit. IEEE transactions on visualization and computer graphics, 24(1), 832-842.
[3] Munkres, J. (2014). Topology second edition.
[4] Hoggard, M. J., Parnell-Turner, R., & White, N. (2020). Hotspots and mantle plumes revisited: Towards reconciling the mantle heat transfer discrepancy. Earth and Planetary Science Letters, 542, 116317.
[5] Dannberg, J., & Sobolev, S. V. (2015). Low-buoyancy thermochemical plumes resolve controversy of classical mantle plume concept. Nature communications, 6(1), 6960.

On the importance of melt to localize large-scale deformation on Venus

Anne Davaille*[1], Gianluca Gerardi[1], and Hélène Massol[2]

[1]FAST, CNRS / Université Paris-Saclay, Orsay, FRANCE
[2]GEOPS, Université Paris-Saclay / CNRS, Orsay, FRANCE
*anne.davaille@universite-paris-saclay.fr

Keywords: Venus, convection, rheology, subduction, laboratory experiments, DEM simulations

Based on Earth's dynamics, water is often considered as a key-ingredient to allow subduction, Plate Tectonics and the continuous resurfacing of a planet, because it softens rocks rheology and lubricates faults and the subduction interface. However, there is another way to strongly localize deformation: two-phase flow.

Subduction and Plate Tectonics require the strong localization of deformation. Based on Earth's dynamics, water is often considered as a key-ingredient since it softens rocks rheology and lubricates faults and the subduction interface. Bands of small-size grains such as mylonites have also been proposed. But melt is also ubiquitous around Earth's plate boundaries. So we studied if and how deformation was localizing in a diphasic fluid using laboratory experiments and DEM (Discrete Element Methods) modeling.

As a model system, we used convection-evaporation in Ludox colloidal dispersions. These fluids are constituted of water, ions and nanoparticles of silica. As the solute (water) is removed, a skeleton of nanoparticles aggregates develops (Gerardi et al, 2026). Therefore as water content decreases, the fluid density increases and its rheology changes from newtonian to visco-elasto-plastic to brittle (Di Giuseppe et al, 2012). Under evaporation, such a system develops solutal convection under a denser and more viscous skin, analogous to the denser and more viscous lithosphere on a planet undergoing thermal convection. The experimental lithosphere is heterogeneous at the meso-scale, with the presence of particle aggregates and free water channels. This results in a highly non-linear rheology at the large scale, capable of producing sufficient shear localization to generate self-consistently asymmetric subduction and rifting.

This suggests that a liquid-solid mixture such as melt-rock could allow subduction on a rocky planet. That could explain why Venus offers evidences of subduction around some large coronae despite the absence of a water ocean on its surface: pervasive melt could do the trick. Indeed, the surface of Venus is littered by volcanoes, suggesting the presence of melt almost everywhere, and lava flows are observed in the trenches of the subduction candidates. Not only water, but melt could also serve as a lubricant of plates interfaces.

References

[1] Gerardi, G., Alba-Simionesco, C., Pépin, M. and Davaille, A. Interplay between gelation and glass formation in silica nanoparticle colloids. Scientific Reports, 16, 10964 (2026). https://doi.org/10.1038/s41598-026-45258-x
[2] Di Giuseppe, E., Davaille, A., Mittelstaedt, E., François, M. Rheological and mechanical properties of silica colloids: from Newtonian liquid to brittle behaviour, Rheol. Acta. DOI 10.1007/s00397-011-0611-9

Combined petrology and physical modelling reveal the thermal evolution of translithospheric diapirs in the French Massif Central

Luc de Hoÿm de Marien[*1], Petra Maierová[1], Karel Schulmann[1], Pavla Štípská[1], Pavel Pitra[1,2], Dimitrios Moutzouris[3], and Simon Couzinié[4]

[1]Czech Geological Survey, CZ-118 21 Prague 1, Czech Republic
[2]Univ Rennes, CNRS, Géosciences Rennes – UMR 6118, F-35000 Rennes, France
[3]Institute of Geosciences, Johannes Gutenberg Universität Mainz, Mainz, Federal Republic of Germany
[4]Université de Lorraine, CNRS, CRPG, 54000 Nancy, France
*luc.dehoym@gmail.com

Keywords: petrology, thermal modelling, translithospheric diapir, Variscan belt, French Massif Central

The Variscan orogeny in the French Massif Central has historically been compared to the Himalayan orogeny, and the geological record has been essentially attributed to a Devonian–Carboniferous continental collision following Silurian oceanic subduction. Mantle peridotite boudins embedded in crustal migmatite and magmatic rocks derived from a mantle reservoir contaminated by continental crust point, however, to a scenario involving continental subduction to mantle depths.

We studied the mineral sequences of mafic eclogite and granulite samples from the exhumed lower plate crust. We used thermodynamic models and petrochronological tools to decipher their pressure–temperature–time (P–T–t) evolutions. Combined, their evolution involve: (1) peak pressure at 20–25 kbar and 850–900 °C at 362 ± 7.7 Ma (U–Pb in zircon), (2) decompression and heating to 12–13 kbar and 900–1000 °C, (3) limited decompression and strong cooling to 10–13 kbar and 700–800 °C at 354.6±8.5 Ma (U–Pb in titanite), and (4) final decompression below 9 kbar. The temperature increase during decompression in stage 2 is not easily explained by exhumation in a subduction channel. To explain such heating event, we consider the exhumation of crustal diapirs through the mantle. Regional evidence of crust–mantle interaction further supports this scenario. Importantly, Devonian–Carboniferous marine sediments deposited on the upper plate suggest attenuated crustal thickness, which implies a Moho pressure < 9 kbar. Thus, both heating during stage 2 and cooling during stage 3 potentially occurred in the mantle.

A simplified physical description of the P–T evolution of crustal diapirs rising through the mantle wedge and lithosphere is used to evaluate this interpretation. The diapir ascent is approximated as the motion of a spherical buoyant, viscous body through a viscous fluid with a non-linear temperature-dependent rheology. Its rising velocity and thermal equilibration with the surrounding mantle are evaluated as two coupled ordinary differential equations. We tested wet and dry mantle rheologies, varied the initial temperature of the diapir between 750 and 950 °C and its initial diameter between 2 and 20 km. Modelled diapirs with diameters of 10–15 km and an initial temperature of 875 °C rising through a wet mantle undergo decompression and heating between 900–950 °C until they cross the modelled mantle geotherm between 45–50 km depth (~ 12–14 kbar), and then decelerate and cool to below 800 °C along with limited decompression. The modelled initial heating and decompression stages are extremely fast (< 1 Myr) while the later stages of near-isobaric cooling occur in 2–20 Myr. The good agreement of the thermal model with the P–T–t data suggests that it captures the main characteristics of the natural process.

Our study presents a new conceptual framework for the exhumation of high-pressure rocks of the French Massif Central. In a broader perspective, contrary to the prevailing consensus, near-isobaric cooling of crustal rocks may not always document the long-term relaxation of a thick orogenic crust but could also be due to swift thermal equilibration of small bodies of crustal rocks directly in the mantle.

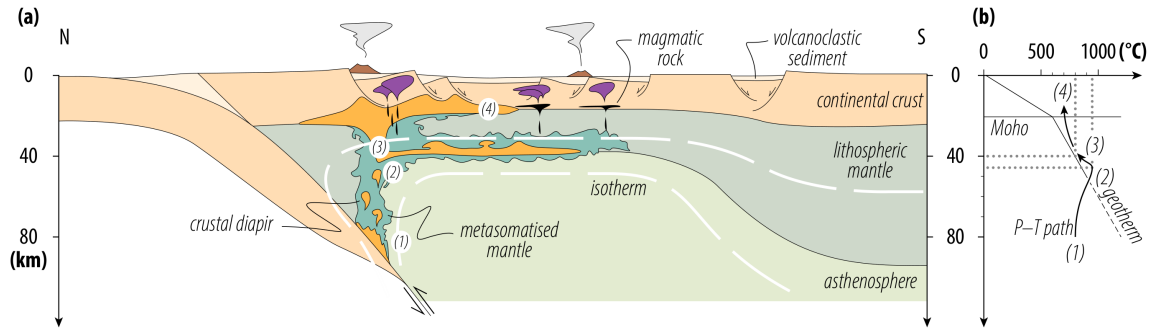


Figure: Geodynamic and thermal evolution of a crustal diapir. (a) Conceptual geodynamic model for the Devonian to Carboniferous transition in the French Massif Central. (b) P–T evolution of a diapir, with a geotherm for reference. The stages (1) to (4) of the figure refer to the metamorphic stages mentioned in the text.

RheologyCalculator.jl: automatically solving arbitrary constitutive relationships

Albert de Montserrat Navarro[*1]

[1]ETH Zürich
[*]albertdemontserratnavarro@eaps.ethz.ch

Much of the challenges in simulating geoscientific processes stems from the (often) non-linear nature and complexity of the constitutive equations. Rheological behavior is often modeled as combinations of individual elements (such as linear elastic springs, viscous dashpots, and plastic sliders), each representing a simple (nonlinear) constitutive relation. These elements are assembled in series and/or parallel to form more complex rheological systems. Solving the resulting constitutive equations typically requires iterative methods, such as Newton-type schemes, which rely on the assembly of local Jacobian matrices.

In most existing codes, constitutive relationships and their corresponding Jacobians are hard-coded, making the implementation of new rheologies a challenging task, as it requires deep modifications to the codebase. Here, we present RheologyCalculator.jl, a Julia package designed to solve constitutive relationships constructed from arbitrary combinations of rheological elements. The package statically determines the computational graph of the constitutive model at compile time, enabling efficient assembly of local Jacobian matrices and the use of local direct solvers without heap allocations, which is crucial for maintaining high performance when employed in large-scale simulations, as the system of equations must be solved in a large number of grid points. RheologyCalculator.jl is also fully differentiable, allowing it to, for example, compute consistent tangent operators or to be differentiated through entire forward simulations for gradient-based analyses. The package is designed for seamless integration into existing geoscientific modeling frameworks, providing a flexible and efficient approach for implementing and experimenting with complex rheological models without extensive code modifications.

Role of water in mantle-lithosphere interactions in the context of Venus

Alexandr Dizov*[1], Ondřej Čadek[1], Petra Maierová[2], Caroline Dumoulin[3], Gaël Choblet[3], and Gabriel Tobie[3]

[1]Charles University, Faculty of Mathematics and Physics, Department of Geophysics, Czechia
[2]Czech Geological Survey, Prague, Czech Republic
[3]Laboratoire de Planétologie et Géosciences, Nantes Université, Nantes, France
*dizov@karel.troja.mff.cuni.cz

Keywords: Venus, mantle plume, melting, water

Present-day Venus has a very hot, dry and uninhabitable surface with a dense, toxic atmosphere. However, the extent and longevity of water presence at its surface, interior and atmosphere is a highly debated topic [1]. Depending on the evolutionary scenario, the mantle could still represent the largest remaining reservoir of water. Here, we investigate how the potential presence of water might influence the formation of Venus' hotspots, presumably manifested at the surface as large topographic rises with a positive gravity signature. To understand the role of water in the plume-lithosphere interaction and the formation of the surface features, we have developed a 3D numerical model in ASPECT [2], incorporating both hydrous and anhydrous melting [3]. The model includes the melting-induced decrease of viscosity associated with dehydration [4] and the density change related to iron depletion of the mantle [5]. We present a qualitative comparison of wet and dry cases illustrating the significance of water in Venus' mantle dynamics, show the resulting thermal structure, viscosity profiles and mantle depletion patterns, and confront our results with the gravity and topography observed in selected regions of Venus. The figure below shows the mantle depletion patterns obtained for plumes with similar width and temperature in the case of a dry (a) and wet (b) mantle, suggesting a significant impact of water on the style of hotspot volcanism. The research was supported by the Grant Agency of Charles University (project no. 252126).

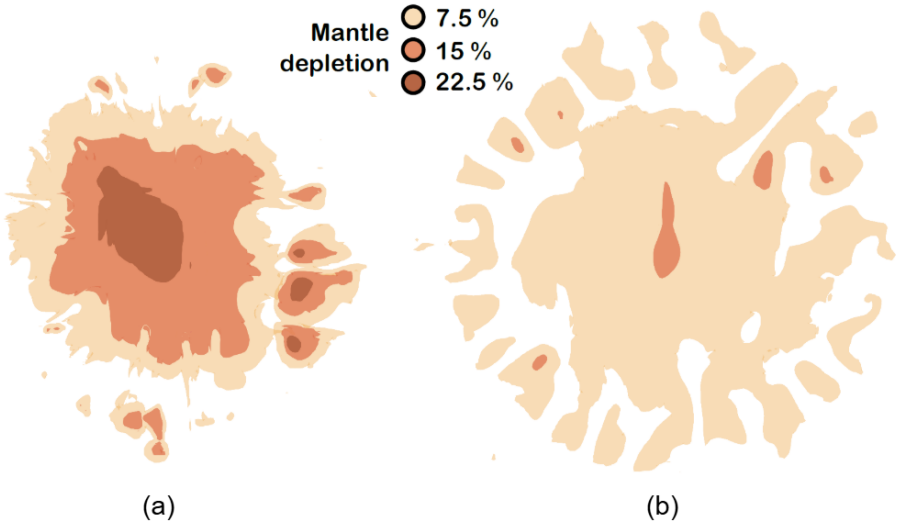


Figure: Mantle depletion patterns obtained for plumes with similar width and temperature in the case of a dry (a) and wet (b) mantle.

References

[1] Gillmann, C. et al. (2022). The Long-Term Evolution of the Atmosphere of Venus: Processes and Feedback Mechanisms: Interior-Exterior Exchanges. Space Science Reviews, 218(7), 56.
[2] Heistler, T. et al. (2017). High Accuracy Mantle Convection Simulation through Modern Numerical Methods II: Realistic Models and Problems. Geophysical Journal International, 210(2), 833-851.
[3] Katz, R., er al. (2003). A new parametrization of hydrous mantle melting. Geochemistry, Geophysics, Geosystems, 4(9).
[4] Hirth, G., & Kohlstedt, D. L. (1996). Water in the oceanic upper mantle: implications for rheology, melt extraction and the evolution of the lithosphere. Earth and Planetary Science Letters, 144(1-2), 93-108.
[5] Sparks, D. W., & Parmentier, E. M. (1993). The Structure of Three-Dimensional Convection Beneath Oceanic Spreading Centres. Geophysical Journal International, 112(1), 81-91.

Linking surface and deep earth processes in geodynamic models: Coupling ASPECT and LandLab

Daniel Douglas[*1], Wolfgang Bangerth[2], Mark Behn[1], Biraj Borgohain[3], Tian Gan[4], Timo Heister[5], Eric Hutton[4], Leif Karlstrom[6], John Naliboff[3], and Greg Tucker[4]

[1]Boston College
[2]Colorado State University
[3]New Mexico Institute of Mining and Technology
[4]Colorado University, Boulder
[5]Clemson University
[6]University of Oregon
[*]daniel.douglas@bc.edu

Keywords: software, geodynamics, surface processes, lithosphere, mantle

Understanding how the Earth evolves as a dynamic, integrated system across vast spatial and temporal scales remains a key goal in the geosciences. Until relatively recently, most numerical modeling studies have treated solid Earth processes separately from surface evolution. Pioneering studies coupling landscape evolution models (LEMs) with geodynamic models have shown that nonlinear feedbacks can strongly influence the evolution of Earth's surface and Earth's interior in settings such as continental breakup, normal faulting, and orogeny. However, these coupled models have largely been limited to 2D "T-models" or small regional 3D simulations due to computational expense.

Two major limitations restrict scalability to larger problems in existing coupling frameworks: (1) requiring the geodynamic and LEM meshes to be identical along the interface, and (2) the lack of parallelization in most LEMs, preventing scaling to the hundreds or thousands of processes required to run large geodynamic simulations. To address these issues, we couple two open-source, modular, community-driven codes: ASPECT and LandLab. While this work is still preliminary, the coupling already demonstrates key advantages over existing coupling frameworks. Critically, the interface between ASPECT and LandLab supports independent meshes, enabling support for adaptive remeshing in ASPECT and diverse grid types in LandLab (raster, hexagonal, unstructured voronoi). This framework also includes support for spherical geometries. ASPECT and LandLab's flexibility and extensibility is also beneficial, enabling the community to easily incorporate new processes based on individual need. While parallelizing LandLab is ongoing work, significant progress has been made through partitioning structured grids for distribution across multiple processes and testing crucial components such as flow routing, stream power, and hillslope diffusion.

We present three use cases that highlight advantages in our framework over existing approaches: (1) the dynamic growth of a volcano on a visco-elasto-plastic plate, (2) an extensional normal fault model with adaptive mesh refinement in ASPECT, and (3) a coupled global mantle convection model. Future work will focus on benchmarking the coupling in serial and in parallel and developing cookbooks to facilitate easy adoption of this framework in the broader community.

Subduction initiation across a magma-poor to magma-rich passive margin transition: preliminary results from 3D numerical modelling

Valeria Fedeli[*1], Alessandro Regorda[1], and Anna Maria Marotta[1]

[1]Università degli Studi di Milano
[*]valeria.fedeli@unimi.it

Keywords: subduction initiation, passive margins, 3D numerical modelling, geodynamics

Subduction Zone Initiation (SZI) at passive margins is a fundamental yet still debated process in plate tectonics, representing the closing phase of the Wilson cycle [1]. The structural and rheological characteristics of passive margins strongly depend on their rifting history and magmatic budget, allowing their classification into magma-poor and magma-rich end-members. These two margin types are characterized by distinct crustal architectures, thermal structures, and sedimentation patterns [2], which may lead to different rheological responses during lithospheric shortening.

Previous studies have shown that several parameters, including margin geometry as well as lithological and rheological inheritance, strongly influence strain localization. therefore magma-rich and magma-poor passive margins respond differently to compression and develop subduction zone initiation through distinct deformation styles and mechanisms [3]. However, the tectonic and mechanical evolution of the transition zone between these two end-members remains poorly constrained.

In this work, we investigate the behavior of the transition zone between magma-poor and magma-rich passive margins through 3D thermo-mechanical numerical modelling performed with the LaMEM code [4]. The model domain includes a fully magma-rich segment, a fully magma-poor segment, and a transitional zone connecting the two end-members. The different lithospheric layers are described using visco-elasto-plastic rheologies. Subduction zone initiation is induced by imposing 50 Myr of convergence at a shortening rate of 2 cm/yr.

Preliminary results highlight how variations in margin geometry influence stress and strain-rate localization during the early stages of convergence, as well as the subsequent evolution of slab geometry over time.

References

[1] Wilson, T. (1966) Did the Atlantic close and re-open? Nature 211, 676–681
[2] Peron-Pinvidic G., Manatschal G. and the "IMAGinING RIFTING" Workshop Participants (2019) Rifted Margins: State of the Art and Future Challenges. Frontiers in Earth Sciences 7:218
[3] Auzemery A., Yamato P., Duretz T., Willingshofer E., Matenco L., Porkoláb K. (2002) Influence of magma-poor versus magma-rich passive margins on subduction initiation. Gondwana Research 103, 172–186
[4] Kaus, B. J., Popov, A. A., Baumann, T., Pusok, A., Bauville, A., Fernandez, N., & Collignon, M. (2016) Forward and inverse modelling of lithospheric deformation on geological timescales. Proceedings of nic symposium 48, 978–983

Intermediate-complexity modeling of magma–tectonic interaction in continental rifts

Menno Fraters*[1,2], Sascha Brune[2], Eleonora Rivalta[2,3], Rene Gassmöller[4], Sibiao Liu[4], Ameha Atnafu Muluneh[2,5], and Cedric Thieulot[6]

[1]University of Graz
[2]GFZ Helmholtz Centre for Geosciences
[3]University of Bologna
[4]GEOMAR Helmholtz Centre for Ocean Research Kiel
[5]University of Bremen, GFZ Helmholtz Centre for Geosciences
[6]Utrecht University
*menno.fraters@uni-graz.at

Keywords: diking, rifting, ASPECT

Continental rifting often induces decompression melting and the ascent of magma that intrudes into the brittle crust in the form of dikes and sills and that extrudes along volcanic fields. At the same time, continental rifts experience stress from topographic loading due to rift flank uplift. It is clear that these two processes interact in magmatic rifts such as the Kenya Rift, the Main Ethiopian Rift, the Afar triple junction, and at the Icelandic plate boundary. However, separating the interplay between tectonic and magmatic processes, the evolving topography and the rift-related stress field, as well as the impact of these processes on dike-fault interactions from field observations alone remains difficult.

Previous modeling studies of time-dependent magma-tectonic interactions in extensional tectonic settings generally fall into two categories: (1) Simple models (e.g. [1]) represent diking by a prescribed fixed rectangular zone of horizontal divergence. While this approach can be applied to model tens of millions of years of dike injection along spreading ridges, its simplicity prevents applications to continental rifts where magmatism manifests over broad areas. (2) More complex setups simulate magma ascent via porous flow and fluid-driven fracture (e.g., [2]). This approach allows to study the evolution of individual dikes, but its computational costs prevent application to lithosphere-scale rifts over geological time scales.

Here, we present a numerical workflow that can be categorized as a model of intermediate complexity. We assume that dikes are nucleated at the brittle-ductile transition above zones of partial melt. They are then propagated perpendicular to the minimum compressive stress, similar to the approach of [3], until they reach their freezing depth or the surface. In this presentation, we show how we approach this problem and how we implement it in the open-source community geodynamics model ASPECT [4,5]. We demonstrate that the generated dikes are being focused in specific regions and we show how the directional dilation and heat injection during dike intrusion influence the long-term rift evolution.

References

[1] Buck, W. Roger, Luc L. Lavier, and Alexei N. B. Poliakov. "Modes of Faulting at Mid-Ocean Ridges." Nature 434, no. 7034 (April 2005): 719–23. https://doi.org/10.1038/nature03358.

[2] Li, Yuan, Adina E Pusok, Timothy Davis, Dave A May, and Richard F Katz. "Continuum Approximation of Dyking with a Theory for Poro-Viscoelastic-Viscoplastic Deformation." Geophysical Journal International 234, no. 3 (September 1, 2023): 2007–31. https://doi.org/10.1093/gji/ggad173.

[3] Maccaferri, Francesco, Eleonora Rivalta, Derek Keir, and Valerio Acocella. "Off-Rift Volcanism in Rift Zones Determined by Crustal Unloading." Nature Geoscience 7, no. 4 (April 2014): 297–300. https://doi.org/10.1038/ngeo2110.

[4] Martin Kronbichler, Timo Heister, and Wolfgang Bangerth. 2012. "High Accuracy Mantle Convection Simulation through Modern Numerical Methods." Geophysical Journal International 191 (1) (August 21): 12–29. doi:10.1111/j.1365-246x.2012.05609.x. http://dx.doi.org/10.1111/j.1365-246X.2012.05609.x.

[5] Timo Heister, Juliane Dannberg, Rene Gassmöller, and Wolfgang Bangerth. 2017. "High Accuracy Mantle Convection Simulation through Modern Numerical Methods – II: Realistic Models and Problems." Geophysical Journal International 210 (2) (May 9): 833–851. doi:10.1093/gji/ggx195. http://dx.doi.org/10.1093/gji/ggx195.

Thermal structure and deformation state of folding slabs : relationship with subduction zones' deep seismicity

Fanny Garel*[1], Nestor Cerpa[1], and Hana Čížková[2]

[1]Géosciences Montpellier, Université de Montpellier, France
[2]Charles University, Faculty of Mathematics and Physics, Prague, Czech Republic
*fanny.garel@umontpellier.fr

Keywords: subduction, transition zone, slab folding, deep-focus earthquakes, thermal parameter

Deep earthquakes in the mantle transition zone occur within or around cold slab anomalies. Although such seismicity has been explained as the result of a metastable olivine wedge in cold slabs, it may occur in slab of intermediate ϕ – the thermal parameter describing the advection of a cold plate within the hot asthenosphere – product of slab velocity and age [2,3]. We investigate here how deformation, and in particular folding, influence both the mean temperature and strain rate within the subducted slab.

First, we analyze with the SubMap tool the occurrence of deep-focus earthquakes as a function of ϕ and of "Kr" – kinematic ratio estimating slab folding at depth [1]. Second, we calculate diagnostics for a variety of subduction simulations exhibiting a large range of morphologies and dynamics – e.g. vertical or horizontal folding, strong rollback, deflected slabs, etc. These diagnostics reveal (i) the temporal variation of slab core temperature and deformation rate during subduction history, (ii) the temporal delay and sometimes large discrepancy between the deep thermal structures and the ones predicted using a ϕ calculation from (surface) velocity and age.

We show that intraslab low-temperature and high-strain rates can be found in a variety of morphology, e.g. vertical folding or inclined slabs. We discuss how present-day morphology and seismicity may reveal past slab folding for a number of subduction zones.

This work is part of ANR project RheoBreak (ANR-21-CE49-0009).

References

[1] Cerpa, N. G., Sigloch, K., Garel, F., Heuret, A., Davies, D. R., & Mihalynuk, M. G. (2022). The effect of a weak asthenospheric layer on surface kinematics, subduction dynamics and slab morphology in the lower mantle. Journal of Geophysical Research: Solid Earth, 127(8), e2022JB024494.
[2] Kirby, S. H., Stein, S., Okal, E. A., & Rubie, D. C. (1996). Metastable mantle phase transformations and deep earthquakes in subducting oceanic lithosphere. Reviews of geophysics, 34(2), 261-306.
[3] McKenzie, D. P. (1969). Speculations on the consequences and causes of plate motions. Geophysical Journal International, 18(1), 1-32.

Testing Compositional Asymmetry Between the African and Pacific LLVPs Using a Bayesian Inversion Framework

Catherine Gower*[1] and Fred Richards[1]

[1]Imperial College London, London, United Kingdom
*c.gower25@imperial.ac.uk

Keywords: large low velocity provinces, Bayesian inversion, core-mantle boundary, thermochemical structure, mantle composition

Large Low Velocity Provinces (LLVPs) above the core-mantle boundary are the largest seismically imaged structures in the Earth's mantle and may play a dominant role in mantle convection. However, their origin, composition, and long-term stability remain debated. In particular, it is unclear whether the African and Pacific LLVPs are compositionally distinct. While they are often assumed to have similar properties, the African LLVP rises significantly higher above the core-mantle boundary, suggesting it may be more buoyant and less dense, perhaps due to lower contributions of recycled crust. Such differences could reflect divergent evolutionary histories and provide insight into past mantle flow and the thermochemical evolution of Earth's interior.

Recent studies have explored the impact of differing evolutionary scenarios for the LLVPs on seismic constraints but have not fully investigated whether these models are consistent with other present-day geophysical observations. Here, we investigate mantle density structure and test for systematic compositional differences between the African and Pacific LLVPs using instantaneous flow modelling within a hierarchical Bayesian inversion framework. We invert for mantle density parameters, including chemically induced density anomalies, constrained by multiple independent geophysical observables: the geoid, dynamic topography, and core-mantle boundary ellipticity. This framework also allows us to quantify parameter uncertainties and covariances, which is particularly important given the trade-off between thermal and compositional effects. We assess whether present-day observations require significant compositional asymmetry between the LLVPs across a range of tomographic and mantle viscosity models.

Preliminary results do not favour strong compositional asymmetry between the African and Pacific LLVPs, suggesting that any chemical differences are insufficient to require fundamentally distinct evolutionary histories. Present-day geophysical observations can be explained using broadly similar chemical density structures for both LLVPs, consistent across numerous tomographic models. If robust, these findings would suggest that subduction history plays a limited role in shaping present-day LLVP density structure, and may point towards a primordial origin, such as early-formed crust or basal magma ocean residue. Ongoing work will further investigate the influence of viscosity structure and prior assumptions on the inferred density contrasts.

Pacific double-subduction drives Gulf of California rifting

Guido Gianni*[1], Xiang He[2,3], Thorsten W. Becker[2,3,4], and Claudio Faccenna[5,6]

[1]Institute of Geophysics, Czech Academy of Sciences, Prague 140, Czech Republic.
[2]Institute for Geophysics, Jackson School of Geosciences, The University of Texas at Austin, Texas 78712, USA.
[3]Department of Earth and Planetary Sciences, Jackson School of Geosciences, The University of Texas at Austin, Texas 78712, USA.
[4]Oden Institute for Computational Engineering and Sciences, The University of Texas at Austin, Texas 78712, USA.
[5]Helmholtz Centre for Geosciences (GFZ), Potsdam 14473, Germany.
[6]Dip. Scienze, Università degli Studi Roma Trè, Roma 00146, Italy.
*gianni@ig.cas.cz

The Gulf of California oblique rift (GOCOR) has experienced rapid rifting at ~6-8 Ma, yet the mechanism behind this acceleration remains debated. During a similar time period, the western Pacific subduction system transitioned from a single- to a double-subduction configuration. We propose that this is no mere temporal coincidence but that the rifting in California during this time was strongly affected by far-field tectonic forces generated from the initiation of Pacific double-subduction. We use 3-D, spherical geodynamic models to compare single- and double-subduction configurations and quantify the resulting stress perturbations transmitted across the Pacific plate. Our results show that while the largest asthenospheric pressure changes are local to the subduction system, the initiation of Pacific double-subduction can generate ~5-15 MPa of horizontal extensional stress in the GOCOR and southern San Andreas Fault system. Sensitivity tests indicate that the magnitude of the stress perturbation depends on lithospheric rheology, in particular the yield stress in visco-plastic formulations and the GOCOR plate boundary strength. However, the extensional stress increment pattern in the GOCOR is robust across these model choices. These results suggest that western Pacific subduction regorganization may have contributed to the rapid rift of GOCOR, highlighting the potential of subduction reorganization as a far-field tectonic driver for continental rifting.

Linking the lower seismic layer in double seismic zones to the oceanic mid-lithospheric discontinuity

Tianyu Hu*[1], Junfeng Zhang[1], Zhensheng Wang[1], Feng Shi[1], Fabio Capitanio[1,2], and Xinnuo Li[1]

[1]State Key Laboratory of Geological Processes and Mineral Resources, School of Earth Science, China University of Geosciences, Wuhan, China.
[2]School of Earth, Atmosphere and Environment, Monash University, Clayton, Victoria, Australia.
*hutianyu@cug.edu.cn

Keywords: double seismic zone, lower seismic layer, oceanic mid-lithospheric discontinuity, eclogitization, stress concentration, subduction zone

The origin of the lower seismic layer (LSL) in double seismic zones (DSZs) remains debated [1-4]. Recent geophysical observations show that oceanic mid-lithospheric discontinuities (MLDs) systematically occur beneath the LSL [1-4], suggesting a possible genetic relationship between them. Here, we investigate whether eclogitization of granulites within the oceanic MLD can generate the stress conditions required for LSL formation [7, 8].

We use two-dimensional thermo-mechanical numerical models of oceanic subduction incorporating melt-related MLD structures composed of residual-melt-derived and intrusive-melt-derived granulites [5, 7, 9]. During subduction, eclogitization of granulites within the MLD promotes grain-size reduction and a transition from dislocation creep to diffusion creep and grain-boundary sliding, producing significant rheological weakening [10-13].

Our models show that weakening of the MLD generates a spatially continuous extensional stress-concentration band in the slab mantle immediately above the MLD. This band reproduces several first-order characteristics of the observed LSL, including its geometry [10-13], depth range [1, 3, 15, 16], extensional stress state [8], and the observed decrease in seismicity with depth [1, 17]. In contrast, models without an MLD fail to develop a comparable shallow and continuous lower stress band.

The predicted position of the modeled lower band is also consistent with geophysical observations showing that the LSL generally overlies the oceanic MLD across slabs of varying ages [5, 6, 18]. Furthermore, MLD-bearing models reproduce a lower brittle seismic band under dry mantle conditions, consistent with the normal Vp/Vs values observed in many LSL regions [19, 20] and previous studies suggesting that the LSL commonly occurs within relatively dry slab mantle domains [2, 21, 22].

These results suggest that eclogitization-driven weakening of the oceanic MLD may provide a key mechanical control on stress concentration and earthquake generation in the lower seismic layer of double seismic zones.

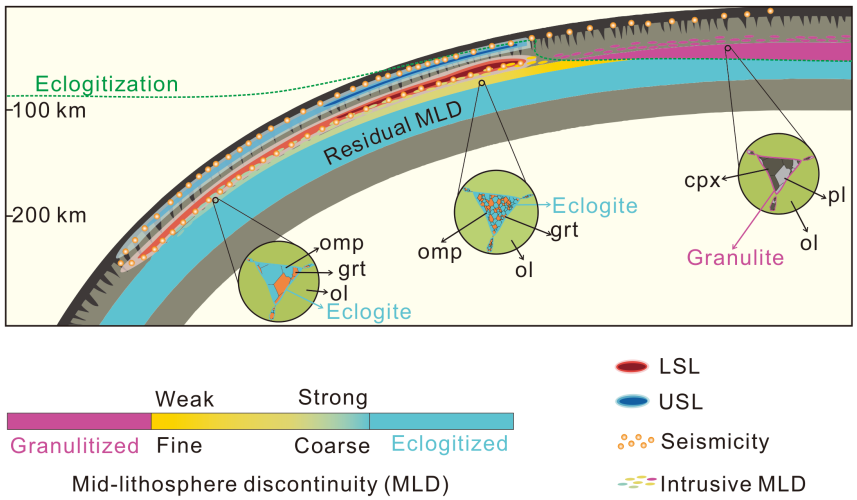


Fig. 1. Schematic illustration of the mechanism for LSL formation. The green dashed line represents the eclogitization boundary. The continuous band represents the MLD derived from residual melts, while scattered ellipsoids represent intrusive MLD bodies. The transition from purple to cyan regions illustrates the progressive eclogitization of metastable granulites within the MLD. Orange circles represent seismicity. The red zone above the MLD indicates LSL, whereas the blue zone indicates USL.

References

[1] Zhan, Z., Mechanisms and Implications of Deep Earthquakes. Annual Review of Earth and Planetary Sciences, 2020. 48(1): p. 147-174.
[2] Shi, F., et al., Metamorphism-facilitated faulting in deforming orthopyroxene: Implications for global intermediate-depth seismicity. Proceedings of the National Academy of Sciences, 2022. 119(11): p. e2112386119.
[3] Peacock, S.M., Are the lower planes of double seismic zones caused by serpentine dehydration in subducting oceanic mantle? Geology, 2001. 29(4): p. 299.
[4] Yang, J., L. Zhao and Y. Li, Tectonic deformation at the outer rise of subduction zones. Geophysical Journal International, 2023. 232(3): p. 1533-1544.
[5] Tharimena, S., et al., Imaging Pacific lithosphere seismic discontinuities—Insights from SS precursor modeling. Journal of geophysical research. Solid earth, 2017. 122(3): p. 2131-2152.
[6] Florez, M.A. and G.A. Prieto, Controlling Factors of Seismicity and Geometry in Double Seismic Zones. Geophysical Research Letters, 2019. 46(8): p. 4174-4181.
[7] Chen, K.X., D.W. Forsyth and K.M. Fischer, A mid-lithospheric discontinuity detected beneath 155 Ma western Pacific seafloor using Sp receiver functions. Geophysical Research Letters, 2024. 51(5): p. e2024GL108347.
[8] Sippl, C., et al., Global constraints on intermediate-depth intraslab stresses from slab geometries and mechanisms of double seismic zone earthquakes. Geochemistry, Geophysics, Geosystems, 2022. 23(9): p. e2022GC010498.
[9] Ohira, A., et al., Evidence for frozen melts in the mid-lithosphere detected from active-source seismic data. Scientific Reports, 2017. 7(1): p. 15770.
[10] Austrheim, H., Eclogitization of lower crustal granulites by fluid migration through shear zones. Earth and Planetary Science Letters, 1987. 81(2-3): p. 221-232.
[11] McNamara, D.D., et al., A key role for diffusion creep in eclogites: Omphacite deformation in the Zermatt-Saas unit, Italian Alps. Journal of Structural Geology, 2024. 179: p. 105033.
[12] Rubie, D.C., Reaction-enhanced ductility: The role of solid-solid univariant reactions in deformation of the crust and mantle. Tectonophysics, 1983. 96(3-4): p. 331-352.
[13] Stünitz, H., et al., Transformation weakening: Diffusion creep in eclogites as a result of interaction of mineral reactions and deformation. Journal of Structural Geology, 2020. 139: p. 104129.
[14] Yamasaki, T. and T. Seno, Double seismic zone and dehydration embrittlement of the subducting slab. Journal of Geophysical Research: Solid Earth, 2003. 108(B4).
[15] Kawakatsu, H., Double seismic zone in Tonga. Nature, 1985. 316(6023): p. 53-55.
[16] Kawakatsu, H., Double seismic zones: Kinematics. Journal of Geophysical Research: Solid Earth, 1986. 91(B5): p. 4811-4825.
[17] Hasegawa, A., et al., Plate subduction, and generation of earthquakes and magmas in Japan as inferred from seismic observations: An overview. Gondwana Research, 2009. 16(3-4): p. 370-400.
[18] Brudzinski, M.R., et al., Global Prevalence of Double Benioff Zones. Science, 2007. 316(5830): p. 1472-1474.
[19] Tsuji, Y., J. Nakajima and A. Hasegawa, Tomographic evidence for hydrated oceanic crust of the Pacific slab beneath northeastern Japan: Implications for water transportation in subduction zones. Geophysical Research Letters, 2008. 35(14).
[20] Wang, J., et al., Seismic Evidence for Large-Scale Intraslab Heterogeneity Beneath Northeast Japan. Journal of Geophysical Research: Solid Earth, 2025. 130(4): p. e2024JB030046.
[21] Fang, H. and R.D. van der Hilst, Earthquake Depth Phase Extraction With P Wave Autocorrelation Provides Insight Into Mechanisms of Intermediate-Depth Earthquakes. Geophysical Research Letters, 2019. 46(24): p. 14440-14449.
[22] Pennacchioni, G., et al., Record of intermediate-depth subduction seismicity in a dry slab from an exhumed ophiolite. Earth and Planetary Science Letters, 2020. 548: p. 116490.

Kinematics and Dynamics of Trumpet-Shaped Strike-Slip Fault Systems: The Western Himalayan Syntaxis Case Study

Yangfan Huang*[1], Adina E. Pusok[1], and Richard T. Walker[1]

[1]Department of Earth Sciences, University of Oxford, Oxford, United Kingdom
*yangfan.huang@stx.ox.ac.uk

Keywords: tectonic escape, trumpet-shaped strike-slip faults, numerical modelling, lithospheric heterogeneity, Western Himalayan Syntaxis

The lateral extrusion of fault-bounded blocks, known as tectonic escape, is a fundamental process accommodating deformation during continental convergence. Tectonic escape may take the form of lateral flow [1,2] or the extrusion of large, strike-slip fault-bounded blocks of the lithosphere [3,4]. Despite significant efforts over the past decades, the dynamics of tectonic escape remain poorly constrained. Here we identify a new class of conjugate strike-slip faults, called trumpet-shaped strike-slip faults (TSFs), that can divert crustal material into adjacent regions and facilitate tectonic escape. In the Western Himalayan Syntaxis, asymmetric TSFs transfer deformation from the Indian indenter into and around the Tajik and Tarim Basins. To investigate the controls on this process, we develop a thin-sheet model incorporating visco-elasto-plastic rheology with basin and belt lithospheric heterogeneities. We systematically explore five key parameters: power-law creep exponent, Argand number, basin- and belt-strength ratios, elastic shear modulus, and yield stress. Our models show that the Argand number (Ar) primarily controls crustal thickening and strain localization in models without basins or belts, with lower Ar values producing thicker crust and more localized deformation adjacent to the indenter. In models containing only a basin, the indenter-basin-strength ratio (λ^{basin}) strongly modulates regional deformation, while in models with both a basin and a belt, the indenter-belt-strength ratio (λ^{belt}) controls the partitioning of deformation and λ^{basin} has a secondary effect. A weak basin ($\lambda^{\text{basin}} < 1$) localizes strain and experiences thickening, whereas a strong basin ($\lambda^{\text{basin}} > 1$) resists deformation, and may rotate or translate laterally. We will also show preliminary 3-D models accounting for depth-dependent rheology to investigate development of shear zones around lithospheric-scale strong basins. Our models demonstrate that basin-belt rheological heterogeneity exerts a fundamental control on the development of TSFs, crustal flow, and strain redistribution during tectonic escape in the Western Himalayan Syntaxis.

References

[1] Dewey, J. F. (1988). Extensional collapse of orogens. Tectonics, 7(6), 1123–1139.
[2] England, P., & McKenzie, D. (1982). A thin viscous sheet model for continental deformation. Geophysical Journal International, 70(2), 295–321.
[3] Tapponnier, P., Peltzer, G., Le Dain, A. Y., Armijo, R., & Cobbold, P. (1982). Propagating extrusion tectonics in Asia: New insights from simple experiments with plasticine. Geology, 10(12), 611–616.
[4] Whitney, D. L., Bezada, M., Hansen, L. N., Teyssier, C., Wada, I., & Zhou, X. (2026). Escape tectonics. Tectonophysics, 920, 231029.

The Coupling of Mechanical Anisotropy to Post Glacial Rebound

Theo Häußler*[1], Clinton P. Conrad[1], and Ágnes Király[1]

[1]University of Oslo
*theoh@uio.no

Keywords: anisotropic viscosity, crystal preferred orientation, geodynamic models

With the increasing melt of polar ice sheets, their weight is continuously redistributed over the surface of the Earth. The resulting post-glacial rebound and gravity perturbations, also known as glacial isostatic adjustment (GIA), can lead to significant changes in relative sea level [1,2] Hypothetically, rock textures in the upper mantle, and in particular a favored crystallographic preferred orientation (CPO), may alter patterns of GIA deformation [3,4]. This may occur due to a preexisting CPO from long time scale geodynamic processes, or if post glacial rebound itself induces or alters a CPO. To model the coupling between CPO and flow, anisotropic viscosity (AV) must be incorporated into the Stokes equations that describe upper mantle deformation. To gauge the importance of CPO-induced AV for GIA processes, we present preliminary modeling results for 3 idealized geodynamic processes: an extreme case of post-glacial rebound, a rising plume sheared by an overriding plate, and a unit convection box.

In general, the speed and magnitude of GIA is sensitive to the vertical and lateral [5] viscosity structure as well as the extent and size of the ice load [6,7]. For East Greenland, Weerdesteijn et. al. [8] have demonstrated that a fast viscous response can be expected where deglaciation happens above a low viscosity region, explaining rapid uplift on decadal time scales. One possible explanation for this low viscosity is that heat from the Iceland plume weakened this area more than ~50 million years ago [9–11]. Under such deformation, polycrystalline samples can also develop a CPO that generates a strong directional dependence in viscosity [12,13]. New rheological models with a realistic treatment of olivine symmetry have been able to model the effect of CPO on flow [14–16]. In addition to GIA, deformation due to a rising plume or plate shear may also generate CPO in the asthenosphere, leading to AV. By tracking the accumulated strain, we probe whether a significantly strong CPO and associated material weakening can emerge from loading and unloading of an ice mass in a series of glacial cycles. Our results show that while the rate of postglacial rebound strongly depends on the viscosity structure and ice load size, even extreme GIA deformations do not lead to a significant CPO. This is because GIA deformation is not sustained for sufficiently long periods of time. By contrast, rising plumes and plate shear may impart asthenospheric deformation over long time periods, inducing CPO. We investigated CPO from a rising plume that is sheared by an overriding plate, in analogy to Greenland passing over the Iceland plume. In our simplistic model, a strong AV contrast emerges above the plume stem. To couple this AV back to post glacial rebound, we aim to develop a benchmark for CPO-induced anisotropic flow. To this extent, we are working to reproduce the results of Rathmann et. al. [16] for coupled flow in an ideal convection box using a new method to compute mechanical anisotropy parameters directly from CPO statistics in situ (Király et al., 2026, in press.)

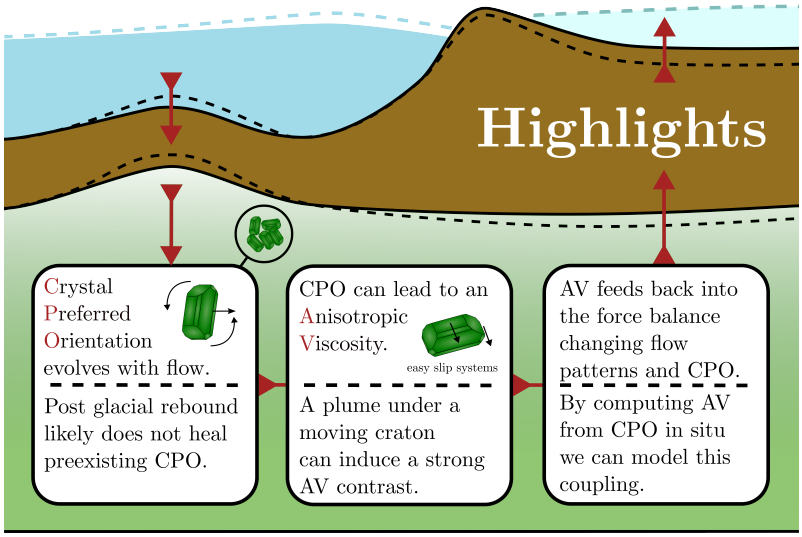


Figure: Graphical Abstract and schematic of Glacial Isostatic Adjustment (GIA). Dotted lines: Previous topography with an ice sheet. Full lines: Adjustment after thousands of years

References

[1] C. P. Conrad, GSA Bulletin 125, 1027 (2013).
[2] J. Ebbing, J. R. Hopper, C. P. Conrad, G. Milne, R. Steffen, J. C. Afonso, V. R. Barletta, A. M. G. Ferreira, J. Freienstein, S. E. Hansen, B. H. Heincke, G. Jones, S. Lebedev, M. Moorkamp, D. L. Schutt, and A. Wansing, Journal of the Geological Society 182, jgs2024 (2025).
[3] U. R. Christensen, Geophysical Journal of the Royal Astronomical Society 91, 711 (1987), number: 3.
[4] N. Gomez, M. Yousefi, D. Pollard, R. M. DeConto, S. Sadai, A. Lloyd, A. Nyblade, D. A. Wiens, R. C. Aster, and T. Wilson, Science Advances 10, eadn1470 (2024).
[5] G. A. Milne, K. Latychev, A. Schaeffer, J. W. Crowley, B. S. Lecavalier, and A. Audette, Geophysical Journal International 214, 1252 (2018).
[6] P. Whitehouse, Earth Surface Dynamics 6, 401 (2018).
[7] M. F. M. Weerdesteijn, C. P. Conrad, and J. B. Naliboff, Geophysical Research Letters 49, e2022GL099731 (2022)
[8] M. F. M. Weerdesteijn and C. P. Conrad, Communications Earth & Environment 5, 791 (2024).
[9] Y. M. Martos, T. A. Jordan, M. Catal´an, T. M. Jordan, J. L. Bamber, and D. G. Vaughan, Geophysical Research Letters 45, 8214 (2018)
[10] N. L. Celli, S. Lebedev, A. J. Schaeffer, and C. Gaina, Earth and Planetary Science Letters 569, 117048 (2021).
[11] B. Steinberger, E. Bredow, S. Lebedev, A. Schaeffer, and T. H. Torsvik, Nature Geoscience 12, 61 (2019).
[12] L. N. Hansen, M. E. Zimmerman, and D. L. Kohlstedt, Nature 492, 415 (2012), number: 7429.
[13] L. N. Hansen, J. M. Warren, M. E. Zimmerman, and D. L. Kohlstedt, Earth and Planetary Science Letters 445, 92 (2016).
[14] Király, C. P. Conrad, and L. N. Hansen, Geochemistry, Geophysics, Geosystems 21, e2020GC009159 (2020), number: 10
[15] L. Mameri, A. Tommasi, J. Signorelli, and R. Hassani, Geophysical Journal International 224, 608 (2021), number: 1.
[16] N. M. Rathmann, K. Mosegaard, I. M. O. Bekkevold, D. A. Lilien, and D. J.
Prior, Geochemistry, Geophysics, Geosystems 25, e2024GC011831 (2024)

Implementing PlateRecipy: an open-access tool utilizing graph theory for detecting tectonic plate boundaries in geophysical datasets and model output

Pejvak Javaheri*[1] and Julian P. Lowman[1,2]

[1]Department of Physics, University of Toronto, Canada
[2]Department of Physical and Environmental Sciences, University of Toronto Scarborough, Canada
*pejvak.javaheri@mail.utoronto.ca

Keywords: plate tectonics, plate modeling, Euler vector, diffuse zones, mantle convection, strain-rate

The emergence of plate-like surface motion in self-consistent mantle convection models is a key behaviour requiring detection in numerical experiment results featuring terrestrial characteristics. However, the identification and verification of candidate plates is a challenging task, in practice. On Earth, narrow divergent, convergent, and strike-slip plate boundaries as well as regions exhibiting widespread diffuse deformation, comprise roughly 10 to 20% of the lithosphere that does not adhere to rigid body motion. Accordingly, the detection of candidate plates must be performed in light of the existence of diffuse deformation occurring regularly as a tectonic characteristic. To address this challenge, we have recently developed a new plate detection tool, 'platerecipy'[1], that utilizes the Random Walker (RW) segmentation algorithm to identify candidate plates in both mantle convection model output as well as global geophysical data sets and terrestrial measurements. We describe how the discrete probability solution arising from RW can be used to both assess confidence in the association of each location with a distinct rigid plate, and to identify diffuse surface regions. Furthermore, we show how utilizing the RW probabilities can significantly improve Euler vector inversion for fitting the plate motion as a probability field allows for a systematic means of incorporating uncertainties inherent to the plate detection process. We demonstrate the effectiveness of our method by applying it to the surface of a mantle convection model and a terrestrial strain-rate dataset. We show how our findings can be used for an Euler vector inversion that allows plate rigidity analysis.

References

[1] Javaheri, P., & Lowman, J. P. (2026). A random walker algorithm for plate boundary detection in spherical mantle convection models and global geophysical data sets: Application to Euler vector determination. Journal of Geophysical Research: Solid Earth, 131, e2025JB032259. https://doi.org/10.1029/2025JB032259

A Global Voxel-Based Analysis of Residence Time and Flux from Backward in Time Mantle Convection

Gabriel Johnston*[1,2], Alessandro Forte[1,2], Molly Anderson[1], and Petar Glisovic[3]

[1]University of Florida
[2]Institut de Physique du Globe de Paris
[3]Department of Geological Sciences and Geological Engineering, Queen's University, Kingston, ON, Canada
*orion1234@ufl.edu

How well mixed is Earth's mantle? Are there primordial reservoirs that have remained isolated from whole mantle convection? What fraction of the mantle feeds present day surface volcanism? We address these questions using large-scale Lagrangian particle tracking flow in time-reversed convection models. We track particles backward in time using a Back-and-Forth Nudging (BFN) method applied to time-reversed thermal convection, initialized with a present-day seismic geodynamic mineral physics model [1]. We use a mantle viscosity structure that has been independently constrained and verified against a wide suite of present-day geodynamic observables, including free-air gravity anomalies, dynamic surface topography, horizontal divergence of plate velocities, excess core–mantle boundary ellipticity, and glacial isostatic adjustment data. We develop a voxel-based analysis framework that quantifies residence time, particle count, and flux density throughout the mantle to identify candidate reservoirs. We use different particle starting conditions, each designed to address a specific aspect of mantle mixing; uniformly distributed particles tracked backward to identify long-lived isolated regions, particles initialized in the D'' layer to assess lower-mantle sampling of the upper mantle, particles placed beneath present-day hotspots to identify plume source regions, particle uniformly spread in the LLSVPs and particles initialized in the upper mantle to quantify upper-to-lower mantle exchange. By combining these approaches, we can find regions of low flux and high residence time, candidates for reservoirs. We identify the core of the African large-low-shear velocity province as being a candidate reservoir having a much larger residence time than the Pacific LLSVP and on the whole is characterized by a dynamical behaviour distinct from the Pacific LLSVP.

References

[1] Glišović, Petar & Forte, Alessandro. (2016). A new back-and-forth iterative method for time-reversed convection modeling: Implications for the Cenozoic evolution of 3-D structure and dynamics of the mantle. Journal of Geophysical Research: Solid Earth. 121. 10.1002/2016JB012841.

Beyond Equilibrium: Kinetic Thresholds and Rheological Feedbacks Create a Potentially Complex 410 in Slab Regions

Buchanan Kerswell*[1], John Wheeler[1], Rene Gassmöller[2], J. Huw Davies[3], Isabel Papanagnou[4], and Sanne Cottaar[4]

[1]Department of Earth, Oceans and Ecological Sciences, University of Liverpool, Liverpool L69 3BX, UK
[2]GEOMAR Helmholtz Centre for Ocean Research Kiel, Kiel, Germany
[3]School of Earth and Environmental Sciences, Cardiff University, Park Place, Cardiff, CF10 3AT, UK
[4]Bullard Laboratories, Department of Earth Sciences, University of Cambridge, Cambridge CB3 0EZ, UK
*b.kerswell@liverpool.ac.uk

Keywords: mantle convection, phase transition, reaction kinetics, geodynamics, numerical modeling

The seismic expression of Earth's 410 km discontinuity varies across tectonic settings, from sharp, high-amplitude interfaces to broad transitions-patterns that cannot be explained by equilibrium thermodynamics without invoking large-scale thermal or compositional heterogeneities. Laboratory experiments show the olivine ⇔ wadsleyite phase transition responsible for the 410 is rate-limited, yet previous numerical studies have not directly evaluated the sensitivity of 410 structure to kinetic and rheological factors. Here we investigate these relationships by coupling a grain-scale, interface-controlled olivine ⇔ wadsleyite growth model to compressible simulations of mantle plumes and subducting slabs. We vary kinetic parameters across seven orders of magnitude and quantify the resulting 410 displacements and widths. Our results reveal an asymmetry between hot and cold environments. In plumes, high temperatures produce sharp 410s (2-3 km wide) regardless of kinetics. In slabs, kinetics exert first-order control on 410 structure through three regimes: (1) quasi-equilibrium conditions producing narrow, uplifted 410s and continuous slab descent; (2) intermediate reaction rates generating broader, deeper 410s with metastable olivine wedges resisting downward slab motion; and (3) ultra-sluggish reaction rates causing slab stagnation with re-sharpened, deeply displaced 410s (< 100 km). Rheological contrasts modulate these kinetic effects by controlling slab geometry and residence time in the phase transition zone. These findings demonstrate that reaction rates strongly influence 410 structure in subduction zones, establishing the 410 as a potential seismological constraint on upper mantle kinetic processes, particularly in cold environments where disequilibrium effects are amplified.

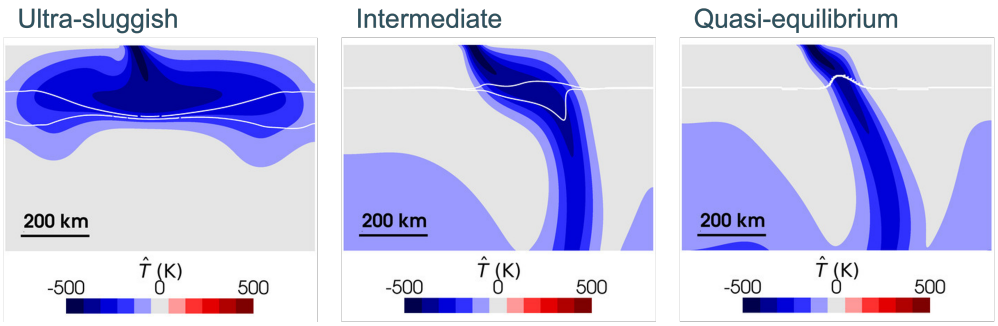


Figure: Simulation snapshots, corresponding to ultra-sluggish (left), intermediate (middle), and fast (right) olivine ⇔ wadsleyite reaction rates in subduction zone settings. The shapshots show the temperature anomaly relative to the background mantle. The white contours mark the 10% and 90% wadsleyite volume fraction, which outline the 410 structure. The numerical setup and boundary conditions are identical in each case, but different kinetic conditions produce distinct seismic structures and slab dynamics.

Investigating the roles of laterally variable surface temperature and tidal heating in Europa's ice shell

Hyunseong Kim*[1], Antoniette Greta Grima[1], and Luke Daly[1]

[1]University of Glasgow
*h.kim.6@research.gla.ac.uk

Observations from past missions, including NASA's Galileo, have revealed a geologically young surface, active ice tectonics and a subsurface ocean on Europa. These imply material recycling within the ice shell, possible compositional exchange with the underlying ocean, and thus the potential conditions for habitability. Therefore, constraining the surface and near-surface properties of Europa's ice shell, such as surface topography, thermal profile and thicknesses of conductive and convective layers, is a key objective of NASA's Europa Clipper mission since they reflect the strength of material recycling. However, the controllers of material recycling remain uncertain. These are likely influenced by the spatial distributions of heat sources on Europa. Insolation raises surface temperatures near the equator, while tidal heating is strongest toward the poles. Because insolation and tidal heating produce opposing latitudinal thermal patterns, their combined effects may either suppress or enhance lateral variations within the ice shell. To investigate the combined effects of insolation and tidal heating, we present numerical models of Europa's ice shell that include laterally variable tidal heating and surface temperature, coupled with visco-elasto-plastic deformation and composite ice rheology. We investigate how these heat sources influence convection within the possible range of ice shell thickness and explore their effects on the global distribution of heat flow, stress accumulation, and topography at the ice surface of Europa. Our results provide new insights into lateral variations in interior properties and the evolution of surface deformation in Europa's ice shell, with implications for surface–interior exchange processes and surface expressions to be observed through future space missions.

Assessment of the Applicability of Smoothed Particle Hydrodynamics to Geodynamic Thermal Convection

Inyup Kim*[1] and Byung-Dal So[2]

[1]Interdisciplinary Program in Earth Environmental System Science & Engineering, Kangwon National University, Chuncheon 24341, Republic of Korea
[2]Department of Geophysics, Kangwon National University, Chuncheon 24341, Republic of Korea
*kiy@kangwon.ac.kr

Keywords: smoothed particle hydrodynamics, thermal convection, convection benchmark, root-mean-square velocity, Nusselt number

Thermal convection forms through the interaction between buoyancy driven by temperature differences and viscous resistance. In planetary interiors, thermal convection transports internal heat and develops circulation patterns between hot and cold materials. The flow patterns of thermal convection depend on thermal boundary conditions and fluid properties such as density and viscosity, so models of planetary interior dynamics frequently examine thermal convection. Simplified thermal convection benchmark models provide comparison of flow structure, heat flux, and domain-averaged velocity among different numerical methods. Smoothed Particle Hydrodynamics (SPH) is a Lagrangian numerical method that approximates continuum fields using particles and kernel functions. The method calculates physical quantities such as density, velocity, pressure, and temperature from particle positions and neighboring particle distributions. Particle-based representation of flow and temperature fields provides a mesh-free structure, which enables flexible construction of thermo-fluid models with complex geometries or moving boundaries. We construct an SPH-based Blankenbach benchmark model to quantitatively compare convective vigor and heat transport efficiency using root-mean-square velocity (V_{rms}) and Nusselt number (Nu). A Rayleigh–Bénard natural convection benchmark model then tests the development of convection induced by a temperature difference. Particle resolution is also considered when evaluating the sensitivity of convective structures and quantitative diagnostics reproduced by the SPH-based thermal convection model. The two benchmark models serve as a validation step for applying SPH to geodynamic thermal convection models. The model configurations, particle resolutions, and quantitative diagnostics established through the validation process provide a basis for extending the particle-based approach to planetary interior dynamics. Potential applications include mantle convection, magma oceans, and other systems involving coupled heat transport and flow structures.

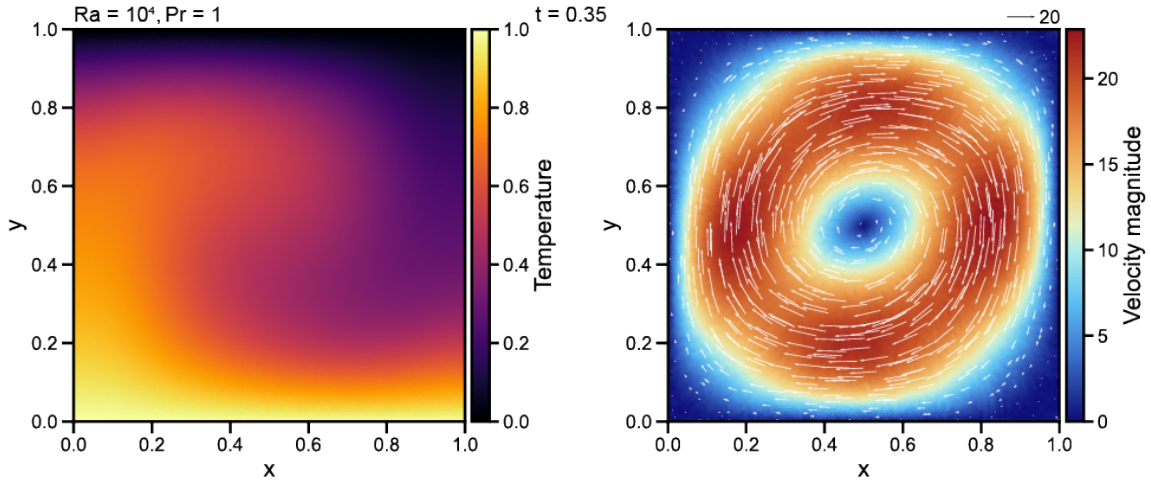


Figure: Temperature and velocity magnitude fields for Blankenbach convection at Ra = 10^4, Pr = 1, and t = 0.35.

The Role of Geophysical Constraints in Assessing of Europa's Interior

Terézia Košíková*[1] and Marie Běhounková[1]

[1]Department of Geophysics, Faculty of Mathematics and Physics, Charles University, Prague, Czech Republic
*terezia.kosikova@mff.cuni.cz

Keywords: icy moons, interior modelling, Europa

Missions Galileo and Juno significantly improved our understanding of the Jovian moons, unveiling the presence of possible subsurface oceans. Building on these discoveries, JUICE and Europa Clipper missions are expected to further constrain internal structures by delivering data, including tidal deformation and magnetic induction measurements ([1–3]).

This study focuses on characterising Europa's internal structure. We combined known material properties ([4–7]) with observational constraints to evaluate plausible structural models. Observational data includes total mass (M), surface radius (R_{surf}), moment of inertia (MOI) [8], magnetic induction amplitude at the synodic period (A_{syn}) measured by Galileo [9], the new ice shell thickness measurement (D_{Ih}) from Juno [10], and the anticipated tidal Love number k_2.

To determine the interior structures that are consistent with measured data, along with their uncertainties, we apply a statistical approach by coupling our model with the emcee sampler [11], which uses the Markov chain Monte Carlo method, which samples posterior distributions of internal structure parameters. We test several combinations of measured data and analyse how used dataset impacts statistical distribution of the parameters.

We assumed models, where Europa is either fully differentiated into the hydrosphere, mantle, and core, or a model with only the hydrosphere and a silicate-iron inner layer, to assess the structure. We analysed the internal structure for two different salts present in the ocean: $MgSO_4$ and NaCl.

We compared the resulting internal structures as additional data information was gradually incorporated. The most significant change was the variation in surface ice shell thickness among tested dataset configurations. Models that incorporated information about A_{syn} preferred very thin ice shell thicknesses, compared to other models.

We then studied resulting structures for models, where the inner layer was not fully differentiated. Our results showed that their structures preferred thicker hydrospheres, when compared with models where we had differentiated mantle and core.

We then plotted the resulting structures as functions of D_{Ih} with respect to A_{syn}, marking the regions where both the measured values of D_{Ih} and A_{syn} fall within one-sigma standard deviation range. The results for $MgSO_4$ are depicted in Figure.

Our results showed that across all plausible models, most of the resulting structures fail to satisfy the one-sigma constraints on D_{Ih} and A_{syn} simultaneously. For the models where 0-10 wt% $MgSO_4$ was present, to be consistent with both measured data, Europa must have at least a partially differentiated core and mantle. In the case of 0.2-4.2 wt% NaCl, we found only a limited number of models that fall within the one-sigma range of both measurements, with or without differentiated mantle and core, due to the higher conductivity of NaCl compared to $MgSO_4$.

This research was supported by Charles University through project No. 142125 and by the Czech Science Foundation (project No. 26-21877S).

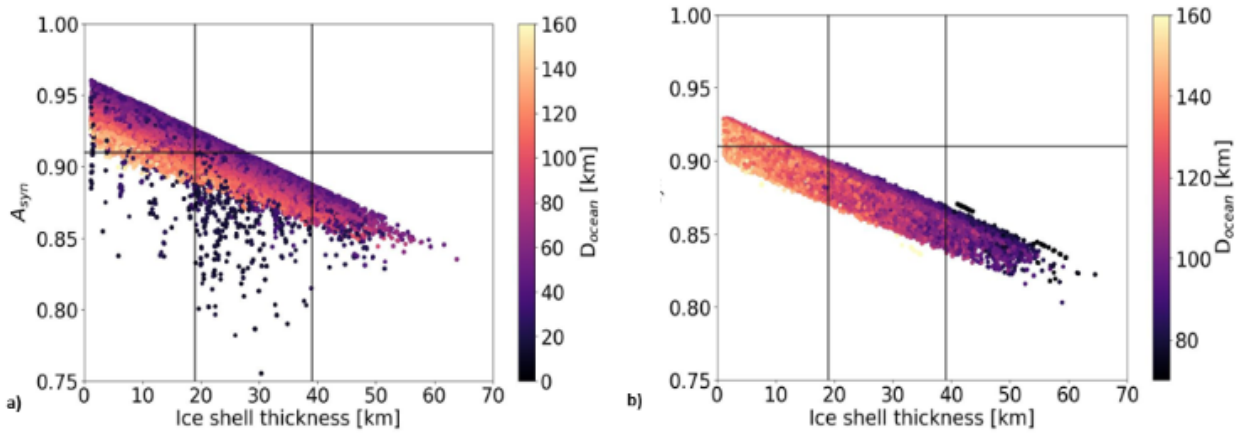


Figure: Scatter plot for amplitude of magnetic induction A_{syn}, ice shell thickness D_{ice} with ocean thickness D_{ocean} depicted in colour, for $MgSO_4$ for concentrations 0-10 wt%, for fully differentiated inner layer models (a) and models where inner layer is composed of silicate-iron mixture (b). In a vertical line, we plot one standard deviation interval for D_{ice}: ± 10 km [10]. In a horizontal line, we depict one standard deviation interval for A_{syn}:± 0.06. It is important to note that the formal uncertainty reported in [9] for A_{syn} is ± 0.02, however this value may be optimistic because it assumes that measurement errors are negligible. Therefore, we used uncertainty that is three times higher, consistent with [12].

References

[1] Cappuccio et al. (2020). https://doi.org/10.1016/j.pss.2020.104902
[2] Cappuccio et al. (2022). https://doi.org/10.3847/PSJ/ac83c4
[3] Mazarico et al. (2023). https://doi.org/10.1007/s11214-023-00972-0
[4] Vance and Brown (2013). https://doi.org/10.1016/j.gca.2013.01.040.
[5] McDougall and Barker (2011). ISBN: 978-0-646-55621-5.
[6] Pan, Yong and Secco (2020). https://doi.org/10.1029/2020GL090192
[7] Journaux et al. (2020). https://doi.org/10.1029/2019JE006176
[8] Gomez Casajus et al. (2022). https://doi.org/10.1029/2022GL099475.
[9] Schilling, Khurana and Kivelson (2004). https://doi.org/10.1029/2003JE002166
[10] Levin et al. (2026). https://doi.org/10.1038/s41550-025-02718-0
[11] Foreman-Mackey et al. (2013). https://doi.org/10.1086/670067
[12] Petricca et al. (2023). https://doi.org/10.1029/2023GL104016

Evolution of hot partially molten orogenic crust during lateral compression: Insights from coupled numerical and analogue models

Ondřej Krýza[*1,2], Petra Maierová[2,3], Prokop Závada[1,3], Vladimír Kusbach[1], Frank Zwaan[4], Karel Schulmann[3,5], and Hana Čížková[2]

[1]Institute of Geophysics, Czech Academy of Sciences, Boční II/1401, 141 31 Prague 4, Czech Republic.
[2]Department of Geophysics, Faculty of Mathematics and Physics, Charles University, V Holešovičkách 2, 180 00 Prague 8, Czech Republic.
[3]Centre for Lithospheric Research, Czech Geological Survey, Klárov 131/3, 118 00 Prague 1, Czech Republic.
[4]Helmholtz Centre Potsdam – GFZ German Research Centre for Geosciences, Section 2.5 Geodynamic Modelling, Potsdam, Germany
[5]Université de Strasbourg, EOST–IPGS, CNRS/Université de Strasbourg UMR 7516, 5 rue René Descartes, 67084 Strasbourg Cedex, France
[*]kryza@ig.cas.cz

Partially molten lower-crustal domains are key features not only of ancient large hot orogens such as the Altai tract of the CAOB or the Variscan Bohemian Massif, but also of currently active systems such as Tibet or the Altiplano–Puna, where seismic imaging reveals extensive low-velocity, high-temperature regions interpreted as crustal mush zones. They form and evolve through the combined action of crustal thickening, mantle-lithosphere removal, and thermally driven weakening. Despite their first-order role in orogenic evolution, the feedback between melt migration, deformation, and the mechanically anisotropic, layered nature of mush systems remains insufficiently understood.

We address this with a multi-method comparison combining semi-scaled thermal paraffin-wax analogue experiments with visco-plastic finite-element numerical models developed in ASPECT, which respect the laboratory scale and adopt analogue material properties; the numerical approach is then extended to orogen-scale control models tuned to natural prototypes. The setup explicitly targets crustal strength, shortening, and basal heating, and how these parameters govern internal deformation, melt coalescence, and plumbing-system architecture.

The analogue experiments reproduced melt migration and coalescence within buckled layers, suggesting that mechanically layered mush domains can localise melt along fold hinges, shear zones, and evolving permeability pathways, with potential transitions from dominantly lateral to buoyancy-driven transfer as deformation proceeds. The corresponding numerical runs successfully reproduce the development of melt-rich regions at both laboratory and orogen scales within a realistic parameter range, but do not fully capture the degree of melt coalescence seen in the analogue experiments, and the two methods differ systematically in the locus of fold initiation — backstop side in the analogue, indenter side in the numerical models. Together with the more homogeneously thickened lower crust produced numerically on orogenic scale, this points to genuinely different effective rheological coupling between deforming and partially molten layers across the two approaches, with the absence of porous melt flow in the numerics as a likely contributor.

A key emerging result is that scaling analysis places our models in a near-transition regime, where the Ramberg number, the ratio of lithostatic to viscous forces, sits close to the threshold separating buoyancy-driven doming and vertical melt extrusion from buckling-driven amplification of partially molten domains. This sensitivity is partly visible at the laboratory scale and clearly expressed at the orogen scale, where melt-rich domains either undergo strong, near-symmetric thickening that drives internal convection within the molten layer, or develop large-amplitude buckling that may trigger Rayleigh–Taylor instability of the buoyant crust. The system thus appears to occupy a regime in which small changes in viscosity, layering, or buoyancy contrast can switch the dominant style of melt transfer — offering a physical explanation for the contrasting deformation styles seen across the two modelling approaches. This motivates us to refine dynamical and thermal scaling, enable porous melt flow, and assume anisotropic permeability in future work. These preliminary results further suggest that natural orogenic systems may undergo spatio-temporal switches in the dominant melt-transfer regime, modulated by crustal chemical stratification, shortening rate, mantle and internal heat input, and the evolving position of melt-rich domains within the system.

The role of the mantle decompaction layer in Hadean volcanism

Yusuke Kubota*[1], John Rudge[2], and Bradford Foley[1]

[1]Pennsylvania State University
[2]University of Cambridge
*kubota@psu.edu

Keywords: Two-phase model, Hadean

How the very early Earth lost its internal heat remains a subject of debate. Early Earth may have been characterized by extensive magmatism due to a hot mantle, which then acted as the primary heat loss mechanism, or been more volcanically quiescent, where heat conduction through the lithosphere served as the primary heat loss mechanism. The primary mode of early Earth heat loss would then strongly influence tectonics and crust formation, the long-term thermal evolution of the interior, and surface environments where life could originate in the Hadean or Eoarchean.

Our recent crustal evolution model suggests that mantle melt production and mafic extrusive volcanism must have been limited prior to 3.6 Ga to remain consistent with Hf isotope data. We hypothesized that these geochemical constraints require a 'quiescent Earth' with a low melt production rate (< 0.6 mm/yr). However, the actual magma supply is governed by complex geodynamic factors: specifically, the mechanics of melt generation, ascent, and accumulation at the mantle-crust boundary. Understanding these physical mechanisms is critical, particularly when evaluating high-flux regimes such as heat-pipe tectonics, which may be incompatible with the low rates inferred from the geochemical record.

A critical phenomenon affecting this supply is the formation of a decompaction layer beneath the mantle-crust interface [1]. Since the crust acts as a rigid thermal boundary, temperatures drop rapidly near this interface. Consequently, ascending melt encounters a freezing horizon that acts as a permeability barrier, causing it to accumulate. Within this zone, the decompaction layer and accumulated magma generate significant melt overpressure relative to the solid matrix, driving magma into the plumbing system and initiating ascent. Therefore, characterizing the dynamics of the decompaction layer is crucial for understanding the physical controls on melt supply.

Recent numerical modeling of Io, an active heat-pipe body [2], demonstrates that crustal thermal structure is controlled by the physics of two-phase melt transport [3]. This model suggests that magma transport is driven by mantle overpressure at the decompaction layer but limited by solidification within the plumbing system. Applying this physical framework to the Hadean, we tested which mantle dynamics and temperature ranges are compatible with the restricted melt fluxes required by the geochemical record. Preliminary results demonstrate the existence of a decompaction layer, where both effective pressure and extraction rates increase significantly with porosity. By systematically exploring the parameter space, we identify the specific mantle geodynamic conditions required to align plateau melting tectonics with the Hf isotope constraints.

References

[1] Sparks D. W., & Parmentier E. M. (1991). Melt extraction from the mantle beneath spreading centers. Earth and Planetary Science Letters, 105, 368–377.
[2] O'Reilly T. C., & Davies G. F. (1981). Magma transport of heat on Io: A mechanism allowing a thick lithosphere. Geophysical Research Letters, 8, 313–316.
[3] Spencer D. C., Katz R. F., & Hewitt I. J. (2020). Magmatic intrusions control Io's crustal thickness. J. Geophys. Res. Planets, 125, e2020JE006443.

Afar Plume Transport Beneath Arabia: Towards Constraining Controls on Sublithospheric Flow

Sreenidhi Kuruvamana Satheeshbabu*[1], Bernhard Steinberger[1], and Sascha Brune[1]

[1]GFZ German Research Centre for Geosciences, Potsdam, Germany
*nidhi@gfz.de

Keywords: mantle plume, Afar plume, Afro-Arabian Rift System, Arabian Shield, plume-lithosphere interaction, ASPECT

Mantle plumes can promote continental breakup by thermally weakening the lithosphere and facilitating rifting under relatively low stresses [1-3]. In addition to vertical upwelling beneath plume centres, plume material may also propagate laterally beneath the lithosphere through sublithospheric channels over distances of hundreds to thousands of kilometres [4,5]. However, the controls governing the direction and persistence of these lateral plume channels remain poorly understood.

The Afro-Arabian Rift System provides a unique natural laboratory for investigating plume-lithosphere interaction because of its exceptional tectonic setting, rich observational constraints, and several unresolved geodynamic features. Plume melt typically propagates along thinned lithosphere confined between regions of thicker lithosphere [5,6]. However, geological and geophysical observations suggest that plume material associated with the Afar plume propagates northward beneath the relatively thick Arabian Shield rather than remaining confined to the Red Sea rift axis. Evidence for this shifted lateral plume flow includes volcanic fields within the Arabian Shield, asymmetric uplift around the southern Red Sea, seismic tomography, and lithospheric structure [7-9]. Despite increasing observational evidence, the mechanisms responsible for this anomalous plume pathway remain unresolved.

Several potential controls have been proposed for the development of the Arabian plume channel, including background mantle flow, interaction with adjacent plume systems, lithospheric thickness variations, and inherited lithospheric structures such as the Ha'il Arch. Beyond these regional elements, sublithospheric transport may be further influenced by plume geometry, inflow position, thermal anomalies, and mantle viscosity structures [10]. However, these competing mechanisms have not yet been systematically evaluated within a unified geodynamic framework.

This project aims to investigate the controls on northward lateral plume flow beneath Arabia using numerical geodynamic modelling with the finite-element code ASPECT [11,12]. Simulations will systematically test the influence of lithospheric structure, plume properties, and mantle flow conditions on sublithospheric plume transport within a regional Afro-Arabian framework. The broader objective is to evaluate whether lithospheric pressure gradients alone can redirect plume material, or whether additional forcing mechanisms—such as regional mantle flow, inherited lithospheric structures, or interaction with another plume system—are required. The modelling strategy builds directly upon established plume-flow and plume-ridge interaction studies [13,14]. Understanding these plume pathways may also provide insight into how sublithospheric plume transport influences regional lithospheric weakening and the localisation of future tectonic activity.

Preliminary, simplified 2D experiments indicate that lithospheric thickness variations exert a major control on plume-head propagation, with thicker-to-thinner lithospheric gradients promoting asymmetric lateral flow. These initial tests also suggest that plume location and interaction with nearby, higher-buoyancy plumes can significantly influence the direction and efficiency of sublithospheric transport. These idealized configurations are currently being scaled into realistic, 3D regional models.

References

[1] C. J. Ebinger and N. H. Sleep, "Cenozoic magmatism throughout East Africa resulting from impact of a single plume," Nature, vol. 395, no. 6704, pp. 788-791, 1998.
[2] A. A. P. Koppers et al., "Mantle plumes and their role in Earth processes," Nat. Rev. Earth Environ., vol. 2, no. 6, pp. 382-401, 2021.
[3] S. Brune et al., "Geodynamics of continental rift initiation and evolution," Nat. Rev. Earth Environ., vol. 4, no. 4, pp. 235-253, 2023.
[4] N. H. Sleep, "Lateral flow of hot plume material ponded at sublithospheric depths," J. Geophys. Res.: Solid Earth, vol. 101, no. B12, pp. 28065-28083, 1996.
[5] S. Leroy et al., "Recent off-axis volcanism in the eastern Gulf of Aden: Implications for plume-ridge interaction," Earth Planet. Sci. Lett., vol. 293, no. 1-2, pp. 140-153, 2010.
[6] G. Davies, "A channelled plume under Africa," Nature, vol. 395, no. 6704, pp. 745-746, 1998.
[7] A. A. Almalki et al., "Lithospheric structure and volcanic distribution in Arabia linked to Afar plume flow," Arabian Journal of Geosciences, vol. 8, no. 12, pp. 10427-10438, 2015.
[8] C. Civiero et al., "Mantle structure and evidence for lateral plume flow beneath Arabia," Geochem. Geophys.

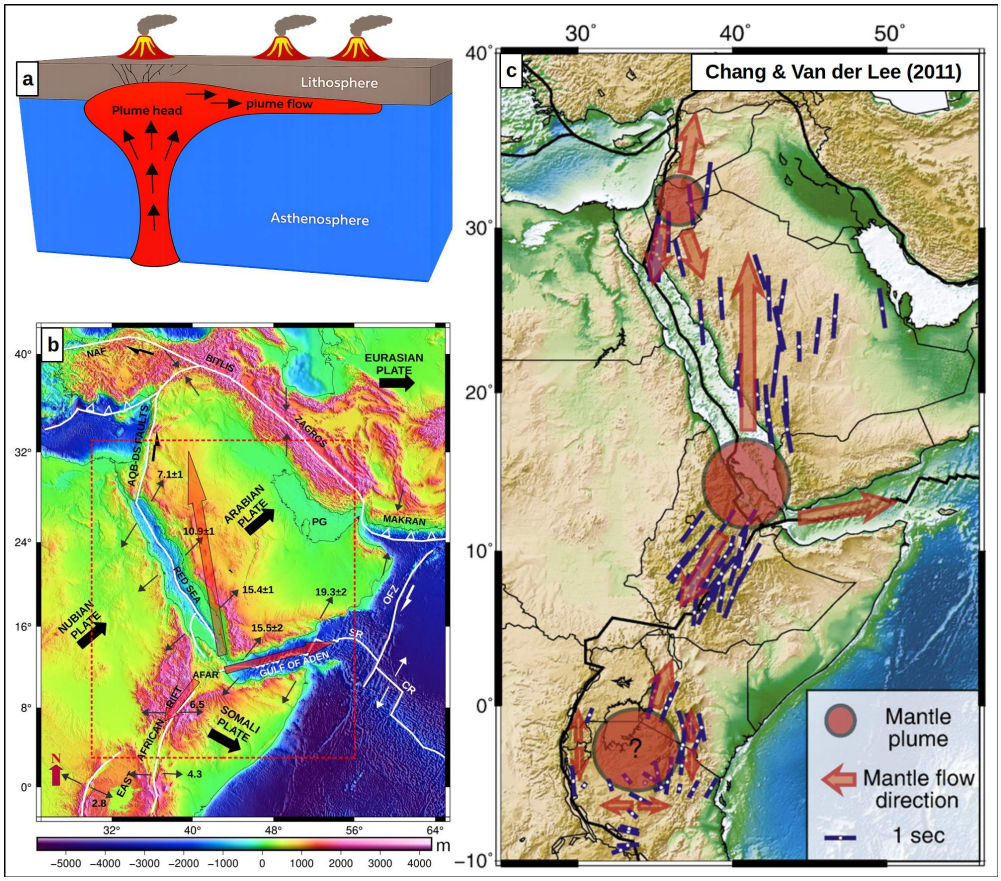


Figure: (a) Schematic illustration of sublithospheric lateral plume transport beneath the lithosphere. (b) Tectonic framework of the Afro-Arabian Rift System showing the Afar Triple Junction, Red Sea, Gulf of Aden, Main Ethiopian Rift, Arabian Shield region, and proposed lateral plume-flow pathways. (c) Inferred lateral transport of the Afar mantle plume based on seismic anisotropy and mantle-flow interpretations modified from [10].

Geosyst., vol. 24, no. 7, e2023GC010911, 2023.
[9] K. S. Sreenidhi, P. G. Betts, M. Radhakrishna, and R. Armit, "Influence of Lateral Plume Channel on the Evolution of Rift Arms of the Afar Triple Junction: Constraints From 3D Gravity Interpretation," J. Geophys. Res.: Solid Earth, vol. 128, no. 8, e2023JB026425, 2023.
[10] S.-J. Chang and S. Van der Lee, "Mantle plumes and associated flow beneath Arabia and East Africa," Earth Planet. Sci. Lett., vol. 302, no. 3-4, pp. 448-454, 2011.
[11] M. Kronbichler, T. Heister, and W. Bangerth, "High accuracy mantle convection simulation through modern numerical methods," Geophys. J. Int., vol. 191, no. 1, pp. 12-29, 2012.
[12] W. Bangerth et al., ASPECT: Advanced Solver for Problems in Earth's Convection, User Manual, 2018.
[13] R. Gassmöller et al., "Major influence of plume-ridge interaction, lithosphere thickness variations, and global mantle flow on hotspot volcanism-The example of Tristan," Geochem. Geophys. Geosyst., vol. 17, no. 4, pp. 1454-1479, 2016.
[14] E. Bredow, B. Steinberger, R. Gassmöller, and J. Dannberg, "How plume-ridge interaction shapes the crustal thickness pattern of the Réunion hotspot track," Geochem. Geophys. Geosyst., vol. 18, no. 8, pp. 2930-2948, 2017.

3D modelling of double out-dip subduction initiation in triangular oceanic basins: the role of slab bending

Laetitia Le Pourhiet[*1,2], Tiphaine Larvet[1], Manuel Pubelier[4], Nicolas Chamot-Rooke[4], and Frederic Mouthereau[5]

[1]Sorbonne Universite
[2]Institut Universitaire de France
[3]Universite Cote d'Azur, France
[4]Ecole Normale Supérieure de Paris
[5]Universite Toulouse P. Sabatier.
[*]laetitia.le_pourhiet@sorbonne-universite.fr

Keywords: subduction initiation, 3D slab folding

Small oceanic plates trapped between larger converging plates are short-lived but important for arc collision, subduction transfer and plate reconstructions. Their evolution is difficult to model because triangular oceanic domains close obliquely, producing along-strike variations in terrane accretion, slab curvature and plate-boundary localisation. We use 3D thermo-mechanical simulations with pTatin3D [1] to test the conditions for double out-dip subduction initiation during closure of a confined triangular oceanic basin.

The model includes an upper oceanic plate and a lower plate carrying a triangular oceanic domain adjacent to a buoyant terrane. One subduction zone is prescribed along one side of the oceanic domain, while the opposite terrane margin is left free to localise deformation and potentially nucleate a second subduction. The domain is 1600 km × 800 km × 670 km, with 12.5 km horizontal resolution and vertical resolution refined to 2.5 km in the crust. We compare two end-member lower-crustal rheologies for the terrane: weak continental-type crust and strong arc-type crust.

In both cases, obliquity drives diachronous terrane entry into the trench and bends the slab parallel to the terrane margin. With weak continental-type crust, the terrane accretes, builds a wide orogenic wedge and increases the trench-parallel bending moment. By conservation of bending moment [2], this strengthens the slab against the perpendicular bending required for second subduction initiation, leading to margin inversion and lithospheric delamination. With strong arc-type crust, accretion remains limited, the slab can bend across the terrane margin, and a transient double out-dip subduction system forms.

The successful double out-dip case individualises a triangular microplate and folds the inherited slab at depth, producing a transient flat-slab segment at ~150–250 km. These results show that double out-dip subduction initiation in confined basins is not controlled by geometry alone, but by the coupling between lower-crustal rheology, topographic loading and 3D slab bending.

This work was supported by supported by ANR COLLISEA

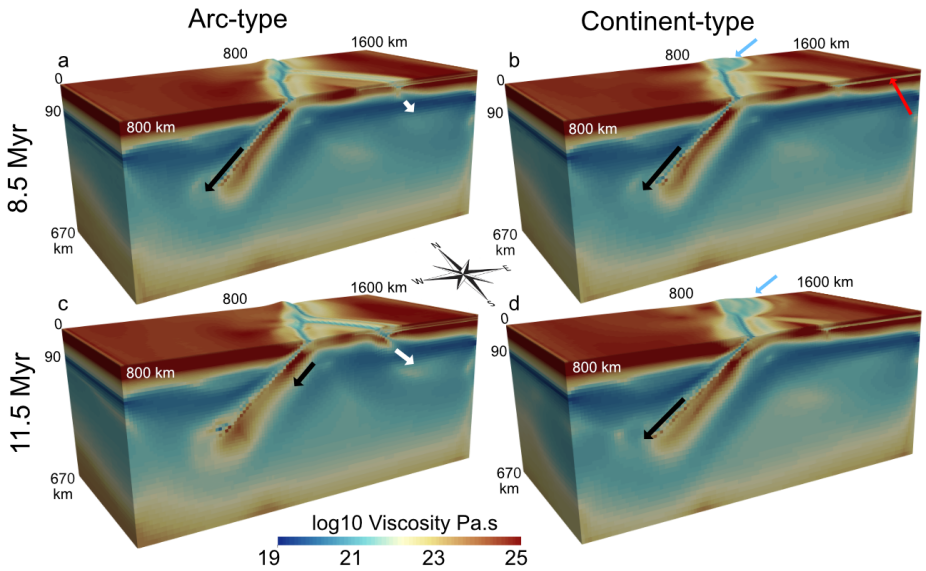


Figure: 3D pTatin3D models of triangular oceanic basin closure. Weak continental-type crust accretes and suppresses double out-dip subduction initiation, whereas strong arc-type crust permits transient double out-dip subduction, microplate formation and deep slab folding.

References

[1] May, D. A., Brown, J., & Le Pourhiet, L. (2014). pTatin3D: High-performance methods for long-term lithospheric dynamics. SC14: International Conference for High Performance Computing, Networking, Storage and Analysis, 274--284.
[2] Pini, V., Ruzzenenti, M., Dal Corso, F., Bigoni, D., & Noselli, G. (2016). How two-dimensional bending can extraordinarily stiffen thin sheets. Scientific Reports, 6, 29627.

Cracking Europa: Dilational bands formation

Laëtitia Lebec*[1], Martin Kihoulou[1], Ondřej Čadek[1], Gabriel Tobie[2], and Gaël Choblet[2]

[1]Department of Geophysics, Faculty of Mathematics and Physics, Charles University, Prague, Czech Republic
[2]CNRS, Laboratoire de Planétologie et Géosciences, UMR 6112, Nantes Université, Université d'Anger, Le Mans Université, Nantes, France
*lebec@karel.troja.mff.cuni.cz

Keywords: Europa, geophysics, dilational bands, extension, interior dynamics

Europa is characterized by a geologically young surface shaped by intense tectonic activity, including linear features such as dilational bands. Observations from the Galileo spacecraft and the Hubble Space Telescope suggest the presence of $MgSO_4$ and/or NaCl on the surface, with their association to specific geological features inferring an internal origin [1,2]. Europa undergoes long-term eccentricity variations driving cycles of global compression and extension over several tens of millions of years, likely promoting the transport of subsurface material to the surface [3–5]. Dilational bands are major tectonic features that record Europa's geological evolution. These structures extend for hundreds of kilometers and are interpreted as extensional features linked to ice shell thickening [6,7]. Bands also commonly expose subsurface material through complete surface opening [6,7]. They are classified according to brightness (dark or bright) and texture (smooth or lineated) [7]. Dark bands, the most common type, appear enriched in non-ice material (NIM) and have a lower albedo than the surrounding terrain [7]. An unresolved stratigraphic correlation between bands' brightness and age has also been inferred [6,8]. Regarding morphology, smooth bands exhibit a hummocky texture, whereas lineated bands are composed of regularly spaced ridges and faults symmetrically distributed around a central depression [6,7,9].

We explore the formation of dilational bands under various extensional tectonic regimes to evaluate the effect of key parameters on their morphology and composition. We also investigate the transport and distribution of NIM and oceanic material at the surface, and seek to explain the origin of the four main band categories based on their formation conditions.

Dilational bands formation is strongly dependent on several key parameters. In particular, high strain rates promotes a more efficient opening of the surface, while a thinner shell limits the amplitude of the topography and the strength of the lithosphere strongly affects the symmetry of the structure. Overall, tectonic extension commonly drives local upwelling within the ice shell, enhancing mass exchanges with the surface. We suggest that various types of bands were formed during distinct extensional events, explaining their brightness and texture differences. In particular, bright bands may form at an early stage of ice shell thickening when a thinner shell promotes the exposure of oceanic material within the fault zone. In contrast, dark bands may form later, when the ice shell is thicker, limiting the exposure of oceanic material and resulting in a higher fraction of NIM within the fault zone. We show that we can constrain the initial vertical profile in the ice shell from the horizontal distribution of material across the band. Finally, we are able to predict the morphology and composition of dilational bands based on the rheological and physical properties of the ice shell at the time of extension.

References

[1] Carlson, R.W. & Calvin, W.M. & Dalton, J.B. & Hansen, G.B. & Hudson, R.L. & Johnson, R.E. & McCord, T.B. & Moore, M.H. (2009). Europa's surface composition. In Europa (eds. Pappalardo, R. T., McKinnon, W. B. and Khurana, K. K.) (p. 283–327). Univ. Arizona Press.
[2] Trumbo, S. K. & Brown, M. E. & Hand, K. P. (2019). Sodium chloride on the surface of Europa. Science Advances, 5 (6), eaaw7123. doi: 10.1126/sciadv.aaw7123
[3] Hussmann, H. & Spohn, T. (2004). Thermal-orbital evolution of Io and Europa. Icarus, 171 (2), 391–410. doi: 10.1016/j.icarus.2004.05.020
[4] Rudolph, M. L. & Manga, M. & Walker, M. & Rhoden, A. R. (2022). Cooling crusts create concomitant cryovolcanic cracks. Geophysical Research Letters, 49, e2021GL094421. doi: 10.1029/2021GL094421
[5] Kihoulou, M. & Choblet, G. & Tobie, G. & Kalousová, K., & Čadek, O. (2025). Subduction-like process in Europa's ice shell triggered by enhanced eccentricity periods. Science Advances, 11 (23). doi: 10.1126/sciadv.adq8719
[6] Prockter, L. M. & Head, J. W. & Pappalardo, R. T. & Sullivan, R. J. & Clifton, A. E. & Giese, B. & Wagner, R. & Neukum, G. (2002). Morphology of Europan bands at high resolution: A mid-ocean ridge-type rift mechanism. Journal of Geophysical Research: Planets, 107 (E5). doi: 10.1029/2000JE001458
[7] Prockter, L., & Patterson, G. (2009). Morphology and evolution of Europa's ridges and bands. In Europa (eds. Pappalardo, R. T., McKinnon, W. B. and Khurana, K. K.) (pp. 237–258). Univ. Arizona Press.
[8] Nimmo, F. & Pappalardo, R. & Giese, B. (2003). On the origins of band topography, Europa. Icarus, 166 (1), 21–32. doi: 10.1016/j.icarus.2003.08.002
[9] Tufts, B. (2000). Lithospheric dilation on Europa. Icarus, 146 (1), 75–97. doi: 10.1006/icar.2000.6369

Estimation of Gravity Field Parameters by thermal evolution modelling of Uranus's icy satellites

Artem Lebedev[*1,2,3], Giuseppe Mitri[2,3], Camilla Cioria[2,3], and Anastasia Consorzi[2,3]

[1]Department of Physics, University of Trento, Trento, Italy
[2]Department of Engineering and Geology, G. d'Annunzio University of Chieti–Pescara, Italy
[3]International Research School of Planetary Sciences
[*]artem.lebedev@unitn.it

Keywords: thermal evolution modeling, gravity studies, icy satellites

Uranus's largest five satellites, Miranda, Ariel, Umbriel, Titania and Oberon, are covered by thick ice shells that surround their rocky interiors. In preparation for potential future space missions such as the Uranus Orbiter and Probe (UOP), it is important to determine the gravitational parameters of the satellites, computed from the internal structure. Different evolutionary scenarios show the possibilities of ocean formation and deep interior dehydration caused by internal radiogenic heating described in previous studies [1]. In our work, to better constrain the satellites' gravity parameters, we present a thermal model coupled with mineral assemblage evolution, focusing on the dehydration of the deep interior.

We develop one dimensional radial evolutionary model solving heat diffusion equation from satellite formation time to present days. Assuming local thermodynamic equilibrium at the evolving pressure-temperature conditions, we estimate mineral assemblages and physical properties of rocky layers using PerpleX [2] as described in [3]. Orgueil (CI) was selected for the mineral assemblages precursor material. Radiogenic heating is computed for the rocky layers from estimated isotope parameters, while tidal heating is applied to ice shell layers and calculated from the tidal Love number k_2 using the ALMA3 code [4].

Figure presents the model results for the largest Uranus' satellite, Titania. Panel A shows the time evolution of the thermal profile, while panel B illustrates the corresponding density profile. We use white lines to separate ocean, ice shell, and rock interior. Thermal evolution results show a peak in maximum temperature within satellite body at 1.7 Ga of about 950 K. From the density profile we can observe a permanent dehydration of the deep interior starting at about 0.7 Ga inducing an increase of density of innermost layers (within 250 km from the center).

By running Monte Carlo simulations we propagate the uncertainties of input parameters and obtain an ensemble of models to estimate the gravity parameter values and their uncertainties. We found that Titania and Oberon are likely to still possess subsurface oceans, and also exhibit the largest interior dehydration among other satellites.

Acknowledgements

A.L., G.M., C.C. and A.C. acknowledge support from the Italian Space Agency (2024-5-HH.0). This abstract was produced while A.L. (CUP E66E24000200005) was attending the PhD program in PhD in Space Science and Technology at the University of Trento, Cycle XL, with the support of a scholarship financed by the Ministerial Decree no. 629 of 24th April 2024, based on the NRRP - funded by the European Union - NextGenerationEU - Mission 4 "Education and Research", Component 1 "Enhancement of the offer of educational services: from nurseries to universities" - In-vestment 4.1 "Extension of the number of research doctorates and innovative doctorates for public administration and cultural heritage"

References

[1] Castillo-Rogez J. et al. (2023) J.G.R. Planets, 128(1)
[2] Connolly, J. A. D. (1990). Am. J. Sc., 290(6), 666-718.
[3] Cioria C. and Mitri G. (2022) Icarus, 388.
[4] Melini, D., Saliby, C. and Spada, G. (2022) Geophysical Journal International.

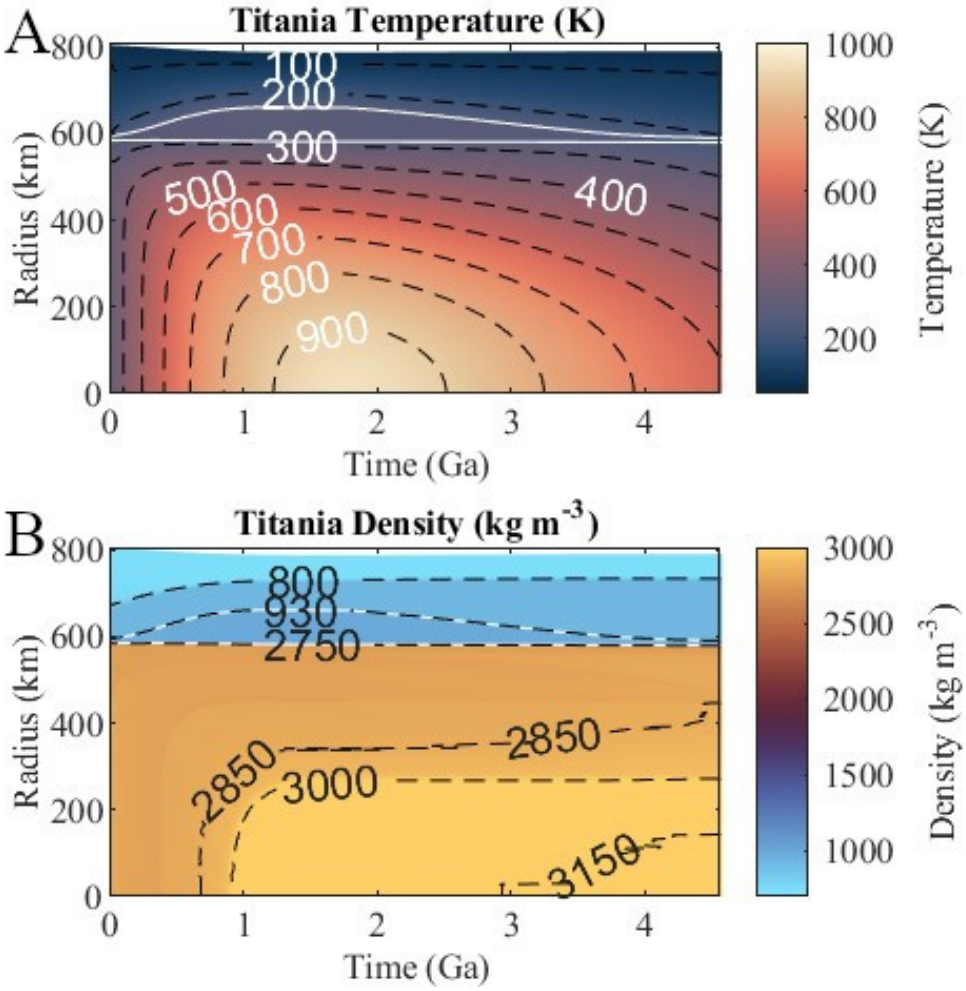


Figure: Titania thermal evolution model results. Panel A shows the temperature profile over time, while Panel B illustrates the evolution of the density profile. The white line marks the boundary between ice shell, subsurface ocean and rocky interior.

Effects of the balance between grain-size reduction and growth on lithosphere–basin evolution and mantle upwelling during continental rifting

Jieun Chang*[1], Minseok Jang[1], and Byung-Dal So[1,2]

[1]Interdisciplinary Program in Earth Environmental System Science & Engineering, Kangwon National University, Republic of Korea
[2]Department of Geophysics, Kangwon National University, Republic of Korea
*bdso@kangwon.ac.kr

Rifting accompanied by lithospheric thinning and mantle upwelling forms structural pathways for deep-sourced fluid migration and rock–fluid interaction. Rift-fault and shear-zone geometries regulate structural pathways favorable for geological resource formation in rift basins. Previous studies identified grain-size evolution associated with grain-size-dependent diffusion creep as a microstructural mechanism for lithospheric weakening, strain localization, and shear-zone development. However, the balance between grain-size reduction and grain growth in controlling mantle upwelling, shear-zone development, and basin formation during rifting remains poorly constrained. Quantifying the reduction–growth balance can connect microstructural evolution with rift-scale architecture and resource-favorable structures.

We performed 2D thermo-mechanical rifting simulations using ASPECT, varying λ (work partitioning factor) and K_g (grain growth rate constant). Larger λ enhanced grain-size reduction and the contribution of diffusion creep in the upper mantle, advancing the onset of mantle upwelling and promoting lithospheric thinning. Larger K_g suppressed sustained shear-zone development and reduced mantle upwelling velocity. The λ- and K_g-dependent variations in mantle upwelling and shear-zone development modified basin geometry and sediment-thickness distribution in the rift center.

The reduction–growth balance couples grain-size evolution with lithospheric deformation and basin–sediment structure during rifting. Grain-size-evolution models provide a rheological basis for interpreting observable rift structures, including basin geometry, sediment distribution, and pathways favorable for natural resource formation.

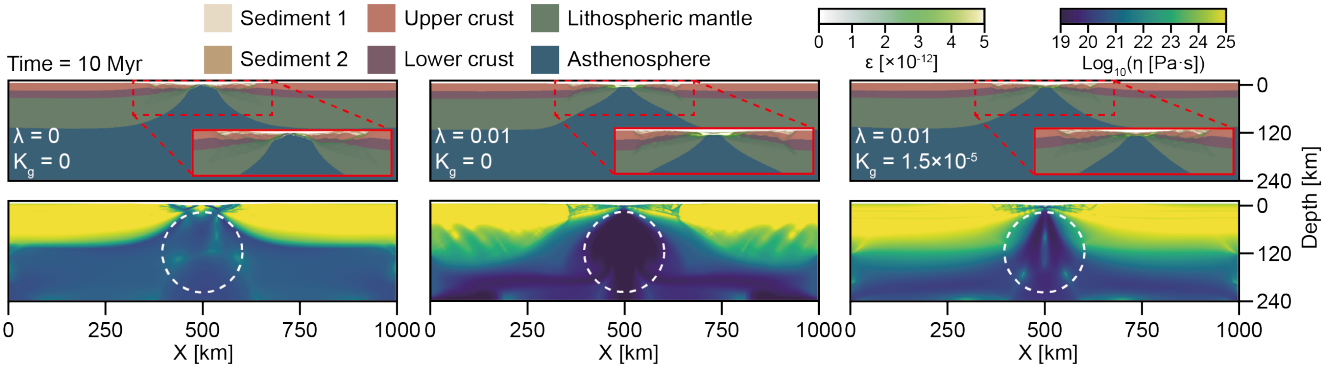


Figure: Model evolution for three grain-size treatments: no grain-size evolution, grain-size reduction only, and coupled grain-size reduction–growth. The upper row shows material composition with strain overlain as a transparent field, where near-zero strain is shown with higher transparency. The lower row shows the logarithm of viscosity. Grain-size reduction enhances focused mantle upwelling along the rift axis, whereas grain growth counteracts the reduction-driven weakening.

The Effect of Multiple Impact Scenarios on the Thermo-Hydrodynamic Evolutionary Path and Core Formation Timing in Terrestrial Planets

Kyeong-Min Lee*[1], Hyo-Im Kim[2], Deok-Kyu Jang[1], and Byung-Dal So[1]

[1]Kangwon National University, Chuncheon, Republic of Korea
[2]Gyeongsang National University, Jinju, Republic of Korea
*kyeong_min@kangwon.ac.kr

Keywords: planetary differentiation, core formation, multiple impacts

Impact heating from planetary collisions partially melts the interior of proto-terrestrial planets, producing a multiphase system in which metal and silicate coexist. With a lower melting point and higher density than silicate, metal segregates as a liquid phase from the solid silicate-metal mixture shortly after heating. The segregated liquid metal then descends toward the planetary center to form the core. Realistically constraining the core-formation timescale is essential for understanding the early evolution of planets and for reproducing the mantle abundances of siderophile elements. However, previous numerical studies of planetary differentiation have often treated impacts merely as an initial heat source, and quantitative assessments of how the spatial distribution of the heat source-dictated by the impact configuration-affects the differentiation timescale remain scarce. In the present study, we employ a multiphase flow model to directly compare the thermo-hydrodynamic evolution paths of single-impactor (one giant impact) and multi-impact (multiple smaller impacts) scenarios under an identical total melt area. In the single giant-impact case, a single metallic diapir forms. Although the diapir descends rapidly, the descent drives a large-scale overturn of the overlying silicate layer that delays the completion of global metal-silicate separation. In contrast, under the multi-impact scenario the melt regions are spatially distributed, so that multiple small diapirs sink independently and suppress large-scale mixing. Consequently, despite the slower descent of each individual diapir, planetary-scale differentiation is completed earlier in the multi-impact case. The results indicate that the impact configuration must be explicitly considered when investigating the early evolution of terrestrial planets.

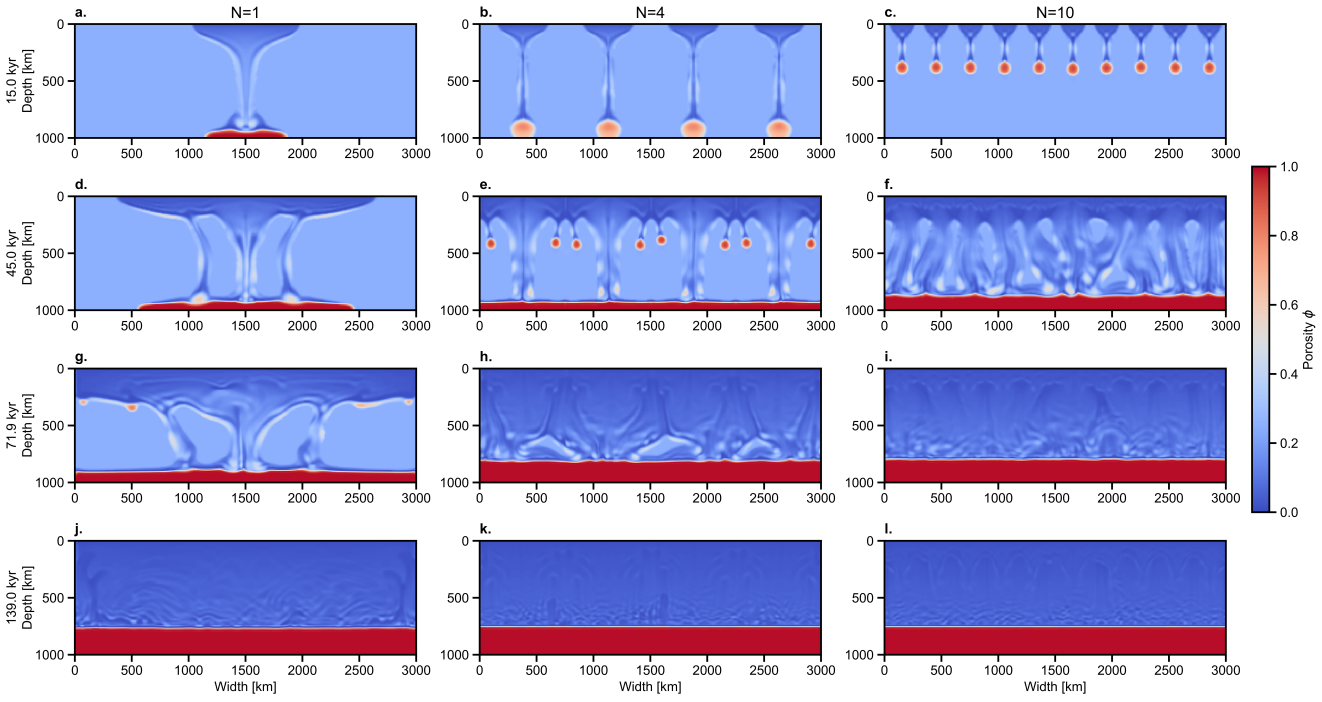


Figure: Comparison of core-formation evolution between the single-and multi-impactor scenarios.

Subduction dynamics in colloidal suspension convection experiments

Victor Lherm*[1], Hugo Remise-Charlot[1], and Anne Davaille[1]

[1]Université Paris-Saclay, CNRS, FAST, 91405, Orsay, France
*victor.lherm@cnrs.fr

Convection controls heat and mass transfers in the mantle, shaping the thermal, compositional, and magnetic evolution of terrestrial planets, as well as their surface geomorphology. Convective patterns critically depend on a temperature-dependent heterogeneous mantle rheology, which leads to complex asymmetric convective dynamics, with a relatively viscous lithosphere acting as an upper boundary layer. This produces a rich diversity of planetary convection regimes, from the Earth's present-day plate tectonics to the stagnant lids of Mercury, Mars, and the Moon. In this context, we aim to better constrain the interplay between mantle rheology, convective dynamics, and surface geomorphology, providing in particular new insights into uncertain convective regimes such as those of the early Earth and Venus.

In this context, we focus on the dynamics of subducting plates using an analogous laboratory convection experiment. We use aqueous colloidal suspensions of silica nanoparticles, named Ludox, which exhibit a wide range of rheological properties, including viscous, elastic, plastic, and brittle behaviors, depending mainly on their water content. Its tunable rheology, rheological transitions, and two-phase nature makes Ludox a powerful analogue system to model planetary interiors. The water content serves as a proxy for temperature in silicate mantles. Convection in Ludox successfully reproduces mesoscale features of mantle convection such as one-sided subduction, and captures the long-term planetary evolution from a vigorously convective magma ocean to solid-state mantle convection.

Here, we investigate subduction-like events by heating colloidal suspensions from below in a quasi-2D tank, while simultaneously allowing the surface to dry through evaporation. We analyze the formation, deformation, and eventual sinking of dense, silica-rich surface layers using a combination of visible and infrared imaging acquired from the side and the top of the tank. We also examine convective patterns using synthetic schlieren to visualize thermocompositional heterogeneities and use optical flow velocimetry to quantify the associated velocity field. By varying temperature gradients, evaporation rates, initial water content, and colloidal suspension type, we identify various kinematic pathways governing the formation and destabilization of stagnant lids, which in turn control the onset and dynamics of subduction-like events. These observations provide new insights on the conditions under which transitions from stagnant lid convection to plate tectonics and asymmetric subduction may occur in planetary mantles.

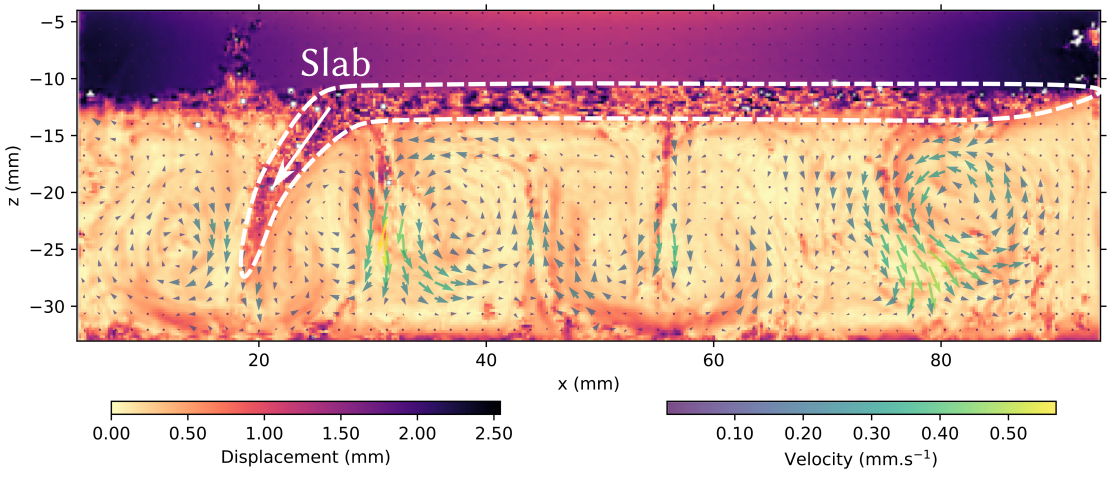


Figure: Side view of a convection experiment during a subduction-like event, with a one-sided subducting slab. The colormap shows the optical displacement field resulting from variations in the refractive index induced by thermocompositional heterogeneities, obtained using synthetic schlieren imaging, and highlights buoyant structures within the flow. The vector field shows the velocity field derived from optical flow velocimetry, capturing the dynamics of convection cells.

Contrasting slab decarbonation patterns control deep carbon cycling efficiency in hot vs. cold subduction zones

Zhong-Hai Li*[1], Hengrui Zhang[1], and Yang Wang[1]

[1]College of Earth and Planetary Sciences, University of Chinese Academy of Sciences, Beijing , China.
*li.zhonghai@ucas.ac.cn

Keywords: deep carbon cycling, decarbonation mechanisms, thermo-petrological modeling

Subducting slabs play a crucial role in deep Earth carbon cycling[1, 2], yet the carbon-cycling efficiency of different subduction zones remains debated [3, 4]. Here, we systematically compare decarbonation characteristics in the extremely cold Tonga and hot Colombia subduction zones using observation-constrained thermo-petrological modeling, integrated with volcanic degassing and arc geochemistry. Two contrasting slab decarbonation patterns are identified: efficient "focused" decarbonation in hot subduction zones versus sluggish "diffuse" decarbonation in cold subduction zones. Hot Colombia exhibits a high decarbonation efficiency >15%, dominated by metamorphic carbon release within a narrow depth range of ~75–115 km and supplemented by partial melting-induced decarbonation. In contrast, cold Tonga shows a much lower decarbonation efficiency of ~1% by dissolution-dominant carbon removal over a broad depth range of ~75–310 km. These surprisingly contrasting decarbonation patterns play critical roles in deep carbon cycling and arc degassing in both present-day and ancient subduction-zone systems, and could further control variations of the global carbon cycle and climate evolution.

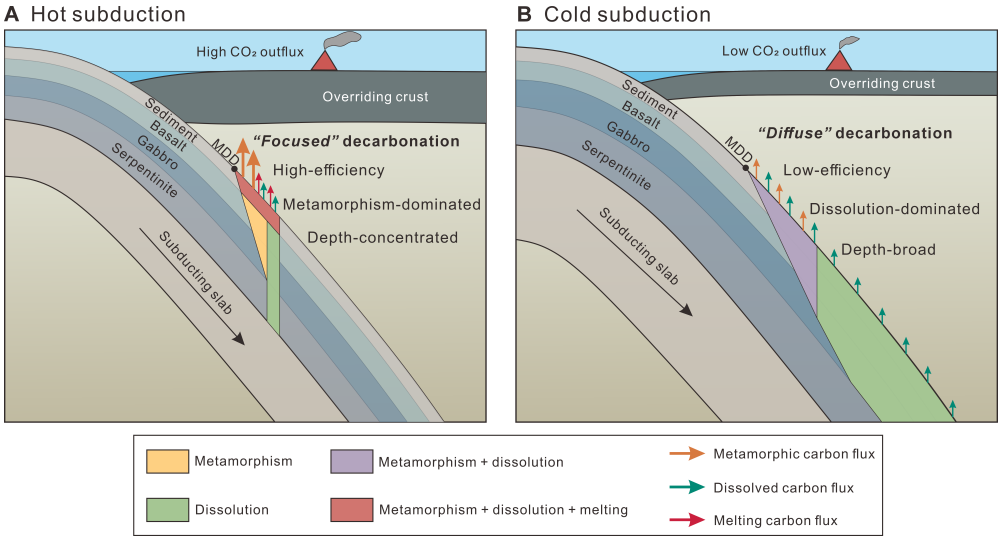


Figure: Contrasting decarbonation characteristics in hot versus cold subduction zones. (A) Efficient "focused" decarbonation in hot subduction zone and (B) sluggish "diffuse" decarbonation in cold subduction zone. Colored areas represent the decarbonation regions via different mechanisms. Colored arrows represent CO2 outfluxes via different mechanisms, with arrow size representing the flux magnitude.

References

[1] Plank, T., & Manning, C. E. (2019). Subducting carbon. Nature, 574, 343–352.
[2] Stewart, E. M., Ague, J. J., Ferry, J. M., Schiffries, C. M., Tao, R.-B., Isson, T. T., & Planavsky, N. J. (2019). Carbonation and decarbonation reactions: Implications for planetary habitability. American Mineralogist, 104, 1369–1380.
[3] Zhong, X., & Galvez, M. E. (2022). The subducting slab as a chromatographic column: Regimes of sub-solidus mass transport as a function of lithospheric hydration state, with special reference to the fate of carbonate. Journal of Geophysical Research: Solid Earth, 127, e2021JB023851.
[4] Arzilli, F., Burton, M., La Spina, G., Macpherson, C. G., Van Keken, P. E., & McCann, J. (2023). Decarbonation of subducting carbonate-bearing sediments and basalts of altered oceanic crust: Insights into recycling of CO2 through volcanic arcs. Earth and Planetary Science Letters, 602, 117945.

Modeling Thermodynamically Consistent Phase Transitions in a Heterogeneous Mantle: A Multi-Component Entropy Method

Ranpeng Li*[1], Juliane Dannberg[1], Rene Gassmöller[1], and Robert Myhill[2]

[1]GEOMAR Helmholtz Centre for Ocean Research Kiel
[2]University of Bristol
*rli@geomar.de

Keywords: numerical method, phase transition, mantle convection, entropy

Accurately incorporating realistic phase transitions in geodynamic models is crucial but challenging. Phase transitions strongly influence mantle convection, as their effects on buoyancy can hinder or accelerate slabs and plumes. In a heterogeneous mantle, different mineral assemblages undergo phase transitions at different depths, leading to lateral buoyancy variations that can cause specific compositions to stagnate or accumulate within characteristic depth ranges. However, complex phase relations, abrupt changes in material properties, and the release or absorption of latent heat pose significant challenges for modeling phase transitions. Dannberg et al. (2022) addressed these challenges by solving the energy equation in terms of entropy rather than temperature, allowing it to capture realistic phase changes in geodynamic models. However, this method was limited to chemically homogeneous systems.

Building on our earlier work, we now present a new multi-component formulation that extends the entropy method to systems with compositional heterogeneities (Li et al., 2026, in review). Our formulation assumes thermal equilibrium below the scales resolved by our mesh, i.e., all components share a single temperature at each point represented in the model. Pressure changes during advection produce an isentropic temperature change. As different chemical components may have different isentropic temperature gradients, which would imply different temperatures for each component at the same location, our multicomponent formulation involves a thermal equilibration step. Using a series of benchmarks and test cases, we show that our implementation in the geodynamic modeling software ASPECT satisfies the conservation of total energy and captures phase transitions self-consistently, regardless of their sharpness, during advection of chemical heterogeneities.

We show the applicability of our new formulation in a series of global convection models. We compare: (1) a single-component pyrolite model, and (2) a two-component mechanical mixture of basalt and harzburgite with the same pyrolitic bulk composition. Our results reveal that small differences in the ringwoodite to bridgmanite + ferropericlase transition between these assemblages with the same composition can significantly affect slab and plume stagnation. Our results highlight the importance of accurately capturing the full effects of phase transitions in a chemically heterogeneous mantle, and our approach enables new investigations into how planetary mantles evolve.

References

[1] Dannberg, J., Gassmöller, R., Li, R., Lithgow-Bertelloni, C., & Stixrude, L. (2022). An entropy method for geodynamic modelling of phase transitions: capturing sharp and broad transitions in a multiphase assemblage. Geophysical Journal International, 231(3), 1833–1849.
[2] Li, R., Dannberg, J., Gassmöller, R., and Myhill, R.: Modeling thermodynamically consistent phase transitions in multi-component assemblages: An entropy method for geodynamic models, EGUsphere [preprint], https://doi.org/10.5194/egusphere-2026-1972, 2026.

Crust–Mantle Separation at the Top of the Lower Mantle: Insights From Numerical Modeling

Xinnuo Li*[1], Zhensheng Wang[2], Junfeng Zhang[1], Jikun Feng[3,4], and Tianyu Hu[2]

[1]School of Earth and Planetary Sciences, China University of Geosciences, Wuhan, China
[2]State Key Laboratory of Geological Processes and Mineral Resources, China University of Geosciences, Wuhan, China,
[3]Laboratory of Seismology and Physics of Earth's Interior,
[4]University of Science and Technology of China,
*LXN2016@cug.edu.cn

Keywords: crust–mantle separation; mantle transition zone; geodynamic modeling; rheological weakening; slab hydration.

Previous geophysical and geochemical studies suggest the accumulation of basaltic materials near the bottom of the mantle transition zone [3, 5]. Recent seismic observations further indicate that oceanic crust may separate from the underlying slab mantle near the 660-km discontinuity, potentially contributing to weak P660P reflections, low-velocity anomalies, and seismic scatterers in the uppermost lower mantle [1, 2]. However, the physical feasibility and controlling mechanisms of this crust–mantle separation process remains debated.

Here we present two-dimensional thermo-mechanical geodynamic models investigating the roles of rheological weakening, plate age, and the Clapeyron slope of the ringwoodite–bridgmanite transition in controlling crust–mantle decoupling during deep slab subduction. Our models incorporate realistic density crossovers between eclogitic crust and surrounding mantle materials near 660–720 km depth, together with viscosity variations associated with hydration and weakening within the slab and surrounding mantle.

The results show that density inversion alone is generally insufficient to produce large-scale crust–mantle separation. Instead, strong rheological weakening is required to mechanically decouple the oceanic crust from the downgoing slab. In particular, two weak zones play critical roles: (1) a hydrated slab mantle layer and (2) a low-viscosity "lower mantle wedge" formed above the penetrating slab tip [4]. When both regions are strongly weakened, the eclogitic crust peels off from the slab and accumulates near the top of the lower mantle, whereas stronger mantle viscosities suppress separation and maintain slab coherence.

By linking numerical modeling with seismic observations, our study suggests that crust–mantle separation may provide a viable mechanism for generating weak P660P phases and localized low-velocity anomalies observed beneath subduction zones. The results further imply that deep water transport and hydration-related weakening may exert a first-order control on basalt recycling pathways and compositional heterogeneity in the mantle transition zone and uppermost lower mantle.

References

[1] Feng, J., Yao, H., Wang, Y., Poli, P., & Mao, Z. (2021). Segregated oceanic crust trapped at the bottom mantle transition zone revealed from ambient noise interferometry. Nat Commun, 12(1), 2531. https://www.ncbi.nlm.nih.gov/pubmed/33953204
[2] Kaneshima, S. (2016). Seismic scatterers in the mid-lower mantle. Physics of the Earth and Planetary Interiors, 257, 105-114.
[3] Tauzin, B., Waszek, L., Ballmer, M. D., Afonso, J. C., & Bodin, T. (2022). Basaltic reservoirs in the Earth's mantle transition zone. Proceedings of the National Academy of Sciences, 119(48).
[4] Yang, J., & Faccenda, M. (2023). On the Dynamics of Water Transportation and Magmatism in the Mid-Mantle. Journal of Geophysical Research: Solid Earth, 128(7).
[5] Yu, C. Q., Goes, S., Day, E. A., & van der Hilst, R. D. (2023). Seismic evidence for global basalt accumulation in the mantle transition zone. Science Advances, 9(22). <Go to ISI>://WOS:001009814700008

Mantle plume formation and dynamics under Central Europe

Yingying Li[*1,2], Bernhard Steinberger[1], Sascha Brune[1,3], Judith Bott[1], and Eline Le Breton[4]

[1]GFZ, Potsdam, Germany
[2]Freie Universität Berlin, Berlin, Germany
[3]Universität Potsdam, Potsdam, Germany
[4]Université de Rennes, Rennes, France
*yingying.li@gfz.de

Keywords: slab-plume interaction, plume dynamics, Central European Volcanic Province, mantle flow, intraplate volcanism

Mantle plumes have been imaged under the Massif Central and Eifel volcanic field, part of the Central European Volcanic Province (CEVP), by seismic tomography models [1,2], and are used to explain the volcanism at the surface. However, how these two plumes formed dynamically remains enigmatic. The plumes exhibit limited horizontal extents in the upper mantle [1,2] and are possibly supported by a broader root in the lower mantle [3]. Notably, both plumes are located near the tips of the slabs stagnating within the mantle transition zone (MTZ) [4]. Based on these observations, we propose that the subducted slab destabilizes the thermal boundary layer created by the lower-mantle plume stagnant at the MTZ, inducing small-scale upper mantle plumes beneath Eifel and Massif Central. To test our hypothesis, we perform 2D upper-mantle geodynamic models with a thermal boundary layer imposed at 670 km depth interacting with a subducting slab. Our models show that slabs of all geometries can destabilize the boundary layer, initiating small-scale plumes ahead of and behind the slab from the bottom of the MTZ [5]. Applying the model to our natural cases, the plumes under Eifel and Massif Central may have been triggered from the MTZ by the subducted Eurasian slab and Calabrian slab, respectively.

The CEVP also includes the volcanic field in the Vosges-Black Forest Dome (VBF), Bohemian Massif (BM) as well as the Pannonian Basin (PB) despite its back-arc setting. However, plume-like upwellings have only been imaged beneath the Eifel and Massif Central, whereas the volcanism in the other regions lacks such focused mantle upwelling [6] and merely exhibits geochemical signatures indicative of plume involvement [7,8]. Moreover, the Canary plume was also proposed to extend a "finger" to Central Europe [9], potentially contributing to the CEVP. A better understanding of plume dynamics beneath Central Europe helps to clarify the spatial relationship between mantle plumes and surface volcanism. To this end, we perform 3D upper-mantle geodynamic models to investigate how the Eifel, Massif Central and Canary plumes are advected at the bottom of the lithosphere under the influence of the mantle flow over the past 70 Myr. Present-day lithosphere thickness variations are derived from freely available tomography models and reconstructed to their past positions. Model results suggest that (1) the Canary plume propagates laterally along a sub-lithospheric corridor beneath the northwest African plate but is stopped by the thick lithosphere beneath the western Mediterranean and cannot reach Central Europe; (2) materials from the Eifel and Massif Central plumes propagate eastward and pass through VBF, BM, PB along the sub-lithospheric corridor beneath Central Europe (Figure), which indicates that the Eifel and Massif Central plumes, assisted by the background mantle flow, are capable of reaching other regions of CEVP, providing heat and material for the surface volcanism there. This also explains why only the geochemical footprint of a mantle plume can be detected in the BM and PB [7,8].

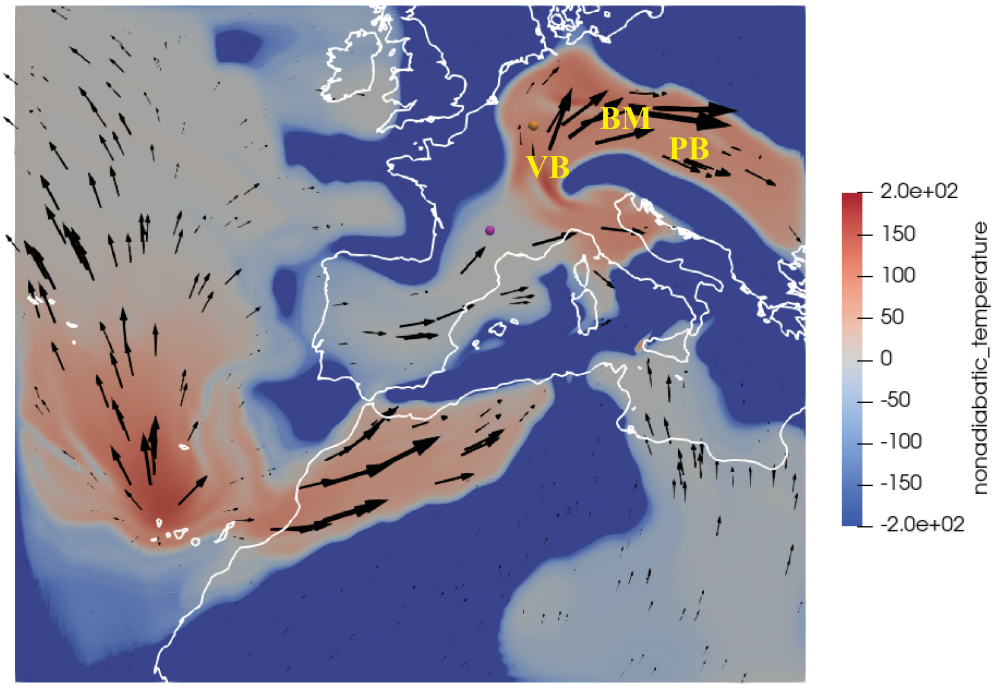


Figure: The distribution of plume materials at the end of the 3D model. Abbreviation: VBF, Vosges-Black Forest Dome; BM, Bohemian Massif; PB, Pannonian Basin.

References

[1] J. R. R. Ritter, M. Jordan, U. R. Christensen, and U. Achauer, "A mantle plume below the Eifel volcanic fields, Germany," Earth and Planetary Science Letters, vol. 186, no. 1, pp. 7–14, Mar. 2001, doi: 10.1016/S0012-821X(01)00226-6.
[2] M. Granet, M. Wilson, and U. Achauer, "Imaging a mantle plume beneath the French Massif Central," Earth and Planetary Science Letters, vol. 136, no. 3–4, pp. 281–296, Dec. 1995, doi: 10.1016/0012-821X(95)00174-B.
[3] S. Goes, W. Spakman, and H. Bijwaard, "A Lower Mantle Source for Central European Volcanism," Science, vol. 286, no. 5446, pp. 1928–1931, Dec. 1999, doi: 10.1126/science.286.5446.1928.
[4] C. Faccenna, T. W. Becker, S. Lallemand, Y. Lagabrielle, F. Funiciello, and C. Piromallo, "Subduction-triggered magmatic pulses: A new class of plumes?," Earth and Planetary Science Letters, vol. 299, no. 1–2, pp. 54–68, Oct. 2010, doi: 10.1016/j.epsl.2010.08.012.
[5] Y. Li, B. Steinberger, S. Brune, E. Le Breton, A. Glerum, and M. Pons, "Intraplate Volcanism Driven by Slab-Plume Interaction: Numerical Modeling and Its Application to the Eifel, Massif Central and Hainan Volcanic Areas," Journal of Geophysical Research: Solid Earth, vol. 131, no. 1, p. e2025JB032799, 2026, doi: 10.1029/2025JB032799.
[6] J. Plomerová, H. Munzarová, L. Vecsey, E. Kissling, U. Achauer, and V. Babuška, "Cenozoic volcanism in the Bohemian Massif in the context of P- and S-velocity high-resolution teleseismic tomography of the upper mantle," Geochemistry, Geophysics, Geosystems, vol. 17, no. 8, pp. 3326–3349, 2016, doi: 10.1002/2016GC006318.
[7] K. Bräuer, H. Kämpf, S. Niedermann, and G. Strauch, "Indications for the existence of different magmatic reservoirs beneath the Eifel area (Germany): A multi-isotope (C, N, He, Ne, Ar) approach," Chemical Geology, vol. 356, pp. 193–208, Oct. 2013, doi: 10.1016/j.chemgeo.2013.08.013.
[8] A. Buikin et al., "Noble gas isotopes suggest deep mantle plume source of late Cenozoic mafic alkaline volcanism in Europe," Earth and Planetary Science Letters, vol. 230, no. 1–2, pp. 143–162, Jan. 2005, doi: 10.1016/j.epsl.2004.11.001.
[9] L. Jolivet et al., "Continental rifts and mantle convection," Earth-Science Reviews, vol. 270, p. 105243, Nov. 2025, doi: 10.1016/j.earscirev.2025.105243.

From Slab Dynamics to Seismicity: A Global Perspective

Yida Li*[1] and Neil Ribe[1]

[1]CNRS/Universite-Paris-Saclay
*yida.li@universite-paris-saclay.fr

Keywords: geodynamics, earthquakes, focal mechanism, ASPECT

Subduction zones host the majority of global earthquakes, including shallow megathrust events, outer-rise earthquakes, and deep intraplate seismicity within subducting slabs. Although subduction-zone earthquakes are concentrated along narrow plate-boundary belts in map view, their three-dimensional distributions and focal mechanisms reveal much more complex, case-dependent patterns. A key question is whether long-term slab deformation can provide a geodynamic framework for explaining where, why, and how earthquakes occur in subduction zones.

Here we develop realistic three-dimensional spherical geodynamic models with ASPECT for subduction zones worldwide, constrained by a range of geophysical observations, including slab geometry, plate reconstructions, and global geodynamic models. By comparing model-predicted slab deformation and stress states with global earthquake catalogs and focal mechanisms, we investigate how long-term slab dynamics controls both the spatial distribution and deformation style of subduction-zone earthquakes.

The models reproduce the first-order distribution of seismicity within subducting slabs: earthquakes occur predominantly within the cold slab core, broadly bounded by T<900°C, and zones of strong long-term deformation systematically coincide with active seismicity. In addition, the modeled stress states reproduce several major classes of observed focal mechanisms, including shallow megathrust and outer-rise events, earthquakes associated with shallow slab bending, and deep intraslab events linked to large-scale slab deformation. However, intermediate-depth earthquakes are poorly reproduced and show large misfits.

These results suggest that large-scale slab dynamics exert a first-order control on where, why, and how subduction-zone earthquakes occur, providing a global geodynamic perspective on the link between long-term deformation and seismicity.

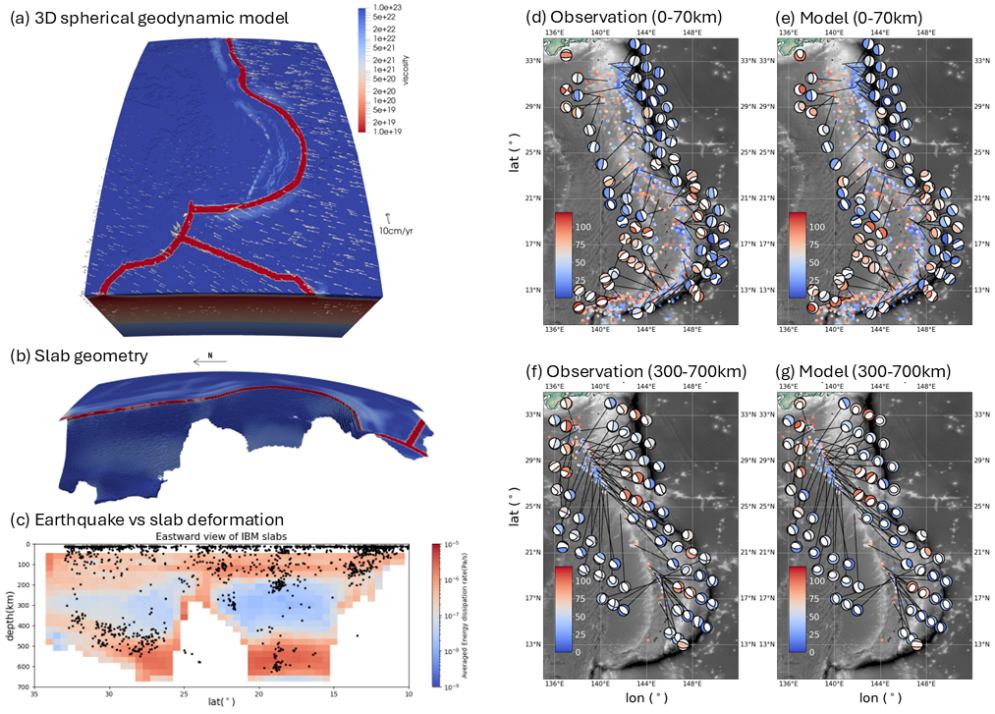


Figure: Izu-Bonin-Mariana model linking slab long-term deformation with seismicity and earthquake focal mechanisms. [1] (a-c) 3D spherical geodynamic model domain, slab geometry, and the correlation between slab energy disspation rate and seismicity distribution. (d-g) Observed vs. modeled earthquake focal mechanisms for shallow (0-70km) and deep (300-700km) events. Colors represent the misfits of focal mechanisms between model and observation, quantified by Kagan angle (°). Blue: small misfit; red: large misfit.

References

[1] Li, Yida, Neil M. Ribe, and Zhe Jia. "Large-scale slab dynamics as drivers of seismicity: Modeling earthquakes

in the izu-bonin-mariana subduction zones." Earth and Planetary Science Letters 679 (2026): 119878.

Geodynamic models of the Hellenic slab: implications for seismicity and stress

Mohit Lohani*[1], Hana Čížková[1], Craig R. Bina[2], Vojtěch Patočka[1], and Paul J. Tackley[3]

[1]Department of Geophysics, Faculty of Mathematics and Physics, Charles University, Prague, Czech Republic
[2]Department of Earth and Planetary Sciences, Northwestern University, Evanston, IL, USA
[3]Institute of Geophysics, Department of Earth and Planetary Sciences, ETH Zurich, Switzerland
*mohit.lohani@matfyz.cuni.cz

The Hellenic subduction zone is characterized by slow convergence (~2 cm/yr), trench rollback (~1–3 cm/yr), and a slab that extends into the lower mantle to depths of ~1200 km, while seismicity is confined to the upper ~200 km. Seismic source analysis further indicates that the stress orientation in the slab transitions from trench-parallel compression at shallow depths to down-dip compression near ~100 km. The aim of this work is to explain such seismicity pattern and stress distribution in the slab in terms of a long-term geodynamic evolution of the Hellenic subduction.

It has been suggested that the cessation of seismicity at ~200 km depth may be attributed to the presence of dry continental material within the subducting slab below this depth. To investigate this, we used 2-D geodynamic models designed in StagYY, where the incoming African plate consists of alternating oceanic and continental stripes proposed by geological reconstructions for Early Cretaceous. Intermediate-depth seismicity is typically linked to dehydration embrittlement. Therefore, only the oceanic crustal and sub-crustal material can host intermediate depth seismicity. Our model slabs show a completely dry slab below ~200 km, precluding dehydration related seismicity at these depths in agreement with the observed cutoff in seismicity.

While 2D models can provide a first order estimate of slab hydration and related seismicity with depth, 3D models are necessary to provide insight into the inherently 3D distribution of stress. We therefore extended our analysis to 3D regional spherical models in StagYY to explore the effects of sphericity, slab heterogeneity and differential rollback due to the presence of a weak zone in the overriding plate. The models show that the trench curvature is largely controlled by spherical geometry and along-strike variations in slab rollback, where the latter is mostly responsible for the transition from along-trench compression at shallow depths to down-dip compression below ~100 km, as indicated by the seismic source models.

Impact of numerical model dimensionality on stagnant-lid convection in extreme curvatures and the influence of dynamically-varying thermal conductivity

Julian P. Lowman*[1,2], Zac Zhang[1], Pejvak Javaheri[1], Frederic Deschamps[3], and Paul J. Tackley[4]

[1]Department of Physics, University of Toronto, Canada
[2]Department of Physical and Environmental Sciences, University of Toronto Scarborough, Canada
[3]Institute of Earth Sciences, Academia Sinica, Taiwan
[4]Institute of Geophysics, Department of Earth Sciences, ETH Zurich, Switzerland
*julian.lowman@utoronto.ca

Keywords: stagnant lid, core size, dimensionality, conductivity, Arrhenius

Terrestrial bodies differ significantly in the curvature of their comprising interior layers (e.g., the mantle of Earth's moon vs. Mercury's mantle), many of which either currently, or sometime in their past, have been suspected to feature stagnant-lid convection. In this study, we investigate the effects of relative core size on the nature of stagnant-lid convection in both 2D annulus and 3D spherical shell geometries. We examine numerical models with a wide range of curvature factors (i.e., ratio of inner-to-outer bounding radii) ranging from 0.2 to 0.9, specifying an Arrhenius thermal viscosity dependence while evaluating the influence of geometry on the convective regime and stagnant lid thickness. We consider rheological parameters representative of both silicate mantles and icy shells. For calculations involving thin shells, we also model a temperature-dependent thermal conductivity to investigate a dynamic conductivity's feedback on the evolution of the convective system. Our results confirm previous speculations in the literature (e.g., [1], [2]) that 2D calculations exaggerate characteristic interior temperatures and stagnant lid thicknesses compared to their 3D counterparts. In addition, a lower surface temperature creates a thicker stagnant lid because it keeps a larger portion of the upper mantle cold and highly viscous, causing the depth where material becomes low enough in viscosity to convect, to occur deeper in the mantle. The inclusion of temperature-dependent thermal conductivity further enhances lid growth by introducing feedback that suppresses basal heat flux. The results demonstrate that both core size and variable material properties exert strong controls on stagnant-lid convection and lithospheric thickness by impacting available energy input into the system.

References

[1] Guerrero, J. M., Lowman, J. P., Deschamps, F., & Tackley, P. J. (2018). The influence of curvature on convection in a temperature-dependent viscosity fluid: Implications for the 2-D and 3-D modeling of moons. Journal of Geophysical Research: Planets, 123(7), 1863–1880.
[2] Javaheri, P., Lowman, J. P., & Tackley, P. J. (2024). Spherical geometry convection in a fluid with an Arrhenius thermal viscosity dependence: The impact of core size and surface temperature on the scaling of stagnant-lid thickness and internal temperature. Physics of the Earth and Planetary Interiors, 349, 107157.

Mantle flow acceleration drives episodic mobile-lid tectonics in Earth-like planets

Tianyang Lyu[*1], Benjun Wu[2], Zhong-Hai Li[3], Guochun Zhao[1,4], Man Hoi Lee[1,5], Fengyuan Cui[3], and Paul J. Tackley[6]

[1]NWU-HKU Joint Center of Earth and Planetary Sciences, The University of Hong Kong, Hong Kong, China
[2]School of Earth Sciences and Engineering, Nanjing University, Nanjing, China
[3]State Key Laboratory of Earth System Numerical Modeling and Application, University of Chinese Academy of Sciences, Beijing, China
[4]State Key Laboratory of Continental Dynamics, Northwest University, Xi'an, China
[5]Department of Physics, The University of Hong Kong, Hong Kong, China
[6]Institute of Geophysics, Department of Earth Sciences, ETH Zürich, Zürich, Switzerland
*tylyu@connect.hku.hk

Keywords: mantle convection, episodic mobile-lid, lithospheric yielding, convective stress, terrestrial planets

The transition between stagnant-lid and mobile-lid tectonics is central to understanding the thermal and geological evolution of Earth and other terrestrial planets. While stagnant-lid and continuous plate-tectonic regimes represent two end-member modes of planetary convection, geodynamic studies have long suggested that an intermediate episodic-lid regime may occur under certain planetary conditions [1,2]. However, the physical mechanisms that allow planets to alternate between stagnant and mobile surface states remain incompletely understood. Here we investigate the generation of episodic mobile-lid tectonics using numerical models of mantle convection with realistic rheological and yielding behavior. By systematically exploring lithospheric strength, mantle viscosity structure, and thermal conditions, we identify the parameter range in which long-lived alternations between stagnant-lid and mobile-lid states can occur. Our results show that episodic mobile-lid behavior can arise as a self-consistent tectonic regime within Earth-like planetary conditions, rather than as a short-lived or purely transient phenomenon. The models further indicate that episodic mobility is controlled by the evolving balance between mantle convective stress and lithospheric yielding strength, a mechanical framework consistent with previous approaches for diagnosing plate-like surface behavior in mantle convection models [3,4]. Mobile-lid phases occur when convective stresses become large enough to overcome lithospheric resistance, whereas stagnant-lid phases develop when the lithosphere remains too strong to yield globally. These results highlight episodic mobile-lid tectonics as a natural transitional regime between permanent stagnant-lid convection and sustained plate tectonics, providing a framework for interpreting the tectonic evolution of Earth, Venus, Mars, and rocky exoplanets.

References

[1] Moresi, L., & Solomatov, V. (1998). Mantle convection with a brittle lithosphere: thoughts on the global tectonic styles of the Earth and Venus. Geophysical Journal International, 133(3), 669–682. https://doi.org/10.1046/j.1365-246x.1998.00521.x

[2] Lyu, T., Ballmer, M. D., Li, Z.-H., Lee, M. H., Yan, J., Wu, B., & Zhao, G. (2025). Dissecting the puzzle of tectonic lid regimes in terrestrial planets. Nature Communications, 16(1), 10037. https://doi.org/10.1038/s41467-025-65943-1

[3] Tackley, P. J. (2000). Self-consistent generation of tectonic plates in time-dependent, three-dimensional mantle convection simulations. Geochemistry, Geophysics, Geosystems, 1(8). https://doi.org/10.1029/2000gc000036

[4] Lourenço, D. L., Rozel, A. B., Gerya, T., & Tackley, P. J. (2020). Efficient cooling of rocky planets by intrusive magmatism. Nature Geoscience, 13, 322–327.

Revisiting Plume-Induced Oceanic Hotspot Swells and Global Plume Buoyancy Fluxes

Ziqi Ma*[1]

[1]University College London
*ziqi.ma.21@ucl.ac.uk

Hotspot swells, the surface topographic expression of plumes, provide key constraints for understanding plume-lithosphere interaction and inform us about the buoyancy flux carried by hot mantle upwellings. Because swell height and cross-section area reflect how plume material spreads beneath moving plates, their geometry can be used to infer the dynamics and physical properties of the underlying plumes. However, previous numerical models studying plume-lithosphere interaction mostly adopt a simplified depth- and/or temperature-dependent rheology and free-slip boundary conditions, and assume that the plume moves at the same speed as the plate. These assumptions may lead to inaccurate estimates of global plume buoyancy flux.

Here, we use 3D regional geodynamic models with composite diffusion-dislocation creep rheology and a free surface to investigate plume-lithosphere interaction for intraplate oceanic hotspots. Model results show that plume material spreads laterally and forms a pancake beneath the lithosphere that is modulated by non-Newtonian rheology in the asthenosphere. In most cases, plume material spreads downstream substantially faster than plate motion, deflating the swell. This behavior indicates that plume spreading is dominated by plume-driven Poiseuille-type flow rather than plate-driven Couette-type flow.

Based on the modelled swell geometry, we derive two sets of empirical scaling laws linking surface topography to mantle plume properties. A simplified set relates swell height, width, and cross-sectional area to plume buoyancy flux and plate velocity, while a second, more comprehensive set links swell geometrical metrics to plume radius, excess temperature, and plate velocity. Applying the first scaling to observations for the Hawai'ian swell yields plume surface buoyancy fluxes well exceeding 4.2 Mg/s. The latter scaling yields either a narrower and hotter (259 km wide, potential excess temperature of 350 K) or a wider and cooler plume (389 km, 164 K), corresponding to plume surface buoyancy fluxes of $5.9 \sim 6.5$ Mg/s.

Finally, we invert these predictive fittings and apply them to intraplate hotspot swells in other ocean basins to quantify the heat and material fluxes carried by plumes on Earth. This approach provides an independent constraint on the contribution of mantle upwellings to Earth's surface heat budget and, by implication, on heat flux from the deep mantle and core-mantle boundary.

The differentiation of the growing mantle-magma ocean system: the primacy of thermodynamic properties

Antonio Manjón-Cabeza Córdoba[*1], Maxim D. Ballmer[1], and Oliver Shorttle[2]

[1]University College London, London, UK
[2]University of Cambridge, Cambridge, UK
[*]a.cordoba@ucl.ac.uk

Keywords: beginning of mantle convection, magma ocean - mantle interaction, planetary interior, planetary dynamics

The beginning of mantle convection conditions the thermo-compositional evolution of rocky planets. Due to the large size and hot temperatures of rocky terrestrial-like planets, solid-state convection begins at the magma ocean (MO) stage, when the mantle growths interacting with a MO. In a previous work [1], we argued that remelting during mantle growth under a MO could buffer the magma ocean composition, limiting the iron enrichment and the density increase, and therefore precluding the formation of a basal layer. That work, based on scaling, cannot deal with chemical heterogeity at the very beginning of convection, which requires a more complex numerical approach, and the question of whether chemical heterogeneities can coalesce to form a secondary MO remains unsolved. We present a new approximation specifically designed to model chemical heterogeneity development for a mantle under a MO. Lagrangian tracers are used to track melt composition and topography of the mantle, and the MO system and the mantle are solved as a P-T continuum to identify the melting relations, which are solved explicitly. We apply these approximations to the mantle convection code StagYY [2]. Preliminary runs show that thermodynamic properties of melts and minerals are the controlling factor of the behavior of the system. In particular, the viscosity and excess density of melts are crucial to understanding the evolution of the newly formed mantle. For low mobility melts, crystallisation happens in a ”freezing” style, which moves the Magma Ocean composition towards a low-Fe buffered scenario, resulting in a homogeneous mantle. For high mobility melts, crystallisation is close to fractional, which moves the Magma Ocean towards a differentiated dense state, resulting in stratified mantles. The potential of overturn is equally affected, if separation of melts and crystals during crystallization is not enough to differentiate the MO, excess topography of the solid mantle results in excess melting, again buffering MO enrichment with the potential to keeping this enrichment below that needed for the overturn.

References

[1] Manjón-Cabeza Córdoba, A., Ballmer, M. D., & Shorttle, O. (2026). Earth and Mars interior structures set by re-melting of the first solid mantle. Preprint uploaded to Arxiv. (To be published in ApJL) arXiv:2605.04840
[2] Tackley, P. J. (2008). Modelling compressible mantle convection with large viscosity contrasts in a three-dimensional spherical shell using the yin-yang grid. Physics of the Earth and Planetary Interiors, 171, 7-18

Variable Thermal Conductivity Induces the Formation of Low-Conductivity Zones in Mantle Convection Models

Enrico Marzotto*[1]

[1]University of Potsdam, Institute of Geoscience
*enrico.marzotto@uni-potsdam.de

Keywords: lattice, radiative, thermal conductivity, ASPECT

Thermal conductivity, Λ (W m^{-1} K^{-1}), is the physical parameter controlling heat diffusion, the dominant heat transport mechanism within thermal boundary layers and thermal anomalies in the mantle (cold descending slabs and hot ascending plumes).

In silicate minerals, diffusive heat transport is the sum of phonon and photon contributions, which are quantified by the lattice (Λ_{lat}) and radiative (Λ_{rad}) conductivities. The effects of pressure (P) and (T) on the thermal conductivity of mantle minerals were investigated by Hofmeister 1999 [1]: pressure increases Λ_{lat} by increasing phonon velocity, whereas temperature reduces Λ_{lat} by increasing phonon scattering. In contrast, Λ_{rad} increases rapidly with temperature, but decreases with increasing opacity of minerals.

Prior to Hofmeister 1999 [1], pressure and temperature dependent thermal conductivity, $\Lambda(P,T) = \Lambda_{lat} + \Lambda_{rad}$, was rarely incorporated into mantle convection models. Hofmeister's work motivated several researchers to investigate the effects of $\Lambda(P,T)$ on mantle convection (e.g., van den Berg [2]). After the initial interest in the early 2000s, however, this line of research remained marginal for almost two decades. In recent years, nonetheless, a growing number of studies have reported the dramatic effects of $\Lambda_{lat}(P,T)$ on subduction dynamics [3]. Moreover, experimental measurements suggest that Λ_{rad} may account for $\sim$40 % of total diffusive heat transport in the upper mantle [4].

The aim of this study is to quantify the effects of $\Lambda(P,T)$ on mantle convection, with a focus on enhanced Λ_{rad} in the upper mantle. For this purpose, we developed a new formulation to compute $\Lambda(P,T) = \Lambda_{lat} + \Lambda_{rad}$ for aggregate rocks based on mineral physics constraints. This formulation was implemented in the geodynamic community software ASPECT [5], which was used to run a series of mantle convection simulations. The model domain consisted of a 3000×6000 km Cartesian box, discretised into a 481×961 mesh of square cells. We employed the Boussinesq approximation and a basal-heated set-up, with isothermal top (273 K) and bottom (3773 K) boundaries. The velocity boundary conditions were free-slip on all four sides of the domain. We tested several convection setups by varying constant viscosity ($10^{24}, 10^{23}, 10^{22}, 10^{21}$ Pa s) or by imposing T-dependent viscosity. We computed three sets of models: 1) $\Lambda = 6$ W m^{-1} K^{-1}; 2) $\Lambda(P,T) = \Lambda_{lat}$; 3) $\Lambda(P,T) = \Lambda_{lat} + \Lambda_{rad}$.

Our results show that the average mantle temperature of the $\Lambda(P,T)$ models is systematically higher than those computed with constant conductivity for all tested viscosities ($\Delta T > 300$ K for 10^{22}). This large ΔT is primarily induced by the formation of low conductivity zones (LCZs) at both thermal boundary layers, which arise from the P–T-dependent formulation of Λ. Such insulating boundaries would modulate the heat extraction from the core (with implications for the geodynamo) and the mantle (slowing down secular cooling). Potentially, the upper LCZ, coupled with the high opacity of silicate melts, might promote partial melting and the formation of the sub-lithospheric low velocity zone (LVZ) layer.

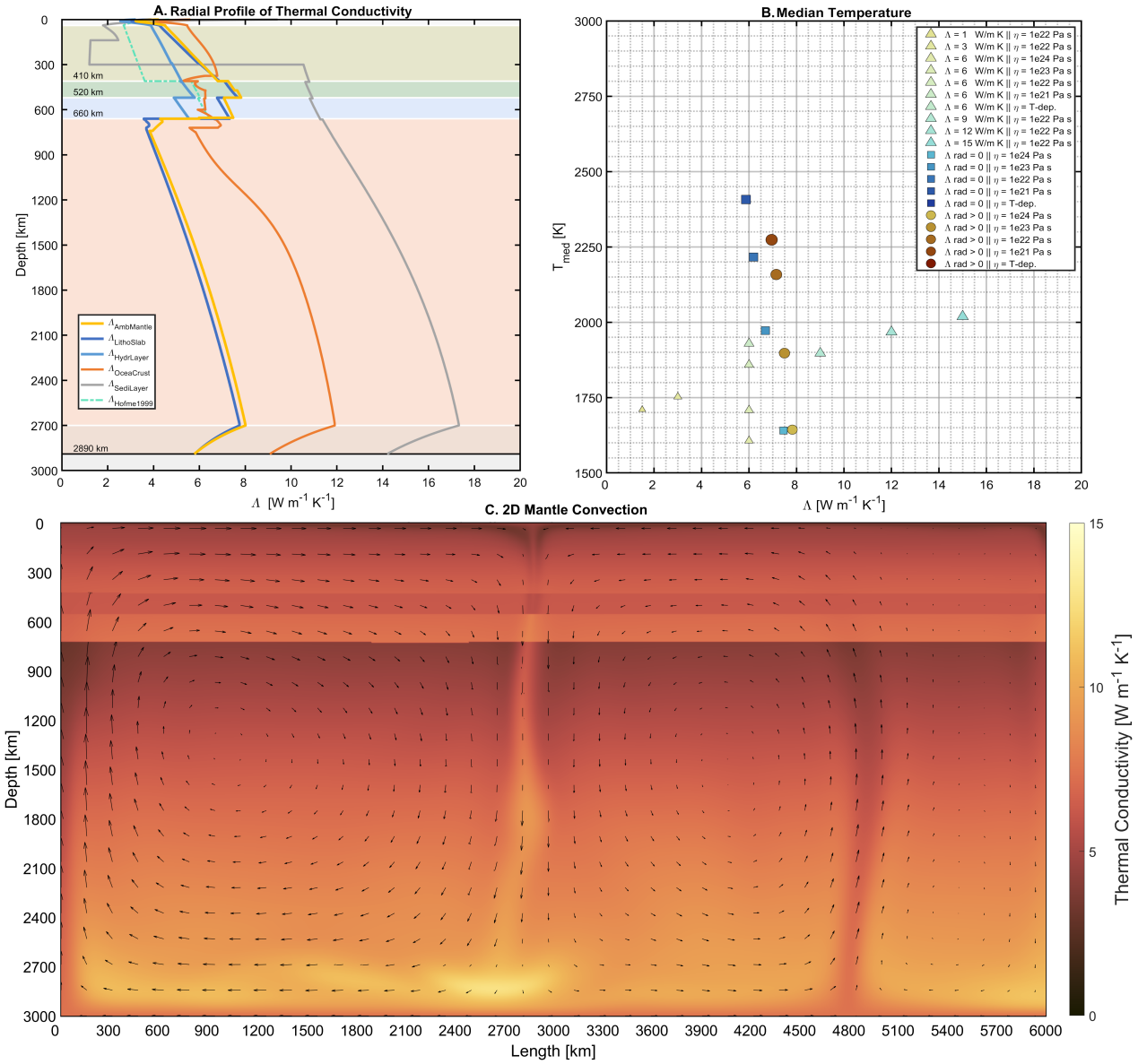


Figure: (A) Radial profile of thermal conductivity. Each profile was computed using the $\Lambda(P,T) = \Lambda_{lat} + \Lambda_{rad}$ formulation based on mineral physics constraints. Five different lithologies are reported here: ambient mantle, lithospheric slab, hydrous slab, oceanic crust, and meta-sediment layer. The Λ profile from [1] is also shown for reference. (B) Median mantle temperature. The markers represent the median temperature of the convection models, computed over 5 Gyr of thermal evolution. Yellow–green triangles represent models with constant thermal conductivity, blue squares represent Λ_{lat}-only models, and red circles represent $\Lambda_{lat} + \Lambda_{rad}$ models. (C) Mantle convection. This panel shows the thermal conductivity field extracted from a $\Lambda(P,T) = \Lambda_{lat} + \Lambda_{rad}$ convection model. Bright colours indicate regions of high Λ (e.g., cold descending slabs), whereas dim colours indicate regions of low Λ (e.g., hot ascending plumes).

References

[1] Hofmeister, A. M. (1999). Mantle values of thermal conductivity and the geotherm from phonon lifetimes. Science, 283(5408), 1699–1706 (https://doi.org/10.1126/science.283.5408.1699)

[2] Van Den Berg, A. P., Yuen, D. A., & Steinbach, V. (2001). The effects of variable thermal conductivity on mantle heat-transfer. Geophysical Research Letters, 28(5), 875–878 (https://doi.org/10.1029/2000GL011903)

[3] Tosi, N., Maierová, P. & Yuen, D. A. (2015). Influence of variable thermal expansivity and conductivity on deep subduction. Subduction Dynamics: From Mantle Flow toMega Disasters. 115–133 (https://doi.org/10.1002/9781118888865.ch6)

[4] Marzotto, E., Koptev, A., Speziale, S., Koch-Müller, M., Abdel-Hak, N., Cichy, S. B., & Lobanov, S. S. (2025). Olivine's high radiative conductivity increases slab temperature by up to 200K. Nat. Comm., 16(1), 6058. (https://doi.org/10.1038/s41467-025-61148-8)

[5] Heister, T., Dannberg, J., Gassmöller, R., & Bangerth, W. (2017). High accuracy mantle convection simulation through modern numerical methods–II: realistic models and problems. GJI, 210(2), 833–851 (https://doi.org/10.1093/gji/ggx195)

From Constant to Nonlinear: Assessing the Role of Rheology in Subduction Interface Behavior

Ana Carolina Maurício Gomes*[1], Whitney Behr[1], Derek Neuharth[2], and Adam Holt[3]

[1]Structural Geology and Tectonics Group, Department of Earth and Planetary Sciences, ETH Zurich, Switzerland
[2]GFZ Helmholtz Centre for Geosciences, Potsdam, Germany
[3]Rosenstiel School of Marine, Atmospheric, and Earth Science, University of Miami, Miami, USA
*cmauricio@erdw.ethz.ch

Keywords: Geodynamics, Subduction Interface, Rheology

Subduction zones drive global plate tectonics [1]. However, their large-scale evolution depends heavily on the narrow, highly sheared plate interface [2]. Numerical models frequently simplify this boundary as a constant-viscosity weak layer [3]. This approach ignores non-linear interactions between strain rate, temperature, and rock strength. Here, we systematically increase interface formulation complexity. By moving from fixed-viscosity to variable Newtonian and power-law rheologies, we isolate how these descriptions change both large-scale geodynamics and fine-scale subduction channel dynamics.

Building upon previous configurations [3], we run two suites of 2D ASPECT subduction models (5120 × 2048 km) [4]. The rheology suite varies oceanic crust formulations across Low-viscosity (LV) and High-viscosity (HV) series by scaling the pre-exponential factor, A, such that the strain-averaged viscosity approaches 10^{19} Pa·s and 10^{20} Pa·s, respectively. These two series act as lower and upper mechanical end-members to bound the uncertainty in subduction channel strength. We compare constant fixed viscosity against two temperature-dependent formulations: Newtonian ($n = 1$) and power-law rheologies. The weak-layer suite embeds a 500×5 km weak layer (Low-viscosity rheology) into a High-viscosity power-law rheology oceanic crust, introduced either before (pre-660) or after (post-660) the slab tip hits the 660 km discontinuity.

The **rheology** suite shows a clear scale-dependence. Large-scale features like slab dip, morphology, maximum velocity, and 660 km arrival time evolve similarly within a given viscosity series. This means bulk kinematics depend primarily on average channel viscosity. Furthermore, the close alignment between Newtonian and power-law outcomes indicates that thermal effects, rather than strain-rate dependence, cause the minor variations between these models. At the channel scale, however, rheology controls the flow. Interaction with the 660 km bottleneck induces a mass-conservative backflow. This backflow peaks at 8 cm/yr in High-viscosity Newtonian models but remains low in power-law settings. While simplified interfaces work well for broad plate kinematics, complex rheologies are required to capture channel-scale deformation and material transport.

The **weak-layer** suite demonstrates that trench entry timing dictates whether the system undergoes a kinematic or stress-based response. Early entry (pre-660 km) directly accelerates plate kinematics, increasing convergence speeds by a factor of approximately 2 to 6, depending on the chosen rheology. Conversely, late entry (post-660 km) has little effect on plate speeds but subdues the overriding plate's horizontal stress. As a direct consequence of these differing regimes, the forearc high in pre-660 km cases is only briefly submerged upon weak-layer entry before recovering, whereas the reduced stress transmission in post-660 km cases triggers a sustained submergence of the forearc high that persists until the end of the 50 Myr simulation.

In summary, our findings demonstrate how specific interface variations control geodynamic evolution across distinct physical regimes. The rheology suite indicates that broad kinematic differences are fundamentally driven by the average channel viscosity. The weak-layer suite reveals that transitioning from a high-viscosity to a low-viscosity formulation yields system-wide impacts, where the exact timing of this rheological shift dictates the duration of both kinematic and overriding plate stress effects.

References

[1] Stern, R. J. (2002). Subduction zones. Reviews of geophysics, 40(4), 3–1. doi:10.1029/2001RG000108
[2] Behr, Whitney M and Holt, Adam F and Becker, Thorsten W and Faccenna, Claudio (2022): The effects of plate interface rheology on subduction kinematics and dynamics. Geophysical Journal International, 230, 796–812. doi: 10.1093/gji/ggac075.
[3] Sandiford, Dan and Moresi, Louis (2019): Improving subduction interface implementation in dynamic numerical models. Solid Earth Sciences Library, 10(3), 969–985. doi:10.5194/se-10-969-2019.
[4] Bangerth, W., Dannberg, J., Gassmoeller, R., & Heister, T. (2020). ASPECT v2. 2.0. Zenodo. doi:10.5281/zenodo.592692.

Rheological Controls on the Plate-Mantle System: Self-Consistent vs. Kinematically Constrained Models

Marla Metternich*[1], Maëlis Arnould[2], Alexandre Janin[3], and Paul Tackley[1]

[1]Institute of Geophysics, Department of Earth and Planetary Sciences, ETH Zürich, Sonneggstrasse 5, CH-8092 Zürich
[2]Laboratoire de Géologie de Lyon, University of Lyon 1, 2 rue Raphaël Dubois, F-69622, Lyon
[3]Laboratoire de Géologie–CNRS UMR 8538, École normale supérieure–PSL University, 24 Rue Lhomond, F-75005, Paris
*marla.metternich@eaps.ethz.ch

Keywords: global mantle convection modelling, self-consistent, plate-driven, plate-like tectonics

Earth's interior processes are co-responsible for shaping the planet's surface environment, the climate system, and habitability over geological timescales. Despite its importance, the history of mantle evolution remains poorly understood because direct imaging methods only capture the present-day mantle. Plate tectonic reconstructions coupled with convection models could provide constraints on the evolution of mantle structure. In this study, we employ both fully self-consistent and plate-driven mantle convection models [1]. The mantle rheology is temperature-, pressure-, phase-, and stress-dependent, with the latter represented through pseudo-plasticity. The novelty of this work lies in employing a composite rheology with "realistic" rheological parameters [2] in a fully three-dimensional geometry and with high Rayleigh number (10^8). By using both fully self-consistent models and plate-driven models, we aim to address the discrepancies in terms of long-term convective and tectonic behaviour that arise when forcing plate velocities onto the surface. The latter is done by imposing time-dependent surface velocity boundary conditions provided by a plate tectonic reconstruction [3].

The reference model with prescribed plate velocities (Figure, right column) shows a wider range of topography than the self-consistent equivalent (Figure, left column). Prescribing velocities at the surface also means stresses are introduced, which leads to the emergence of sharp plate boundaries and a large topographic variation (−13 to +5 km), compared to the topography for self-consistent cases (−7 to +2 km, Figure c,d). However, the magnitude of surface velocity for self-consistent cases does approximate that of imposed plate velocities, or sometimes even exceeds it. Consequently, forcing velocities from a plate tectonic reconstruction can then have a decelerating effect regionally. Hence, we observe more mantle-driven drag (negative drag in Figure h) for the plate-driven cases, as opposed to predominantly surface-driven drag for self-consistent equivalents. Furthermore, plate-driven models produce a systematically thicker lithosphere relative to self-consistent models, as these portions of the oceanic lithosphere resist recycling as per the tectonic reconstruction.

To evaluate the extent to which the models reproduce plate-like tectonics, we explore several sources of constraints. Slab sinking rates are computed to compare to estimates inferred from seismic tomography [4]. Sinking rates in self-consistent models provide insight into the mantle's rheology, as they are highly sensitive to viscosity. Furthermore, a tessellation algorithm [5] is applied to the surface of the models to detect plates in the self-consistent models with plate-like behaviour. Based on these results, a plate-size frequency distribution can be calculated and compared to that of the plate-driven models. A low surface yield stress (i.e. a weak lid) generates too many small plates and underestimates the largest plate's size. On the other hand, a high yield stress may result in a stagnant lid without any active plate-like activity. So, to generate Earth-like plate tectonics, yield stress needs to be sufficiently high to reproduce realistic slab sinking rates and yield an adequate plate-size frequency distribution, but also sufficiently low to facilitate a long-term mobile lid regime.

References

[1] Tackley, P. J. (2008). Phys. Earth Planet. Inter. 171, 1–4.
[2] Tackley, P. J., Ammann, M., Brodholt, J. P., Dobson, D. P., & Valencia, D. (2013). Icarus 225, 50–61.
[3] Merdith, A. S., Williams, S. E., Collins, A. S., et al. (2021). Earth-Sci. Rev. 214, 103477.
[4] Van der Meer, D. G., van Hinsbergen, D. J. J., & Spakman, W. (2018). Tectonophysics 723, 309–448.
[5] Janin, A., Coltice, N., Chamot-Rooke, N., & Tierny, J. (2025). Nat. Geosci. 18, 1041–1047.
[6] Coltice, N., Husson, L., Faccenna, C., & Arnould, M. (2019). What drives tectonic plates? Science Advances, 5(10), https://www.doi.org/10.1126/sciadv.aax4295.

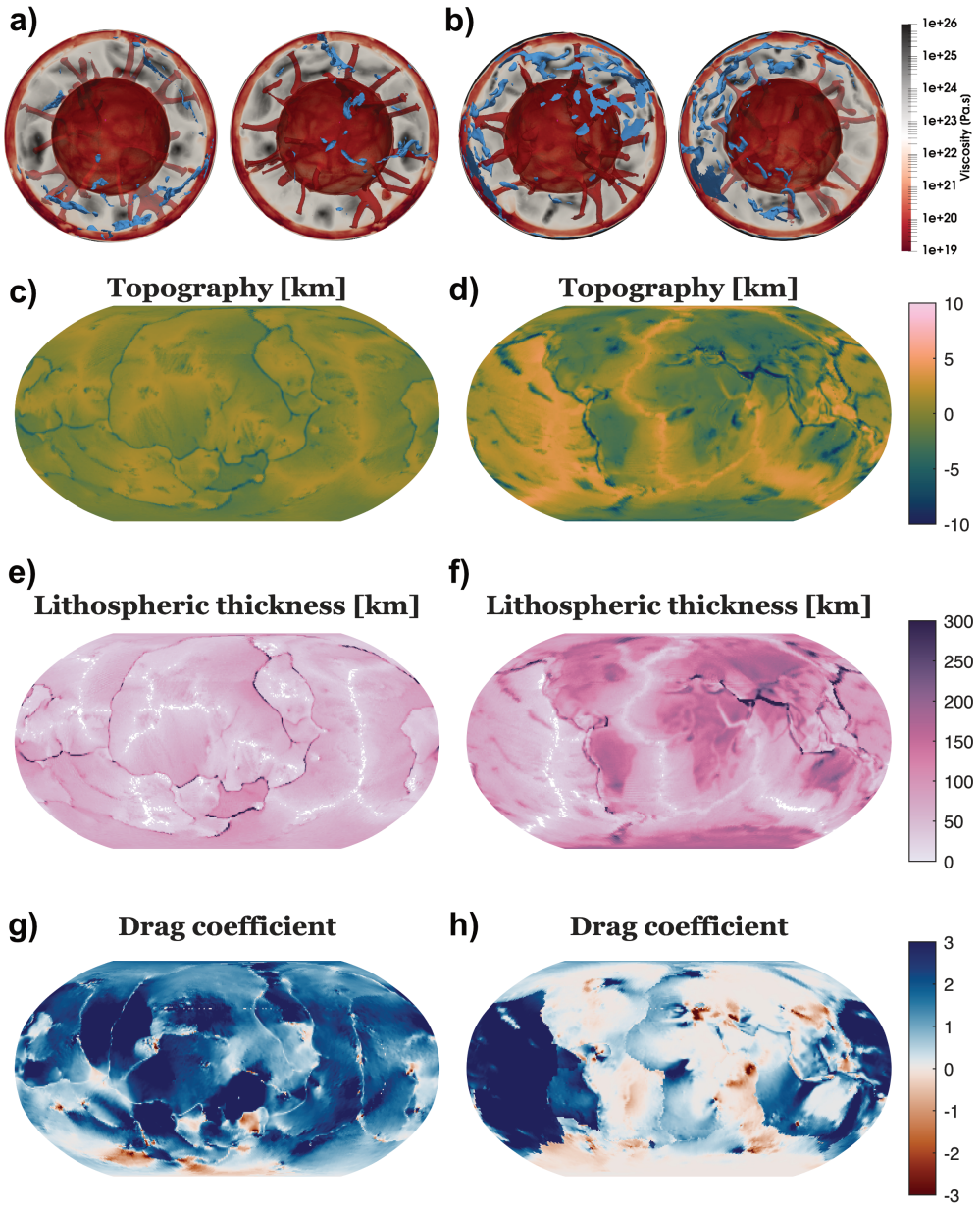


Figure: Cross-sections showing viscosity, downwellings (blue) and upwellings (red) for an Africa-centred view (a-b, left) and a Pacific-centred view (a-b, right), surface fields of topography (c-d), lithospheric thickness (e-f), and drag coefficient (g-h, calculated after [6]). Plotted are the self-consistent case (left column) and the plate-driven case (right column) for surface yield stress 30 MPa and $\eta_0 = 10^{21}$ Pa s.

Effects of Surface Mobility on Relevant Mantle H_2O Fluxes and Distribution

Nickolas Moccetti Bardi*[1]

[1]ETH Zürich
*nickolas.moccetti@eaps.ethz.ch

Keywords: water, mantle, hydrous

Using Gibbs free energy solvers combined with published experimental data, we assess the structurally bound water capacity of nominally anhydrous minerals, as well as low- and high-pressure hydrous phases. These maps are incorporated into a global mantle convection model [1] to investigate the long-term evolution of mantle water content. A parameter study spanning a range of yield stresses is performed, with particular emphasis on the role of surface mobility in controlling volatile exchange fluxes between the mantle and the atmosphere. Across multiple simulation ensembles, surface mobility emerges as the primary control on the intensity of ingassing between the two reservoirs.

Time-series autocorrelation analysis of reservoir H2O mass indicates that the mantle transition zone (MTZ) behaves as a transient, high-capacity layer that is unable to sustain long-lived hydrated states in the absence of frequent water-rich slabs penetrating beyond 410 km depth. This highlights the tendency of overturn-dominated regimes to sequester water at greater mantle depths relative to continuously active tectonics.

Bottom-up integration of our models suggests a total stored mantle H2O on the order of 1–1.5 ocean masses, an amount significantly lower than previous estimates [2, 3]. This reduction results from the rapid decrease in water storage capacity beyond 660 km depth and the subsequent ease of outgassing. Because supercriticality-enhanced extraction processes are not accounted for, vertical water transport is limited to percolation speeds, which decrease sharply as hydrous material progresses deeper into the mantle, suggesting this estimate to be an upper bound.

In addition, recent advances in high-pressure thermodynamic databases enable the assessment of oxygen fugacity profiles down to core–mantle boundary depths. Building on this, we present a conceptual redox tracking framework for an upcoming suite of simulations that integrate carbon into the system both as an independent component and as a feedback pathway to water through the production of C-O-H fluids.

References

[1] P. J. Tackley. Modelling compressible mantle convection with large viscosity contrasts in a three-dimensional spherical shell using the yin-yang grid. Physics of the Earth and Planetary Interiors 171, 7–18 (2008).
[2] Nakagawa, T., Iwamori, H., Yanagi, R. et al. On the evolution of the water ocean in the plate-mantle system. Prog Earth Planet Sci 5, 51 (2018).
[3] Karato, Si., Karki, B. & Park, J. Deep mantle melting, global water circulation and its implications for the stability of the ocean mass. Prog Earth Planet Sci 7, 76 (2020).

Explaining d410-d660 correlation using MCMs?

Gwynfor T. Morgan*[1,2] and J. Huw Davies[1]

[1]School of Earth and Environmental Sciences, Cardiff University
[2]now at Institutt for Geovitenskap, Universitetet i Bergen
*gwynfor.morgan@uib.no

Keywords: mantle dynamics, MTZ, seismic discontinuities

The topography on d410 and d660 [e.g. 1] is potentially a useful constraint on geodynamic models, sensitive to both the dynamics in the mid-mantle and the dynamics of the upper and lower thermal boundary layers that control the positions and geometries of upwellings (warm anomalies) and downwellings (cool anomalies) in the mid-mantle. Recently, using tables of seismic properties calculated from mineral physics models, workers [2, 3] have calculated synthetic discontinuity topographies from previously published Mantle Circulation Models (MCMs). Interestingly, neither of these studies reproduced the positive correlation between d410 and d660 recovered by recent global seismology studies [e.g. 4, 5, 6].

In order to evaluate the discriminating power of the predicted topographies on mantle dynamics, a suite of mantle circulation models are presented where CMB temperature, initial compositional condition and radial viscosity structure are varied. The MCMs are then evaluated with reference to the d410 and d660 structure of the Waszek et al model [6]. None of the MCM-predicted topographies provide a good match with all aspects of observed seismic discontinuity structure, but an improved match is observed on d660 with models where the viscosity is reduced near 670 km depth. Various putative explanations (including the overall vigour of convection, enrichment of the lower MTZ in basalt affecting d660, metastable olivine affecting d410, and some complications arising from the sensitivity of the SS-precursor) for the correlation of d410 and d660 are evaluated, although none of the simple implementations reproduce the positive correlation recovered by modern seismology for this set of simulations, initially presented in [7].

References

[1] Shearer and Masters (1992) https://doi.org/10.1038/355791a0
[2] Papanaganou et al (2023) https://doi.org/10.1093/gji/ggac478
[3] Morgan et al (2025) https://doi.org/10.1093/gji/ggaf344
[4] Houser (2016) https://doi.org/10.1016/j.epsl.2016.04.018
[5] Guo & Zhuo (2020) https://doi.org/10.1093/gji/ggz546
[6] Waszek et al (2021) https://doi.org/10.1038/s41561-021-00850-w
[7] Morgan (2025, pp 121–170) https://orca.cardiff.ac.uk/id/eprint/184145/

Strain Localisation in 2D models of continental rifting coupled to surface processes.

Gwynfor T. Morgan*[1], Huismans, R. S.[1], Nixon, C.[2], Gawthorpe, R.[1], and Theunissen, T.[1]

[1]Institut for Geovitenskap, Universitetet i Bergen, Bergen, Norway,
[2]Equinor, Bergen, Norway
*gwynfor.morgan@uib.no

Keywords: continental rifting, coupled surface processes

During continental rifting, strain is accommodated both by the viscous flow and plastic deformation localised on faults in the crust. Initially distributed over a broad region, strain progressively localises as extension increases and the mantle lithosphere necks. Slip along these faults forms basins that are subsequently filled with sediments.

Additionally, erosion and deposition of sediments deform the Earth's surface, modifying the loading of the crust-lithosphere system. This can influence dynamics of normal faulting (e.g. [1]), and Wolf et al. [2] showed that, at the scale of continental rifts, increased sediment supply can promote fault localisation.

In this work we explore the factors that control the role surface processes play in effecting fault localisation by systematically varying extension rate, crustal strength, and surface erodibility in a suite of 2D thermo-mechanical tectonic models (Fantom; [3]) coupled to the landscape evolution model FastScape [4,5]. We also vary the mode of marine sediment deposition, treating it either as 'aggrading', where the rift is filled from the deepest point in the basin representing sediment supply from out of the plane of the 2D geodynamic model, or 'prograding', where sediments are deposited from the shoreline, representing deltaic deposition due to sediment supply in the plane of the model which is implemented using a diffusion scheme [6]. Finally, we compare our results with the North Sea, where strain progressively localised onto major faults (e.g. [7,8]), with significant along-strike variations in basin morphology.

References

[1] Olive et al. (2014) doi.org/10.1002/2014GL061507
[2] Wolf et al. (2022) doi.org/e2021JB023490
[3] Thieulot (2011) doi.org/10.1016/j.pepi.2011.06.011
[4] Braun & Willett (2013) doi.org/10.1016/j.geomorph.2012.10.008
[5] Wolf et al. (2021) doi.org/10.1029/2020JB021168
[6] Yuan et al. (2019) doi.org/10.1016/j.epsl.2019.115728
[7] Cowie et al. (2005) doi.org/10.1016/j.epsl.2005.01.039
[8] Phillips et al. (2019) doi.org/10.1029/2019TC005756

Sensitivity of hydrothermal vent temperatures to changes in crustal permeability profiles

Kim Moutard*[1], Jean-Arthur Olive[2], Thibaut Barreyre[3], and Milena Marjanović[4]

[1]Laboratoire de Géologie - École normale supérieure - PSL University Paris, France
[2]Laboratoire de Géologie - École normale supérieure, CNRS, France
[3]Geo-Ocean, Univ. Brest, CNRS, Ifremer, Plouzané, France
[4]Institut de Physique du Globe de Paris, CNRS, 75005 Paris, France
*kim.moutard@ens.psl.eu

Keywords: hydrothermal systems, mid-ocean ridge, permeability, magmatic inflation

Hydrothermal circulation at mid-ocean ridges is enabled by the highly permeable young oceanic lithosphere and the presence of a shallow heat source, both of which can fluctuate on different time scales in response to tectonic and magmatic activity. Seafloor observatories increasingly permit us to quantify how hydrothermal discharge responds to these changes, by continuously measuring key properties of vent fluids such as temperature, chemical composition, or flow rate. Barreyre et al. [1] for example demonstrated that hydrothermal vent temperatures at the East Pacific Rise (EPR) 9°50'N steadily increase between eruptions, as the axial melt lens (AML) inflates. The models used to interpret these measurements, however, have thus far stipulated a uniform permeability along the fluid upflow path, when magmatic inflation likely imparts depth-dependent changes to the permeability field.

To remedy this, we developed SAPHYR, a semi-analytical framework to study the behavior of an axisymmetric (1-D) hydrothermal upflow zone with a depth-dependent permeability profile, subjected to lateral heat loss. SAPHYR specifically forecasts the steady-state temperature and velocity of upwelling fluids, from heat source to seafloor, given a basal heat input and background permeability profile. It is validated against standard models [2] that assume both uniform and exponentially-decaying permeability profiles.

We use SAPHYR to evaluate how exit fluid temperatures may evolve in response to depth-dependent perturbations of the upflow zone permeability profile. At the EPR, such perturbations could arise from changes in the mean stress of the upper oceanic crust caused by an inflating axial melt lens. To test this hypothesis, we run a large parametric study where we compare the state of the hydrothermal discharge zone before and after imposing a perturbation, and do so for a wide range of basal heat inputs, background permeability profiles, and degree of lateral heat loss. We find that an inflating melt lens can either trigger an increase or a decrease in hydrothermal vent temperatures depending on the basal heat-flow and the vent location with respect to the inflating body. Our findings elucidate why neighboring hydrothermal vents may respond differently to the same sub-seafloor deformation process, as was documented at the EPR. They further open a window to inverting changes in sub-seafloor permeability and stress from time series of black smoker temperatures.

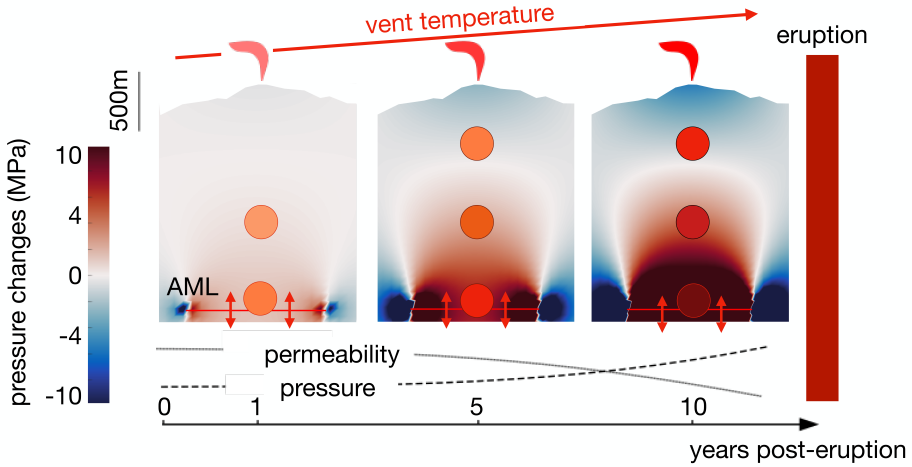


Figure: Conceptual model of inter-eruptive hydrothermal heating driven by AML inflation. Color contours represent the spatial distribution of pressure changes induced by the AML inflation. Decompression and compression lobes are denoted in blue and red, respectively. The model posits that the thermal evolution of hydrothermal fluids is coupled to the compressive stress field within the upper crust during the inter-eruptive period.

References

[1] Barreyre, T., Olive, J. A., Fornari, D. J., McDermott, J. M., Parnell-Turner, R., Moutard, K., Wu, J. N. & Marjanović, M. (2025). Hydrothermal vent temperatures track magmatic inflation and forecast eruptions at the East Pacific Rise, 9 50'N. Proceedings of the National Academy of Sciences, 122(42), e2510245122.
[2] Driesner, T. (2010). The interplay of permeability and fluid properties as a first order control of heat transport, venting temperatures and venting salinities at mid-ocean ridge hydrothermal systems. Geofluids, 10(1-2), 132-141.

How surface temperature changes surface magmatism and the tectonic regime

Laura Murzakhmetov[*1], Cédric Gillmann[1], Diogo Lourenco[1], and Paul Tackley[1]

[1]ETH Zurich, Switzerland
[*]mulaura@ethz.ch

Keywords: Venus, surface temperature, magmatism, mantle convection

Venus is, in terms of size, density and composition, the most similar planet to Earth. Still, the two planets differ greatly in their surface conditions, tectonic regime and volcanic signatures. Solving the enigma of how and why they evolved to be so different is of particular importance to understand habitability in the universe. This study investigates the influence of Venus' high surface temperature on the surface dynamics and tectonic regime, which in turn influences the interior evolution of the planet.

For this, the numerical convection code StagYY [1] is used to model the 2-D thermochemical evolution and convection of a Venus-like planet. Our work aims to explain how higher surface temperature promote more surface magmatism, and in turn the generation of younger surfaces and thicker crusts. We aim to explain the influence of the surface temperature on the viscosity structure of and partial melting in the lithosphere. More magmatism shifts the tectonic regime gradually and we strive to explain the underlying mechanism. Our results could be used to understand the positive feedback loop between surface temperature and surface magmatism. Ultimately, we aim to refine our understanding of conditions necessary for planetary habitability and deepen our understanding of the evolution of rocky planets.

References

[1] Tackley, P.J., 2008. Modelling compressible mantle convection with large viscosity contrasts in a three-dimensional spherical shell using the yin-yang grid. Physics of the Earth and Planetary Interiors, 171(1-4), pp.7-18.

Exploring geodynamic controls of orogenic gold systems under Paleoproterozoic and Phanerozoic thermal conditions.

Maria Elisa Muñoz*[1], Leevi Tuikka[1], and David Whipp[1]

[1]University of Helsinki, Finland
*elisa.munoz@helsinki.fi

Keywords: orogenic gold, Paleoproterozoic, thermal regime, DOUAR

Orogenic gold deposits are an economically important and distinct class of gold-only deposits associated with active accretionary or collisional tectonic settings. To date, models aiming to explain their formation remain debated as most are conceptual, address elements separately, or consider only deposit-scale features [1]. With the demand for mineral resources, including gold, continuously increasing and shallow deposits being exhausted, new approaches are needed to understand the orogenic gold system and thus improve the prediction of the locations of deeper undiscovered deposits.

We have conducted a preliminary study using generic lithospheric-scale 3D models to explore how thermal conditions influence the distribution and preservation of orogenic gold deposits. This study used the numerical code DOUAR [2], coupled with the landscape evolution model FastScape, to model the latest stage of subduction leading to continental accretion/collision over a 20 Myr timeframe. The model design features an older craton and younger continental lithosphere, reflected by contrasting thermal fields, separated by an oblique convergent margin in the middle and normal convergent margins on the sides. Phanerozoic and Paleoproterozoic-like scenarios were tested by systematically increasing mantle potential temperature in steps of 50 °C and crustal radiogenic heat production by up to two times higher relative to the reference model. The results revealed that elevated crustal radiogenic heat production, not mantle potential temperature, was the main factor controlling upper crustal temperatures and deformation, promoting wider and deeper zones favorable for orogenic gold formation in the Paleoproterozoic scenario. Moreover, oblique convergence may play a significant role in the formation of deep hypozonal deposits and overall preservation potential in the Paleoproterozoic by promoting deformation of deeper crustal levels and lower uplift and erosion compared to normal convergence.

While these 3D models were useful to resolve primary regions of orogenic gold deposition at a regional scale, they were insufficient to resolve smaller crustal structures, known to allow fluid flow and host most deposits. Furthermore, the spatial and temporal scale of the models allows for a restricted view in the orogenesis evolution, neglecting additional processes that contribute to the formation and preservation of deposits. Ongoing research is using the ASPECT software [3,4] to create high-resolution 2D models that capture a longer period of the accretionary/collisional orogenesis process. This study also aims to integrate phase equilibria and fluid flow modelling to explore the timing of ore-bearing fluid generation and release, and the location of potential fluid migration pathways, as well as the physical mechanisms that contribute to the migration of such fluids from source to depositional sites.

References

[1] Groves, D.I., Santosh, M., Müller, D., Zhang, L., Deng, J., Yang, L.-Q. & Wang, Q.-F. (2022). Mineral systems: Their advantages in terms of developing holistic genetic models and for target generation in global mineral exploration. Geosystems and Geoenvironment 1, 100001.
[2] Braun, J., Thieulot, C., Fullsack, P., DeKool, M., Beaumont, C. & Huismans, R. (2008). DOUAR: A new three-dimensional creeping flow numerical model for the solution of geological problems. Physics of the Earth and Planetary Interiors 171, 76–91.
[3] Kronbichler, M., Heister, T. & Bangerth, W. (2012). High accuracy mantle convection simulation through modern numerical methods. Geophysical Journal International 191, 12–29.
[4] Heister, T., Dannberg, J., Gassmöller, R. & Bangerth, W. (2017). High accuracy mantle convection simulation through modern numerical methods - II: Realistic models and problems. Geophysical Journal International 210, 833–851.

A cyclo-steady-state model for inter-rifting deformation in magmatic rifts

Ivan Navarrete*[1] and Jean-Arthur Olive[2]

[1]Laboratoire de Géologie, École normale supérieure—PSL, Paris, France
[2]Laboratoire de Géologie, École normale supérieure—PSL, CNRS UMR, Paris, France
*ivan.navarrete@ens.psl.eu

Keywords: continental rifting, inter-rifting deformation, visco-elastic relaxation, cyclo-steady state, fractional diffusion, analytical model

The inter-rifting phase of the rifting cycle, the strain that accumulates between discrete magmatic episodes, remains the least-constrained component of rift kinematics. One class of models borrows the backslip framework of [1], locking the rift above the brittle-ductile transition and imposing continuous slip below, an assumption incompatible with the viscous rheology expected at depth beneath magmatic rifts [3]. A second class represents the rift as a dislocation opening continuously at depth [2], which is equally problematic: dike intrusions are discrete, episodic events, and a continuously opening source at depth has no geological basis. Analytical diffusion models [4] capture the post-diking transient but require an a priori specification of the viscous layer thickness as a free parameter and cannot satisfy a non-zero far-field plate velocity.

We develop a fully analytical model in which a thin elastic plate (thickness H, Young's modulus E, Poisson's ratio ν) overlies a Newtonian viscous half-space of viscosity η. Dike intrusions recur periodically at interval T, each opening the rift by 2ω. The viscous half-space exerts a non-local shear traction on the plate base, coupling surface velocity at all points through the Stokes kernel, and the governing integro-differential equation reduces, after a Fourier transform, to a fractional (half-Laplacian) diffusion equation $\partial_t \hat{u} = -a|k|\hat{u}$, parameterized by a single characteristic velocity $a = EH/[2\eta(1-\nu^2)]$. The single-intrusion step response is the arctangent profile $u^{\mathrm{STEP}} = (\omega/\pi)\arctan(at/x)$, with a Lorentzian velocity field whose diffusion front advances as at.

After many cycles the system reaches a Cyclo-Steady State (CSS), expressed in closed form through the Digamma function:

$$v_{\mathrm{CSS}}(x,\tau) = \frac{2\omega}{\pi T}\,\mathrm{Im}\left\{\psi\left(\frac{\tau}{T} + i\frac{x}{aT}\right)\right\}$$

where $\tau \in [0, T)$ is time elapsed since the last intrusion. Integrating over one full cycle analytically recovers the dike half-opening ω at every distance from the rift: far-field plate divergence is satisfied by construction, with no prescribed boundary conditions. The width of the CSS velocity profile scales as aT, providing a direct geodetic constraint on the ratio EH/η.

We extend the model to a Maxwell visco-elastic asthenosphere via the elastic-visco-elastic correspondence principle [5], recovering two relaxation regimes separated by the Maxwell timescale $\tau_R = \eta/\mu_m$: near-field elastic rebound at $t \ll \tau_R$ converging to far-field viscous diffusion at $t \gg \tau_R$, with both limits reaching the same CSS.

References

[1] Savage, J.C. & Prescott, W.H. (1978). J. Geophys. Res., 83, 3369–3376.
[2] LaFemina, P.C. et al. (2005). J. Geophys. Res., 110.
[3] Bürgmann, R. & Dresen, G. (2008). Annu. Rev. Earth Planet. Sci., 36, 531–567.
[4] Foulger, G.R. et al. (1992). Nature, 358, 488–490.
[5] Hetland, E.A. & Hager, B.H. (2005). J. Geophys. Res., 110, B10401.

Dynamics of Carbonated Melt Migration in an Evolving Continental Rift

Derek Neuharth[*1], Sascha Brune[1,2], Juliane Dannberg[3], and Anne Glerum[1]

[1]GFZ Helmholtz Centre for Geosciences, Potsdam, Germany
[2]University of Potsdam, Potsdam-Golm, Germany
[3]GEOMAR Helmholtz Centre for Ocean Research, Kiel, Germany
*neuharth@gfz.de

Keywords: rift, two-phase flow, carbon

Continental rifting can remobilize carbon stored within the lithosphere and transfer it to the atmosphere through magmatism and degassing. In particular the base of the continental lithosphere could be a significant carbon store as it likely has been metasomatized by carbon-rich material from the underlying mantle over geological timescales. Because CO_2 lowers mantle solidus temperatures, these enriched domains are expected to melt at lower temperatures than the surrounding mantle during extension, potentially generating carbonated melts that migrate toward developing rift axes and influencing CO_2 release throughout rift evolution. While previous studies have examined the effects of volatiles on magma dynamics [1] or the rifting of metasomatized lithosphere without melt transport [2], the coupled evolution of volatile-rich melt transport and heterogeneous lithospheric carbon during rifting remains poorly understood.

To investigate these processes, we use the geodynamic code ASPECT [3] to model rifting with two-phase flow of magma through a deforming medium. Our models implement the Reactive Disequilibrium Multi-Component (R_DMC) melting formulation [4] allowing melt composition to evolve dynamically. We additionally include the carbonate "ledge" [5], a sharp increase in solidus temperature at pressures below 2 GPa that can promote partial crystallization of carbonated melts and thereby limit their upward transport. The model setup contains an initial carbon-rich metasomatized layer at the base of the lithosphere, and we systematically vary both its CO_2 concentration and reference melt permeability to evaluate their influence on melt migration and carbon focusing beneath the rift axis.

Our preliminary results show that melting initiates within the metasomatized layer prior to widespread asthenospheric melting, producing volatile-rich melts that further enrich the overlying lithosphere. With continued extension, melt becomes focused into channels along the base of the lithosphere and is transported laterally toward the rift center. The carbonate ledge strongly influences this transport behavior: at lower CO_2 contents, melts commonly crystallize at the ledge, whereas higher volatile contents and permeabilities promote channelization through the barrier by transporting melt into warmer regions (Figure). This channelization leads to enhanced carbon accumulation beneath the rift axis, where remelting and focused melt ascent subsequently increase surface degassing. Variations in channelization efficiency and remelting of solid carbon above the ledge produce dynamically variable CO_2 output throughout rift evolution.

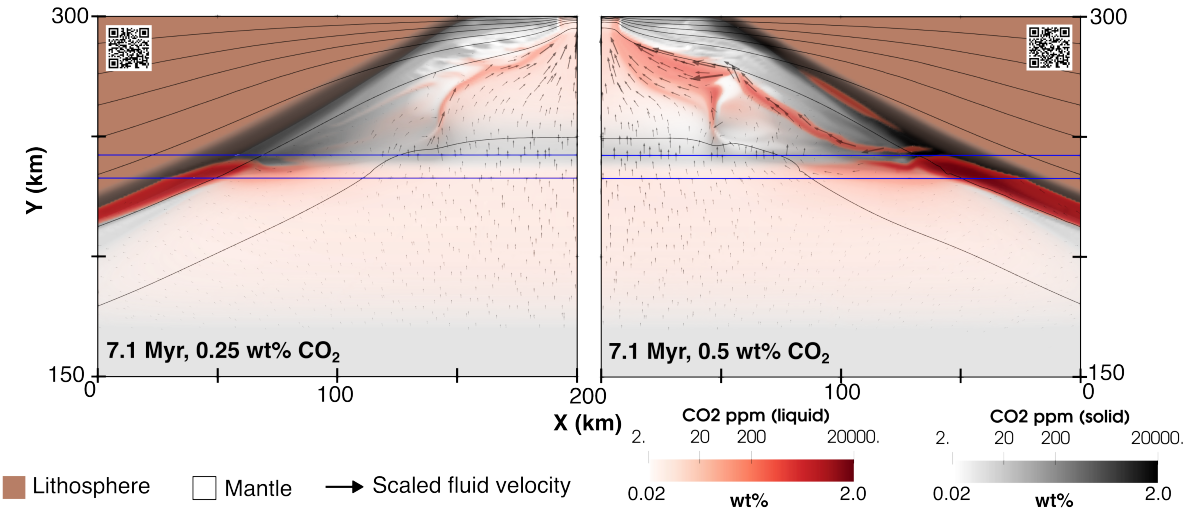


Figure: Figure showing how higher CO_2 contents lead to greater channelization through the carbonate ledge (blue lines) and towards the surface.

References

[1] Keller, T., Katz, R. F., and Hirschmann, M. M. (2017). Volatiles beneath mid-ocean ridges: Deep melting,

channelised transport, focusing, and metasomatism. Earth and Planetary Science Letters, 464, 55–68.
[2] Gorczyk, W., and Gonzalez, C. M. (2019). CO2 degassing and melting of metasomatized mantle lithosphere during rifting – Numerical study. Geoscience Frontiers, 10(4), 1409–1420.
[3] Bangerth, W., Dannberg, J., Fraters, M., Gassmoeller, R., Glerum, A., Heister, T. et al. (2024). ASPECT v3. 0.0. Zenodo.
[4] Keller, T., and Katz, R. F. (2016). The role of volatiles in reactive melt transport in the asthenosphere. Journal of Petrology, 57(6), 1073–1108.
[5] Dasgupta, R., and Hirschmann, M. M. (2010). The deep carbon cycle and melting in Earth's interior. Earth and Planetary Science Letters, 298(1–2), 1–13.

Lithospheric mechanisms leading to rift failure

Tina Neumann*[1,2], Sascha Brune[1,3], Susanne Buiter[1,2], and Michael Pons[1,4]

[1]GFZ Helmholtz Centre for Geosciences, Potsdam, Germany
[2]Tectonics and Geodynamics, Faculty of Georesources and Materials Engineering, RWTH Aachen University, Germany
[3]University of Potsdam, Germany
[4]Department of Science, Roma Tre University, Italy
*tneumann@gfz.de

Keywords: continental rifting, rift failure, extension, deformation, lithospheric dynamics, continental breakup, geodynamical modelling

Lithospheric rifting represents an irreversible geodynamic process that often culminates in continental breakup and the formation of rifted continental margins. However, Earth's geological record preserves numerous examples of aborted continental rifts—so-called "failed rifts"—in which rifting ceased prior to lithospheric rupture. Understanding the mechanisms that govern rift success or failure is therefore essential for constraining lithospheric dynamics and the fundamental processes controlling plate tectonics evolution.

Here, we first present a classification framework for rift evolution using selected natural examples. This framework accounts for the competition between internal rift processes and external forcing mechanisms operating across spatial and temporal scales. These factors determine whether deformation localizes and promotes breakup or delocalizes and inhibits rift propagation. We then investigate these processes at the lithospheric scale employing thermo-mechanical simulations using the finite-element code ASPECT. Our models explore the impact of lithospheric weakening and strengthening mechanisms on the onset of the initial rift localization and the long-term tectonic evolution.

Our results provide new insights into the physical conditions controlling continental rift success and failure and contribute to a broader understanding of large-scale geodynamic processes.

Layered bubble-rich structures on icy worlds: near-vacuum experiments with large volumes of low-salinity water

Vojtěch Patočka[*1], Petr Brož[2], Kristian Chan[3], Priyanka Biju Sindhu[1,2], Mark G. Fox-Powell[4], Matthew Sylvest[5], Zoe Emerland[5], and Manish R. Patel[5]

[1]Charles University, Faculty of Mathematics and Physics, Department of Geophysics, Prague, Czechia
[2]Institute of Geophysics of the Czech Academy of Sciences, Prague, Czechia
[3]Johns Hopkins University Applied Physics Laboratory, Laurel, United States
[4]School of Environment, Earth and Ecosystem Sciences, The Open University, Milton Keynes, United Kingdom
[5]School of Physical Sciences, STEM, The Open University, Milton Keynes, United Kingdom
[*]vojtech.patocka@matfyz.cuni.cz

Keywords: effusive cryovolcanism, icy moons, low-pressure physics

Icy bodies of the outer Solar System display evidence of remarkable surface activities, including explosive and potentially effusive cryovolcanism. When water is released into their extremely low-pressure surface environments, or when the surface ice melts in response to an impact, the liquid water has traditionally been expected to form solid ice with a porous outer layer. Here, we expose 40 kg of low-salinity water in a specialist chamber at The Open University, UK, and show that freezing under near-vacuum conditions is a complex, dynamic process during which vapor puffs through the growing ice sheets, building previously unobserved ice structures. Millimeter-thin, sheet-like ice layers form, separated by centimeter-thick, large-aspect-ratio pockets of vapor. The overall height of this layered, bubble-rich ice is controlled by a balance between its weight and the equilibrium vapor pressure. In the laboratory, the height reaches approximately ten centimeters, which could plausibly extend to tens of meters in the low-gravity environments of icy bodies. The high porosity of such ice has significant implications for the interpretation of remote sensing observations, and its fragile character makes terrains created by effusive cryovolcanism risky for landed spacecraft.

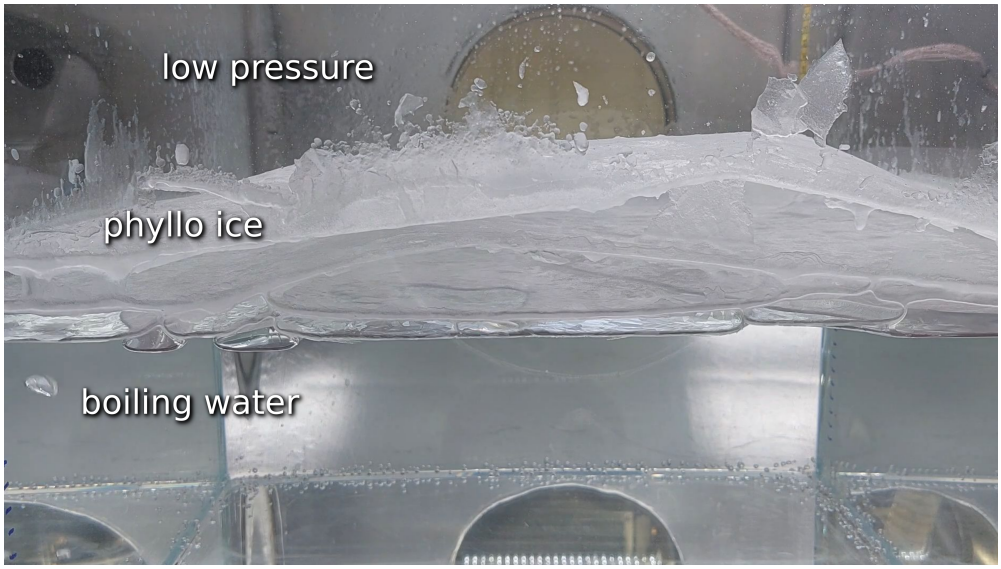


Figure: Three stages of low-pressure-formed ice

References

[1] Patočka, V., Brož, P., Chan, K., Biju Sindhu, P., Fox-Powell, M.G., Sylvest, M., Emerland, Z., Patel, M.R. (2026): Layered bubble-rich structures on icy worlds: near-vacuum experiments with large volumes of low-salinity water, Earth. Planet. Sci. Lett., 685, 119999

Coupled Damage and Ocean Overpressure Dynamics in Enceladus' Ice Shell

Barbora Piláriková*[1], Ondřej Souček[2], and Marie Běhounková[1]

[1]Department of Geophysics, Charles University, Czech Republic
[2]Mathematical Institute, Charles University, Czech Republic
*pilarikovabarbora@gmail.com

Keywords: icy moons, damage mechanics, fractures

The origin of many tectonic features observed on the surface of Enceladus remains uncertain, with several mechanical and thermal processes proposed as potential formation mechanisms operating over a wide range of timescales. In this study, we investigate the evolution of microscopic mechanical damage within Enceladus' ice shell on tidal timescales using a three-dimensional mechanical model. We consider an initially intact ice shell model based on Čadek et al. 2019 [1] subjected to two sources of forcing: (1) overpressure of the subsurface ocean generated by freezing at the ice–ocean interface and the associated volumetric expansion of ice, and (2) tidal forcing arising from Enceladus' orbital dynamics, including the effects of the thinned shell beneath the south polar terrain.

Damage is represented by a scalar field describing the density of microcracks and evolves nonlinearly as a function of the local stress state [2]. Damage initiation is restricted to regions where the extensional stress regime dominates. Both forcing mechanisms contribute to the development of extensional stresses within the ice shell, promoting the nucleation and growth of microcracks. The damage evolution is coupled to the pressure evolution of the subsurface ocean. Ocean overpressure is determined by the competition between water freezing at the ice-ocean interface and the volumetric response of the deformable ice shell. Treating the ocean as a compressible fluid and the ice shell as a compressible solid, we investigate how ocean-shell interactions modify the stress field and influence the spatial distribution of damage.

Our simulations produce both global and regional maps of stress and damage accumulation, with particular focus on the south polar terrain. These results provide new constraints on the role of tidal forcing and ocean overpressure in initiating fracture networks and shaping the tectonic evolution of Enceladus' ice shell. Future developments of the model will explore the conditions for damage initiation both at the top and bottom shell boundaries along with the possible hydrofracturing impact of the pressurized ocean on the crack propagation for the basal crevasses.

References

[1] Čadek et al. (2019). Long-term stability of Enceladus' uneven ice shell. doi: 10.1016/j.icarus.2018.10.003
[2] Duddu et al. (2020). A non-local continuum poro-damage mechanics model for hydrofracturing of surface crevasses in grounded glaciers. doi: 10.1017/jog.2020.16.

Controls on the spatio-temporal distribution of plume-related excess melting during continental rifting

Abigail Plimmer*[1], Ritske Huismans[1], and Sebastian Wolf[1]

[1]University of Bergen
*abigail.plimmer@uib.no

Keywords: rifting, plumes, rheology

The complexity in the relationship between mantle and lithosphere processes may be most directly exemplified in the coupling between upwelling plumes and extending lithosphere at rifted margins, and the distribution of excess melting across these regions through space and time. Rifted margins are often described in two end-member classes; magma-rich and magma-poor, typified by the emplacement of seaward dipping reflector sequences (SDRs) and high velocity lower crustal bodies (HVLC) or the exhumation of serpentinised mantle with little extrusive melt, respectively. Previous studies have linked margin architecture and magmatic budget to extension velocity, lithosphere thickness, and rheology. The role of mantle plumes remains poorly constrained, with plumes associated with both magma-poor and magma-rich margins, implying that their influence on excess melt production is not straightforward. Our study aims to better constrain the relationship between mantle plumes and excess melting at rifted margins by exploring the interaction of plumes originating from the mantle transition zone and rifting.

We present two-dimensional numerical simulations to investigate how mantle plumes interact with lithosphere extension during continental rifting. Rifting is simulation using the ALE finite-element code FANTOM [3], incorporating a thermal anomaly at the base of the upper mantle to represent an ascending plume. We compare these models with the models of [1, 2] to explore how plumes modify the rifting behaviours and melting patterns associated with varying crustal rheologies.

Our results indicate that excess melting associated with mantle plumes is heterogenous in space and time. The timing, magnitude and lateral distribution of excess melting depends non-linearly on the interaction between hot upwelling plumes and the rheological contrast in the lithosphere. Stronger crusts are most sensitive to the timing of plume arrival beneath the lithosphere, but all rheologies exhibit a threshold behaviour which controls the extent of excess melting. These results demonstrate that plume-driven excess melting may be highly time-dependent with an elevated background melting relative to non-plume models, and pulses in plume material in time.

References

[1] Gang Lu and Ritske S. Huismans. Melt volume at Atlantic volcanic rifted margins controlled by depth-dependent
extension and mantle temperature. Nature Communications, 12(1):3894, June 2021.
[2] Thomas Theunissen and Ritske S. Huismans. Long-Term Coupling and Feedback Between Tectonics and Surface Processes During Non-Volcanic Rifted Margin Formation. Journal of Geophysical Research: Solid Earth, 124(11):12323–
12347, November 2019.
[3] Cedric Thieulot. Fantom: Two-and three-dimensional numerical modelling of creeping flows for the solution of geological problems. Physics of the Earth and Planetary Interiors, 188(1-2):47–68, 2011.

Surface expression of global tectonic regimes on Earth and Venus

Michael Pons*[1], Stephan V. Sobolev[2,3], Charitra Jain[2], Menno Fraters[4], Sascha Brune[2,3], Francesca Funiciello[1], and Claudio Faccenna[1,2,5]

[1]Università degli Studi Roma Tre, Dipartamento di scienze, Laboratory of Experimental Tectonics, Rome, Italy
[2]GFZ Helmholtz Centre for Geosciences, Potsdam, Germany
[3]Institut für Geowissenschaften, Universität Potsdam, Potsdam, Germany
[4]University of Graz, Department of Earth Sciences, NAWI Graz Geocenter, Graz, Austria
[5]Institute of Geosciences, Johannes Gutenberg University Mainz, Germany
*michaelpons.geo@gmail.com

Keywords: subduction, networks, Earth, Venus, global tectonics, modelling

Earth and Venus are similar in size and bulk composition, yet their surfaces record fundamentally different tectonic regimes. On Earth, plate tectonics and efficient lithospheric recycling are sustained by widespread subduction networks, which play a key role in plate reorganization, supercontinent breakup, and long-term mantle and lithosphere evolution [1]. In this study, we propose that the development of global subduction networks on Earth is promoted by water-rich continental sediments, which reduce frictional strength along convergent margins and facilitate the initiation and maintenance of large-scale plate motion.

To test this hypothesis, we use the ASPECT code [2] to perform a series of 3D global geodynamic models. For Earth, we investigate two end-member scenarios: first, plume-driven regional subduction that progressively evolves into a global subduction network; and second, a model initialized with prescribed plate boundaries and subduction zones at 1 Ga, showing that long-lived subduction can be sustained when friction is locally reduced. On Earth, such frictional weakening may vary through time and could be linked to climatic episodes such as Snowball Earth events, during which enhanced erosion and sediment supply may have increased lubrication along plate boundaries [3].

We compare these results with Venus-like models, where the absence of surface water leads to higher frictional strength at the lithosphere-mantle interface and along potential plate boundaries. In the absence of efficient local weakening mechanisms, subduction-like structures on Venus remain regional and short-lived, preventing the formation of a self-sustaining global subduction network. However, over longer timescales, Venus's lithosphere may thicken, become gravitationally unstable, and founder into the mantle, potentially triggering episodic resurfacing events associated with the development of rift networks.

By comparing Earth and Venus (Figure), we highlight the critical role of surface water, sediment supply, and frictional weakening in controlling lithospheric recycling efficiency. Our results suggest that the surface expression of tectonic regime evolution is strongly linked to the ability of a planet to develop and maintain global subduction networks.

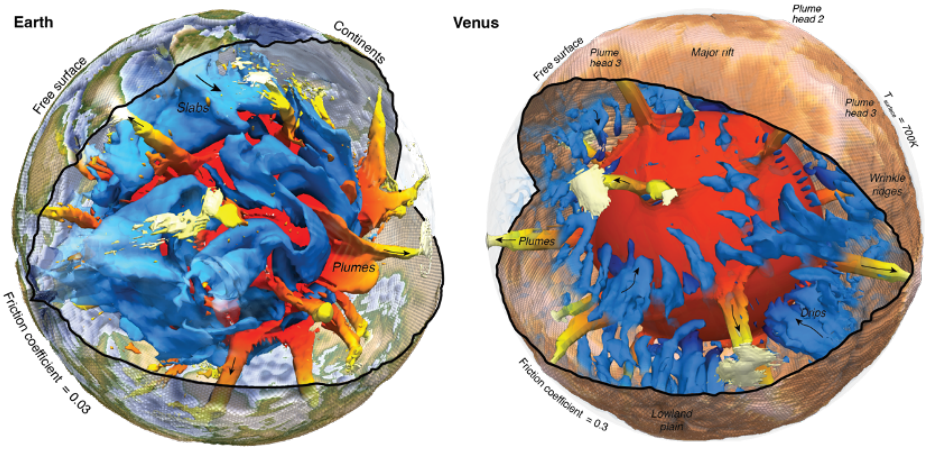


Figure: Reference 3D Earth and Venus model computed with ASPECT. Cold material (blue), such as subduction zones on Earth and mantle drips on Venus, sinks into the mantle, while warm mantle plumes (red) rise toward the surface.

References

[1] Faccenna, C., Becker, T. W., Holt, A. F., & Brun, J. P. (2021). Mountain building, mantle convection, and super-

continents: Revisited. Earth and Planetary Science Letters, 564, 116905.
[2] Kronbichler, M., Heister, T., & Bangerth, W. (2012). High accuracy mantle convection simulation through modern numerical methods. Geophysical Journal International, 191(1), 12-29. http://dx.doi.org/10.1093/gji/ggx195.
[3] Sobolev, S. V., & Brown, M. (2019). Surface erosion events controlled the evolution of plate tectonics on Earth. Nature, 570(7759), 52-57.

Modeling True Polar Wander from Time-Dependent Mantle Convection Using Self-Gravitating Geoid and Dynamic Topography in ASPECT

Hang Qian*[1,2], Bernhard Steinberger[1], Michael Pons[3], Sascha Brune[1,4], and Poulami Roy[5]

[1]GFZ Helmholtz Centre for Geosciences, Potsdam, Germany
[2]Freie Universität Berlin, Berlin, Germany
[3]Università degli Studi Roma Tre, Rome, Italy
[4]University of Potsdam, Potsdam, Germany
[5]Durham University, Durham, United Kingdom
*hang.qian@gfz.de

Keywords: true polar wander, mantle convection, geoid, self-gravitation, LLSVPs

True polar wander (TPW), the reorientation of the solid Earth relative to its spin axis, provides a key constraint on the long-wavelength evolution of mantle mass anomalies. TPW is controlled by perturbations to Earth's inertia tensor, which are determined by the degree-two components of Earth's non-hydrostatic mass distribution and its associated geoid response. However, many mantle convection studies focus on present-day geoid or dynamic topography, while the dynamical link between time-dependent mantle structure, the maximum moment of inertia axis, and TPW remains less explored. Here we develop a numerical framework in ASPECT to compute self-gravitating geoid and dynamic topography in global, time-dependent mantle convection models, with particular emphasis on the degree-two geoid components that control TPW.

We first implement a self-gravitation correction for geoid and dynamic topography calculations following the formulation of Zhong et al. [1]. In this approach, self-gravitation modifies the interpretation of pressure and boundary stresses, while leaving the Stokes flow field unchanged. The implementation is benchmarked against semi-analytical propagator-matrix solutions and published CitcomS benchmarks for incompressible Stokes flow in a spherical shell [1,2]. These comparisons show that self-gravitation has a significant influence on long-wavelength topography and geoid kernels, especially for $l = 2$, and is therefore essential for robust TPW calculations.

We then apply the method to layered incompressible mantle models spanning the last 140 Ma to compute the evolution of the degree-two geoid, dynamic topography, and the associated maximum moment of inertia axis. Finally, we extend the framework to compressible thermo-chemical mantle convection models spanning the last 250 Ma, in which temperature, composition, and density heterogeneities jointly contribute to the evolving inertia tensor. This allows us to investigate how large low-shear-velocity provinces (LLSVPs), subduction-induced density anomalies, and lower-mantle viscosity structure influence the predicted TPW path.

Our preliminary results suggest that the degree-two thermo-chemical structure of the lowermost mantle exerts a first-order control on the stability and migration of the maximum moment of inertia axis. Long-lived LLSVP-like structures may stabilize the rotation axis by maintaining a persistent degree-two mass distribution [3,4], whereas changes in subduction history and lower-mantle viscosity can produce substantial variations in modeled TPW trajectories. This study provides a self-consistent geodynamic framework for linking mantle convection, geoid evolution, inertia-tensor perturbations, and TPW, and offers a pathway for comparing numerical mantle models with paleomagnetic constraints on Earth's rotational history.

References

[1] Zhong, S., McNamara, A., Tan, E., Moresi, L., and Gurnis, M. (2008). A benchmark study on mantle convection in a 3-D spherical shell using CitcomS. Geochemistry, Geophysics, Geosystems, 9, Q10017.
[2] Liu, S. and King, S. D. (2019). A benchmark study of incompressible Stokes flow in a 3-D spherical shell using ASPECT. Geophysical Journal International, 217, 650–667.
[3] Dziewonski, A. M., Lekic, V., and Romanowicz, B. A. (2010). Mantle anchor structure: An argument for bottom up tectonics. Earth and Planetary Science Letters, 299, 69–79.
[4] Steinberger, B., Seidel, M.-L., and Torsvik, T. H. (2017). Limited true polar wander as evidence that Earth's nonhydrostatic shape is persistently triaxial. Geophysical Research Letters, 44, 827–834.

Understanding the Evolution of Venusian Rifts through Integrated Observations and Modeling

Alessandro Regorda*[1], Iris van Zelst[2], Julia Maia[3], Zoltán Erdős[4], and Cédric Thieulot[5]

[1]Università degli Studi di Milano, Milan, Italy
[2]School of GeoSciences, University of Edinburgh, Edinburgh, UK
[3]Institute of Space Research, German Aerospace Center (DLR), Berlin, Germany
[4]The Helmholtz Centre Potsdam, GFZ German Research Centre for Geosciences, Potsdam, Germany
[5]Department of Earth Sciences, University of Utrecht, Utrecht, the Netherlands
*alessandro.regorda@unimi.it

Keywords: Venus rifting, numerical models, Venus topography

Recent numerical modelling and observational evidence suggest that Venus may have experienced tectonic-like processes in the past and could still be tectonically active today. In fact, the surface of Venus is characterized by a global network of chasmata, extending for thousands of kilometres and displaying strong imilarities to terrestrial rift systems [1, 2]. Yet their driving mechanisms, temporal evolution, and lithospheric structure remain poorly understood because of the sparse observational constraints. Investigating the evolution of Venusian chasmata is therefore essential to better understand Venus' interior dynamics and history.

Here, we used a forward 2D numerical model [3] to constrain the rates, durations, and lithospheric structures of Venus' rifts, integrating observational evidence from topography and gravity anomalies. In particular, we tested different extensional velocities and lithospheric and crustal thicknesses.

For comparison with natural observation, we extracted topographic and gravity profiles spaced every 50 km along 30 Venusian rift axis. Successively, we selected subsets consisting of at least 3 topographic profiles from each rift, evaluating their homogeneity and, therefore, limiting 3D effects not evaluable by means of 2D models. For this analysis, we used the normalized mean absolute error and the Pearson correlation index to provide a robust evaluation of the similarities of the topographic profile between the average extracted and each profile of the subsets. We then used the average topography of each subset for comparison with Venus' observation.

We observed that models with a lithospheric thickness of 100 km and a crustal thickness of 15 km show the best agreement with the observed topography across the largest number of Venusian rifts, with exceptions located in the Thetis Regio. In addition, we identified one group of rifts with a duration of 2-5 Myr and an extension velocity of 1-2 cm/yr, and one group with a duration of 10-12.5 Myr and an extension velocity of 0.5-1 cm/yr. Finally, we were also able to distinguish asynchronous evolutions and a variation of crustal thickness along the axis of some rifts.

References

[1] Brossier, J., Gilmore, M. S., & Head, J. W. (2022). Extended rift-associated volcanism in Ganis chasma, venus detected from magellan radar emissivity. Geophysical Research Letters, 49(15):e2022GL099765. doi: 10.1029/2022GL099765.
[2] Gülcher, A. J., Gurnis, M., & Smrekar, S. E. (2025). Dynamics of venusian rifts and their interactions with plumes and intrusions. Earth and Planetary Science Letters, 667:119514. doi:10.1016/j.epsl.2025.119514.
[3] Regorda, A., Thieulot, C., van Zelst, I., Erdős, Z., Maia, J., & Buiter, S. (2023). Rifting venus: Insights from numerical modeling. Journal of Geophysical Research: Planets, 128(3):e2022JE007588. doi:10.1029/2022JE007588

Petit-Spot Volcanism: Flexure-Driven Melt Transport in the Oceanic Lithosphere

Marko Repac*[1] and Adina Pusok[1]

[1]Department of Earth Sciences, University of Oxford, Oxford, United Kingdom
*marko.repac@earth.ox.ac.uk

Keywords: petit-spot volcanism, plate flexure, melt transport

Petit-spots are volcanoes with relatively small volumes of magma production found on the seafloor of subducting plates [2, 3]. Geochemical observations suggest petit-spots are derived from low-degree asthenospheric melts with a crustal and/or carbonatitic component [6], while others suggest additional interaction with metasomatic zones during migration [1]. Their occurrence near the outer-rise region within the concave curvature—where plate bending generates extension at the base of the lithosphere and compression at the top—suggests the creation of rapid melt pathways through otherwise cold, thick lithosphere [3]. However, the extent to which flexure-induced stresses influence melt migration, especially in a lithosphere with strong rheological contrasts, remains poorly quantified.

Here, we use numerical models of melt transport across the brittle–ductile transition zone in the lithosphere [4, 5, 7] to investigate how plate flexure influences melt transport. We introduce flexure into our models via prescribed boundary loading and imposed velocities, producing depth-dependent compression and extension separated by a neutral surface. We systematically test how lithospheric age and flexural stresses affect the style of melt transport and melt ascent rates. Our results show that the lowermost, ductile domain is not affected by tectonic forcing. Melt ascent rates in the brittle domain monotonically increase with an increasing extension strain rate. Under compression, melt ascent rates reach a maximum at low stresses, enough to overpressurise the magma, but not enough to close the pores and suppress melt extraction. Above a certain compressive threshold, melt ascent is arrested in the crust to form sills. Petit-spot-like forcing exhibits a combined effect depending on the position of the brittle–ductile transition in relation to the stress neutral surface, a relationship inherently governed by plate age. This work provides a quantitative basis for understanding when flexure promotes upward melt transport versus trapping melt within the oceanic lithosphere.

References

[1] Buchs et al. (2013). Low-volume intraplate volcanism in the Early/Middle Jurassic Pacific basin documented by accreted sequences in Costa Rica. G-cubed 14, doi:10.1002/ggge.20084.
[2] Harmon et al. (2025). Evidence for petit-spot volcanism in the Puerto Rico Trench. GRL 52, doi:10.1029/2024GL114362.
[3] Hirano et al. (2006) Volcanism in response to plate flexure. Science 313, doi:10.1126/science.1128235.
[4] Li et al. (2023), Continuum approximation of dyking with a theory for poro-viscoelastic–viscoplastic deformation, GJI, doi:10.1093/gji/ggad173.
[5] Li et al. (2025), Models of buoyancy-driven dykes using continuum plasticity and fracture mechanics: a comparison, GMD 18, doi:10.5194/gmd-18-6219-2025.
[6] Mikuni et al. (2024) Contribution of carbonatite and recycled oceanic crust to petit-spot lavas on the western Pacific Plate, Solid Earth 15, doi:10.5194/se-15-167-2024.
[7] Pusok et al. (2025). Inefficient melt transport across a weakened lithosphere led to anomalous rift architecture in the Turkana Depression. GRL 52, doi:10.1029/2025GL115228.

Flexural and Membrane Stresses in Doubly Curved Subducting Slabs

Neil M. Ribe[*1], Gianluca Gerardi[1], and Yida Li[1]

[1]Lab FAST, Universite Paris-Saclay, CNRS, Orsay, France
[*]neil.ribe@universite-paris-saclay.fr

Keywords: subduction, membrane deformation, flexural deformation, Gaussian curvature, hoop stress, buckling instability

A subducting slab is a thin doubly curved shell with complex shape that deforms in interaction with the surrounding mantle. The midsurface of such a shell can deform in two distinct ways: by in-plane stretching and shear (membrane deformation) and by bending and twisting (flexural deformation). Using boundary-element numerical models of subducting viscous shells together with thin-shell theory, we study how the stress depends on the geometry of the slab, focusing on the influence of the Gaussian curvature G (the product of the two principal curvatures) of the midsurface. The main results, based on an idealized model of the Mariana slab comprising portions with both $G > 0$ and $G < 0$, are (1) the downdip membrane stress changes from compressive to tensile with increasing depth when $G > 0$, and from compressive to tensile to compressive when $G < 0$; (2) the longitudinal ("hoop") membrane stress is tensile at shallow depths and compressive at greater depths when $G > 0$, and the reverse when $G < 0$; (3) the downdip flexural stress at the upper surface of the slab is tensile at shallow depths and compressive at greater depths. The stress distributions predicted by a three-dimensional model of the Mariana slab with realistic geometry and rheology agree qualitatively with those predicted by the idealized Mariana model. However, the hoop stress distribution predicted by the realistic model agrees poorly with that inferred from centroid moment tensors of earthquakes in the Mariana slab. We propose that the presence in the Mariana slab of distinct regions with $G > 0$ and $G < 0$ is the result of a longitudinal buckling instability driven by compressive hoop stresses.

From Mantle to Atmosphere: Quantifying the Geodynamic and Climatic Impacts of Large Igneous Provinces

Sandrine Ritter*[1], Julian Rogger[1], Attila Balazs[1], Dominic Stemmler[1], and Taras Gerya[1]

[1]Department of Earth and Planetary Sciences, ETH Zurich, Zurich, Switzerland
*sandrine.ritter@eaps.ethz.ch

Keywords: large igneous provinces, CO_2 outgassing, climate modeling

The dynamics of large igneous provinces connect complex processes in the Earth's interior with surface global climate changes. These processes include the nonlinear dynamics of deep mantle plume-lithosphere interaction, the variable spatial and temporal evolution of melt and volcanic emplacement. The extensive CO_2 emissions that occur during such events can be a major driver of mass extinctions. However, the severity of this event depends heavily on the initial properties of the plume and the geological setting in which it is emplaced. The goal of this study is to reveal the combined processes of this multiscale event that require further understanding.

Therefore, we couple the thermomechanical numerical geodynamic model i3evlis with a simplified geological carbon cycle model. This model considers the balance of degassing from the solid Earth and silicate weathering as the sole carbon sink. Using i3evlis, we model mantle dynamic processes, such as partial melting, and study the CO_2 emission of large igneous provinces. Then, we study its surface environmental and climatic consequences based on the resulting CO_2 evolution. This approach provides a better understanding of the deep mantle and the climatic crisis during and after an LIP event.

Our results indicate that the intensity of CO_2 emissions depends on geological settings and does not always coincide with volcanic activity. Furthermore, the balance between carbon sources and sinks cannot always be restored within a given time frame.

Broad thermochemical plumes - morphology, melt production, and volatile release

Maxwell Rudolph*[1] and Qianyi Lu[1]

[1]Department of Earth and Planetary Sciences, University of California, Davis
*maxrudolph@ucdavis.edu

Keywords: mantle plume, large igneous province, melting, volatiles, climate, biogeodynamics

The mantle plume paradigm provides the most compelling explanation for long-lived intraplate volcanism on Earth. The long-held view [1] is that plumes are generated by boundary layer instabilities within the lowermost mantle and that plumes ascend through the mantle with an inflated, bulbous head, followed by a long-lived tail. Plume heads generate large igneous provinces (LIPs) and tails give rise to long-lived volcanic hostpots [2].

Several lines of evidence suggest that mantle plumes are not purely thermal upwellings. First, the geologic record suggests that the kilometer-scale pre-magmatic uplift that would be associated with a buoyant thermal plume head is generally not observed [3]. Second, the plume conduits (tails) imaged in global and regional tomographic models are wider than would be expected for a purely thermal plume. Third, geochemical and petrological considerations require that plumes sample a mantle reservoir that is compositionally distinct from the ambient upper mantle [e.g., 4,5,6]. Fourth, plumes appear to pond or become offset within the mid-mantle, often below the mantle transition zone, in the 400–1000 km depth range (the extended transition zone, ETZ) [e.g., 7,8,9]. The incorporation of eclogite into deep mantle upwellings (recycled subducted oceanic crust) may explain all of these observations. Eclogite is denser than pyrolite at most mantle depths and the difference in buoyancy between pyrolite and eclogite may drive plume ponding or stagnation. The incorporation of eclogite into plume heads reduces their buoyancy and hence, pre-magmatic uplift [10]. Eclogite melts at higher pressures and temperatures and thus may produce more melt [11,12].

We use ASPECT to model the ascent of thermochemical mantle plumes. We adopt equation of state properties for eclogite and pyrolite from thermodynamic lookup tables computed using HeFESTo with the latest thermodynamic database [13]. We adopt depth- and temperature-dependent transport properties [14]. We demonstrate that depending on the temperature and composition structure of the lowermost mantle, a variety of plume dynamics can arise, including the generation of broad, headless plumes that are minimally deflected in the lower mantle but become strongly sheared by plate motions in the upper mantle. We also demonstrate using cylindrical axisymmetric geodynamic models that thermochemical mantle plumes can generate the volumes of melt and carbon release that are necessary to explain the volume of large igneous provinces as well as the long-lasting carbon cycle and climate perturbations that may drive mass extinctions. We show that owing to the competition between eclogite's negative buoyancy and more fusible melting behavior, maximum melt production and volatile release are achieved for a specific intermediate amount of entrained eclogite [15].

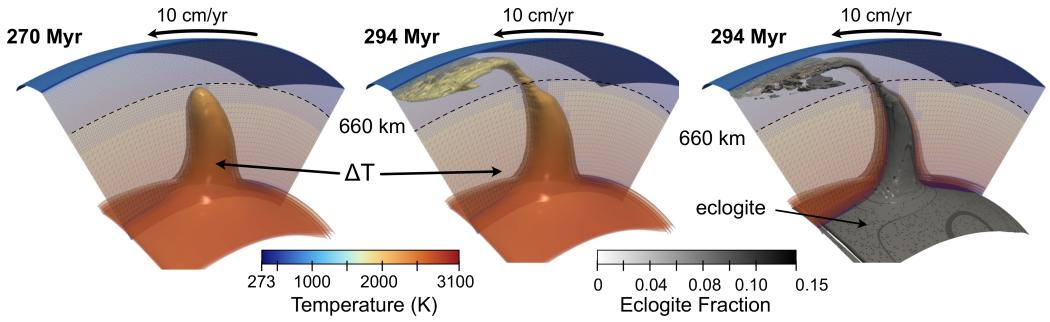


Figure: Visualization of an ASPECT calculation in 3D spherical cap geometry showing the ascent of a broad thermochemical plume through the lower mantle (left) and impingement on the lithosphere. The lithosphere is moving leftward at a rate of 10 cm/yr, generating deflection of the plume. The plume is sourced from a thermal boundary layer enriched in eclogite (15 %) relative to the background pyrolitic mantle and the plume rises through a mantle with depth-dependent viscosity and transport properties. The plume is represented by isosurfaces of temperature anomaly (150 K) relative to the adiabat, and colored based on temperature. The adaptively refined ASPECT mesh is shown.

References

[1] Morgan, W.J., 1971. Convection Plumes in the Lower Mantle. Nature 230, 42–43.
[2] Richards, M.A., Duncan, R.A., Courtillot, V.E., 1989. Flood Basalts and Hot-Spot Tracks: Plume Heads and

Tails. Science 246,103–107.
[3] Saunders, A.D., Jones, S.M., Morgan, L.A., Pierce, K.L., Widdowson, M., Xu, Y.G., 2007. Regional uplift associated with continental large igneous provinces: The roles of mantle plumes and the lithosphere. Chemical Geology, The Great Plume Debate: Testing the Plume Theory 241, 282–318.
[4] Hofmann, A. W., & White, W. M. (1982). Mantle plumes from ancient oceanic crust. Earth and Planetary Science Letters, 57 (2), 421–436.
[5] Jackson, M. G., Hart, S. R., Koppers, A. A. P., Staudigel, H., Konter, J., Blusztajn, J. et al. (2007). The return of subducted continental crust in Samoan lavas. Nature, 448 (7154), 684–687.
[6] Sobolev, A. V., Hofmann, A. W., Kuzmin, D. V., Yaxley, G. M., Arndt, N. T.,538 Chung, S.-L. et al. (2007). The Amount of Recycled Crust in Sources of Mantle-Derived Melts. Science, 316 (5823), 412–417.
[7] French, S.W., Romanowicz, B., 2015. Broad plumes rooted at the base of the Earth's mantle beneath major hotspots. Nature 525, 95–99.
[8] Davaille, A., Romanowicz, B., 2020. Deflating the LLSVPs: Bundles of Mantle Thermochemical Plumes Rather Than Thick Stagnant "Piles." Tectonics 39, e2020TC006265.
[9] Munch, F.D., Romanowicz, B., Mukhopadhyay, S., Rudolph, M.L., 2024. Deep mantle plumes feeding periodic alignments of asthenospheric fingers beneath the central and southern Atlantic Ocean. Proceedings of the National Academy of Sciences 121, e2407543121.
[10] Dannberg, J., Sobolev, S.V., 2015. Low-buoyancy thermochemical plumes resolve controversy of classical mantle plume concept. Nature Communications 6, 6960.
[11] Leitch, A.M., Davies, G.F., 2001. Mantle plumes and flood basalts: Enhanced melting from plume ascent and an eclogite component. Journal of Geophysical Research: Solid Earth 106, 2047–2059.
[12] Sobolev, S.V., Sobolev, A.V., Kuzmin, D.V., Krivolutskaya, N.A., Petrunin, A.G., Arndt, N.T., Radko, V.A., Vasiliev, Y.R., 2011. Linking mantle plumes, large igneous provinces and environmental catastrophes. Nature 477, 312–316.
[13] Stixrude, L., Lithgow-Bertelloni, C., 2024. Thermodynamics of mantle minerals — III: the role of iron. Geophysical Journal International 237, 1699–1733.
[14] Steinberger, B., Calderwood, A.R., 2006. Models of large-scale viscous flow in the Earth's mantle with constraints from mineral physics and surface observations. Geophysical Journal International 167, 1461–1481.
[15] Lu, Q., and Rudolph, M.L. in review. Melt production and volatile release from broad thermochemical plumes. Submitted to Geophysical Research Letters.

Updated lunar crustal thickness distribution from global geodynamic models

Sabatino Santangelo*[1], Adrien Broquet[1], Gael Cascioli[1,2], Ana-Catalina Plesa[1], Doris Breuer[1], and Hauke Hussmann[1]

[1]German Aerospace Center (DLR)
[2]Technische Universität Berlin
*sabatino.santangelo@dlr.de

Keywords: moon, crust, crustal thickness, geodynamics, lunar evolution, heat producing elements

Introduction: An asymmetrical concentration of radiogenics in the lunar mantle has been suggested to cause a long-standing thermal anomaly of several hundreds of K, which could have lasted up to present-day [1,2]. Such a subsurface temperature distribution at present-day will induce gravity field anomalies that can affect crustal thickness inversions. Interestingly, thermal anomalies have also been suggested to affect the degree-3 component of the tidal response of the Moon [2].

Here, we combine thermal evolution models that account for crustal thickness variations [1] with gravity and topography inversions for crustal thickness that take thermally-induced density anomalies as input [3,4]. Thus, we provide a coupled, self-consistent estimate of the lunar mantle temperature and its crustal structure.

Methods: This work focuses on the best-fit model in [1] (Figure a), which is consistent with both Apollo heat flow experiments [5], Blue Ghost Mission 1 LISTER [6], and LMS [7] experiments.

The setup in Figure a consists of a geodynamic model overlaid with a crustal thickness model, as described in [1]. At present-day, this model produces a temperature field which predicts a positive thermal anomaly of ~100-200 K underneath the nearside Procellarum KREEP Terrane (PKT), and two smaller anomalies (~50-100 K) underneath the farside highlands terrane (positive) and south pole-Aitken basin (negative).

The 3D temperature field is then discretized into layers from the surface to the core and converted into a density field assuming a mantle density and thermal expansion coefficient of 3400 kg/m^3 and $2 \cdot 10^{-5}$ K^{-1}, respectively. Thereafter, the gravity anomaly associated with density variations within each layer is computed following [8], using the DSP code [9]. These anomalies are then fed into a global inversion model that self-consistently solves for mare and feldspathic crustal thickness from observed gravity and topography [9].

Results: The update in crustal thickness resulting from our approach is shown in Figure b. As expected, regions where subsurface temperatures were higher than average result in a crustal thinning (e.g., PKT, Farside Highlands). Conversely, regions of colder-than-average interior, such as basins, show crustal thickening subsequent to our calculation (e.g., SPA).

The most prominent variation in crustal thickness is related to the nearside temperature anomaly and reflects the shape of the modeled PKT area. Within this area, we obtain a crustal thinning of ~20 % (~8.5 km) with respect to the original crustal thickness model which did not account for a variable mantle density [4]. The secondary temperature anomalies associated with the farside highlands and the south pole-Aitken basin induce a crustal thinning and thickening, respectively, of about 3 km. Outside of these three regions, we see moderate crustal thickening throughout the lunar surface.

Conclusion: In this work we successfully quantify the effect of mantle thermal anomalies predicted by geodynamic models on lunar crustal thickness inversions. We build a self-consistent model of the present-day thermal state and crustal structure of the Moon, where the thickness of the lunar crust is up to 20 % different with respect to previous inversions.

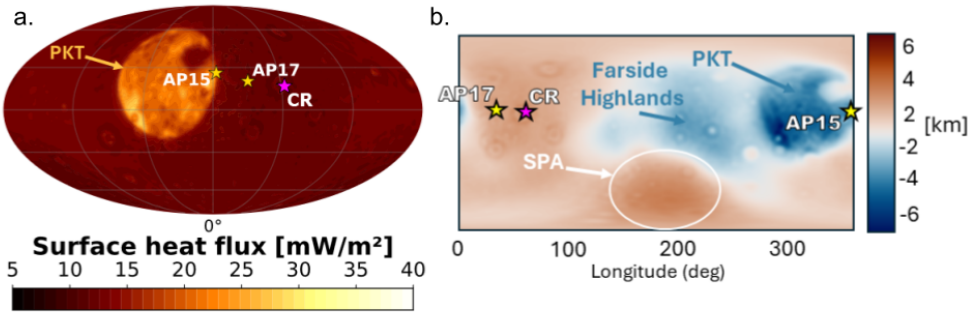


Figure: a) Surface heat flux distribution from one of the best-fit models in [2]. This setup consists of a radiogenic anomaly of ~1200 km in radius, and 30 ppm Th equivalent concentration for a 1.6 km thick layer. Bulk abundance of radiogenics is equivalent to 90 ppb Th. b) Variations in crustal thickness inversion induced by temperature anomalies in the mantle. Locations of Procellarum KREEP Terrane (PKT), farside highlands, south pole-Aitken, Apollo 15, Apollo 17, and mare Crisium are annotated in the map.

References

[1] Santangelo, S., Plesa, A.-C., Broquet, A., Breuer, D., & Grott, M. (2025). Present-day thermal state and surface heat flux of the Moon. Journal of Geophysical Research: Planets, 130, e2025JE009458. https://doi.org/10.1029/2025JE009458
[2] Park, R.S., Berne, A., Konopliv, A.S. et al. Thermal asymmetry in the Moon's mantle inferred from monthly tidal response. Nature 641, 1188–1192 (2025). https://doi.org/10.1038/s41586-025-08949-5
[3] Mark A. Wieczorek et al., The Crust of the Moon as Seen by GRAIL. Science 339, 671–675 (2013). doi:10.1126/science.1231530
[4] Broquet, A., Maia, J., & Wieczorek, M. A. (2025). On the crustal architecture of the terrestrial planets. Journal of Geophysical Research: Planets, 130, e2025JE009139. https://doi.org/10.1029/2025JE009139.
[5] Langseth, M. G., Keihm, S. J., & Peters, K. (1976, April). Revised lunar heat-flow values. In In: Lunar Science Conference, 7th, Houston, Tex., March 15-19, 1976, Proceedings. Volume 3.(A77-34651 15-91) New York, Pergamon Press, Inc., 1976, p. 3143–3171. (Vol. 7, pp. 3143–3171).
[6] Nagihara, S., Zacny, K., Ngo, P., Sanasarian, L., Misra, R., Grott, M., et al. (2026). First robotic attempt to measure heat flow of the Moon: Deployment of LISTER on Blue Ghost Mission One to Mare Crisium (No. EGU26-6066). Copernicus Meetings.
[7] Johnson, C. L., Grimm, R. E., Espley, J., Garrick-Bethel, I., Howard, S. K., Maxwell, R. E., et al. (2026). Results from the Lunar Magnetotelluric Sounder on Blue Ghost Mission 1 (No. EGU26-8526). Copernicus Meetings.
[8] Wieczorek, M. A., & Phillips, R. J. (1998). Potential anomalies on a sphere: Applications to the thickness of the lunar crust. Journal of Geophysical Research: Planets, 103(E1), 1715–1724.
[9] Broquet, A., & Andrews-Hanna, J. C. (2024). The moon before mare. Icarus, 408, 115846.

Role of Local and Far-Field Forces in Central and Eastern U.S. Intraplate Seismicity

Arushi Saxena*[1], Maria Beatrice Magnani[2], and Eunseo Choi[3]

[1]University of California Davis
[2]Southern Methodist University
[3]Center for Earthquake Research and Information, University of Memphis
*ahsaxena@ucdavis.edu

Keywords: intraplate seismicity, tectonics

The Central and Eastern United States (CEUS), located in the cratonic interior far from active plate boundaries, exhibits ongoing seismicity and a complex near-surface stress state. While several local and plate-boundary mechanisms have been proposed to explain this deformation, the relative contributions of these sources remain poorly quantified. With the increasing availability of high-resolution seismological and geodetic constraints, we address this question using geodynamic models.

We develop instantaneous 3-D numerical models representing CEUS that incorporate heterogeneities from surface to the mantle-transition zone. These input models are implemented in the community geodynamics code ASPECT in a modular framework, enabling smooth integration of input from different observational models. Our models utilize a strain-weakening viscoplastic rheology where materials creep by dislocation up to a deviatoric stress limit, which is defined by the Drucker-Prager yield criterion and decreases as strain accumulates. We apply far-field plate stresses along the side boundaries, and quantify which of the major sources of heterogeneities considered here primarily increase stresses along the preexisting faults in the CEUS.

Our models reveal a positive correlation between observed seismicity and surface deformation driven by upper mantle flow, highlighting the importance of deep mantle dynamics in controlling intraplate stress. Removing gravitational potential energy contributions due to topographic variations reduces this correlation, suggesting that this force partially opposes the overall shearing motion rather than supplementing it. Together, these results provide a present-day, physically consistent representation of the CEUS stress field and offer a framework for exploring the interplay among mantle dynamics, lithospheric structure, and intraplate seismicity in cratonic settings.

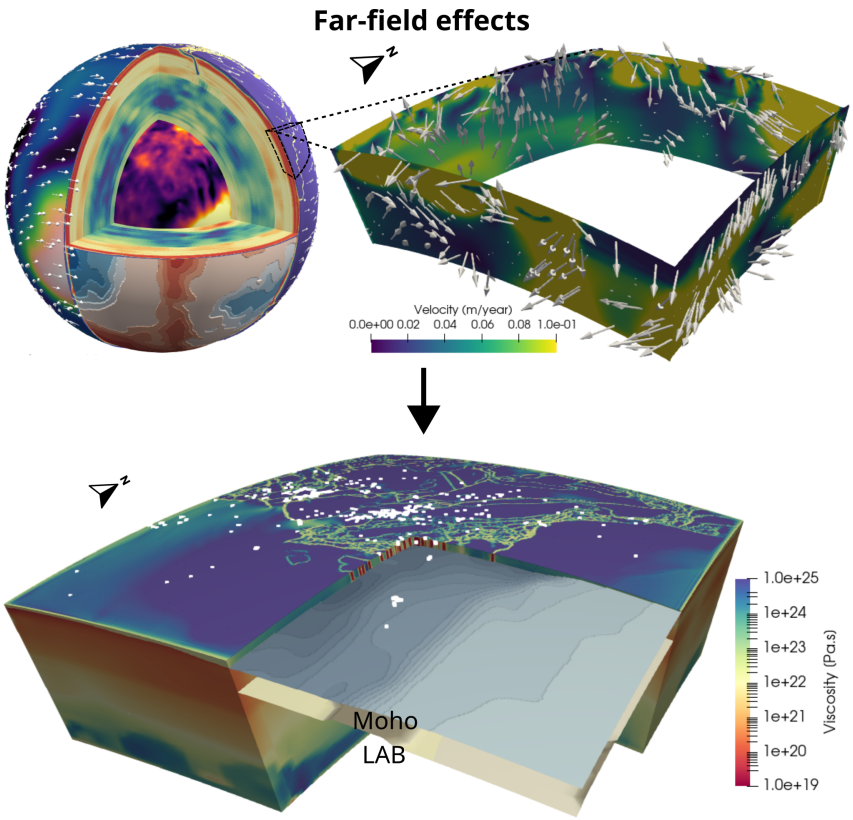


Figure: (top) Velocities extracted from a global mantle-flow model as boundary constraints for our regional model. (bottom) Viscosity distribution in our model with contours showing crustal and lithospheric mantle structure discontinuities.

Two-phase flow modelling with FEniCSx: benchmarking and first steps into studying deformation and fluid flow feedback in simple shear

Felipe Sáez Leiva*[1], Néstor Cerpa[1], and Andréa Tommasi[1]

[1]Géosciences Montpellier, CNRS & Université de Montpellier, France
*felipe.saez-leiva@umontpellier.fr

Keywords: two-phase flow, Finite Element Method, benchmark

Study of natural shear zones, both in the crust and mantle, often highlights both fluid-controlled weakening and deformation-controlled focusing of fluids. Indeed, fluids, which can be either melts or aqueous, induce softening in rocks, even in small proportions (< 10%) [1,2,3,4]. This feedback loop between deformation and fluids result in highly effective strain localization. Fluid transport in deformable media has been studied in numerous work [5, 6]. Nonetheless, the effect of large strain deformation of the solid matrix in response to external stresses on this interaction is still poorly understood.

To address the nature of this coupling, as well as the effect it has on deformation, we have implemented the three-field formulation [7] of the two-phase flow problem in FEniCSx, a finite element model library that provides an interface to create simple, flexible and efficient Python scripts to solve a boundary value problem. In this contribution, we present the benchmarking of our code by (1) comparison of our results on a instantaneous viscous inclusion test with those from a similar formulation implemented in a finite difference software, and (2) comparison to the 1D and 2D solitary wave benchmark. We also show preliminary results on the behaviour of a solitary wave in a solid medium deforming by simple shear.

References

[1] Tommasi, A., Vauchez, A., Fernandes, L.A.D., Porcher, C.C., (1994). Magma-assisted strain localization in an orogen-parallel transcurrent shear zone of southern Brazil. Tectonics 13, 421–437.
[2] Zimmerman, M., Zhang, S., Kohlstedt, D. & Karato, S. (1999). Melt distribution in mantle rocks deformed in shear. Geophys. Res. Lett. 26, 1505–1508.
[3] Katz, R.F., Spiegelman, M., Holtzman, B., (2006). The dynamics of melt and shear localization in partially molten aggregates. Nature 442, 676–679
[4] Chardelin, M., Tommasi, A., Padrón-Navarta, J.A., 2024. Progressive Strain Localization and Fluid Focusing in Mantle Shear Zones during Rifting: Petrostructural Constraints from the Zabargad Peridotites, Red Sea. J. Petrol. 65, egae081
[5] Yarushina, V. M., & Podladchikov, Y. Y. (2015). (De)compaction of porous viscoelastoplastic media: Model formulation. Journal of Geophysical Research: Solid Earth, 120(6), 4146–4170. https://doi.org/10.1002/2014JB011258
[6] Keller, T., May, D. A., & Kaus, B. J. P. (2013). Numerical modelling of magma dynamics coupled to tectonic deformation of lithosphere and crust. Geophysical Journal International, 195(3), 1406–1442. https://doi.org/10.1093/gji/ggt306
[7] Lu, G., May, D. A., & Huismans, R. S. (2024). A three-field formulation for two-phase flow in geodynamic modeling: Toward the zero-porosity limit. Journal of Geophysical Research: Solid Earth, 129, e2023JB027469. https://doi.org/10.1029/2023JB027469

Thermal structure modeling of subduction zones incorporating two-phase fluid flow

Minji Seong*[1] and Byung-Dal So[1,2]

[1]Interdisciplinary Program in Earth Environmental System Science and Engineering, Kangwon National University, Chuncheon 24341, South Korea
[2]Department of Geophysics, Kangwon National University, Chuncheon 24341, South Korea.
*bdso@kangwon.ac.kr

Keywords: subduction zone, two-phase flow, numerical modeling, finite element method

Subduction is a fundamental geodynamic mechanism driving the recycling of material and energy within Earth as lithospheric plates descend into the mantle at convergent boundaries. The descent of cold oceanic lithosphere influences the thermal structure of the mantle wedge by controlling the temperature distribution and flow pattern. Such thermal-dynamic coupling contributes to arc volcanism and the long-term evolution of oceanic lithosphere.

In subduction zones, thermal structure, mantle flow, and viscosity structure are interrelated. Dehydration reactions in the subducting oceanic crust supply fluids to the mantle wedge. The supplied fluids further affect the viscosity structure and thermal structure of mantle materials. Therefore, a model that incorporates thermal structure, mantle flow, viscosity structure, and fluid flow enables a more realistic interpretation of subduction zone thermal structure.

In this study, we develop a thermal structure model that incorporates two-phase flow in subduction zones using Firedrake, an open-source finite element platform. The two-phase formulation describes the coupled motion of a solid mantle matrix and a fluid phase released by dehydration reactions. The governing equations simulate fluid migration through the mantle wedge. Compaction pressure serves as an additional variable for analyzing fluid distribution and migration pathways in the modeled domain. The model offers a framework for interpreting the thermal, hydrological, and mechanical structures of subduction zones, including metamorphic reactions in the oceanic crust, arc volcanism, and estimates of mantle wedge viscosity structure.

Model-derived temperature and pressure structures serve as input parameters for mineral metamorphism experiments simulating subduction zone environments. Temperature and pressure conditions in subduction zones constrain mineral stability and magnetic properties in the subducting oceanic crust. Magnetic anomaly surveys in subduction zones show reduced anomaly amplitudes along the subducting oceanic plate. Such reduction is associated with demagnetization caused by metamorphism of magnetic minerals during subduction. These model-derived conditions guide uniaxial compression experiments using natural magnetic minerals. Measurements of magnetization changes under these conditions enable integrated modeling-experiment investigation of magnetic anomaly reduction in subduction zones.

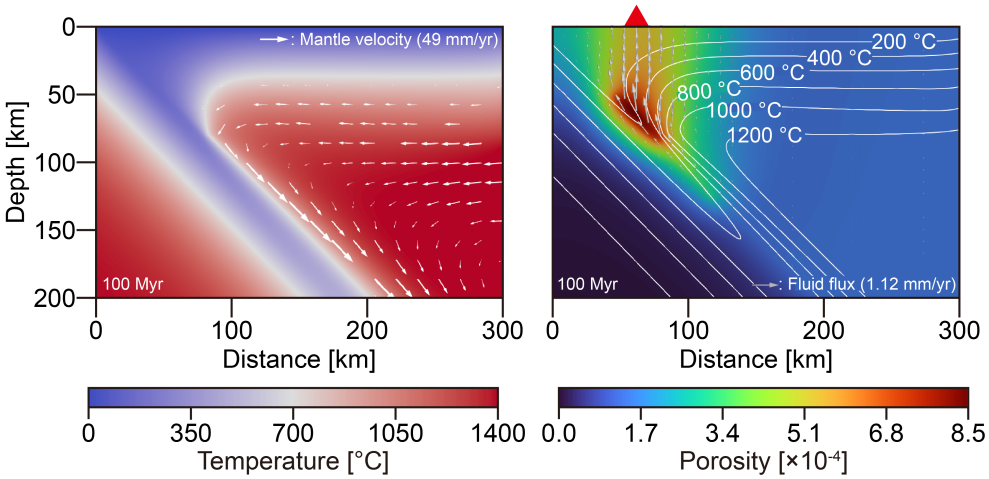


Figure: Temperature field (left) and porosity distribution (right) at 100 Myr. White arrows indicate solid mantle velocity in the left and fluid flux in the right. White contours denote isotherms at 200 °C intervals, and the red triangle marks the volcanic arc.

Did supracrustal materials build Archean continents? Evidence from coupled S-Si isotopes

Kun Shang*[1], Jian Zhang[1], Zaicong Wang[2], Ian Cawood[1], Yawen Cui[3], Ming Li[2], Ruihong Chang[1], Yanan Shen[3], and Guochun Zhao[1,4]

[1]The University of Hong Kong
[2]China University of Geosciences, Wuhan
[3]University of Science and Technology of China
[4]Northwest University
*kshang@connect.hku.hk

Keywords: sulfur and silicon isotopes, Archean continent, TTG

The formation of Archean continental crust by partial melting of hydrous mafic protoliths is widely acknowledged, yet the nature and origin of the mafic protolith itself remains strongly debated. One school of thought proposes hydrothermally altered basaltic rocks as the protolith, whereas another argues that lower crustal mafic cumulates can equally account for the geochemical signatures of TTGs. Coupled silicon and quadruple sulfur isotopes serve as particularly powerful tools in this debate, as their distinctive fractionation mechanisms and chemical behavior exclude the influence of secondary processes and directly trace the source reservoirs of felsic crust. Here, we present integrated whole-rock silicon and sulfur isotopic data for Neoarchean granitoids from the North China Craton to elucidate the origin and evolution of their protoliths. Most granitoids display non-zero $\Delta^{33}S$ (0.01 ‰ to −0.24 ‰) and elevated $\delta^{30}Si$ (−0.09 ‰ to −0.05 ‰), indicative of a supracrustal source and notably distinct from previously reported mantle-like zircon $\delta^{18}O$ values. A global dataset demonstrates that granitoids younger than 3.8 Ga consistently exhibit elevated $\delta^{30}Si$ and non-zero $\Delta^{33}S$, implying that the vast majority—if not all—of Archean continental crust was generated by partial melting of supracrustal materials rather than unaltered mafic cumulates.

Volatile distribution in a Crystallizing Venusian Magma Ocean with hydrodynamic escape

Brandon Lopez*[1] and Shi J. Sim[1]

[1]Georgia Institute of Technology
*blopez49@gatech.edu

Keywords: magma ocean, volatiles, Venus, hydrodynamic escape

The initial distribution of volatiles between the interior and atmosphere of a rocky planet is largely determined during the magma ocean crystallization phase of planetary development. Water and carbon dioxide dissolved in the magma outgas into the primordial atmosphere as the magma ocean cools, providing greenhouse effect that affects the thermal evolution of the interior. Volatile-rich magma can be trapped into the freezing residual mantle especially if the magma ocean cools rapidly. The balance of these processes determines both the atmospheric and interior volatile budget, setting the stage for secular planetary evolution and the thermochemical surface conditions for potential life. The trapping of volatiles into the freezing residual mantle has previously been modeled with a constant fraction of melt trapped in the freezing volume. However, this process is dynamic and scales with the rate of cooling of the magma ocean. This work models the magma ocean crystallization phase and the effects of constant and dynamic melt trapping on the volatile distribution for rocky planets in the inner Solar System based on previous work [1]. A grey atmosphere model for a coupled carbon dioxide and water atmosphere with hydrodynamic escape is simulated with a one-dimensional thermochemical evolution model of the magma ocean for a range of initial water masses from 0.01 to 20 Earth oceans, H:C ratios from 0.1 to 100, and a range of orbits from 0.2 to 2 AU. KLB-1 peridotite is used for the solidus and liquidus and all simulated planets has Earth-like masses and gravity. Results show that dynamic melt trapping sequesters more volatiles into the mantle relative to constant-fraction models, producing drier primordial atmospheres for Earth-relevant H:C ratios. Furthermore, results suggest that considering carbon dioxide into the mix has more effect while hydrodynamic escape is less influential compared to previous study [2]. These differences have significant implications for the long-term volatile cycling and potential habitability of Earth-sized planets across the inner Solar System.

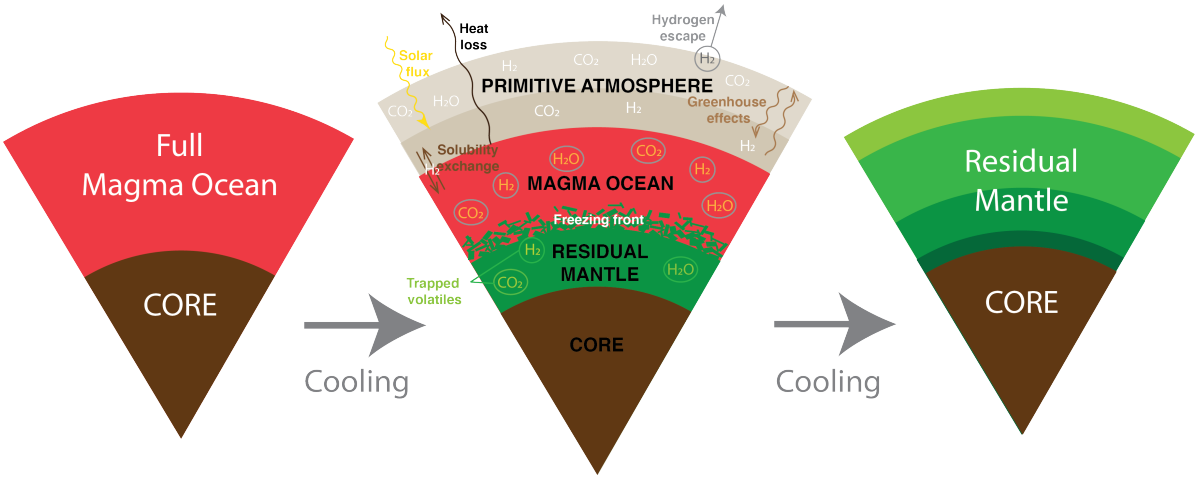


Figure: Schematic on magma ocean evolution

References

[1] Sim, S. J., Hirschmann, M. M., & Hier-Majumder, S. (2024). Volatile and trace element storage in a crystallizing martian magma ocean. Journal of Geophysical Research: Planets, 129(8), e2024JE008346.
[2] Hamano, K., Abe, Y., & Genda, H. (2013). Emergence of two types of terrestrial planet on solidification of magma ocean. Nature, 497(7451), 607–610.

Investigating the Stability of Thermochemical Piles for Different Origins

Henry W. Sitte*[1], Claudia Stein[1], and Ulrich Hansen[1]

[1]Institute of Geophysics, University of Münster, Münster, Germany
*h.sitte@uni-muenster.de

Keywords: LLSVPs, mantle convection, rheology, thermochemical piles, stability

The presence of large regions with strongly reduced seismic velocities (LLSVPs) in the lower mantle of the Earth raised many questions about the nature and origin of these structures. Many of which are still open for debate. From seismological observations, it is known that the LLSVPs extend over several hundred kilometers, vertically and horizontally, and are likely thermochemical. Different hypothesis exist in regards to the origin of the chemically distinct material that forms the LLSVPs. It could originate from a basal layer enriched in iron that formed during the magma ocean phase due to fractional crystallization or from interaction between core and mantle material in which iron-rich material diffuses from the outer core into the lower mantle. Another theory proposes the accumulation of subducted oceanic crust at the core-mantle boundary.

We investigate the stability of thermochemical piles in 2D Cartesian mantle convection simulations for different origin scenarios. This includes, for example, the longevity of the pile structures, as well as the spatial stability (strong horizontal movement or localized stagnation). Modelled structures formed from a material influx through the bottom boundary are usually smaller but longer-lived compared to piles from a primordial layer. Additionally, the effect of different rheological parameters on the stability of the thermochemical piles is investigated. Increasing the top (stress dependence) or bottom viscosity (composition or depth dependence) yields longer-lived piles that are spatially more stable due to less turbulent convection. Likewise, a thermal expansivity decreasing with depth reduces the convective vigor and, hence, stabilizes the thermochemical structures. First modelling results featuring thermochemical structures at the core-mantle boundary resulting from subducted material will also be presented.

To conclude, our mantle convection models show that thermochemical piles could have formed at the core-mantle boundary following the magma ocean phase and survive until the present day. The stabilizing effect of rheological parameters is similar for different origin scenarios, but longevity and size can vary depending on the source of the material.

From Thermochronology to Geodynamics - Adapting Uncertainty Analysis for Lithosphere and Mantle Modeling

Stephanie A. Sparks*[1] and Kip V. Hodges[2]

[1]The College of Wooster, Ohio, USA
[2]Arizona State University, Arizona, USA
*ssparks@wooster.edu

Keywords: uncertainty quantification, sensitivity analysis, Taguchi method, Earth systems' modeling

Numerical geodynamic models are increasingly used to investigate coupled Earth system processes across a wide range of spatial and temporal scales. Despite the importance of these models, formal uncertainty quantification and systematic parameter influence analysis remain comparatively uncommon in geodynamic workflows. This limitation is due in part to the large and complex parameter spaces characteristic of Earth system simulations, as well as the substantial computational cost associated with running replicate experiments. As a result, many studies rely on limited one-at-a-time parameter exploration or qualitative assessments of model sensitivity, making it difficult to rigorously evaluate uncertainty and parameter interactions.

This work proposes the adaptation of computationally efficient uncertainty analysis approaches, including the Taguchi method, to lithospheric deformation and mantle convection modeling contexts. These methods were initially developed and tested within thermal–kinematic modeling frameworks during my dissertation research, where they were applied across models of increasing complexity. Benchmark experiments ranged from simple geothermal gradient calculations and closure temperature models to full one-dimensional thermal–kinematic simulations. By comparing multiple approaches to parameter influence analysis, including one-at-a-time methods, full factorial design, and orthogonal array–based Taguchi designs, this work demonstrated that dominant first-order parameter influences consistently emerge even in relatively high-dimensional parameter spaces.

These results suggest that computationally tractable uncertainty frameworks can be implemented both within and across modeling platforms while substantially reducing the number of simulations required relative to traditional experimental designs. In particular, orthogonal array methods provide an efficient strategy for identifying dominant controls on model behavior while preserving interpretability in computationally expensive systems. This creates an opportunity to expand these approaches into broader geodynamic applications where uncertainty analysis remains limited by computational cost and model complexity.

Future work will investigate how efficient experimental design and parameter influence analysis can be incorporated into lithospheric deformation and mantle convection simulations. These systems introduce additional challenges associated with strongly coupled thermal, mechanical, and rheological processes, as well as emergent behaviors that may depend sensitively on parameter selection. Extending computationally efficient uncertainty quantification approaches to these models may improve the interpretability, reproducibility, and comparative analysis of geodynamic simulations while helping identify which parameters most strongly influence predicted tectonic and lithospheric behavior.

More broadly, this work aims to contribute toward transferable uncertainty analysis frameworks that can be adapted across Earth system modeling applications. By improving the tractability of systematic parameter exploration in computationally intensive simulations, these approaches may help bridge methodological gaps between thermal–kinematic, lithospheric, and mantle-scale modeling studies while supporting more robust interpretation of geodynamic model results.

Revisiting Thermal Evolution Models of Rocky Planets using Asymmetric Thermal Boundary Layers

Dave Stegman*[1] and Victoria Auerbach[1]

[1]Institute of Geophysics and Planetary Physics, Scripps Institution of Oceanography, University of California, San Diego, La Jolla, CA, USA
*dstegman@ucsd.edu

Keywords: basal magma ocean, stagnant lid, mantle convection

We describe several suites of 1D thermal evolution models using parameterized convection for a variety of scenarios including a Mars-sized planet in the stagnant lid regime, and Earth-sized and Venus-sized planets in mobile lid regime with a crystallizing basal magma ocean (BMO). The interiors of the planets are modeled as compressible fluids with adiabatic increases in pressure and temperature, which lead to associated depth-dependent changes in mantle viscosity. We develop a method that allows the upper and lower thermal boundary layers (TBLs) to be locally defined and evolve independently, which leads to asymmetries in their viscosity, thickness, and heat flow. Our results indicate the widely used assumption of symmetric TBLs within parameterized convection models imposes an artificial constraint on the system that can lead to spurious outcomes. As an example, symmetric TBLs do not allow for the possibility of heat transfer from the mantle into the core, which can arise under certain conditions (e.g. within stagnant lid planets at larger Urey ratios) and can extend for over 1 billion years in duration. This treatment for separate TBLs in mantles with a crystallizing BMO is particularly important since the lower TBL defines the coupling between the overlying solid mantle to the BMO. Our results show the longevity of the BMO is strongly dependent on initial conditions that directly effect the properties and subsequent evolution of the lower TBL. We further show that the most important uncertainties is the activation volume (and assumed deformation mechanism) for the lowermost mantle and the extent to which current rheological formulations are appropriate.

A new approach to estimate oceanic upper mantle viscosity structure

Bernhard Steinberger and Shipboard Party SO319*[1]

[1]GFZ Helmholtz Centre for Geosciences
*bstein@gfz.de

Keywords: plume, viscosity, mantle

Mantle viscosity is one of the most important parameters that determine the structure of convection in the Earth's mantle, hence the evolution of the mantle. Yet, even 90 years after the classic estimate by Haskell, it remains poorly determined with various recent estimates for any given depth often differing by an order of magnitude or more. Here we present a new approach to estimate the radial profile of upper mantle viscosity below the Pacific plate: It makes use of the fact that the motion of the Pacific plate relative to the Hawaii hotspot has changed at ≈47 Ma, giving rise to the bend in the Hawaiian-Emperor Seamount chain: Until ≈47 Ma, relative plate motion was ≈northward, and material emplaced beneath the Emperor Chain would have remained beneath. Yet after the relative plate motion changed after ≈47 Ma, this material should have been sheared off by an amount that depends on how well it is coupled to the overlying plate, i.e. mantle viscosity structure: it should be sheared off more, if the plate is decoupled from the underlying mantle by a zone of low viscosity.

Here we present both analytical and numerical results. Numerical results were computed with ASPECT. The modelling domain is a cartesian box of length x width x depth = 4620 km x 3960 km x 660 km, i.e. with aspect ratio 7:6:1. Viscosity is explicitly depth-dependent (for a given adiabatic reference temperature profile) and temperature-dependent for deviations from the adiabatic profile. We test four different radial viscosity profiles: One without low-viscosity asthenosphere, one with a thin channel of reduced viscosity, one with a wider channel and one where the entire upper mantle has reduced viscosity. Plume influx is prescribed at the bottom of the box, and plate motions are prescribed at its surface. Velocities inferred from a global mantle flow model are prescribed at the sides of the box. Through comparison to results without, the influence of this large-scale flow can be seen: Regional flow in the upper mantle shifts from aligned with the plates immediately below the lithosphere towards northward at greater depth, hence influences the advection of plume material in the upper mantle.

To obtain results for the the seismic velocity and electrical conductivity distribution that can be compared to the computed temperature distribution for different models, ocean bottom seismometers and electromagnetometers have been deployed during a cruise with the Japanese research vessel Hakuhomaru in October 2025 and collected again during a cruise with the German research vessel Sonne in spring 2026.

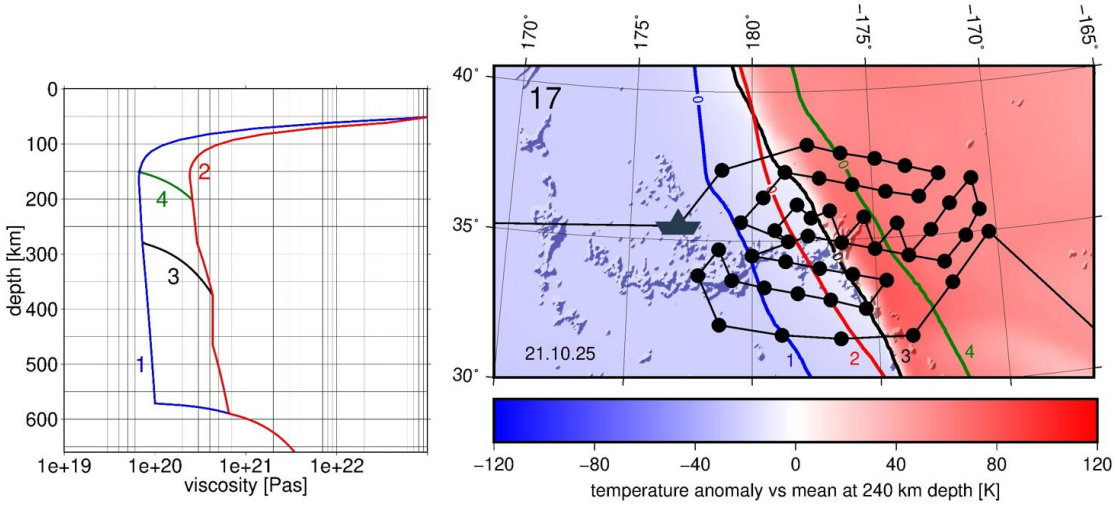


Figure: Different upper mantle viscosity structures (left) and resulting temperature anomalies at 240 km depth for the reference case (black line). The zero isocontours are also shown for the other viscosity structures, with the same colors

Using ASPECT to construct a fully coupled 3D geodynamic landscape evolution model - Preliminary results and Outlook

Simran Suresh*[1], Menno Fraters[1], and Daniel Douglas[2]

[1]Department of Earth Sciences, University of Graz, Austria
[2]Boston College (MA, USA)
*simran.suresh@uni-graz.at

Keywords: New Zealand, subduction, LPO, seismic anisotropy, uplift

New Zealand is undergoing rapid uplift and exhumation since 5 Ma [1]. Subduction of the Pacific plate at the Hikurangi restarted 25–30 Ma ago [2,3], since then, the crustal thickness of the Pacific plate has increased making it buoyant and inhibiting subduction [2,4]. Compressional stresses between the Pacific-Australian plates increased to compensate for this resistance, thereby making the strike-slip regime to oblique strike-slip one [5,6]. In the recent 5 Ma, all these tectonic forces, along with orographic precipitation and erosion related isostasy, lead to rapid uplift across the island and total uplift of 20 km since 12 Ma [5,7]. An understanding of this uplift pattern from the mantle to surface is essential. Several modelling studies focus on only the lithospheric deformation affecting the surface processes [4,7] without considering the deeper interaction with the mantle like Lattice preferred orientation (LPO) in this region. We aim to fill this gap by developing a fully coupled 3D thermo-mechanical model using ASPECT [8] and GWB [9] of the lithosphere-mantle with the surface features. This will enable a better understanding of the recent uplift rates and topography evolution.

A recent study [10] has shown that interface viscosity of $5 \cdot 10^{20}$ Pa s best suits the observed plate motion, hydrated olivine agrees well with the seismic anisotropy and slab dehydration correlates with the seismic attenuation and volcanism in the region. These models were run for 6 Myr advecting the particles without updating the Stokes solution. To investigate the sudden 5 Ma uplift, we will construct a set of models starting at 10 Ma and run it forward in time, tracking the LPO evolution and comparing with present day seismic anisotropy observations. Coupling ASPECT to the surface evolution model OpenLEM [11] with allow for topography evolution developed by surface evolution processes like erosion and sedimentation in a complex tectonic setting. We plan to perform sensitivity tests by varying the slab structure and material parameters — slab dip, mantle wedge viscosity and convergence rates which directly control the topography wavelength, amplitude [12,13], and uplift rates. Currently, we present the initial setup of the region and planned experiments.

References

[1] Tectonics, 23, TC4001. Batt, G.E., Baldwin, S.L., Cottam, M.A., Fitzgerald, P.G., Brandon, M.T. & Spell, T.L. (2004). Cenozoic plate boundary evolution in the South Island of New Zealand: new thermochronological constraints. Tectonics, 23, TC4001.
[2] Nicol, A., Mazengarb, C., Chanier, F., Rait, G., Uruski, C. & Wallace, L. (2007). Tectonic evolution of the active Hikurangi subduction margin, New Zealand, since the Oligocene. Tectonics, 26, TC4002.
[3] Ballance, P.F. (1976). Evolution of the Upper Cenozoic magmatic arc and plate boundary in northern New Zealand. Earth and Planetary Science Letters, 28, 356–370.
[4] Herman, F., Cox, S.C. & Kamp, P.J.J. (2009). Low-temperature thermochronology and thermokinematic modeling of deformation, exhumation, and development of topography in the central Southern Alps, New Zealand. Tectonics, 28, TC5011.
[5] Walcott, R.I. (1998). Modes of oblique compression: Late Cenozoic tectonics of the South Island of New Zealand. Reviews of Geophysics, 36, 1–26.
[6] Sutherland, R. (1999). Cenozoic bending of New Zealand basement terranes and Alpine Fault displacement: a brief review. New Zealand Journal of Geology and Geophysics, 42, 295–301.
[7] Batt, G.E. & Braun, J. (1999). The tectonic evolution of the Southern Alps, New Zealand: insights from fully thermally coupled dynamical modelling. Geophysical Journal International, 136, 403–420.
[8] Bangerth, W., Dannberg, J., Fraters, M., Gassmöller, R., Glerum, A., Heister, T., Myhill, R. & Naliboff, J. (2024). ASPECT: Advanced Solver for Problems in Earth's ConvecTion User Manual. Zenodo.
[9] Fraters, M.R.T., Thieulot, C., van den Berg, A. & Spakman, W. (2019). The Geodynamic World Builder: a solution for complex initial conditions in numerical modelling. Solid Earth, 10, 1785–1807.
[10] Douglas, D., Fraters, M. & Billen, M. (2025). Constraining Solid Dynamics, Interface Rheology, and Slab Hydration in the Hikurangi Subduction Zone Using 3-Dimensional Fully Dynamic models. Geochemistry, Geophysics, Geosystems, 26, e2024GC011824.
[11] Hergarten, S. (2020). Transport-limited fluvial erosion - simple formulation and efficient numerical treatment. Earth Surface Dynamics, 8, 841–854.
[12] Crameri, F., Lithgow-Bertelloni, C.R. & Tackley, P.J. (2017). The dynamical control of subduction parameters on surface topography. Geochemistry, Geophysics, Geosystems, 18, 1661–1687.

[13] Billen, M.I. & Gurnis, M. (2001). A low viscosity wedge in subduction zones. Earth and Planetary Science Letters, 193, 227–236.

Tracking the Geochemical Evolution of the Oceanic Crust Using a Multi-Component Geodynamic Model of Mid-Ocean Ridge Magmatism

Shona A. Swan*[1], Tobias Keller[2], Derek Keir[1], and Thomas Gernon[1]

[1]University of Southampton
[2]University of Glasgow
*S.A.Swan@soton.ac.uk

Mid-ocean ridge processes of melt generation, transport, and crust formation are indirectly observable across both spatial and temporal scales. Our current understanding of these systems relies primarily on geophysical imaging and geochemical signatures preserved in erupted products. Numerical geodynamic models are essential tools for investigating the coupled dynamics of mantle melting and magmatic transport beneath spreading centres.

Two-phase mantle magma dynamic models have improved our understanding of melt generation and focusing beneath mid-ocean ridges. However, many of these existing approaches simplify the treatment of oceanic crustal formation. Additionally, they typically neglect the tracking of geochemical evolution. This limits their ability to make direct comparisons between model predictions and observed mid-ocean ridge basalt (MORB) compositions.

We present a new model based on the framework of [1], which includes the first 4-field solver with a compressible formulation for mid-ocean ridge systems. The model includes non-linear rheologies and applies plastic failure in a MOR setup, enabling adaptive softening along the ridge axis in a more realistic manner than previous approaches.

We also implement a melt extraction and emplacement algorithm that enables simulation of oceanic crust formation within the model domain for the first time. This is coupled with a geochemical solver, allowing us to directly predict the full major, trace, and isotopic compositional variability and evolution of newly formed oceanic crust as well as the mantle residue. This enables direct comparison to extensive global datasets of MORB and abyssal peridotite compositions and the systematic study of how petrological and geochemical signatures arise from the coupled fluid mechanics and thermochemistry of a dynamic sub-ridge mantle. Preliminary parameter tests demonstrate the capabilities of the model and the types of dynamic and geochemical behaviour it can reproduce.

References

[1] Keller, T., Katz, R.F. and Hirschmann, M.M., 2017. Volatiles beneath mid-ocean ridges: Deep melting, channelised transport, focusing, and metasomatism. Earth and Planetary Science Letters, 464, pp. 55–68.

Viscous response of Enceladus' ice shell to hydrothermal vents

Klára Anna Šindlerová*[1], Martin Kihoulou[1], and Ondřej Čadek[1]

[1]Department of Geophysics, Faculty of Mathematics and Physics, Charles University, Prague, Czech Republic
*klara.anna@sindler.cz

Keywords: numerical modeling, thermal convection, phase transitions, Enceladus, icy moons, hydrothermal vents

Saturn's icy moon Enceladus is highly intriguing due to its potentially habitable subsurface ocean. The liquid state of the ocean is maintained by the thermal power generated by tidal dissipation in the moon's porous silicate core [1]. Recent studies [2–4] highlighted interesting features on Enceladus' surface: 100-km-scale oval-shaped depressions of unknown origin with a depth of 1–1.5 km. These regional depressions appear to be too smooth to be of impact or tectonic origin, but as suggested by Schenk and McKinnon [4], they might be a viscous response of the ice shell to local thinning caused by hydrothermal vents located at the seafloor.

To investigate this scenario, we developed a numerical code that solves viscous deformation of the ice shell using finite element software FEniCS [5]. We solve equations of thermal convection, incorporating free-surface boundary conditions at both the surface and the ice-ocean interface, where we also account for the ice-water phase transition. The shape of the domain is evolved using the ALE method [6]. Boundary temperatures are fixed for each simulation; however, we test various surface temperatures across runs (59 K, 100 K, and 140 K) to account for the insulating effect of a hypothesized regolith layer [7]. The ice-ocean interface is kept at 270 K. The hydrothermal vents are mimicked by a Gaussian peak in the heat flux coming from the subsurface ocean, with amplitudes ranging from 0.1 to 0.5 W/m^2 and a width of 60 km.

We used this model to test the scenario where localized heat flux from the subsurface ocean induces thinning of the ice shell. This thinning drives a flow of ice toward the affected region, resulting in a topographic surface depression of up to 1.5 km deep in our models and thinning the ice shell to less than 2 km in some cases. Through our parametric study, we varied the heat flux amplitude, the ice shell thickness, and the surface temperature, and compared the resulting topography with observations [4]. The amplitude of the heat flux correlates with the final depth of the depression. On the other hand, surface temperature has little effect on the final depth of the depression, though it does affect the rate at which the depression forms. In general, thinner ice shells result in a deeper final topography. The best fit is found for models featuring a heat flux amplitude of 0.25 W/m^2 and a 20-km-thick ice shell, with the depression developing on a time scale of tens to hundreds of millions of years.

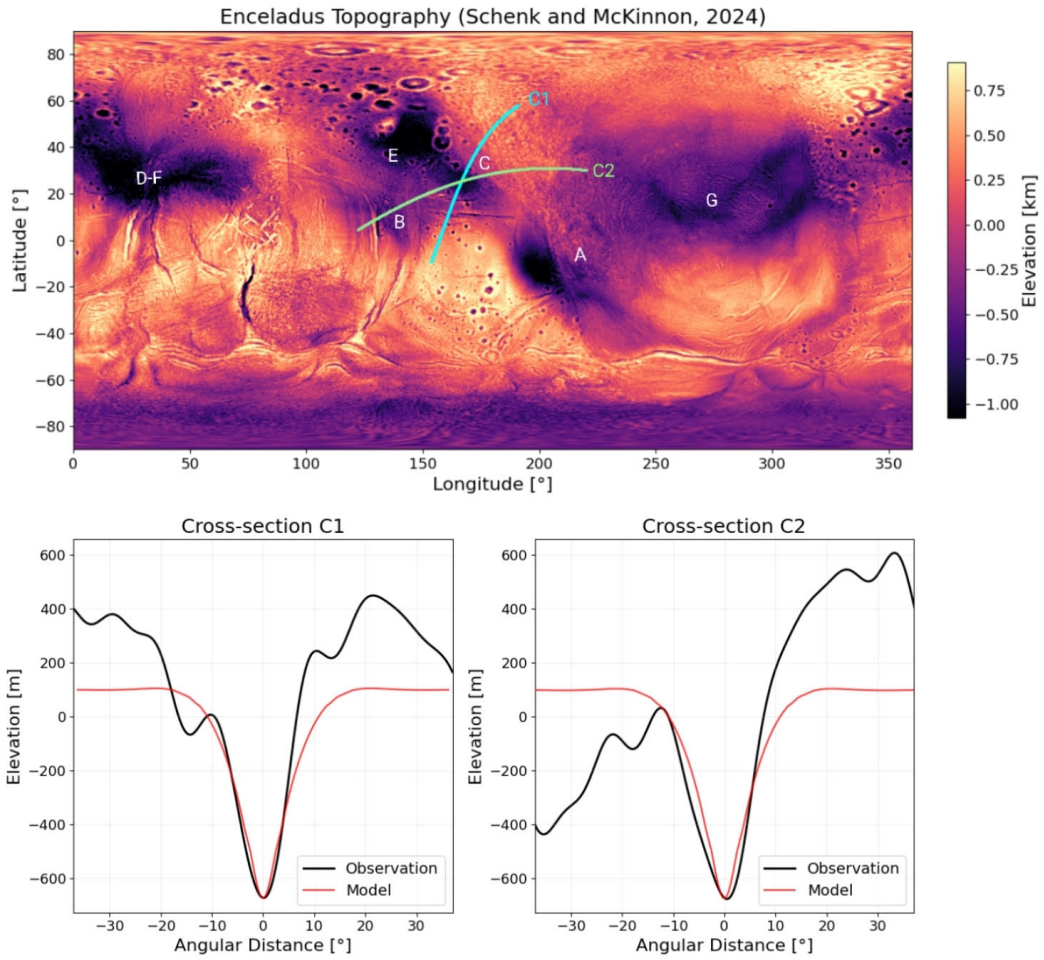


Figure: On the top, we show Enceladus' topography with the depressions labeled A-G [4]. The topography predicted in our model is compared with the observation in two cross-sections (blue and green lines C1 and C2), see the bottom panel (black line observation, red line model). The observed topography corresponds to spherical harmonic degrees 4–40.

References

[1] Choblet et al. (2017), Nat. Astron., 1, 841–847.
[2] Tajeddine et al. (2017), Icarus, 295, 46–60.
[3] Park et al. (2024), J. Geophys. Res. Planets, 129, e2023JE008054.
[4] Schenk and McKinnon (2024), Icarus, 408, 115827.
[5] Logg et al. (2012), The FEniCS Book, Springer–Verlag.
[6] Donea et al. (2004), Encyclopedia of Computational Mechanics, John Wiley & Sons, pp. 413-437.
[7] Martin et al. (2023), Icarus, 392, 115369.

Strength and sensitivity: Toward an a priori quantification of deformation localization potential in the ductile lithosphere

Catherine Thoraval*[1], Fanny Garel[1], Etienne Van Broeck[1], and Diane Arcay[1]

[1]Géosciences Montpellier, Université de Montpellier, CNRS, Montpellier, France
*catherine.thoraval@umontpellier.fr

Keywords: lithosphere, rheology, non-newtonian, ad-hoc yield stress, dislocation creep, deformation localization

A long-standing question regarding plate tectonics is how deformation localizes in a strong lithospheric 'intraplate' mantle up to a weak plate boundary. Geodynamical simulations reveal that deformation localization is the result of rheological feedbacks which allow mantle material weakening through temperature and/or strain rate increases. Such weakening can arise directly from the rheology's dependence on strain rate and/or indirectly by modifying material properties (e.g. grain size reduction) or by impacting fields characteristics (e.g. shear heating).

Classical creep rheologies yield unrealistically high viscosities for olivine below 1200 K ($> 10^{24}$ Pa·s), but recent numerical deformation *ab-initio* models and laboratory experiments suggest lower viscosities for olivine at these low temperatures.

To numerically reproduce a 'mobile-lid regime' atop a convective mantle, a pragmatic approach in rheological parameterization introduces an ad-hoc 'yield stress' leading to a strain-rate dependent viscosity limitation. However, this 'yielding' deformation is predicted throughout most of the lithospheric mantle up to 1500 K, far exceeding the domain of brittle deformation.

Meanwhile, the classical "Christmas tree" representation of rheological features highlights rheological variations at depths - but such representations are ill-suited for predicting the evolution of a geodynamical system.

Here, we propose a theoretical analysis of lithosphere rheological parameterizations to evaluate an *a priori* 'potential for deformation localization' by incorporating weakening dependencies on strain rate and temperature. This 'potential for deformation localization' is calculated for various rheological parameterizations such as

- dislocation creep flow laws (at high and low to high temperatures)
- 'yield-stress' pseudo-brittle approximation
- grain-boundary sliding
- diffusion creep.

The estimated potentials agree with (i) actual geodynamical simulations that feature the detailed non-newtonian feedbacks between plate weakening and deformation, and (ii) large-scale independent constraints on plate and asthenosphere macro-scale 'effective' viscosity.

Our results reconcile the effective yield stress estimates used in mobile-lid geodynamical convection simulations with realistic rheology based on actual deformation processes. This 'potential for deformation localization' can be extended to account for other physical processes that possibly impact rheological properties, such as grain size evolution or shear heating, and may serve as a screening tool for rheological parameterizations in large-scale dynamical models.

This study has benefited from funding by the French National Research Agency for the project RheoBreak (ANR-21-CE49-0009, PI F. Garel).

Modeling Iron Droplets Settling in Magma Ocean: Timescales of Core Formation

Sushilkumar Thounaojam[*1], Dr. Jun Yan[1], and Prof. Dr. Lena Noack[1]

[1]Freie Universität Berlin
[*]sushilkus99@zedat.fu-berlin.de

Keywords: iron droplets, metal-silicate differentiation, compressible magma ocean

During planetary accretion, core formation primarily occurs through the separation of iron-rich metal from silicate mantle as impactor-derived metal sinks through a magma ocean. The timescale and chemical equilibration of this metal-silicate separation critically depend on the dynamics of iron droplets within the magma ocean, governed by their size, buoyancy, and the viscosity contrast with the surrounding silicate mantle. With increasing size and mass of exoplanets, the sinking distance from surface to core-mantle boundary (CMB) increases which would increase the time of sinking with different sinking behaviours. Here, we investigate the sinking behaviour of iron droplets in magma ocean, deriving scaling laws for the iron-segregation timescale based on droplet size, buoyancy, and viscosity contrast. Our numerical simulations confirm that the settling velocity of a single droplet aligns with the analytical Stokes settling regime. We demonstrate that the sinking time is proportional to viscosity but inversely proportional to droplet surface area and buoyancy. Furthermore, different configurations for same number of iron droplets results in different sinking times; for instance, an adjacent configuration of two iron droplets sinks faster than the vertical configuration. Future work should extend this model to compressible two-phase flow and incorporate the effects of high pressure on local redox conditions, particularly relevant for understanding oxygenation of the lower mantle due to the core growth on rocky super-Earths.

References

[1] Shun-Ichiro Karato, and V. Rama Murthy. "Core formation and chemical equilibrium in the Earth—I. Physical considerations." Physics of the Earth and Planetary Interiors 100.1-4 (1997): 61-79.
[2] D.C. Rubie, F. Nimmo, H.J. Melosh. "Formation of Earth's Core." Treatise on Geophysics, edited by David J. Stevenson, 2nd ed., vol. 9, Elsevier, 2015, pp. 43-78.
[3] Stevenson, D. J. "Models of the Earth's Core." Science 214.4521 (1981): 611-619.

Modelling ductile strain localization with evolutive stochastic rheologies

Andréa Tommasi*[1], Felipe Sáez-Leiva[1], Lilou Zeller[1], Michel Peyret[1], Riad Hassani[2], and Maurine Montagnat[3]

[1]Géosciences Montpellier, CNRS & Université de Montpellier, France
[2]Géoazur, Observatoire de la Côte d'Azur, Université Côte d'Azur, France
[3]Université Grenoble-Alpes, CNRS, IRD, G-INP, IGE, France
*andrea.tommasi@umontpellier.fr

Keywords: strain localization, shear zones, plate tectonics, numerical modelling, rheology, stochasticity, microstructural evolution, damage, regime diagram, softening, anisotropy

Plate Tectonics requires strain localization over the entire thickness of the plates. However, modelling strain localization in the deep sections of the plates, which deform by ductile processes, remains a challenge, prompting the use of ad hoc schemes to model plate boundaries. We posit that the bottleneck for self-consistent generation of ductile strain localization in geodynamical models is poor representation of the intrinsic mechanical heterogeneity of rocks, in particular at small scales. This prevents its effects from being accounted for at larger scales, notably emergent properties that arise during upscaling, like anisotropy. To model this heterogeneity and its evolution, we adopt a stochastic description of the rheology, which evolves in time and space as a function of the local work-rate. This approach enables to reproduce the full variety of responses observed in nature, from heterogeneous deformation at the local scale, but homogeneous at the system-scale, with or without softening, to spontaneous development of system-scale shear zones. It enables, thereby, the construction of regime diagrams for ductile strain localization using three adimensional parameters. These parameters describe the degree of heterogeneity and potential for evolution of the rheology, function of (1) the constitutive equation, which represents the active deformation processes, (2) the evolution law for the rock mechanical properties, (3) the initial properties, and (4) the energy input to the system. It also allows the prediction of the intensity of localization and the resulting system-scale anisotropic softening, paving the way for self-consistent modelling of plate boundaries in geodynamics.

This work was supported by the European Research Council (ERC) under the European Union Horizon 2020 Research and Innovation programme [grant agreement No 882450 – ERC RhEoVOLUTION].

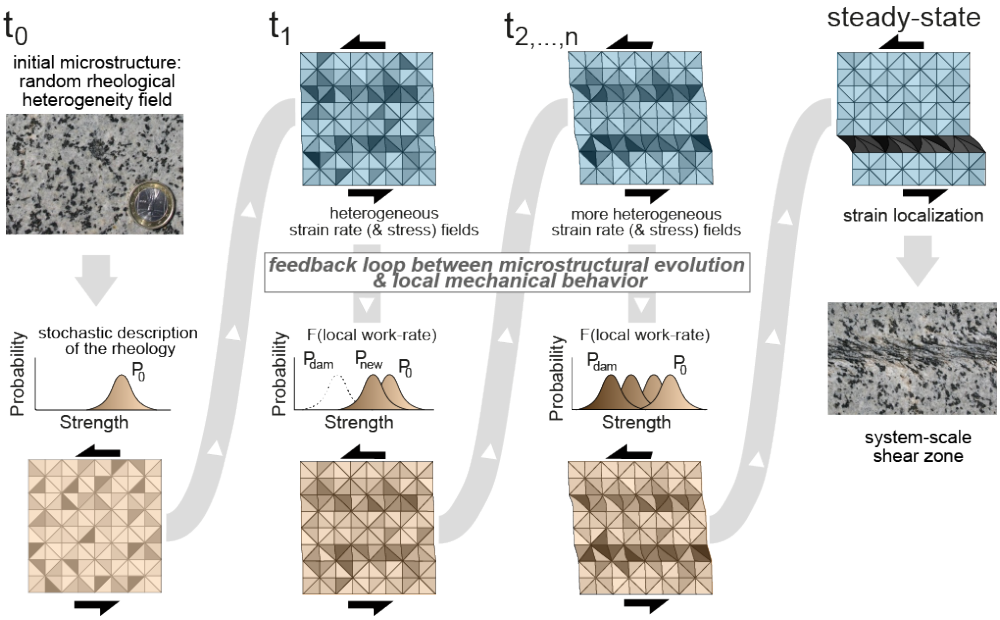


Figure: Graphical summary of the approach proposed to self-consistently model system-scale strain localization arising from rheological heterogeneity. At time t_0, rheological heterogeneity at the sub-mesh scale is modelled by randomly sampling a density probability function, which describes the initial spatial variability in a property controlling the material strength (P_0). Spatial variation in strength produces heterogeneous strain rate and stress fields at time t_1. The material strength is then updated as a function of the local work-rate. If the latter is higher than a threshold, the mesh element is progressively damaged (its strength decreases). This is modeled by sampling the rheological property in another density probability function (Pnew, which varies linearly between P0 and Pdam) Otherwise, the mesh element either retains or progressively recovers its initial strength. Repetition over time ($t_{2,..,n}$) of this process may produce spatial organization of the rheological heterogeneity field, leading to a steady-state characterized by strain localization in a small number (here, one) system-scale shear zones.

Linking elastic and viscous anisotropy in the upper mantle through neural networks

Andrea Tommasi*[1], Audrey Sabri[1], Nestor Cerpa[1], Riad Hassani[2], and Javier Signorelli[3]

[1]Géosciences Montpellier, CNRS & Université de Montpellier, France
[2]Géoazur, Observatoire de la Côte d'Azur, Université Côte d'Azur, France
[3]IFIR, CONICET, Rosario, Argentina, in memoriam
*andrea.tommasi@umontpellier.fr

Keywords: upper mantle, olivine, deformation, textures, seismic anisotropy, viscous anisotropy

The upper mantle displays a strong anisotropy of both its elastic and viscous properties. This anisotropy stems from the convolution of the intrinsic elastic and viscous anisotropy of olivine, the main mineral phase in the upper mantle, and from the crystal preferred orientations (CPO) produced by deformation. The elastic anisotropy may be probed by seismic methods, like shear wave splitting or anisotropic tomography, which show that most of the upper mantle is anisotropic [1]. The viscous anisotropy cannot be probed in situ, but numerical models demonstrate that it plays an important role in mantle convection and plate tectonics [2–4].

Both the elastic and the viscous anisotropies are controlled by crystal orientations, but their relationship is not straightforward. Their prediction also involves different computational costs. The elastic anisotropy can be estimated by averaging the anisotropy of all crystals composing the rock, requiring only knowledge of the single crystal elastic properties and the CPO. Estimating the viscous anisotropy of a polycrystal is more challenging. It requires mechanical tests (laboratory or numerical experiments) in at least 6 different orientations [5,6] (more if the tests are not performed along the CPO eigenvectors). Moreover, given the non-linearity of the flow law describing deformation by dislocation creep, which is the source of viscous anisotropy, the mechanical behavior of an anisotropic mantle volume has to be computed in the orthotropic olivine CPO reference frame, where the viscous anisotropy can be described by the 6 Hill coefficients [5,6]. Estimation of this reference frame has also a non-negligible computational cost.

To reduce the computational cost of modeling the viscous anisotropy of olivine-rich rocks in geodynamical simulations, we trained neural networks (NN) to predict the rotation matrix relating the CPO to the geodynamical reference frame and the Hill coefficients describing the viscous anisotropy given the aggregate elastic compliance tensor expressed in the external (geodynamics) reference frame. The training database was constructed using viscoplastic self-consistent simulations of the deformation of olivine polycrystals, with parameters representative of deformation in the lower lithospheric and asthenospheric mantle [4,6,7]. It is composed of 906 000 triplets of 21 elastic constants (input), 6 Hill coefficients (output1), and a rotation angle (output2, described by 4 scalars). We trained two types of NN: a simple Multi-layer Perceptron (MLP) with a 70:20:10 data split and a Bayesian NN with a 80:20 data split. Both successfully predict the Hill coefficients and the rotation matrix, but with distinct performance characteristics. The MPL achieves a mean average error of 0.06 (mean R-squared of 0.99) for the Hill coefficients and 6.6° for the rotation angle with a computational cost of 0.005ms per prediction on CPU and 64.5Mb. Even higher accuracy is achieved with BNN: mean average error of 0.04 (mean R-squared of 0.998) for the Hill coefficients and 3.8° for the rotation angle, with a computational cost of 3.2ms per prediction on CPU and 120.7Mb.

This work was supported by the European Research Council (ERC) under the European Union Horizon 2020 Research and Innovation programme [grant agreement No 882450 – ERC RhEoVOLUTION].

References

[1] Montagner, J. & Mainprice, D. Anisotropic Seismology. (Cambridge University Press, 2026). doi:10.1017/9781139031271.
[2] Tommasi, A. et al. Structural reactivation in plate tectonics controlled by olivine crystal anisotropy. Nat. Geosci. 2, 423–427, doi: 10.1038/NGEO528 (2009).
[3] Lev, E. & Hager, B. H. Anisotropic viscosity changes subduction zone thermal structure. Geochemistry, Geophys. Geosystems 12, (2011).
[4] Mameri, L., Tommasi, A., Signorelli, J. & Hassani, R. Modelling olivine-induced viscous anisotropy in fossil mantle strike-slip shear zones and the resulting strain localization in the crust. Geophys. J. Int. 224, 608–625 (2021).
[5] Hill, R. A theory of yielding and plastic flow of anisotropic metals. Proc. Roy. Soc. Lond. A193, 281–297 (1948).
[6] Signorelli, J. W., Hassani, R., Tommasi, A. & Mameri, L. An effective parameterization of texture-induced viscous anisotropy in orthotropic materials with application for modeling geodynamical flows. J. Theor. Comput. Appl. Mech. 6737 (2021) doi:https://doi.org/10.46298/jtcam.6737.
[7] Tommasi, A., Mainprice, D., Canova, G. & Chastel, Y. Viscoplastic self-consistent and equilibrium-based modeling of olivine lattice preferred orientations. Implications for upper mantle seismic anisotropy. J. Geophys. Res.

105, 7893–7908 (2000).

How do you drive sinking and translation of a warm, oceanic plate? A geodynamic-petrological model of Paleoproterozoic flat-slab subduction

Leevi Tuikka*[1], David Whipp[1], and Cedric Thieulot[2]

[1]Institute of Seismology, University of Helsinki, Helsinki, Finland
[2]Utrecht University, Utrecht, Netherlands
*leevi.tuikka@helsinki.fi

Keywords: precambrian, subduction, eclogite

Broad observational and modeling evidence suggests, that plate tectonics began at roughly 3.0 Ga (e.g. [1,2]), prior to the start of the Paleoproterozoic era (2.5-1.6 Ga). The protracted transformation from the very early, buckling Archean plate tectonics to the modern style featuring cold and steep subduction was slow due to the gradual secular cooling of Earth. Several studies (e.g. [3,4]) have suggested an intermediate tectonic style called transitional plate tectonics, proposed to operate roughly from Neoarchean to Mesoproterozoic time, based on estimated mantle potential temperatures. Such a mode would retain some characteristics from early tectonics but have more similarity to plate tectonic processes that we observe today.

The key matter behind the transition of plate tectonic regimes was gradual transformation over time from positively or neutrally to negatively buoyant oceanic plates. This evolution has likely been driven by two related factors: more voluminous melting producing thicker oceanic crust due to higher mantle temperatures at MORs and a much thicker depleted oceanic mantle layer from the melt removal. Oceanic mantle melting reached up to 50% in volume at MORs within the Paleoproterozoic mantle potential temperatures. Such a significant depletion could reduce the slab buoyancy enough to produce horizontal translation in the shallow asthenosphere before the thick oceanic crust becomes fully eclogitized and subducts.

Our oceanic-continental subduction models explore the conditions under which flat-slab subduction occurs during the transitional plate tectonic regime with a focus on the Paleoproterozoic era. The problem is addressed using regional-scale, 4500×1200 km models in the geodynamic modeling software ASPECT [5] coupled with lookup tables generated by MAGEMin [6]. The MAGEMin tables determine several important material properties, including density and the flow law parameters. An essential component of the models is quantifying the basalt to eclogite transition in the thick oceanic crust, as it governs slab dynamics to a great extent [3]. Instead of modeling the basaltic composition metastability directly, we use a density scaling factor similar to [3], which includes the effect of the kinetic delay in phase transition at lower temperatures. This scaling factor is defined separately for the upper and lower oceanic crust, as their water content, grain size, and accumulated strain differs substantially. These variations exert a key control on the rate of eclogitization.

The results suggest that flat-slab subduction would have been viable and likely the principal plate tectonic mode for the Paleoproterozoic conditions and a 20-km thick oceanic crust. By modifying the kinetic delay scaling factor or density reduction due to depletion in the oceanic mantle, the horizontal extent over which subduction is "flat" can vary by several hundred kilometers. However, with intermediate scaling and density values, the length of the flat region is roughly 600 km from the trench. In addition, we found that either permeable boundary conditions on the side walls or distant enough side walls are important for producing flat-slab subduction. Such boundary conditions allow continuous flattening of the slab rather than curving during subduction [7].

References

[1] Cawood P. A., Hawkesworth C. J., Pisarevsky S. A., Dhuime B., Capitanio F. A., and Nebel O. (2018). Geological archive of the onset of plate tectonics. Phil. Trans. R. Soc. A. 37620170405.
[2] Palin R. M. and Santosh, M. (2020). Plate tectonics: What, where, why, and when? Gondwana Research, 100, p. 3–24.
[3] Perchuk A. L., Zakharov V. S., Gerya T. V., Griffin W. L. (2023). Flat subduction in the Early Earth: The key role of discrete eclogitization kinetics. Gondwana Research, 119, p. 186–203.
[4] Cawood P. A., Kröner A., Pisarevsky S. (2006). Precambrian plate tectonics: Criteria and evidence. GSA Today, 16:7.
[5] Heister T., Dannberg J., Gassmöller R., and Bangerth W. (2017). High Accuracy Mantle Convection Simulation through Modern Numerical Methods – II: Realistic Models and Problems. Geophysical Journal International 210:2.
[6] Riel N., Kaus B. J. P., Green E. C. R., Berlie N. (2022). MAGEMin, an Efficient Gibbs Energy Minimizer: Application to Igneous Systems. Geochemistry, Geophysics, Geosystems, 23.
[7] Chertova M. V., Geenen T., van den Berg A., and Spakman W. (2012) Using open sidewalls for modelling self-consistent lithosphere subduction dynamics, Solid Earth, 3, p. 313–326.

Diagnosing rheological feedbacks during plate boundary formation

Etienne Van Broeck*[1], Fanny Garel[1], Catherine Thoraval[1], Diane Arcay[1], and D.Rhodri Davies[2]

[1]Géosciences Montpellier, Université de Montpellier, CNRS, Montpellier, France
[2]Research School of Earth Sciences, The Australian National University, Canberra, ACT, Australia
*etienne.van-broeck@umontpellier.fr

Keywords: numerical modeling, strain localisation, weakening, softening, feedbacks, plate boundary, plate tectonics

Numerical models are designed to isolate and explore the key mechanisms driving Earth dynamics. Yet, they incorporate increasingly complex rheologies, where strain localization emerges from multiple interacting weakening mechanisms that are not always straightforward to interpret. Mantle rheology is strongly temperature-dependent, but rheological parameterizations may also include strain-rate dependence (e.g. non-Newtonian dislocation creep), as well as additional dependencies such as grain size or fluid content. In addition, various physical processes may promote weakening, including shear heating, melting , anisotropy, or chemical and mineralogical transformations, in some cases acting simultaneously, which can make disentangling the resulting sequence quite hard. To address this complexity, we develop diagnostics to quantify weakening rate and evaluate the relative contributions to weakening, thereby unraveling the rheological feedbacks governing strain localization during incipient plate boundary formation. We apply these diagnostics to 2-D lithospheric scale extension models (2 cm yr^{-1}) with an initially 50 Myr old thermal structure and a homogeneous olivine mantle. We compare different olivine flow law combinations including pressure, temperature, strain rate and/or grain size dependencies. Grain size evolution is calculated using the paleowattmeter and tracked using Lagrangian particles. We quantify the relative contributions of temperature, strain rate, and grain size to weakening for the different rheologies investigated in this study. Across all simulations, the large-scale evolution remains broadly similar, with progressive strain localization associated with asthenosphere upwelling leading to the formation of a new plate boundary. However, the timing and duration of localization vary significantly between rheologies. Our diagnostics reveal that these differences are not controlled by a single weakening mechanism, but result from the evolving partitioning of weakening between thermal, mechanical, and grain-size contributions. This highlights that strain localization depends not only on the overall strength evolution of the lithosphere, but also on how weakening mechanisms interact and are activated through feedbacks. Because these feedbacks are highly context-dependent, rheological parameterizations that produce similar large-scale behavior in one tectonic setting may lead to significantly different evolutionary pathways in others, with important implications for the interpretation and comparison of geodynamic models.

Topographic diffusion parameterization for rift dynamics: application to an ultraslow Arctic ridge

Nhat Le Vo[*1,2], Javier García-Pintado[1,2], Karim Noruzi-Moghanjoghi[1,2], and Marta Pérez-Gussinyé[1,2]

[1]MARUM – Center for Marine Environmental Sciences, University of Bremen
[2]Faculty of Geosciences, University of Bremen
*nvo@marum.de

Keywords: ultraslow spreading ridge, Arctic mid-ocean ridge, surface processes, topographic diffusion, sediment transport, thermomechanical modeling

The ultraslow-spreading Mohns Ridge, at its intersection with the Knipovich Ridge, exhibits an asymmetric distribution of sediment thickness, with the eastern flank showing greater sediment accumulation than the western flank. This sediment cover may influence the mechanics and act as a thermal blanket, potentially influencing ridge tectonics as well as hydrothermal fluid pathways. To better understand controls on hydrothermal systems such as Loki's Castle, located at the ridge intersection, it is essential to assess how variations in sediment thickness affect both spreading processes and hydrothermal circulation.

As a first step towards this goal, we show here an extended topographic diffusion formulation that jointly describes sediment transport, erosion, and deposition for rifted margins and spreading ridges from shallow water to the distal margin areas and oceanic seafloor. Building on diffusive surface-process models of Kaufman et al., 1991 [1], alongside the existing subaerial framework [2], we implement a generalized diffusion coefficient that accounts for water depth, tidal effect, slope-dependent transport efficiency, and variable sediment supply for the submarine domain. This formulation is integrated into the geodynamic code *Rift2Ridge*, which has previously been used to simulate rifting and seafloor spreading [3,4].

We present standalone tests of the diffusion module on synthetic 2-D topographic profiles, exploring how asymmetric sediment supply and variable diffusion coefficients control topography, erosion patterns, and deposition. These tests provide a basis for its coupling to thermo-mechanical models.

We are currently setting up the extended diffusion scheme in a coupled configuration for the Mohns–Knipovich ultraslow ridge intersection, with an asymmetric pelagic sediment flux representative of the observed sediment distribution. The coupled models are designed to quantify how sediment burial history modify the geothermal gradient of the crust and upper mantle, as well as potential feedbacks on ridge tectonics. Our results aim to clarify how realistic surface processes influence this ultra-slow spreading ridge, and provide a process-based framework for assessing the impact of sediment cover on potential hydrothermal fluid pathways at the Mohns–Knipovich ridge intersection.

References

[1] Kaufman, P., Grotzinger, J. P., & McCormick, D. S. (1991). Depth-dependent diffusion algorithm for simulation of sedimentation in shallow marine depositional systems. Bulletin (Kansas Geological Survey), (233), 489-508.
[2] Andrés-Martínez, M., Pérez-Gussinyé, M., Armitage, J., & Morgan, J. P. (2019). Thermomechanical implications of sediment transport for the architecture and evolution of continental rifts and margins. Tectonics, 38(2), 641-665.
[3] Mezri, L., García-Pintado, J., Pérez-Gussinyé, M., Liu, Z., Bach, W., & Cannat, M. (2024). Tectonic controls on melt production and crustal architecture during magma-poor seafloor spreading. Earth and Planetary Science Letters, 628, 118569.
[4] Yang, P., Pérez-Gussinyé, M., Liu, S., García-Pintado, J., & RaghuRam, G. (2025). Interactions between syn-rift magmatism and tectonic extension at intermediate rifted margins. Earth and Planetary Science Letters, 671, 119682.

The effect of Mercury's spin rate and eccentricity variations on past tidal heating

Michaela Walterová[*1]

[1]Department of Geophysics, Faculty of Mathematics and Physics, Charles University, Prague, Czech Republic
[*]michaela.walterova@matfyz.cuni.cz

Keywords: Mercury, tidal torque, tidal dissipation, orbital evolution

Mercury, the innermost planet of the solar system, is currently locked in a 3:2 spin-orbit resonance: it undergoes exactly three rotations around its axis during two revolutions around the Sun. This unique spin state is a result of solar tides which tend to drive a prolate planet into an equilibrium embodied by a semi-integer ratio of the rotational frequency to the mean motion. While moons and (exo)planets on circular orbits evolve towards fully synchronous (1:1) rotation, celestial bodies on eccentric orbits might get locked into higher-order resonances, such as 3:2, 2:1, or similar.

Mercury's orbit around the Sun is also subject to secular variations. A combined effect of Jupiter and Venus produces large-amplitude changes in the innermost planet's orbital eccentricity, which varies between 0.1 and about 0.3 on a few-million-year timescale. In addition to this "short-period" component, the orbital eccentricity can also experience longer periods of increased or decreased average value [1]. The chaotic nature of inner solar system's evolution may even drive the eccentricity up to 0.5 [2]. Any considerable changes in the orbital eccentricity, coupled with a relaxation of Mercury's shape and ongoing thermal evolution under different insolation patterns [3], may also affect the stability of the spin-orbit resonance.

Both the rotation state and the orbital eccentricity then determine the distribution and magnitude of tidal heating within the planet. On its present orbit and in its current spin-orbit resonance, Mercury experiences tidal dissipation that is orders of magnitude smaller than radiogenic heating [4]. Nevertheless, in past high-eccentricity excursions coupled with a potentially different rotation state [5,6], tidal heating in parts of its interior might have been non-negligible.

In this work, we analyse the stability of different past spin-orbit resonances under varying orbital eccentricity (Figure) and evaluate the tidal dissipation pattern that might have influenced Mercury's thermal evolution. The orbital variations are calculated numerically with the N-body integrator Rebound [7]. Mercury is modelled as a differentiated viscoelastic sphere with radial interior structure consistent with the latest observational data [e.g., 8] and its tidal deformation is evaluated semi-analytically, using the normal mode theory approach [e.g., 9]. Tidal deformation, parameterised by the Love number k_2 and the phase lag ε_2 at multiple frequencies, and the permanent shape of Mercury are then used to evaluate the secular tidal torque and determine for which spin-orbit resonances it equals zero [10]. Finally, we discuss the tidal heating pattern under different spin rate and eccentricity evolution scenarios.

Acknowledgement: The work on this project has been supported by the Czech Science Foundation grant nr. 23-06513I.

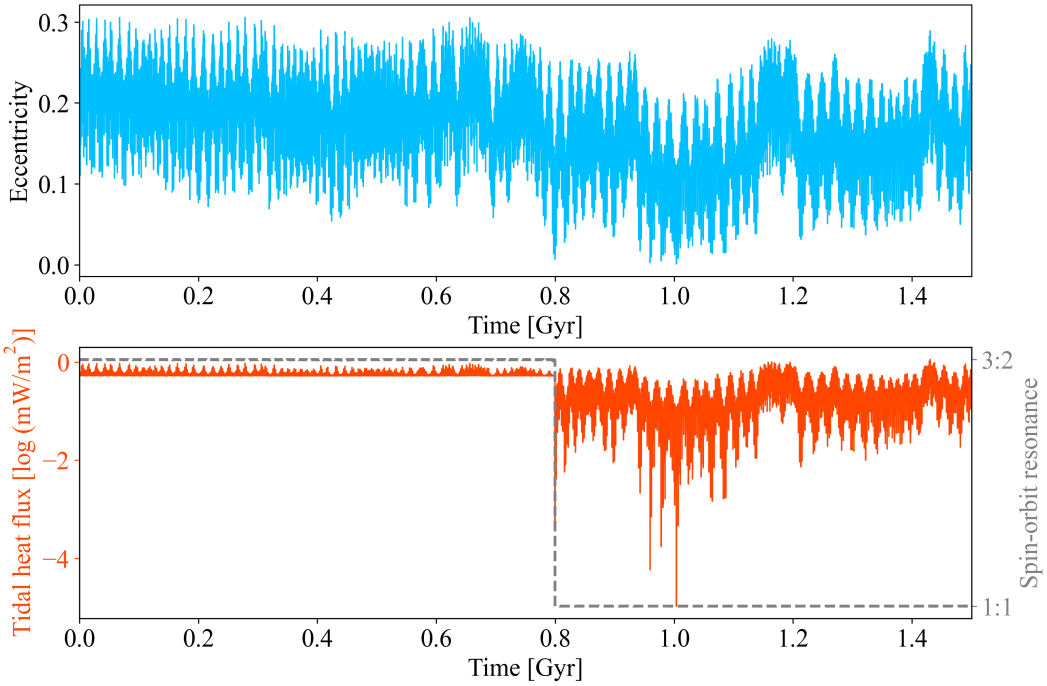


Figure: Evolution of Mercury's orbital eccentricity (upper panel), surface tidal heat flux (lower panel, solid orange line), and spin-orbit resonance (lower panel, dashed gray line) over 1.5 Gyr from now, starting in the present-day configuration of the solar system. The triaxiality of Mercury was set to the present-day value of $C_{22} = 8 \times 10^{-6}$ and the mantle viscosity to a constant value of $\eta = 10^{16}$ Pa s.

References

[1] Lithwick, Y. & Wu, Y. (2014). Secular chaos and its application to Mercury, hot Jupiters, and the organization of planetary systems. Proc. Natl. Acad. Sci. U.S.A., 111(35), 12610–12615.

[2] Laskar, J. & Gastineau, M. (2009). Existence of collisional trajectories of Mercury, Mars and Venus with the Earth. Nature, 459(7248), 817–819.

[3] Tosi, N., et al. (2025). The influence of spin–orbit resonances on the evolution of Mercury's mantle and crust. Icarus, 439, id. 116630.

[4] Rivoldini, A., et al. (2010). Past and present tidal dissipation in Mercury. Abstract nr. EPSC2010-671, EPSC 2010, held in Rome, Italy.

[5] Wieczorek, M., et al. (2012). Mercury's spin-orbit resonance explained by initial retrograde and subsequent synchronous rotation. Nature Geoscience, 5(1), 18–21.

[6] Knibbe, J. S. & van Westrenen, W. (2016). On Mercury's past rotation, in light of its large craters. Icarus, 281, 1–18.

[7] Rein, H. & Spiegel, D. S. (2015). IAS15: a fast, adaptive, high-order integrator for gravitational dynamics, accurate to machine precision over a billion orbits. Mon. Not. R. Astron. Soc., 446(2), 1424–1437.

[8] Goossens, S., et al. (2022). Evaluation of Recent Measurements of Mercury's Moments of Inertia and Tides Using a Comprehensive Markov Chain Monte Carlo Method. The Planetary Science Journal, 3(2), id. 37.

[9] Takeuchi, H. & Saito, M. (1972). Seismic Surface Waves. Methods in Computational Physics, 11, 217–295.

[10] Noyelles, B., et al. (2014). Spin-orbit evolution of Mercury revisited. Icarus, 241, 26–44.

Maximum Decoupling Depth controls the Point of No Return in oceanic subduction zones

Yang Wang*[1], Zhong-Hai Li[1], Taras V. Gerya[2], and Hengrui Zhang[1]

[1]College of Earth and Planetary Sciences, University of Chinese Academy of Sciences, Beijing , China
[2]Department of Earth Sciences, ETH-Zurich, Zurich, Switzerland
*yangwang-geo@ucas.ac.cn

Keywords: Maximum decoupling depth, the point of no return, subduction channel, exhumation, eclogite

Mechanical decoupling to coupling transition between subducting slab and mantle wedge fundamentally influences subduction processes [1,2]. Global compilation of pressure-temperature conditions from oceanic metamorphic rocks suggests that tectonic exhumation of eclogites from depths exceeding 80±10 km is unlikely [3], thus defining the "point of no return" (PNR) [4]. This depth coincides with the maximum decoupling depth (MDD) between slab and mantle wedge observed in mature subduction zones worldwide, yet this striking coincidence remains unexplained. Here, we combine thermo-petrological modelling with analytical study to evaluate three key MDD-regulated processes governing exhumation: crustal detachment, metamorphic densification, and subduction-channel flow. It reveals that slab-mantle coupling near MDD (1) triggers sharp temperature increase that drives metamorphic densification of oceanic crust, (2) reverses slab–mantle rheological strength, and thereby (3) induces downward channel flow along the slab surface, which precludes exhumation of subducted oceanic crust from depths below MDD and explains its coincidence with PNR. We further demonstrate that the proposed mechanism also operates in nascent subduction zones, where a shallow MDD-controlled PNR explains low peak pressures of metamorphic soles worldwide. Finally, we explain why MDD-controlled PNR is absent in continental subduction settings where intrinsically buoyant and rheologically weak continental crust can exhume from greater depths below MDD.

References

[1] Agard, P., Yamato, P., Huet, B., Angiboust, S., & Schmalholz, S. M. (2020). Slabitization: Mechanisms controlling subduction development and viscous coupling. Earth-Science Reviews, 208, 103259.
[2] Wada, I., & Wang, K. (2009). Common depth of slab-mantle decoupling: Reconciling diversity and uniformity of subduction zones. Geochemistry, Geophysics, Geosystems, 10(10).
[3] Agard, P., Plunder, A., Angiboust, S., Bonnet, G., & Ruh, J. (2018). The subduction plate interface: rock record and mechanical coupling (from long to short timescales). Lithos, 320–321, 537–566.
[4] Whitney, D. L., Teyssier, C., Seaton, N. C. A., & Fornash, K. F. (2014). Petrofabrics of high-pressure rocks exhumed at the slab-mantle interface from the "point of no return" in a subduction zone (Sivrihisar, Turkey). Tectonics, 33(12), 2315–2341.

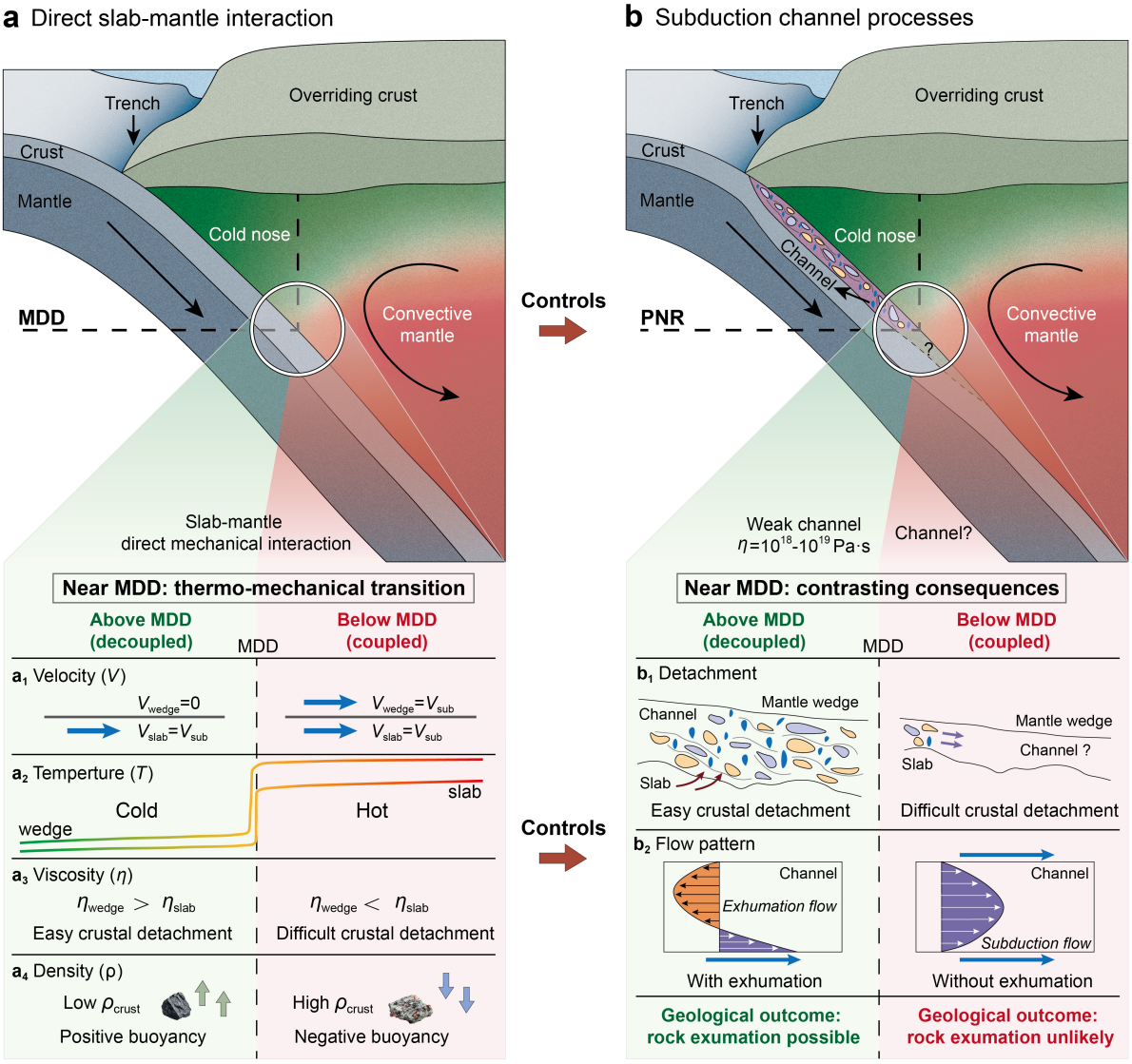


Figure: Conceptual model illustrating how MDD controls the PNR of subducted oceanic rocks. (a) Thermo-mechanical transition near MDD during direct interaction of the subducting slab and mantle wedge before subduction-channel development. The mechanical decoupling-to-coupling transition across MDD generates a fundamental contrast in mantle-flow velocities above and below this boundary. Above MDD, the forearc mantle remains mechanically decoupled from the subducting slab, forming a cold, stagnant mantle wedge with zero velocity. Below MDD, slab–mantle coupling drives hot, vigorous sub-arc and back-arc mantle flow with velocities comparable to subduction rate (a_1). This enhanced mantle flow induces sharp temperature increase in both oceanic crust and mantle wedge (a_2). The resulting thermal contrast exerts two key effects: (1) above MDD, the rheological contrast between the stronger mantle wedge and weaker oceanic crust promotes crustal detachment, whereas below MDD, the rheologically weak mantle wedge suppresses crustal detachment (a_3); (2) relatively low P-T conditions above MDD maintain low crustal density and positive buoyancy, whereas phase-transition-induced metamorphic densification below MDD increases crustal density (a_4). (b) MDD-controlled contrasting consequences for subduction-channel flow. Above MDD, the rheologically strong forearc mantle promotes crustal detachment and the development of a weak subduction channel ($\sim 10^{18}$–10^{19} Pa·s) (b_1). Together with the low density of subducting crust and a no-slip overriding mantle wedge, these favorable conditions enable upward exhumation flow and the eventual exhumation of HP metamorphic rocks from depths above MDD (b_2). In contrast, below MDD, slab-mantle coupling suppresses crustal detachment (b_1) and promotes metamorphic densification of the oceanic crust. Combined with shear drag from both the subducting slab and overriding mantle wedge, the downward subduction flow dominates, making exhumation from depths below PNR unlikely (b_2).

Composition-dependent erosion in subduction zones: Implications for slab dynamics and Andean margin evolution

Yijun Wang[*1], Sascha Brune[1,2], Derek Neuharth[1], and Michael Pons[3]

[1]GFZ Helmholtz Centre for Geosciences, Potsdam, Germany
[2]University of Potsdam, Potsdam, Germany
[3]Roma Tre University, Rome, Italy
[*]ywang@gfz.de

Surface processes have been proposed to influence subduction dynamics by modulating sediment flux to trenches, which may enhance subduction and the overall plate velocity. However, the combined effects of lithology-dependent erosion and sediment frictional/rheological properties remain poorly constrained. Natural landscapes exhibit large variations in erodibility related to lithology, climate, and tectonic setting. However, existing subduction models have simplified surface processes drastically by prescribing initial sediment distribution or relying on linear surface diffusion with uniform erosional parameters. Here, we investigate how lithology-dependent variations in erodibility influence the evolution of subduction zones using high-resolution two-dimensional thermo-mechanical models coupled with surface processes.

To explore the effects of erosion across a range of subduction styles characterized by varying slab dynamics and trench motions, including trench advance and retreat, as well as slab rollback and rollover, we developed a series of visco-plastic subduction models that capture these settings while incorporating free-surface deformation and landscape evolution. Using these models, we vary the overall erosion efficiency and compare our results to Andean settings spanning the humid Northern Andes, arid Central Andes, and glaciated Southern Andes, where differences in erosion rates and sediment fluxes to the trench may influence subduction dynamics. For each case, we compare models with uniform erosional properties against models with lithology-dependent erodibility and depth-dependent marine sediment transport.

Our results aim to quantify the extent to which surface erosion variability can feed back into slab geometry, trench migration, and crustal deformation. In particular, we test whether changes in erosional efficiency due to lithological variations can enhance the localization of deformation, modify sediment transportation efficiency, or alter the balance between tectonic uplift and surface erosion rates. This work highlights the importance of integrating realistic surface-process parameterizations into geodynamic models of convergent margins.

The dense MORB fraction controls the dynamic stability and water-storage potential of the Mantle Transition Zone

Zhensheng Wang*[1,2], Sierd Cloetingh[2,3], Alexander Koptev[2,4], Qin Wang[4], Alessio Lavecchia[2,5], István J. Kovács[2], and Timothy Kusky[1,6]

[1]China University of Geosciences, Wuhan, China
[2]Institute of Earth Physics and Space Science ELKH, Sopron, Hungary.
[3]Utrecht University, Utrecht, The Netherlands.
[4]Nanjing University, Nanjing, China.
[5]University of Bari "Aldo Moro", Bari, Italy.
[6]China University of Geosciences, Wuhan, China.
*jasonwang@cug.edu.cn

Keywords: mantle transition zone, deep-water cycle, water-storage potential, hydroweakening, mid-ocean ridge basalt, mid-lithospheric discontinuity

The mantle transition zone (MTZ; ~410–660 km depth) is widely regarded as Earth's largest internal water reservoir and a key interface linking the deep-water cycle, mantle convection, and lithospheric evolution [2,4,6]. High-pressure mineral physics experiments demonstrate that transition-zone minerals, particularly wadsleyite and ringwoodite, can incorporate up to ~2–3 wt% H_2O [2,7]. However, geophysical and geochemical estimates of actual MTZ water content remain highly variable and commonly below this mineralogical storage capacity [8,10], suggesting that additional geodynamic processes regulate long-term water retention. At the same time, increasing evidence indicates that the MTZ contains substantial proportions of dense, Fe-rich mafic materials compositionally similar to recycled mid-ocean ridge basalt (MORB) [1,3], which possess limited water-storage capacity [5] but significantly enhance mantle density [1,3]. How the interplay between hydration and MORB enrichment controls MTZ stability and realistic water-storage potential remains poorly constrained.

Here we use high-resolution geodynamic numerical models to investigate the coupled effects of water content and MORB fraction on the density, viscosity, convection, and long-term evolution of the MTZ. Our results demonstrate that MTZ stability is governed by a narrow range of MORB-to-water ratios. Excess hydration reduces viscosity and density, promoting buoyancy-driven instabilities, convective upwelling, and progressive dehydration. In contrast, MORB enrichment suppresses these instabilities by increasing mantle density and stabilizing hydrated domains. The balance between these competing effects determines whether hydrated MTZ layers remain dynamically stable over geological timescales.

By combining modeled stability limits with global estimates of MTZ MORB abundance, we further constrain the realistic physical water-storage potential of the MTZ. The results indicate that MTZ water storage is strongly laterally heterogeneous and controlled not only by intrinsic mineralogical capacity but also by dynamic stability. Regions with moderate MORB contents can preserve larger volumes of water by dynamically stabilizing hydrated mantle domains, whereas MORB-rich regions may suppress the intrinsic mineralogical water-storage capacity of the MTZ, and MORB-poor domains are more susceptible to buoyancy-driven instability and dehydration. Under present-day Earth conditions, most of the MTZ likely resides in stable or slowly dehydrating regimes, characterized by gradual water release from the lower MTZ over hundreds of millions of years. These findings support the existence of a long-lived and self-regulating deep-water cycle and suggest that the coupled evolution of hydration and compositional heterogeneity in the MTZ plays an important role in sustaining long-term lithospheric stability and Earth's surface habitability.

References

[1] Ballmer, M. D., Schmerr, N. C., Nakagawa, T., & Ritsema, J. (2015). Compositional mantle layering revealed by slab stagnation at ~1000-km depth. Science Advances, 1(11), e1500815. https://doi.org/10.1126/sciadv.1500815
[2] Bercovici, D., & Karato, S. (2003). Whole-mantle convection and the transition-zone water filter. Nature, 425(6953), 39-44.
[3] Dannberg, J., & Sobolev, S. V. (2015). Low-buoyancy thermochemical plumes resolve controversy of classical mantle plume concept. Nature Communications, 6, 6960.
[4] Hirschmann, M. M., Tenner, T., Aubaud, C., & Withers, A. C. (2009). Dehydration melting of nominally anhydrous mantle: the primacy of partitioning. Physics of the Earth and Planetary Interiors, 176(1), 54-68.
[5] Iwamori, H. (2004). Phase relations of peridotites under H_2O-saturated conditions and ability of subducting plates for transportation of H_2O. Earth and Planetary Science Letters, 227(1), 57-71.
[6] Karato, S. (2011). Water distribution across the mantle transition zone and its implications for global material circulation. Earth and Planetary Science Letters, 301(3), 413-423.

[7] Kohlstedt, D. L., Keppler, H., & Rubie, D. C. (1996). Solubility of water in the α, β and γ phases of $(Mg,Fe)_2SiO_4$.

Contributions to Mineralogy and Petrology, 123(4), 345-357. https://doi.org/10.1007/s004100050161
[8] Wang, W., Walter, M. J., Peng, Y., Redfern, S., & Wu, Z. (2019). Constraining olivine abundance and water content of the mantle at the 410-km discontinuity from the elasticity of olivine and wadsleyite. Earth and Planetary Science Letters, 519, 1-11. https://doi.org/https://doi.org/10.1016/j.epsl.2019.04.018
[9] Wang, Z., & Wang, Y. (2022). Global water distribution in the mantle transition zone from a seismic isotropic velocity model and mineral physics modeling. Frontiers in Earth Science, 10
[10] Zhou, W., Hao, M., Zhang, J. S., Chen, B., Wang, R., & Schmandt, B. (2022). Constraining composition and temperature variations in the mantle transition zone. Nature Communications, 13(1), 1094. https://doi.org/10.1038/s41467-022-28709-7

Pure necking or strain localization: Rheological and geometrical controls of the lower crust on slab detachment

Tatjana Weiler*[1], Andrea Piccolo[2], Arne Spang[1], and Marcel Thielmann[3]

[1]University of Bayreuth
[2]University of Leeds
[3]University of Bonn
*tatjana.weiler@uni-bayreuth.de

Keywords: slab detachment, Hindu Kush, lower crust, strain localization, necking

Earthquake nests are defined as volumes of intense intermediate-depth seismicity which are isolated from any surrounding seismic activity. The high seismic activity within these earthquake nests occurs continuously and thus sets them apart from other seismic sequences such as earthquake swarms or aftershocks. The three most studied earthquake nests are the Vrancea (Romania), Bucaramanga (Colombia) and Hindu-Kush (Afghanistan) earthquake nests. The intermediate-depth seismicity in all three nests has been linked to the occurrence of slab detachment. To determine the nucleation and rupture mechanisms of the intermediate-depth seismicity within these nests, it is necessary to constrain the conditions at which they occur.

Here, we use two-dimensional thermomechanical models with a nonlinear visco-elasto-plastic rheology to determine the deformation state and answer the questions whether either pure shear necking or simple shear are the controlling mechanisms of the detachment process in the Hindu Kush.

We focus on the effect of the lower crust on the detachment process which is up to now insufficiently constrained. We therefore concentrate on the question how the viscosity ratio ($\eta_{\mathrm{lith}}/\eta_{\mathrm{lc}}$) between the lithosphere and the lower crust and the depth (d_{lc}) to which the lower crust may have been subducted influence the detachment process. We varied the viscosity ratio ($\eta_{\mathrm{lith}}/\eta_{\mathrm{lc}}$) between 0.01 and 1000, and the subduction depth of the lower crust (d_{lc}) between 160 km and 240 km. The deformation behaviour of the 270 models can be classified into five different regimes based on stress, strain rate, detachment depth, and coupling between subducting and overriding plate. The five regimes represent the dependency of the detachment depth (d_{det}) on the viscosity ratio ($\eta_{\mathrm{lith}}/\eta_{\mathrm{lc}}$). Settings with small viscosity ratios and/or deeper lower crust detach slowly via necking in a range from 110 km to 470 km, whereas large viscosity ratios in combination with shallower lower crust leads to fast detachment in about 230±15 km depth. The characteristics of depth, duration, and mechanism are consistent with the young age of the Hindu Kush slab and the deeper peak of seismicity in the Hindu Kush nest where $M_w > 7$ earthquakes are interpreted to occur by thermal shear instabilities [1]. Therefore, we suggest that beneath the Hindu Kush, a strong lithosphere with a comparably weak lower crust which extends down to 180 km depth favor detachment via simple shear.

References

[1] Poli, P., Prieto, G., Rivera, E., & Ruiz, S. (2016). Earthquakes initiation and thermal shear instability in the Hindu Kush intermediate depth nest. Geophysical Research Letters, 43(4), 1537–1542.

Thermomechanical modeling of the Archean thermal state: Evidence for a hot, thin lithosphere

Chenying Yu[*1], Ting Yang[2], Guochun Zhao[1], Peter A. Cawood[3], Shoufa Lin[4], Jin Liu[5], Xiao Wang[1], Qihang Wu[1], Min Sun[1], and Jian Zhang[1]

[1]The University of Hong Kong
[2]Southern University of Science and Technology
[3]Monash University
[4]University of Waterloo
[5]Jilin University
*jian@hku.hk

Although the stability of present-day cratons is traditionally attributed to their cold, thick, and mechanically strong lithospheric roots, the thermal state of their Archean precursors remains poorly constrained. Here, we integrate 1D thermal and 2D numerical models to reproduce the tectonic processes that operated during the Archean and to quantitatively constrain the early Earth's thermal state. Our model results demonstrate that the thermal state of the lithosphere is significantly controlled by variations in basal heat flux and crustal heat production, which consequently govern the lithospheric thickness and crustal dynamics. Higher crustal heat production and mantle heat flux lead to the development of a super-thin and hot lithosphere (generally < 75 km), characterized by intense and rapid crustal convective overturn. In contrast, low heat values result in a thick and stable lithosphere (typically > 150 km), analogous to present-day cratons. Intermediate values of these thermal parameters successfully reproduce the typical dome-and-keel architectures observed in Archean granite-greenstone assemblages, consistent with geological evidence. Under these conditions, the Archean Moho temperature is further constrained within the range of 880–1082°C. This indicates that a hot and thin Archean lithosphere (75–150 km) was essential to drive the extensive crustal partial melting responsible for forming Archean continental nuclei. Therefore, our findings reveal that the Archean thermal lithosphere was significantly hotter and thinner than its modern cratonic counterpart, offering a new geodynamic perspective on early craton formation.

Geodynamic controls on the Upper Rhine Graben: from transtensional basin architecture to thermo-hydro-mechanical processes

Alan J. Yu*[1,2], Sascha Brune[1,2], Judith Bott[1], Magdalena Scheck-Wenderoth[1,3], Anne C. Glerum[1], and Mauro Cacace[1,3]

[1]GFZ Helmholtz Centre for Geosciences, Potsdam, Germany
[2]Institute of Geosciences, University of Potsdam, Potsdam, Germany
[3]Institute of Applied Geosciences, Technische Universität Berlin, Berlin, Germany
*alan.yu@gfz.de

Keywords: oblique rifting, Upper Rhine Graben, multi-scale coupled modelling

The Upper Rhine Graben, situated along the border of France and Germany, is a major segment of the intraplate European Cenozoic Rift System with significant geothermal potential. Despite decades of geophysical surveys and increasingly high-resolution subsurface models, fundamental gaps remain in our understanding of its long-term deformation: (i) a kinematic transition from normal to strike-slip faulting with unresolved driving mechanisms; (ii) half-graben structures with alternating polarity, often attributed to poorly constrained crustal inheritance; and (iii) an unusually narrow width (~30–40 km) despite the absence of basin-scale inversion or lateral confinement.

Using coupled lithosphere–surface geodynamic modelling with ASPECT and Fastscape, we show that these first-order features can emerge from sustained transtension alone. First, as rifting progresses, deformation self-organizes from normal faulting along pre-existing weaknesses to strike-slip faulting aligned with regional kinematics, without requiring changes in far-field plate motion. Second, within a suitable range of rift obliquity, conjugate border faults develop along the rift axis, producing opposing half-grabens independently of inherited transverse anisotropies. Third, along-strike shortening from Alpine–Pyrenean compression limits crustal thinning and enhances strike-slip partitioning, thereby preserving graben narrowness.

These results indicate that the observed complexities reflect intrinsic transtensional mechanics rather than site-specific controls. This framework may hence provide a first-order explanation for oblique segments of the East African Rift, the Gulf of California, and the North Sea. Moreover, the deformation fabric provides a foundation for subsequent thermo-hydro-mechanical modelling with GOLEM, where strain-dependent dilation and permeability govern transient fluid and heat transport, with implications for geothermal resource prediction.

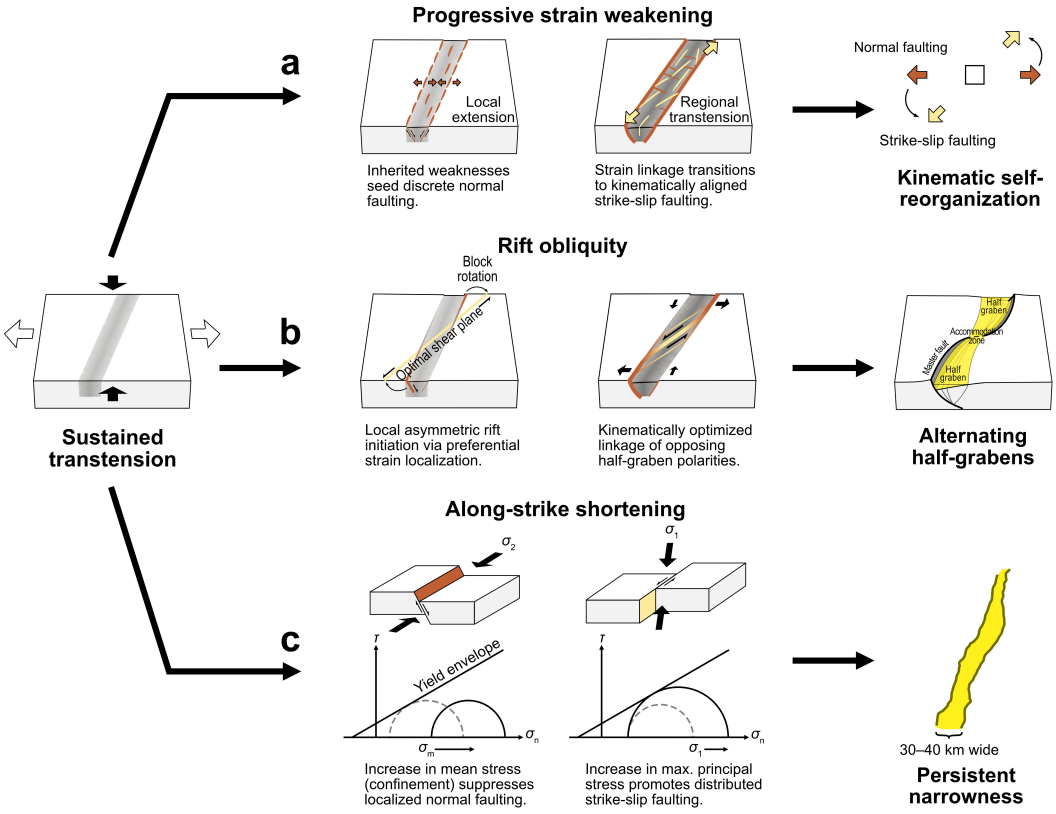


Figure: Unified conceptual model for the evolution of transtensional rifts, exemplified by the Upper Rhine Graben. (a) Progressive strain weakening drives self-organized kinematic transition. (b) Rift obliquity promotes the formation of alternating half-grabens. (c) Along-strike shortening maintains rift narrowness.

Strain localisation in anisotropic materials

Filippo Zarabara*[1], Thibault Duretz[1], Anna Bardroff[1], Albert De Montserrat[2], and Carolina Giorgetti[3]

[1]Goethe University Frankfurt
[2]ETH Zurich
[3]CNRS
*Zarabara@uni-frankfurt.de

Keywords: anisotropy, numerical modelling, strain localisation, bifurcation analysis, rock mechanics

The aim of the project is to study strain localisation in anisotropic geo-materials by integrating two tools: bifurcation analysis and mechanical modelling. We take advantage of a newly developed Julia-based tool to perform bifurcation analysis on frictional materials and predict the critical orientation of shear bands. This tool has been validated through the reproduction of classical results from the literature and is further supported by 2D mechanical modelling. We apply the two-step methodology to study the orientation of shear bands in anisotropic rocks first with Hill-type elastoplastic rheology, calibrated through direct numerical simulations of a layered elastoplastic medium. This work may help to elucidate the origin of shear bands in orientations not predicted by the classical isotropic theory, and provide an explanation for the occurrence in nature of non-Andersonian tectonic structures such as low angle normal faults, whose physical explanation remains elusive. Furthermore, it may provide insights from a rock mechanics perspective on the deformation structures and strain localisation in layered media.

Adeli2024 : The new version of a 3D versatile software for elasto-visco-plastic deformations on geological time scales

Lilou Zeller*[1], Riad Hassani[2], Michel Peyret[1], and Andréa Tommasi[1]

[1]Géosciences Montpellier, Université de Montpellier, CNRS, France
[2]Géoazur, Université Côte d'Azur, CNRS, IRD, Observatoire de la Côte d'Azur, France
*lilou.zeller@umontpellier.fr

Keywords: finite-element software, elasto-plasticity, elasto-viscosity, pseudo-transient methods

ADELI is a finite element software program developed to simulate the thermomechanical behavior of the lithosphere over geological time scales.

Written in a Lagrangian formulation for large deformations, this code employs hypoelastic constitutive models ranging from elastoplasticity (Von Mises, Drucker-Prager) to linear viscoelasticity (Maxwell) and nonlinear viscoelasticity (power-law and exponential models). Faults can also be accounted for using Coulomb friction contact.

The time discretization is based on a dynamic relaxation method, allowing the use of an explicit numerical scheme to integrate the equation of motion. The material constitutive models and interface laws, on the other hand, use implicit or semi-implicit methods.

This software differs from other open-source codes in geodynamics in several ways:

- Explicit time step, which allows for the cost-effective use of highly nonlinear constitution laws, such as a viscoelastic law combining stress dependence in power and exponential forms.
- Lagrangian formalism for natural tracking of domain boundaries and the evolution of material properties.
- Stochastic module for representing sub-mesh heterogeneity in material rheology using probability density functions.

This software, developed in the 1990s, has been used by several research teams to study issues such as fault behavior, interactions between the convective mantle and lithospheric plates, or the localization of deformation at different scales.

Using a test case, we present a new version of this code, rewritten in modern Fortran and featuring a more user-friendly configuration file. We will see how the use of object-oriented programming leads to greater efficiency, modularity, and ease of use.

This work was supported by the European Research Council (ERC) under the European Union Horizon 2020 Research and Innovation programme [grant agreement No 882450 – ERC RhEoVOLUTION]



Figure: Logo

Multiscale modeling of viscous strain localization : from rocks sample to lithospheric scale

Lilou Zeller*[1] and Andréa Tommasi[1]

[1]Geosciences Montpellier, CNRS, France
*lilou.zeller@umontpellier.fr

Keywords: strain localization, viscosity, multi-scale

Strain localization in ductile shear zones is the dominant deformation mode in most of the crust and lithospheric mantle. These ductile shear zones occur at every spatial scale from the centimeter up to the plate scale and with scale invariance (eg. [1,2]). This is usually taken into account in the design of numerical studies of strain localization by using spatially invariant rheological laws (eg. [3]). Yet, even those spatially invariant models only represent a narrow range of shear-zone scales.

This study aims to investigate how ductile shear zones form and how the development of a shear zone affects the mechanical behavior of a rock volume at increasing larger spatial scales. We focus on the ductile layers of the lithosphere, which deform mainly by dislocation creep. To that end, we adopt a bottom-up approach going from the heterogeneities of the rocks at the sample scale to the lithospheric scale.

We start by the development of a two-scale heterogeneous model, where the link between microscopic and macroscopic models is assured by a phenomenological state-variable evolution law. This approach allows studying how the properties emerging of strain localization at small scales affect the deformation at larger scales.

The micro-scale behavior is determined based on simulations with a stochastic representation of time-evolving rock rheology. They run using the finite-element software Adeli2024 code. The evolution of the rheology (softening or hardening due to an evolution of the rock structure in response to deformation) is controlled by the local work-rate. These models allow, for the same material, for both steady-state strain localization and homogeneous deformation, depending on the initial microstructure and the imposed boundary conditions [4].

Strain localization in these models results in anisotropic softening of the material which has been parameterized as an evolution law for the state variables of the macro-scale model. This law associates, to a set of material parameters and boundary conditions, the bulk strength, anisotropy and orientation of the anisotropy that would be generated by viscous strain localization. It has been implemented in the 2D anisotropic geodynamical code MDoodz7 [5].

The poster will develop on the framework and show preliminary results of this two-scale modeling.

This work was supported by the European Research Council (ERC) under the European Union Horizon 2020 Research and Innovation programme [grant agreement No 882450 – ERC RhEoVOLUTION]

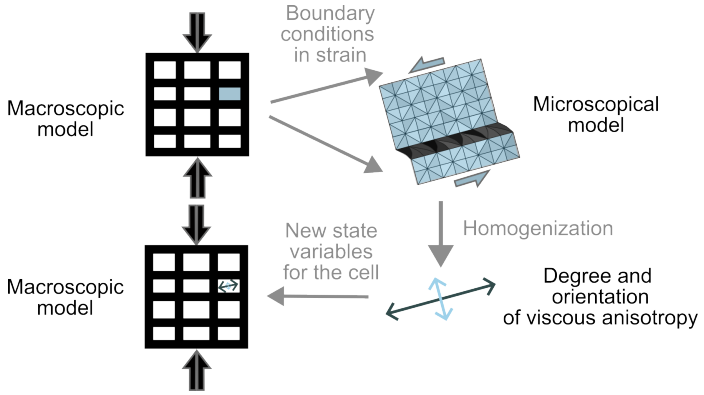


Figure: Graphic summary of the approach.

References

[1] Carreras, J. (2001), "Zooming on Northern Cap de Creus shear zones", Journal of Structural Geology
[2] Fossen and Cavalcantes (2017). "Shear zones – A review", Earth-Science Reviews
[3] Gardner, Robyn et al. (2017). "Patterns of strain localization in heterogeneous, polycrystalline rocks – a numerical perspective". Earth and Planetary Science Letters
[4] Tommasi, Andréa, Felipe Sáez-Leiva et al. (in revision). "Modelling spontaneous ductile (viscous) strain localisation on Earth". EPSL.

[5] Duretz, Thibault, René de Borst et Philippe Yamato (2021). "Modeling Lithospheric Deformation Using a Compressible Visco-Elasto-Viscoplastic Rheology and the Effective Viscosity Approach". Geochemistry, Geophysics, Geosystems

Numerical Simulation of Fully Compressible Two-Phase Flow in Subduction Zones

Rui-Min Zhang*[1] and Zhong-Hai Li* [supervisor of Rui-Min Zhang][1]

[1]College of Earth and Planetary Sciences, University of Chinese Academy of Sciences, Beijing, China
*zhangruimin22@mails.ucas.ac.cn

Keywords: Two-Phase Flow, Fully Compressibility

During slab subduction, dehydration of hydrous minerals via phase transitions generates free fluids [1]. These volatile-bearing fluids decouple from the solid matrix and migrate as porous flow through the slab and both the large and small mantle wedges [2]. Their weakening effect promotes stress concentration and triggers deep-focus earthquakes; fluid-induced melting forms the core mechanism for volcanic island arcs and subduction-related intraplate volcanoes [3]; and fluids act as the primary carrier for volatile cycling between Earth's shallow and deep interiors.

Developed in an object-oriented C++ framework using the open-source PETSc solver toolkit, the code offers high maintainability, extensibility, and portability. It employs a coupled staggered grid finite difference (StagGrid-FDM) and particle-in-cell (PIC) algorithm [4] with distributed-memory parallelism across grids, particles, and solvers, efficiently supporting high-precision geological models with tens of millions of degrees of freedom and hundreds of millions of particles. By incorporating thermodynamic phase diagrams covering rock densities and water capacities, the code enables accurate modeling of realistic geological scenarios.

To elucidate deep fluid migration laws and quantify their dynamic effects, we adopt fully compressible [5] mass and momentum conservation equations [6]:

$$\frac{1}{\rho^s}\frac{\mathcal{D}^s\rho^s}{\mathcal{D}t} + \nabla\cdot\vec{v^s} + \frac{P^t - P^f}{(1-\phi)\eta^\phi} = \frac{\Gamma^{mass}}{1-\phi}\left(\frac{1}{\rho^f} - \frac{1}{\rho^s}\right),$$

$$-\nabla\cdot\left[\eta^t\left(\nabla\vec{v^s} + \vec{v^s}\nabla\right) - \frac{2}{3}\eta^t\left(\nabla\cdot\vec{v^s}\right)\mathbf{G}\right] + \nabla P^t = \rho^t\vec{g},$$

These equations accurately describe mass transfer between the fluid and solid phases, correctly capture material volumetric changes, and ensure strict global mass conservation.

Focusing on fluid-solid coupling problems including mineral phase transition dehydration, fluid transport, and fluid-induced weakening in subduction zones, the code enables quantitative simulation of the complete deep fluid release-migration-reaction chain and its induced mechanical, thermal, and thermodynamic responses. We have successfully simulated oceanic lithosphere dehydration in the upper mantle, clearly resolving the co-evolution of porosity, water content, and rock viscosity,which preliminarily validating the code's stability and reliability. This work provides essential theoretical support and numerical tools for research on volatile cycling, deep-focus earthquake genesis, and arc/intraplate volcanism.

References

[1] Cerpa, N. G., & Wada, I. (2025). Hydration State and Updip Fluid Migration in the Slab Mantle. Journal of Geophysical Research: Solid Earth, 130(6), e2024JB030609. https://doi.org/10.1029/2024JB030609
[2] Wada, I., & Behn, M. D. (2015). Focusing of upward fluid migration beneath volcanic arcs: Effect of mineral grain size variation in the mantle wedge. Geochemistry, Geophysics, Geosystems, 16(11), 3905–3923. https://doi.org/10.1002
[3] Lee, C., Cerpa, N. G., Lee, J., & Huh, M. (2026). Intraplate volcanism induced by magmatic solitary waves ascending from the mantle transition zone. Geology, 54(2), 143–147. https://doi.org/10.1130/G53800.1
[4] Gerya, T. V. (2019). Introduction to Numerical Geodynamic Modelling (2nd ed.). Cambridge: Cambridge University Press. https://doi.org/10.1017/9781316534243
[5] Gassmöller, R., Dannberg, J., Bangerth, W., Heister, T., & Myhill, R. (2020). On formulations of compressible mantle convection. Geophysical Journal International, 221(2), 1264–1280. https://doi.org/10.1093/gji/ggaa078
[6] McKENZIE, D. (1984). The Generation and Compaction of Partially Molten Rock. Journal of Petrology, 25(3), 713–765. https://doi.org/10.1093/petrology/25.3.713

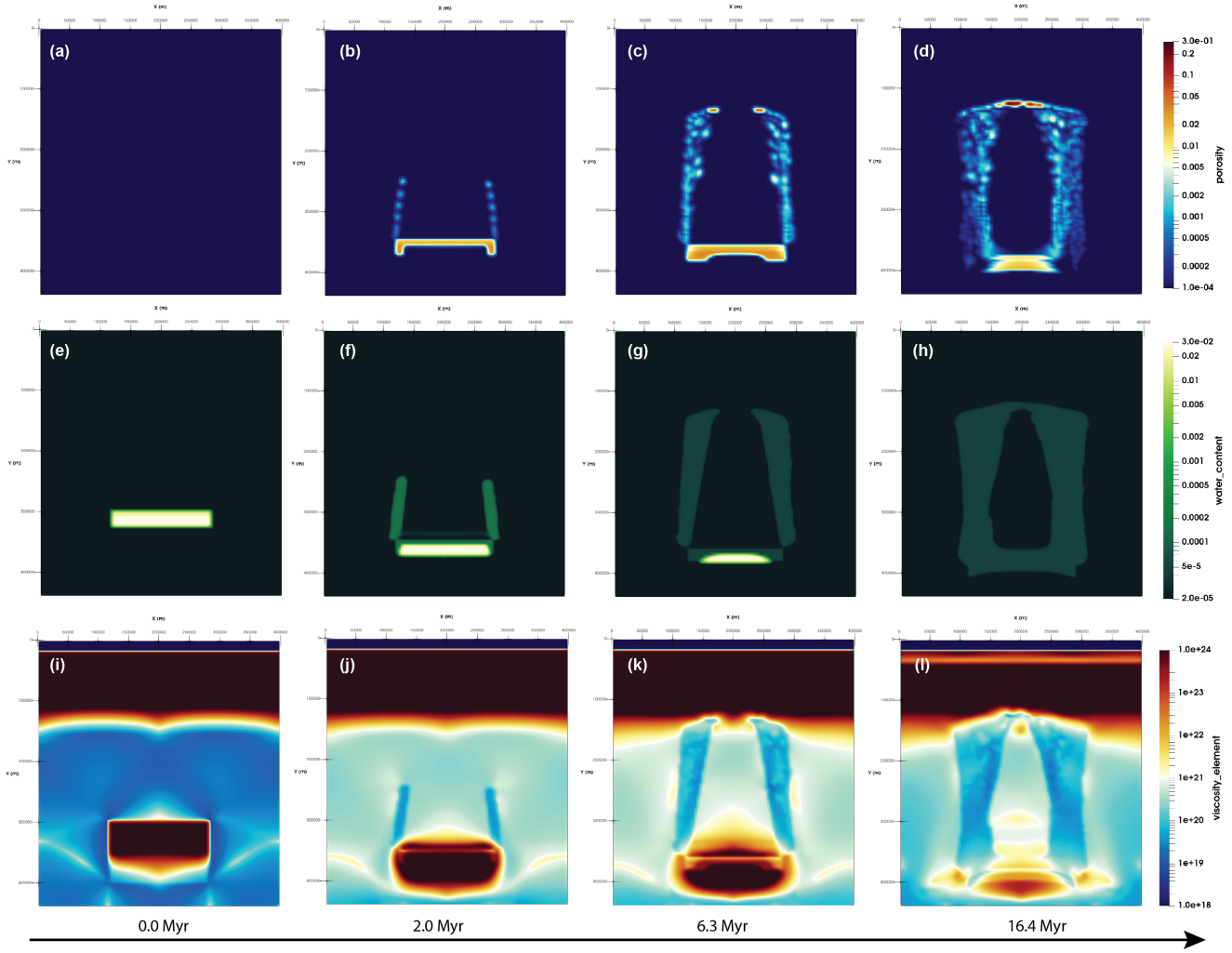


Figure: Numerical simulation results of the dehydration process of 60 Myr-old oceanic lithosphere. Evolution of porosity, water content, and viscosity fields at model times 0.0 Myr (a,e,i), 2.0 Myr (b,f,j), 6.3 Myr (c,g,k), and 16.4 Myr (d,h,l): (a-d) porosity fields; (e-h) water content fields; (i-l) viscosity fields.

Applying geodynamic tools to 3D large-scale ice-sheet modelling

Yu Zhang[*1,2], Ágnes Király[1], Till Sachau[2], Haibin Yang[3], and Paul D. Bons[2]

[1]NJORD Centre, Department of Geosciences, University of Oslo, Oslo, Norway
[2]Department of Geosciences, Tübingen University, Tübingen, Germany
[3]School of Earth Sciences, Zhejiang University, Hangzhou, China
[*]yu.zhang@geo.uio.no

Keywords: Underworld, ASPECT, ice dynamics, fold, shear zone

Ice in ice sheets behaves primarily as a ductile material, i.e. it can flow as a thick viscous fluid. Its flow properties are also anisotropic due to the development of crystallographic preferred orientation (CPO) of the ice crystals. Satellite and airborne sensors have provided detailed data on ice surface flow velocities, englacial structures of ice sheets and bedrock elevations. These data give insight into the flow behaviour of ice sheets. One significant structural phenomenon observed is large-scale folds (over 100 m in amplitude) in the englacial stratigraphy in polar ice sheets. Some folds can reach km-scale amplitudes and show plume-like geometries. A large population of folds is associated with ice streams. Ice streams, such as the over 500-km-long Northeast Greenland Ice Stream (NEGIS), are corridors of distinctly faster ice flow with lateral boundaries primarily defined by marginal shear zones, known as shear margins. Fast-flowing ice streams drain most of the inland ice from the Antarctic and Greenland ice sheets. Despite their critical role, the formation mechanisms of these large-scale folds and shear zones remain debated.

Geodynamic modelling tools provide a complementary framework for investigating solid-state ice flow and deformation, especially for processes that resemble problems in mantle and lithosphere dynamics, such as full-Stokes flow, strong rheological contrasts, evolving internal stratigraphy, anisotropic rheology, and thermo-mechanical coupling. Here, we apply two well-established full-Stokes geodynamic codes, Underworld and ASPECT, to three-dimensional, large-scale ice-sheet modelling. Underworld combines an Eulerian finite-element mesh with Lagrangian material points, making it well suited for particle-in-cell modelling of ice with highly non-linear rheology (stress exponent $n = 4$), localized shear deformation, and strong viscosity contrasts between ice, air, and bedrock. ASPECT provides a flexible, community-developed framework with a wide range of plugins for modelling complex geophysical and geological processes. Its established particle-in-cell methods also provide a useful basis for tracking CPO and anisotropic viscosity, as commonly applied to orthotropic materials such as olivine in the mantle.

By incorporating anisotropic, non-linear ice viscosity and evolving CPO, together with temperature evolution, we can model the formation of large-scale folds, ice streams and their shear margins. This approach highlights how geodynamic modelling tools can help bridge solid-Earth and ice-sheet modelling, providing a framework for investigating complex ice-sheet deformation.

Invert for the length scale of lunar mantle heterogeneity in the source region of Chang'E-5 mare basalts

Wenbo Zhang[*1,2], Meng Tian[1], and Nan Zhang[2]

[1]Faculty of Physics, Ludwig Maximilian University, Munich, Germany
[2]School of Earth and Space Sciences, Peking University, Beijing, China
*Meng.Tian@physik.lmu.de

Keywords: Chang'E-5 mare basalts, chemical heterogeneity, trace-element compositional variation, melting column model, Markov Chain Monte Carlo

The lunar mantle is widely thought to preserve chemical heterogeneity inherited from lunar magma ocean crystallization and subsequent cumulate mantle overturn. A compelling line of evidence for this heterogeneity is the large variation in incompatible trace-element patterns among lunar mare basalts, which record the composition and melting history of their mantle sources. However, most previous interpretations have treated these sources as binary mixtures of heterogeneous end-members, thereby preventing constraints on the spatial scale and distribution of mantle heterogeneity. Here we compile incompatible trace-element concentration data for Chang'E-5 mare basalts and invert these observations using a one-dimensional melting column model with Markov Chain Monte Carlo sampling. This framework links trace-element variability in erupted melts to the scale of source heterogeneity while accounting for partial melting and melt transport through the lunar mantle. Preliminary inversions indicate that the characteristic length scale of chemical heterogeneity in the Chang'E-5 source region is on the order of tens of kilometers. Such a scale is comparable to estimates for Earth's mantle, suggesting that the ancient lunar interior may have experienced vigorous mixing and convection.